

Tissue engineering strategies for biomaterial-based
anticancer drug delivery and enhancement of angiogenesis
in tumor-resected bone

Dissertation

Zur Erlangung des Grades

Doktor der Naturwissenschaften

Am Fachbereich Biologie

Der Johannes Gutenberg-Universität Mainz

Iris Bischoff

geb. am 15.07.1980 in Wiesbaden

Mainz, 2014

Dekan:

1. Berichterstatter:
2. Berichterstatter:

Tag der mündlichen Prüfung: 07.07.2014

Abbreviations

Abbreviations

ACA	Anticancer Agents
ALK	Activin receptor-like kinase
ALP	Alkaline phosphatase
APS	Ammonium persulfate
ATM	Ataxia telangiectasia mutated
ATR	Ataxia telangiectasia and Rad3 related
BD	Becton Dickinson
bFGF	Basic Fibroblast Growth Factor
BSA	Bovine serum albumin
°C	Degree Celsius
Calcein AM	Calcein acetoxymethyl ester
CBP	CREB binding protein
CD	Cluster of Differentiation
CIS	Cisplatin
CHK2	Checkpoint kinase-2
cm ²	Square centimetre
CO ₂	Carbon dioxide
CREB	cAMP response element-binding protein
CV	Crystal violet
dest.	Destillata
DMEM	Dulbecco's Modified Eagle Medium
DMSO	Dimethyl Sulfoxide
DNA	Deoxyribonucleic acid
DOX IV	Doxorubicin

ECGS	Endothelial Cell Growth Supplement
EDTA	Ethylenediaminetetraacetic acid
ELISA	Enzyme-linked immunosorbent assay
ERK	Extracellular-signal-regulated kinases
EtOH	Ethanol
GFP	Green Fluorescent Protein
h	Hour(s)
HA	Hydroxyapatite
HACD	Poly-Cyclodextrin-functionalized Hydroxyapatite
HCMEC	Human Cerebral Microvascular Endothelial Cell
HDMEC	Human Dermal Microvascular Endothelial Cell
HEPES	4-(2-hydroxyethyl)-1-piperazineethanesulfonic acid
HRP	Horseradish peroxidase
HUVEC	Human Umbilical Vein Endothelial Cell
LD	Lethaldosis
LDH	Lactate dehydrogenase
MeOH	Methanol
nd	Not detectable
min	Minute
ml	Milliliter
mM	Millimolar
MMP	Matrix metalloproteinase
MTS	3-(4,5-dimethylthiazol-2-yl)-5-(3-carboxymethoxyphenyl)-2-(4-sulfophenyl)-2H-tetrazolium

Abbreviations

nm	Nanometer
NO	Nitric oxide
OSA	Osteosarcoma
P	Passage
PA	Plasminogen activators
PAA	Polyacrylamide
PBS	Phosphate Buffered Saline
PCAF	p300/CBP-associated factor
PFA	Paraformaldehyde
PMA	Phorbol-12-myristate-13-acetate
poly(CD)	Poly-Cyclodextrin
pOB	Primary Osteoblast
P/S	Penicillin/Streptomycin
RNA	Ribonucleic acid
rpm	Rounds per minute
RPMI	Rosswell Park Memorial Institute
SDS-PAGE	Sodium Dodecyl Sulfate Polyacrylamide Gel Electrophoresis
SMC	Smooth muscle cells
TEMED	N,N,N',N'-Tetramethylethylenediamine
UMET	Unité Matériaux Et Transoformations
v/v	Volume to Volume
µg	Microgram

Index of contents

1	Introduction	- 1 -
1.1	Tissue engineered bone constructs for bone replacement.....	- 1 -
1.1.1	Tissue engineering.....	- 1 -
1.1.2	Bone tissue engineering.....	- 1 -
1.1.3	Bone formation.....	- 3 -
1.1.4	General aspects and clinical relevance of angiogenesis.....	- 4 -
1.1.5	Vascularization strategies: Advantages of co-cultures for engineered constructs with regard to vascularization and bone regeneration.....	- 8 -
1.1.6	Macrophages as tools for the improvement of the co-culture strategy	- 10 -
1.2	Cancer	- 11 -
1.2.1	Cancer background.....	- 11 -
1.2.2	Cancer and cell cycle.....	- 11 -
1.2.3	Cancer and the role of hypoxia	- 14 -
1.3	Treatment of osteosarcoma	- 17 -
1.3.1	Cancer treatment agents.....	- 18 -
1.3.2	Substitutes for tumor-resected bone	- 20 -
1.3.3	Drug delivery systems as implants for tumor-afflicted bone	- 20 -
1.4	Aim of the study	- 23 -
2	Materials and methods	- 25 -
2.1	Materials	- 25 -
2.1.1	Instruments	- 25 -
2.1.2	Consumables	- 26 -
2.1.3	Chemicals	- 26 -
2.1.4	Cell culture media	- 28 -

2.1.5	Buffers	- 29 -
2.1.6	Antibodies.....	- 29 -
2.1.7	Primers	- 30 -
2.1.8	Kits and Assays	- 31 -
2.1.9	Inhibitors.....	- 31 -
2.1.10	Biomaterials.....	- 31 -
2.1.11	Cell lines.....	- 32 -
2.2	Methods.....	- 32 -
2.2.1	Isolation and culture of cells	- 32 -
2.2.2	Conditions for co- and triple-cultures	- 37 -
2.2.3	Matrigel® angiogenesis assay	- 38 -
2.3	Cytotoxicity Assays.....	- 38 -
2.3.1	Cell viability test: MTS Assay	- 38 -
2.3.2	Cytotoxicity test: Release of Lactate dehydrogenase (LDH) ...	- 38 -
2.3.3	Cell viability test: alamarBlue®	- 39 -
2.3.4	LIVE/DEAD® viability/toxicity assay	- 39 -
2.3.5	DNA Quantification	- 40 -
2.3.6	Cytotoxic effect of cisplatin and doxorubicin on various cell types	- 41 -
2.3.7	Determination of median lethal dose (LD ₅₀).....	- 41 -
2.3.8	Biomaterial	- 41 -
2.3.9	Extraction Assay	- 43 -
2.3.10	Quantification of doxorubicin-release from poly(CD)-functionalized or unfunctionalized hydroxyapatite	- 46 -
2.3.11	Cell adhesion and growth on hydroxyapatite granules	- 46 -
2.3.12	Anoxic culture	- 47 -
2.3.13	Inhibition of HIF-1 α	- 47 -
2.4	Gene expression	- 47 -

2.4.1	RNA isolation	- 47 -
2.4.2	Reverse transcription	- 48 -
2.4.3	Quantitative real-time reverse transcriptase-polymerase chain reaction (Quantitative real-time RT-PCR)	- 48 -
2.5	Protein expression	- 49 -
2.5.1	Enzyme-linked immunosorbent assay (ELISA)	- 49 -
2.5.2	Sodium dodecyl sulfate polyacrylamide gel electrophoresis - SDS-PAGE	- 50 -
2.5.3	Western Blot	- 51 -
2.5.4	NanoOrange® protein quantification	- 51 -
2.6	Immunofluorescence staining	- 52 -
2.6.1	Image quantification	- 53 -
2.7	Statistical analysis	- 53 -
3	Results	- 54 -
3.1	Treatment of osteosarcoma cell lines and human primary cells with chemotherapeutic agents	- 54 -
3.2	Cytotoxic effect of chemotherapeutically treated biomaterials on human primary cells and human cancer cells	- 67 -
3.3	Cell growth on the biomaterials	- 82 -
3.4	Effect of anoxia on anticancer drug-treated cells	- 85 -
3.5	Analysis of the cell cycle in anticancer drug-treated cells	- 93 -
3.6	Analysis of cell cycle under hypoxic conditions	- 98 -
3.7	Angiogenic activation of OEC in co-culture with pOB	- 101 -
4	Discussion	- 110 -
4.1	Drug delivery systems for osteosarcoma	- 110 -
4.2	Enhancement of angiogenesis in bone tissue regeneration	- 117 -
4.3	Effect of hypoxia and drug-treatment on the cell cycle	- 117 -
5	Summary	- 129 -

6	Zusammenfassung	- 131 -
7	References	- 133 -
8	List of figures	- 152 -
9	List of tables	- 155 -
10	Publications and scientific presentations	- 156 -
10.1	Publications	- 156 -
10.2	Scientific presentations.....	- 156 -

1 Introduction

1.1 Tissue engineered bone constructs for bone replacement

1.1.1 Tissue engineering

The loss or impairment of organs and tissues is generally associated with therapies which include medication, the application of non-biological materials, surgical resection to remove diseased organs and sometimes replacement with healthy tissues or other transplantation methods (Ono et al. 1999). All these approaches are accompanied by major side effects and long-term complications. Tissue engineering has gained more attention in the field of regenerative medicine during the last decades. The aim is the successful replacement, modification or restoration of tissues or organs (Baradari et al. 2011) through the application of viable cells or tissues, biological substitutes such as scaffolds and growth factors or signaling molecules. The goal is to replace tissue with a functional tissue analogue that is designed for implantation to provide the needs for any individual patient (Zhou et al. 1998; Martel et al. 2002). These viable implants should offer the advantage of restoring, maintaining and improving the function of diseased or lost tissues and organs in order to optimize the healing process and to avoid severe adverse effects.

One possibility is the use of drug delivery systems such as lipid- or polymer-based nanoparticles or cyclodextrins, which can be designed to improve medication and the therapeutic efficacy of drugs (Allen and Cullis 2004; Uekama et al. 1998). Drug delivery systems, which release drugs such as anticancer agents in a time-dependent manner, without the alteration of their physical, chemical or biological properties, might be combined with a transplantable scaffold in order to stabilize the resected area and provide a localized drug therapy at the same time.

1.1.2 Bone tissue engineering

The challenge in bone tissue engineering is the successful reconstruction of bone defects resulting from trauma, tumor surgery, infections, biochemical disorders or abnormal skeletal development (Meijer et al. 2007). The essential elements of successful bone graft integration are osteogenesis, osteoconduction, osteoinduction and biocompatibility (Albrektsson and Johansson 2001). Different approaches with the

use of allografts (the transplantation of bone from one individual to another) or the application of materials from a different species (xenograft) go along with the risk of an immune rejection and involve the life-long administration of immunosuppressors (Cypher and Grossman 1996). Until now, the gold standard of bone grafting is the use of autologous bone material (healthy bone e. g. iliac crest, from the same individual) to reconstruct the lost bone. A disadvantage of this treatment is the necessity of an additional surgical intervention which can be accompanied with complications such as infection, severe pain, cosmetic disadvantages or even mortality (Giannoudis et al. 2005; Gitelis and Saiz 2002).

Bone tissue engineering constitutes an alternative for the regeneration of new bone. The aim is to restore the lost bone with its natural function by combining progenitor or mature cells with a stabilizing biocompatible bone graft in order to reconstruct the deficit (Rose, Felicity R A J and Oreffo, Richard O C 2002). The application of growth factors or their incorporation into the scaffold might improve the regenerative process (Hutmacher 2000). Vallet-Regí *et al.* highlight the *in vitro* procedure and processing of scaffolds that should be used for a successful bone substitution by suggesting two approaches. On the one hand prior to implantation, the scaffold might be soaked with tissue-inducing growth factors such as bone morphogenetic proteins and cells or on the other hand chemically treated with osteoinducing substances such as growth factors or peptides (Figure 1). All factors are applied in order to support the regeneration process in bone (Vallet-Regí et al. 2011).

A



B

Figure 1: Scheme of tissue engineered bone regeneration constructs.

Two approaches in bone tissue engineering. A shows the *in vitro* application of growth factors and cells to the bone construct prior to implantation. In B the surface of the scaffold is chemically prepared with osteoinductive substances such as peptides or growth factors before implantation (Vallet-Regí et al. 2011).

1.1.3 Bone formation

The vertebrate skeleton consists of more than 200 bones that can be divided into two categories. Flat bones like the skull consist of compact bone with a layer of interspersed bone marrow (Garzón-Alvarado et al. 2013). Long bones such as limb bones encompass most parts of the skeleton. These consist of a diaphysis in the central part of the bone composed of dense cortical or compact bone. Inside the diaphysis is the medullar cavity. Both ends of the long bone are formed by the epiphyses. The part between the diaphysis and epiphysis is termed the metaphysis.

There are two different mechanisms in the process of bone formation (ossification). Four cell types dominate in the bone-forming tissue, namely osteoblasts, osteocytes, osteoclasts and osteoprogenitor cells. During intramembranous ossification, which forms the flat bones such as skull, clavicle and mandible, the bone is formed by mesenchymal cells that condensate and subsequently differentiate into osteoblasts. Osteoblasts secrete large amounts of collagen I and low amounts of collagen type V that later mineralizes by the deposition of calcium hydroxyapatite (Caetano-Lopes et al. 2007). The activity of the enzyme alkaline phosphatase (ALP) is one of the osteoblastic differentiation markers (Eleniste et al. 2014). Bone morphogenic proteins (BMP) play a crucial role in the regulation of the activity and differentiation of osteoblasts (Rao and Stegemann 2013). Long bones are formed via endochondral ossification, a more complex process that requires a hyaline cartilage precursor (Shum et al. 2003). The ossification starts in the perichondrium, a layer of dense connective tissue that surrounds the cartilage. The cells differentiate into osteoblasts and form the "bone collar" where mineralization and the initiation of the cortical bone takes place. The bone collar forms the dense outer part of the compact bone (Dirckx et al. 2013). Chondrocytes located in the center of the diaphysis start to increase in size (hypertrophy) and to secrete alkaline phosphatase, which is crucial for mineral deposition. Subsequently, the cartilage is invaded by blood vessels, osteoclasts and osteoprogenitor cells resulting in cartilage replacement by trabecular bone and bone marrow which constitute the primary ossification center (Kronenberg 2003). Macrophage-derived osteoclasts generate space for the bone marrow by breaking down the spongiosa (Dirckx et al. 2013). The development of bone is characterized by a balance between osteoclast-derived bone resorption and osteoblast-stimulated bone formation (Mercatali et al. 2011).

After resection or loss of bone due to factors such as cancer, a cascade of healing processes is initiated. Bone fracture is accompanied by disruption of the vasculature

that is followed by an inflammatory response leading to the formation of new bone (Figure 2) (Rao and Stegemann 2013).

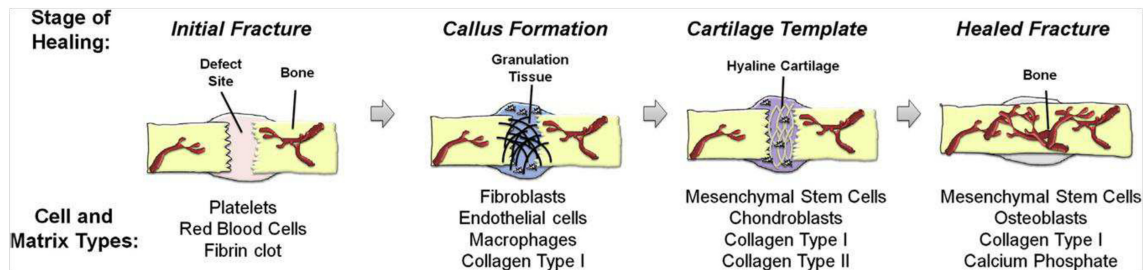


Figure 2: Schematic of the process of bone fracture healing, shows the major cell and matrix types involved at each stage (from Rao and Stegemann 2013).

As bone is a metabolically active tissue, a supply of oxygen and nutrients is constantly required. High vascularization of bone tissue guarantees the nourishment of the cells on the one hand and waste removal on the other hand.

1.1.4 General aspects and clinical relevance of angiogenesis

Angiogenesis plays a crucial role in tumor formation (Koch et al. 1992). It is a highly regulated process that is also involved in growth, tissue repair and bone remodeling (Villars et al. 2000). It requires formation of new blood vessels by the process of sprouting from preexisting blood vessels in the microvasculature. In contrast to vasculogenesis, a process that is defined to be limited to early embryogenesis, the process of angiogenesis occurs during development and post-natal life. During hypoxia pro-angiogenic factors such as VEGFA, eNOS or angiopoietin 2 are up-regulated (Auguste et al. 2005). Angiogenesis can be divided into an activation phase and a resolution phase (Pepper 1997). The activation phase is composed of the initiation process and progression, including increase of vascular permeability and extravascular fibrin deposition, followed by basement membrane degradation, cell migration into the surrounding matrix, cell division and the formation of a lumen in the proximal sprout (Stetler-Stevenson 1999).

In a first step VEGFA induces the increased release of nitric oxide (NO), resulting in the widening of blood vessels, named vasodilatation. The basal lamina and the extracellular matrix are degraded by extracellular proteolytic enzymes such as matrix

metalloproteinases (MMP) or plasminogen activators (PA) (Pepper 2001). Subsequently, endothelial cells invade and migrate towards the angiogenic stimulus into the extracellular space where they proliferate and form a capillary lumen (Oh et al. 2000). Finally, endothelial cells perform mitosis at the tip of a sprouting vessel (Zhou et al. 1998). The resolution phase includes the termination of cell migration as well as the inhibition of cell division. The newly formed vessels are stabilized and the maturation of the vascular network indicated by the reconstitution of the basement membrane, with the subsequent promotion of intercellular junction complex maturation completing the angiogenic process (Pepper 1997). The process of maturation requires angiogenic and arteriogenic factors that lead to the coating of the newly formed blood vessels with mural cells such as pericytes or vascular smooth muscle cells (SMC). Pericytes are associated with small blood vessels such as arterioles, venules or capillaries and share the basement membrane with the endothelium while vascular SMC form a concentric layer around arteries or veins (Hellström et al. 1999).

There are three major signaling pathways during the maturation of new blood vessels. In the platelet-derived growth factor (PDGF-B) and its receptor-beta (PDGFR- β) pathway, endothelial cells secrete PDGF-B as a chemoattractant, leading to the recruitment of pericytes in the microvasculature through the activation of PDGFR- β (Ferrara and Kerbel 2005). PDGFR- β is expressed by vascular SMC and pericytes. Studies of PDGF-B-negative embryos that lack the presence of pericytes exhibit microaneurysms and rupture (Hellström et al. 1999; Lindahl et al. 1998). The Tie/angiopoietin signaling system is another important pathway during vascular development. The main components of this pathway are angiopoietin-1 and angiopoietin-2 which are ligands of the receptor tyrosine kinase Tie-2 (Thurston and Daly 2012). Studies by Visconti *et al.* indicate that angiopoietin-2 and VEGFA collaborate and induce the formation of capillary structures (Visconti et al. 2002). Koblizek *et al.* found that in an *in vitro* assay using endothelial cells the formation of capillary-like sprouts in a fibrin gel occurred when recombinant angiopoietin-1 was applied (Koblizek et al. 1998). These studies underline the important role of the Tie/angiopoietin pathway during vessel maturation. The third pathway leading to the formation of new blood vessels is the transforming growth factor beta 1 (TGF- β 1) pathway. Studies by Goumans *et al.* outlined the importance of the TGF- β 1 signaling pathway for normal vessel development (Goumans et al. 2003). Two signaling cascades involve the activin receptor-like kinase 5 (ALK-5)-Smad-2/3 or the ALK-1-Smad-1/5 pathway, initialized by TGF- β 1. Both pathways play a crucial role in endothelial cell proliferation, migration during the activation phase and vessel maturation in the resolution phase of angiogenesis (Jain 2003).

Vascular endothelial growth factor (VEGF) and tumor necrosis factor α (TNF- α) are the major angiogenic-stimulating factors (Abbassi et al. 1993). TNF- α , in addition to other factors, is known to play a role in the inflammatory response to various stimuli, among them macrophages (Vassalli 1992). Its primary function is the regulation of immune cells resulting in apoptosis, cell proliferation, cell differentiation of cells or the release of additional cytokines. VEGF is a sub-family of the platelet-derived growth factor (PDGF) family that can be divided into six members, VEGFA, VEGFB, VEGFC, VEGFD, VEGFE and the placental growth factor protein (PGF) (Clauss 2000). In angiogenesis, VEGFA represents the most important member of the family. As a result of alternative splicing, there are five different isoforms of VEGFA produced (VEGFA₁₂₁, VEGF₁₄₅, VEGFA₁₆₅, VEGFA₁₈₉ and VEGFA₂₀₆) (Girling and Rogers 2009), whereby VEGF₁₆₅ is the most relevant variant during angiogenesis (Yue and Tomanek 2001). VEGFA is a major contributor to angiogenesis as it is necessary for endothelial cell proliferation and the formation of tube structures by integrating activated endothelial cells into angiogenic structures, resembling capillaries (Shibuya 2006). VEGFA evokes a cellular response by binding to the tyrosine kinase receptor, VEGFR1 or VEGFR2, resulting in the transmission of extracellular signals into the cell leading to the promotion of endothelial cell differentiation, proliferation and sprouting (Adams and Alitalo 2007). Inflammation or low oxygen supply is associated with a high expression of VEGFA. During hypoxia, the VEGFA gene is under the control of the transcription factor hypoxia-inducible factor-1 (HIF-1) (Mohamed et al. 2004).

Under physiological conditions the activation phase of angiogenesis is mainly induced by hypoxia or inflammation. During inflammation platelets of the fibrin clot are the first cells that are recruited at sites of injury. They aggregate at the end of the damaged blood vessels and release growth factors like platelet-derived growth factor (PDGF) and transforming growth factor beta (TGF- β) (Martin and Leibovich 2005), attracting inflammatory cells such as neutrophils and monocytes (chemotaxis). Monocytes from the bloodstream enter the inflammatory area through the blood vessel walls. Once the monocytes are in the wound, they differentiate into macrophages at sites of inflammation. Macrophages regulate tissue repair by secretion of several growth factors and pro-inflammatory cytokines/chemokines or acute-phase proteins, including TNF- α or interleukins like IL-8 or IL-6 that amplify the inflammatory response (Werner and Grose 2003). IL-8 is a chemokine providing chemotactic activity for neutrophils and lymphocytes (Baggiolini et al. 1989). It is involved in the invasion of neutrophils by shedding neutrophil lectin adhesion molecule-1 (LECAM-1), the up-regulation of leukocyte β_2 integrins and finally the attachment and transmigration of the neutrophils through the vessel wall (Huber et al. 1991). Studies by Koch *et al.* suggested an

important function of macrophage-derived IL-8 in tumor growth and wound repair (Koch et al. 1992). In addition, IL-8 is relevant in terms of angiogenesis as it directly enhances endothelial cell proliferation and their formation of capillary structures (Li et al. 2003). Besides macrophages, endothelial cells are also known to release IL-6 (Motro et al. 1990). As a mediator of inflammatory signals, IL-6 is mainly induced by other cytokines like TNF- α or IL-1 β (Topley et al. 1993). IL-6 induces the C-reactive protein (CRP), a member of the acute phase reactants that activates the complement system (Steensberg et al. 2003; Steel and Whitehead 1994).

The presence of macrophages is followed by lymphocytes, which release a number of cytokines which influence the function of macrophages (Greenhalgh 1998). The interaction of leukocytes with endothelial cells is mediated through cell adhesion molecules that bind to integrins such as $\alpha_L\beta_2$ or $\alpha_M\beta_2$ on the leukocyte surface, initially starting with a weak adhesion to selectins. This process is called leukocyte rolling. In the next step a stronger adhesion mediated by intercellular adhesion molecule-1 (ICAM-1) or vascular cell adhesion molecule (VCAM-1) takes place (Tsaryk et al. 2007). The transmigration process of leukocytes across the endothelial lining is mediated by platelet endothelial cell adhesion molecule (PECAM) or CD99 (Peters et al. 2003; Ley et al. 2007) (Figure 3). Selectins are expressed after cytokine activation of endothelial cells by tissue macrophages. Initially, P-selectin is expressed on the surface of endothelium or platelets. E-selectin is induced shortly after P-selectin expression (Boyle, MD, Edward M et al. 1997). E-selectin and ICAM-1 are adhesive proteins induced on endothelium for the binding of granulocytes, monocytes and T-lymphocytes as a response to several cytokines, including TNF- α , IL-1 or interferon- γ (IFN- γ) (Leeuwenberg et al. 1992; Carlos et al. 1991).

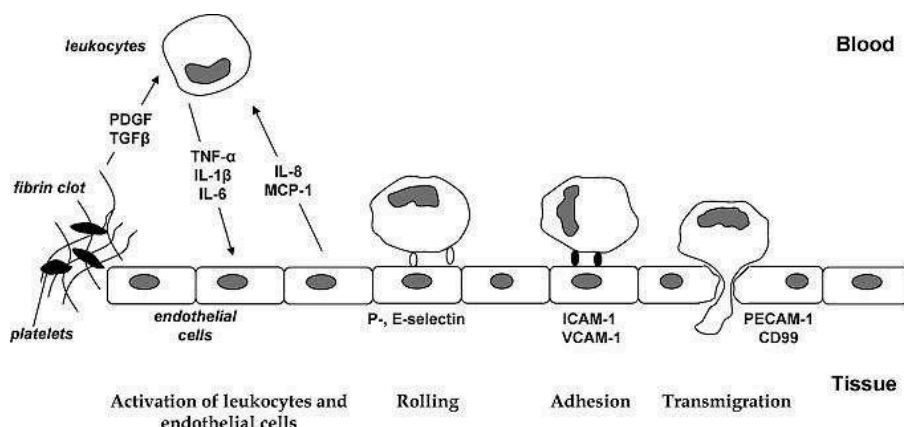


Figure 3: Activation phase of wound healing (from Tsaryk et al. 2007)

During the activation phase of wound healing platelets of the fibrin clot secrete growth factors like PDGF or TGF- β and attract leukocytes. Leukocytes like monocytes differentiate into macrophages at the site of action and release inflammatory factors like TNF- α , IL-6 or IL-8 to amplify the inflammatory response. Via integrins, the leukocytes bind to selectins and adhesion molecules to the endothelial surface. Finally, the transmigration of leukocytes through the endothelial border is mediated by PECAM or CD99.

During the proliferative phase of wound healing, granulation tissue consisting of inflammatory cells, newly formed blood vessels and fibroblasts is formed (Figure 4). In order to recruit cells to the sites of wound healing, macrophages secrete PDGF and TGF- β that induce the migration and proliferation of fibroblasts (Diegelmann et al. 2004). When fibroblasts enter the wound they form the granulation tissue that is composed of collagen and fibronectin.

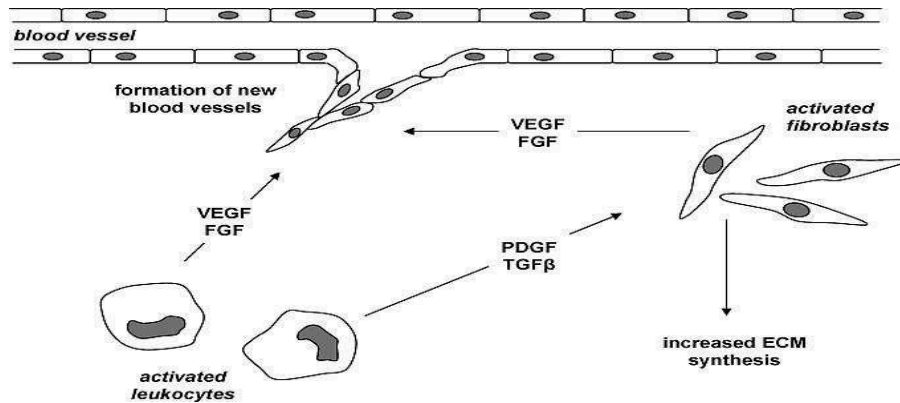


Figure 4: Proliferative phase of wound healing (from Tsaryk et al. 2007)

During the proliferative phase of wound healing macrophages secrete growth factors like PDGF or TGF- β . Both factors induce the migration and proliferation of fibroblasts, which secrete proangiogenic growth factors such as VEGF and bFGF finally leading to the formation of new blood vessels.

Concurrently, macrophages and fibroblasts secrete pro-angiogenic factors like VEGF and basic fibroblast growth factor (bFGF) which finally lead to new blood vessel formation (Nissen et al. 1998; Adams und Alitalo 2007). When the vascularization of inflamed and damaged tissue is completed, the fibroblasts differentiate into myofibroblasts and contract the matrix in order to bring the margins of the wound together, leaving a collagen-rich scar tissue that is remodeled over time (Midwood et al. 2004).

1.1.5 Vascularization strategies: Advantages of co-cultures for engineered constructs with regard to vascularization and bone regeneration

Once the tissue engineered bone graft is incorporated into the host's skeleton, there is a need for nutrients and oxygen for the tissue (Santos et al. 2009). In addition, the removal of waste products must be guaranteed. Therefore, a sufficient and well developed vasculature around the implanted area is required. Rouwkema *et al.* described an inflammatory wound healing response following the implantation process that induces the formation of new blood vessels (Rouwkema et al. 2008). Unfortunately, this neovessel formation is too slow to provide adequate blood vessels.

As a consequence, vascularization strategies are needed to guarantee the successful long-term incorporation of a bone substitute. These strategies might be (i) designing the scaffold to facilitate the vascularization process (Malda et al. 2004), (ii) the delivery of growth factors such as VEGF (Ehrbar et al. 2004), *in vivo* prevascularization (Kneser et al. 2006) or *in vitro* prevascularization (Levenberg et al. 2005). As *in vitro* prevascularization strategies proved able to enhance the formation of angiogenic structures at the site of implantation, recent research has focused on the use of co-culture systems and the research on their complex interactions (Simunovic et al. 2013). The processes of angiogenesis and osteogenesis depend on factors that play a crucial role during the interaction of endothelial cells and osteoblasts during bone repair (Collin-Osdoby 1994). During the past decade, complex co-culture systems have become a promising instrument for clinical applications in the field of bone tissue engineering and regenerative medicine, mimicking the natural conditions in the bone. With regard to the formation of new blood vessels, it would be useful to work with autologous cells that are easy to isolate. Outgrowth endothelial cells (OEC), isolated from human peripheral blood, or human dermal microvascular endothelial cells (HMDEC) can serve as a potential cell source for the process of neovascularization in co-cultures. The co-culture of human primary endothelial cells with human primary osteoblasts, isolated from human cancellous bone fragments, constitutes an approach in bone tissue engineering (Unger et al. 2011). Previous studies reveal that the co-cultivation of pOB with human primary HMDEC (Santos et al. 2009) or OEC (Fuchs et al. 2007) resulted in the formation of angiogenic structures of endothelial cells after three to four weeks of cultivation, induced by pOB or the osteosarcoma cell line MG-63, providing pro-angiogenic factors for the endothelium such as VEGF or matrix components like collagen. The studies performed by Villars *et al.* have shown that there is a reciprocal regulation and functional relationship between endothelial cells and osteoblasts during osteogenesis (Villars et al. 2000). Systemic hormones and paracrine growth factors such as IL-6, prostacyclin or endothelin-1 that are secreted by endothelial cells play a significant role in this interaction (Brandi and Collin-Osdoby 2006). On the other hand, osteoblasts influence the activity of endothelial cells by the secretion of pro-angiogenic growth factors such as VEGF or bFGF (Deckers, Martine M L et al. 2002). Further studies suggest intercommunication between endothelial cells and osteoblasts that not only require diffusible regulatory molecules, but involve gap junction communications for a multicellular network (Villars et al. 2002).

1.1.6 Macrophages as tools for the improvement of the co-culture strategy

During the last decade, co-cultures represented a successful model in tissue engineering and a promising tool for the reconstruction of bone after trauma. As angiogenic structures need three to four weeks to form *in vitro*, it might be useful to improve the beneficial effect of the co-culture on the angiogenic activation of OEC and to accelerate the formation of microvessel-like structures *in vitro*. For a clinical application it would enhance the chances of an advanced and more successful healing accompanied with an upgraded quality of life. Several approaches have been proposed to improve the neovascularization process of engineered tissues, including the use of endothelial cells or endothelial progenitor cells (Rivron et al. 2008) (Rouwkema et al. 2006), strategies based on the natural interaction of the different cell types during the process of bone regeneration using co-culture systems (Fuchs et al. 2007; Kaigler et al. 2003) or additional treatment of tissue engineered constructs with growth factors or morphogens (Dohle et al. 2010; Dohle et al. 2011). Nevertheless, treating co-cultures with growth factors or morphogens has several limitations and drawbacks, e.g. relatively short half-lives of growth factors or the induction of leaky and unstable vessels in response to VEGF treatment (Sundberg et al. 2002). Mimicking the natural responses of the human body to accelerate the formation of angiogenic structures might be another possibility. As inflammation is a physiological reaction to initiate healing processes, our group has considered the possibility of using pro-inflammatory stimuli as a tissue engineering strategy, especially with respect to enhancing vascularization. Macrophages play a key role during the process of inflammation regarding angiogenesis, due to their presence in normal and inflamed tissue and their potential to release growth factors and cytokines that are of major importance during the formation of new blood vessels. Previous studies have shown that activated macrophages may have an influence on each phase of angiogenesis, that is, the alteration of the local extracellular matrix and the induction of endothelial cells either to migrate or to proliferate (Sunderkötter et al. 1994). *In vivo* studies by Arras *et al.* showed that by the application of LPS monocytes and thus macrophages accumulated and proliferated rapidly at sites of the wound, resulting in a higher density of capillaries (Arras et al. 1998). Therefore, addition of this type of cell might have positive influences on the formation microvessel-like structures via inflammatory processes in a co-culture system of OEC and pOB.

1.2 Cancer

1.2.1 Cancer background

Cancer is one of the leading causes of death worldwide, accounting for about 13% of all deaths in humans per year (Ferlay et al. 2010). It can affect diverse parts of the body by invasion (primary) or metastasis (secondary) of tumor cells and cause morbidity with severe functional and structural defects, leading to death. Metastases are the major cause of death from cancer. The main types of cancer are lung, stomach, liver, colorectal, breast and cervical cancer (Jemal et al. 2011). In general, cancer arises from a single cell, whereby the transformation of a normal cell to a cancer cell is a multistage process with the progression from a pre-cancerous lesion to malignant tumors. This transformation is due to various factors, including genetic predisposition or external agents like ultraviolet radiation, tobacco smoke or biological carcinogens such as infections from viruses, bacteria or parasites (Venitt 1996). Aging is an additional factor, as the risk for cancer rises dramatically as the person gets older. Early detection and treatment can markedly reduce cancer mortality (WHO 2013).

1.2.2 Cancer and cell cycle

When DNA damage occurs, induced by e.g. irradiation or the application of anticancer agents (Renbin Zhao et al. 2000), the cell initiates mechanisms to prevent genome mutation that might give rise to carcinogenesis. After DNA impairment, the tumor suppressor protein p53 is posttranslationally stabilized and accumulates. p53 is sustained through a series of posttranslational modifications. The activation of the transcription factor results in cell cycle arrest or apoptosis. p53 is a sequence-specific DNA-binding protein and its primary role has been attributed to its function as a transcription factor that controls hundreds of cellular genes that are implicated in a variety of physiological responses to genome instability, DNA damage or metabolic stress such as hypoxia (Maclaine and Hupp 2009). Under normal conditions, p53 is constantly inactive in healthy cells. p53 levels are regulated in large part by murine double minute 2 homolog (Mdm2), the product of a p53-inducible gene. Mdm2 interacts with the N-terminus of p53 resulting in an inhibition of the transcriptional activity of p53 by interfering with its ability to contact transcriptional co-activators such as p300/CBP (Prives and Hall 1999). Furthermore, Mdm2 promotes the ubiquitination of p53 which leads to the transport of p53 from the nucleus to the cytoplasm where it is degraded by

proteasomes (Chen et al. 2003). When cells are exposed to stress, signal mediators such as ATM (ataxia telangiectasia mutated), ATR (ataxia telangiectasia and Rad3 related) and checkpoint kinase-2 (CHK2) perform a phosphorylation of the transcription factor, leading to the inhibition of its instabilization by Mdm2. Besides, Mdm2 is deactivated by p14ARF which thus promotes p53. Additionally, p53 is no longer exposed to ubiquitination and hence degradation by proteasomes can no longer take place. p53 is furthermore stabilized through modifications by acetyltransferases like CBP, p300 or PCAF or methyltransferases such as SET9 which increases its site-specific DNA binding (Masatsugu and Yamamoto 2009). In further steps, p53 recruits cofactors that are needed for the transcription of the target genes, but in general, p53 can also mediate their transcriptional regression. The transcription of many genes into proteins that are involved in various pathways are induced by p53. This pathway finally leads to cell cycle arrest, DNA repair or apoptosis (Figure 5) (Riley et al. 2008).

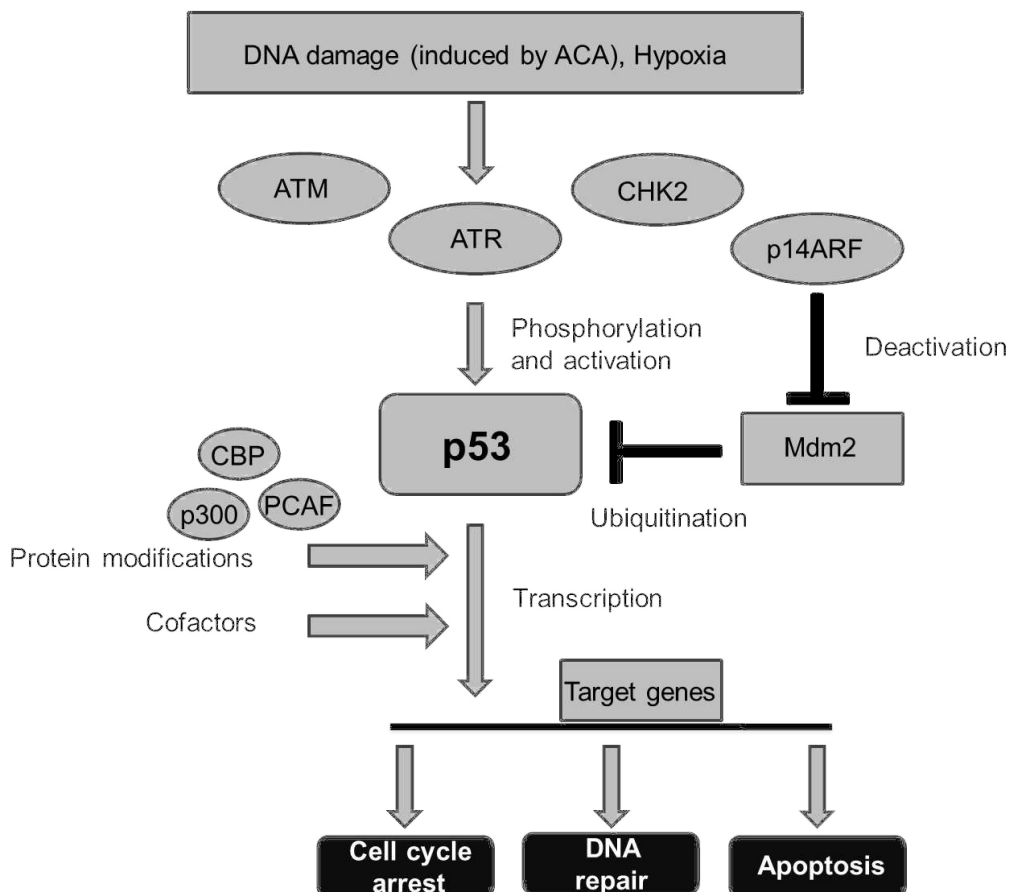


Figure 5: p53 pathway

Under normal conditions p53 is constantly down regulated by Mdm2. DNA damage or hypoxia lead to the stabilization of p53 through several protein modifications. Accompanied by cofactors, p53 targets genes that transcribe for proteins that initiate cell cycle arrest, DNA repair or apoptosis.

p21, the cyclin-dependent kinase (CDK) inhibitor is the primary mediator of the p53-dependent G1 cell cycle arrest (Adimoolam and Ford 2003; He et al. 2005). The main target of p21 is the inhibition of the cyclin-dependent kinase 2, which inhibits the cell at the transition from the G1-phase to the S-phase (Brugarolas et al. 1999; Bunz et al. 1998) remain in the G0-phase of the cell cycle. In addition, p21 seems to play a significant role in the G2-phase arrest of the cell cycle in response to DNA damage (Figure 6) (Cazzalini et al. 2010).

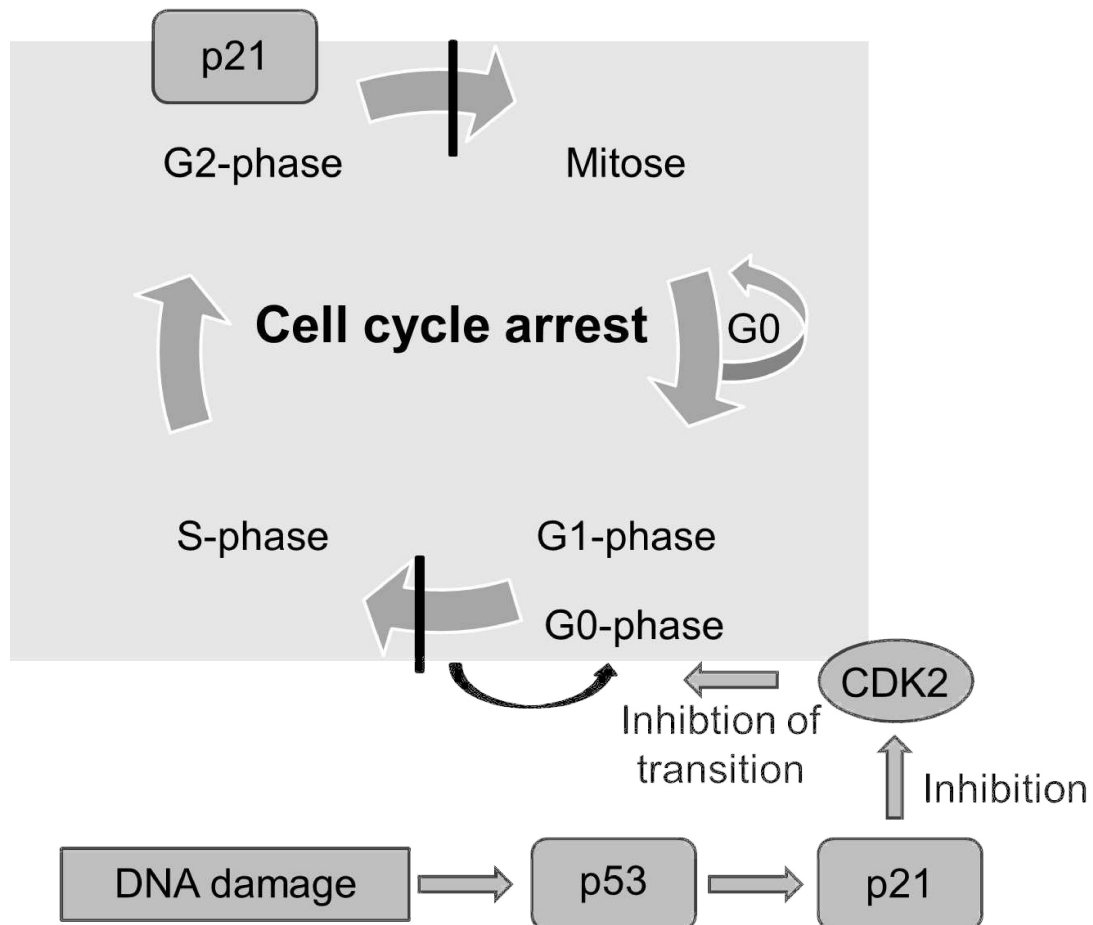


Figure 6: DNA damage induced cell cycle arrest

When DNA damage occurs and p53 is stabilized, the transcription factor promotes the induction of p21, a CDK inhibitor. Thus the transition of the cell cycle from the G1-phase to the S-phase is interrupted and the cell remains in the G0-phase. Additionally, p21 when can hinder the cell from the transition from the G2-phase to the mitose resulting in cell cycle arrest.

In case of irreversible damage, the induction of apoptosis is induced by p53 through the up-regulation of genes that play a crucial role in apoptosis preventing genome mutation that might give rise to carcinogenesis. The target genes of p53 can be divided into three categories. The first group encodes for proteins of the cell membrane such as CD95, DR5 or PERP. The second group encodes for proteins that localize to the cytosol (Pidd, PIG8) and the third group encodes proteins of the mitochondria such as

the p53 up-regulated modulator of apoptosis (PUMA) Bcl-2 associated X protein (BAX) or Noxa (Benchimol 2001; Chipuk et al. 2004). The expression of BAX proteins leads to the release of cytochrome c from the mitochondria and the activation of apoptotic protease activating factor 1 (Apaf-1) that binds and thus activates caspase-9 (Figure 7) (Shen and White 2001; Soengas et al. 1999).

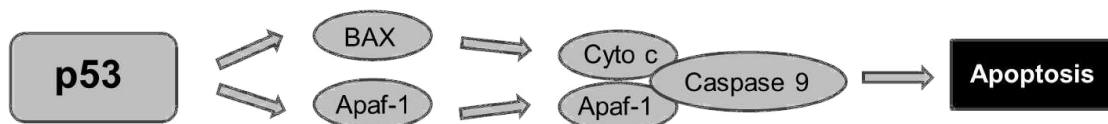


Figure 7: Apoptosis pathway

In the apoptosis pathway of p53, the expression of BAX leads to the release of cytochrome c from the mitochondria. Apaf-1 is activated and binds together with cytochrome c to caspase 9 what finally leads to the induction of apoptosis.

In more than 50% of all human tumors, p53 loses its function due to mutations (Ryan et al. 2001). Many of the tumors which retain wild-type p53 lose the ability to induce the p53 response. Others exhibit a lack of the ability to respond to p53 (Hainaut et al. 1997; Woods and Vousden 2001). Therefore, potentially malignant cells are not able to enter apoptosis (Hannan et al. 2013). The tumor cells can thus proliferate and spread, finally leading to metastasis and death in the worst case scenario.

1.2.3 Cancer and the role of hypoxia

Cellular hypoxia occurs both in normal physiology and pathological conditions such as cancer (Harris 2002). In rapidly proliferating malignant tumors, hypoxic conditions are common due to the abnormal tumor vasculature, characterized by leaky and fragile blood vessels. This is the main reason that cancerous tissue often contains vast areas with low oxygen concentrations (Leite de Oliveira, Rodrigo et al. 2012; Boyle and Travers 2006). In addition, hypoxia promotes the invasion and metastasis of cancer cells (Arsenault et al. 2012).

Many adaptive responses are induced by hypoxia, mainly mediated by hypoxia inducible factor 1 (HIF-1). The oxygen sensor HIF-1 is a heterodimer, consisting of the subunits HIF-1 β and HIF-1 α . The latter is, as an O₂ sensor, a key regulator of cellular responses to hypoxia, and acts as a transcription factor. In a normoxic environment, HIF-1 α is constantly hydroxylated by specific prolyl hydroxylases (PHD) at the two proline residues P402 and P564 that are localized inside the oxygen-dependent

degradation (ODD) domain. Subsequently, polyhydroxylated HIF-1 α binds to the van Hippel-Lindau (VHL) tumor suppressor protein, which is an E3 ubiquitin ligase, resulting in proteasomal degradation of HIF-1 α (Liu et al. 2013; Fels and Koumenis 2005). When the oxygen tension in cells drops, the hydroxylation of HIF-1 α decreases and the transcription factor is stabilized. In response to hypoxia, PHD are less active, leading to inhibited proline hydroxylation of HIF-1 α resulting in its accumulation. VHL is no longer able to target by ubiquitination of HIF-1 α for proteasomal degradation (Harris 2002). Subsequently, HIF-1 α is translocated to the nucleus, where it dimerizes with HIF-1 β and binds to the hypoxia-response elements (HRE) in the promoter region of the target genes. The HIF-1 α /HIF-1 β dimer binds to the transcriptional co-activators p300/CBP and target genes that are responsible for a range of adaptive responses including angiogenesis, metabolic reprogramming, erythropoiesis and scavenging of reactive oxygen species (ROS) are transcribed (Figure 8) (Giaccia et al. 2003; Aragonés et al. 2008).

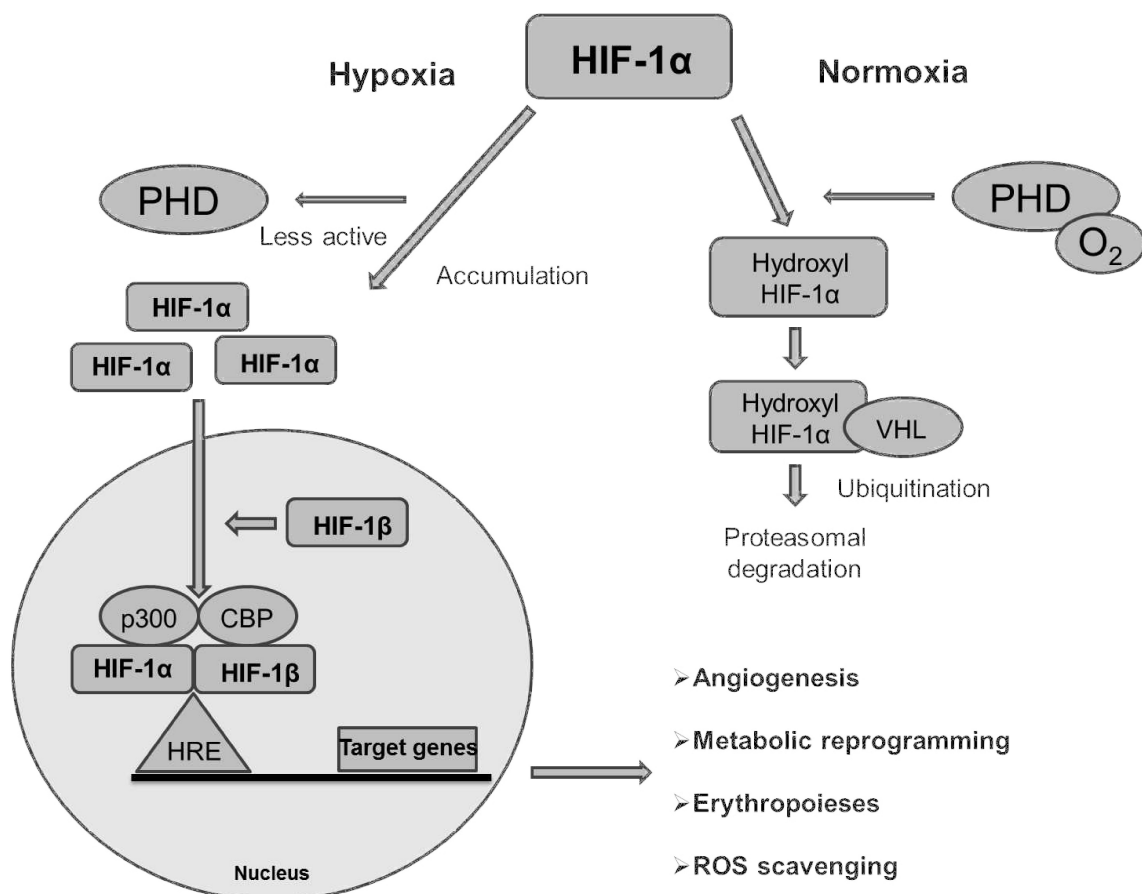


Figure 8: HIF-1 α pathway

Under normoxia HIF-1 α is constantly degraded due to hydroxylation by PHD. In the absence of oxygen PHD are less active and HIF-1 α is stabilized. Together with HIF-1 β the transcription factor binds to the transcriptional co-activators p300/CBP and target genes that are responsible for processes that regulate the oxygen requirement in the cell.

Previous studies indicate an interaction between HIF-1 α and the tumor suppressor p53. Under hypoxic or anoxic conditions, p53 is stabilized and binds to the ODD domain of the accumulated HIF-1 α resulting in its inhibition, e.g. by enabling Mdm2 to degrade the protein, leading to decreased secretion of pro-angiogenic factors and thus to reduced tumor cell survival (Rajani Ravi et al.; Fels and Koumenis 2005). This interaction might be promising in cancer therapy of tumors that express wild-type p53. Other studies suggest a direct interaction of HIF-1 α and Mdm2 resulting in a protection of p53 Mdm2-induced ubiquitination and degradation.

1.2.3.1 Primary bone cancer

In general, bone cancer that arises from the skeletal system is rare. Only 0.001% of all new cancers are primary bone tumors. Nevertheless, bone cancer can affect any part of the bone. Benign or malignant tumors can rise in cartilaginous, osteoid (unmineralized bone matrix), fibrous tissue or bone marrow (Malawer et al. 2008). Among malignant tumors of bone there are different types of myeloma, chondrosarcoma, fibrosarcoma or osteosarcoma (OSA), just to name a few (Jaffe and Selin 1951). Malawer et al. describes three mechanisms of tumor growth and extension (Malawer et al. 2008). Benign tumors grow and expand by compression of normal tissue or resorption of bone by reactive osteoclasts. Malignant bone tumors arise through direct destruction of normal tissue by destroying the cortex of the bone and invading the soft tissue. Surgery is the most common treatment of bone cancer although cancer recurrence occurs frequently due to incomplete tumor removal (Malawer et al. 2008).

1.2.3.2 Osteosarcoma and metastasis

Among malignant tumors in bone, the most common primary bone cancer is osteosarcoma, accounting for 35.1% of all primary sarcomas in bone, followed by chondrosarcoma and Ewing's sarcoma (Howard D. Dorfman 1995). According to the World Health Organization (WHO), there are eight classification categories of OSA: conventional, telangiectatic, small cell, low-grade central, secondary, parosteal, periosteal, and high-grade surface. These are distinguished histologically and on the basis of typical radiographic appearances (Yarmish et al. 2010). OSA usually affects the appendicular skeleton and often originates in the metaphysis of long bones of

children or juveniles (Bielack et al. 2002), particularly in the knee region. In osteosarcoma, the tumor cells produce bone or osteoid and cartilage matrix and fibrous tissue. Conventional OSA can be divided into three subtypes, that is osteoblastic, chondroblastic and fibroblastic. It can arise in the medullary cavity of the metaphysis of the long bone but it also may occur on the surface of the bone (juxtacortical) (Klein and Siegal 2006). Patients that are afflicted with OSA mostly suffer from severe pain that greatly impairs the quality of life, but draws attention to the tumor

In addition, bone metastasis is even more frequent than OSA and causes severe pain which limits the cancer patient's quality of life and often results in death (Parkin et al. 2005; Jemal et al. 2008).

1.3 Treatment of osteosarcoma

Surgery is the usually applied treatment for bone cancer to remove the entire tumor and the surrounding area of normal bone and soft tissue to remove residual cancer cells. For better control of cancer, pre-/post-operative radiotherapy or chemotherapy are administered. In spite of significant improvements in surgery and radio- or chemotherapy, the optimal therapy and the sequence of treatments in combined therapy, show only modest improvement in overall survival of the patient (Lamoureux et al. 2007). Besides, lethal risks and severe adverse effects are present with each treatment of bone cancer (Love et al. 1989). Despite all attempts of bone cancer treatment, it exhibits one of the highest rates of recurrence, which occurs mostly as a result of incomplete surgical resection and the existence of residual neoplastic cells in the soft tissue of the surgical site after marginal resection (Loree and Strong 1990; Partridge et al. 2000). There is little doubt that residual cancer will yield local persistence and nearly always an increased mortality (Upile et al. 2007). The adequate resection of bone and the bone tumor results in large bone defects, leading to a grave impairment of the patient's quality of life (Gotay et al. 1992). Additional attempts to eliminate residual cancer cells after tumor resection such as high-dose radio- or chemotherapy are considered mandatory to avoid cancer recurrence, but have severe adverse effects making the curative potency questionable (Brennan et al. 1995). Therefore, novel strategies for cancer treatment after tumor surgery which effectively kill the remaining cancer cells in soft tissue but accompanied with less side effects without compromising survival and the quality of life are required and need to be investigated. The traditional concept of radical excision is challenged by the "less is

more" concept with greater consideration of maintaining structure and function as well as the patient's quality of life (Shah and Gil 2009).

Adjuvant high-dose systemic radio- or chemotherapy in cancer therapy is applied in order to damage cells in such a way that they die. The optimal treatment is to target replicating cells, which unfortunately also include healthy cells. Thus, many cancer patients die of complications from the high doses of systemic administered medication or radiation that is needed to kill the surviving cancer cells (Lavertu et al. 1997).

1.3.1 Cancer treatment agents

Besides radiotherapy, chemotherapeutic drugs are commonly used in cancer therapy. Various drug types are divided in different groups such as mitotic inhibitors, anti-metabolites, alkylating agents or anti-tumor antibiotics (Malhotra and Perry 2003). The anti-tumor drug cisplatin is related to alkylating agents while doxorubicin belongs to the anti-tumor biotics, anthracyclines (Pujol et al. 2000; Gewirtz 1999). One of the most effective chemotherapeutic agents is the drug cisplatin $[\text{Pt}(\text{NH}_3)_2\text{Cl}_2]$ that is widely used to treat cancer, including sarcoma, small cell lung cancer, germ cell tumors, lymphoma, and ovarian or testicular cancer (Bassett et al. 2004; Price et al. 2004). The cisplatin treatment in patients involves a series of intravenous applications every 3-4 weeks at a dose of 50-120 mg/m² body surface (Jamieson and Lippard 1999). After application, cisplatin enters the cells by passive diffusion. In the aqueous environment of the body the chlorine atom in cisplatin can be replaced and activated by two hydroxide ions or water molecules (Jamieson and Lippard 1999). When aqueous cisplatin reacts with DNA, its molecules are able to bind to the primary target DNA. The water molecules of cisplatin easily react with the N7 atom of guanine or adenine to form intrastrand and interstrand crosslinks (Hou et al. 2009) (Figure 9).

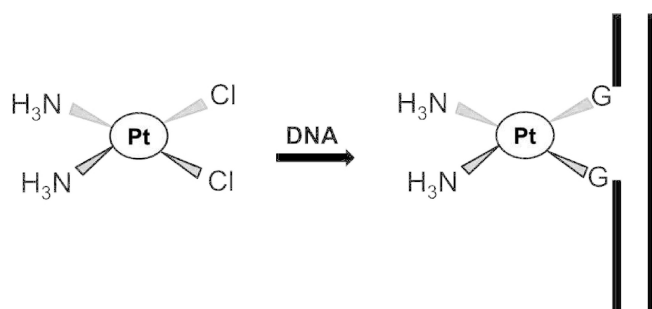


Figure 9: Crosslinks in DNA formed by cisplatin

In an aqueous solution, cisplatin reacts with the N7 atom of the guanine in the DNA resulting in the formation of interstrand or intrastrand crosslinks.

The blocking of the DNA polymerase by cisplatin results in the inhibition of DNA replication which takes place in the S-phase of proliferating cells, leading to an arrest in the G2 phase of the cell cycle (Sorenson and Eastman 1988). Furthermore, RNA polymerase II, which is responsible for transcribing most eukaryotic genes, is blocked by platinum-DNA lesion which evokes various cellular responses such as nucleotide excision repair, polymerase degradation and apoptosis (Jung and Lippard 2003; Galluzzi et al. 2012; Kelland 2007; Prestayko et al. 1979).

Anthracyclines are the class of anti-tumor drugs with the widest spectrum of activity in human cancers (Weiss 1992). Doxorubicin is a potent antitumor drug in clinical use (Figure 10). It is administered for the treatment of several types of cancer, such as multiple myeloma, breast, bladder, ovarian, sarcomas, leukemia and lymphomas (Young et al. 1981).

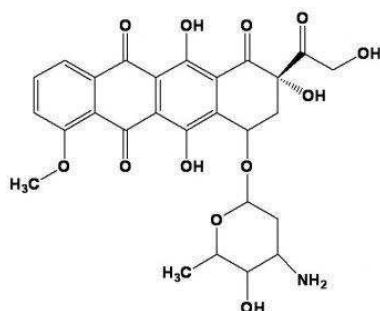


Figure 10: Doxorubicin

Structural formular of doxorubicin. (Source: inspiralis.com. 2006)

As an intercalative antitumor drug it interacts with nucleic acids and cell membranes and induces single- and double-strand breaks in DNA (Tewey et al. 1984). In addition, doxorubicin inhibits the type II topoisomerase which cuts DNA double strands temporarily in order to manage DNA tangles and supercoils for DNA repair (Thorn et al. 2011). In addition, doxorubicin generates free radicals, resulting in damage of cellular membranes, DNA and protein (Bachur et al. 1977, 1978). The cells' most sensitive phase for doxorubicin is during the S-phase as well as the G2-phase, where the anthracycline causes cell cycle arrest (Giacinta Del Bino, and Zbigniew Darzynkiewicz 1991). According to this fact, rapidly proliferating (including healthy) cells and tumor cells are highly affected by the agent and during chemotherapeutic treatment using doxorubicin major side effects occur such as cardiotoxicity, in addition to others (Bristow et al. 1978; Thorn et al. 2011).

1.3.2 Substitutes for tumor resected bone

The major challenge remains to reconstruct the defect caused by the removal of diseased bone to maintain function and address aesthetic considerations. Smaller areas can be filled either by bone cement or an autologous or a bioceramic bone substitute graft such as hydroxyapatite (HA) or highly purified beta-tricalcium phosphate (β -TCP) (Ogose et al. 2005). For larger defects bioceramic bone grafts for bone reconstruction are combined with macro- or mini-metal fixation plates such as titanium, for maintaining mechanical and structural stability (Yamamoto et al. 2000). Preferably, the substitute should be implanted at the same time as the tumor resection, otherwise the surrounding tissue will collapse. During the last decades, hydroxyapatite (HA) has been investigated extensively and is widely used as bone substitute due to the high biocompatibility and the absence of impairment of host metabolism. In addition, the material offers the function as scaffold that supports natural bone formation (osteoconductivity). The material also permits proliferation and adherence of osteoblasts and their precursors to the surface of the implant (osseointegration). The extremely slow resorption of the material, the promotion of new bone formation combined with the similarity in composition to the mineral phase of natural bone make HA a highly suitable material for bone replacement in clinical applications (Bernhardt et al. 2011).

1.3.3 Drug delivery systems as implants for tumor-afflicted bone

Residual cancer cells often remain in the soft tissue after tumor resection. The efficacy of post-operative chemo- or radiotherapy is uncertain and is often accompanied by severe adverse effects. Therefore, an effort was made to extend the protocol of chemotherapy by using high-dose chemotherapy with or without autologous peripheral blood stem cell transplantation (Fratino et al. 2013) and tumor-targeted drug delivery systems (Hu et al. 2013). Unfortunately, these methods did not show significant advantages over standard chemotherapy (Thabet et al. 2000). Therefore, a localized chemotherapeutic strategy (Moore et al. 1991) as an alternative to overcome the major disadvantages of systemically administered chemotherapy, including toxic effects on healthy cells, has attracted much attention. The application of high local chemotherapeutic concentrations may effectively kill residual neoplastic cells after incomplete tumor resection. In addition, the elimination of tumor cells might be enhanced due to sustained exposure to chemotherapeutic agents throughout the cell cycle (Ehrhart et al. 1999). The advantages of generating a drug delivery system that

can maintain a constant drug release rate have been discussed (Lin and Kawashima 2012; Colombo 1993). Furthermore, releasing the drug at the specific site would have further advantages. Implantable drug delivery systems, which associate anticancer agents with bone substitutes, were developed to optimize the therapeutic properties of the drugs and make them safer and more effective (Lee et al. 1999). Several advantages over the administration of drugs by conventional methods are present in the application of drug delivery implants. Initially, a lower drug dose may be needed since the anticancer agent is protected from rapid *in vivo* metabolism (Iyer and Ratain 1998). In addition, the effectiveness of the drug at the site of action is increased and the delivery of tumor cell-inhibiting drugs can continue over a period of time directly at the site needed. As the side effects of anticancer agents are reduced to a minimum, the patient's well-being is increased. Currently, different synthetic polymers such as poly(lactic-co-glycolic acid) are often used as drug carriers (Hines and Kaplan 2013). Although some are successful for human application, fabrication problems, difficulties in processing limited organic solvent and irreproducible drug release kinetics remain (Jeong et al. 1999).

Bone substitute materials that can be used for the reconstruction of bone defects after trauma can serve as carriers for a variety of drug types, such as steroids, proteins, hormones, amino acids, phenolics, vaccines, antibiotics or anticancer agents (Sinha et al. 2004). The most commonly used bioceramic bone substitute materials include hydroxyapatite (HA) and β -tricalcium phosphate (β -TCP) or β -TCP/HA biphasic ceramics. These materials feature good tissue biocompatibility and are often applied for filling cavities after surgery, alone or combined with a metal scaffold to replace the removed bone segment and prevent the soft tissue from collapsing. The influence of physicochemical properties of the bioceramic such as 3D structure, porosity, pore size, surface area and ionic composition of the equilibrating solution on the binding and release of the drug is of high importance and requires further studies (Baradari et al. 2011; Chai et al. 2007).

For a convenient inclusion and release of chemotherapeutic drugs in a bioceramic bone graft, cyclodextrins (CD) have been shown to be useful. β -cyclodextrins consist of seven glycopyranose units (Figure 11). On account of the C-H bonds, the cavities of the cyclodextrin molecules exhibit a hydrophobic character, which enables the formation of inclusion complexes with many lipophilic compounds (Gunay 2013).

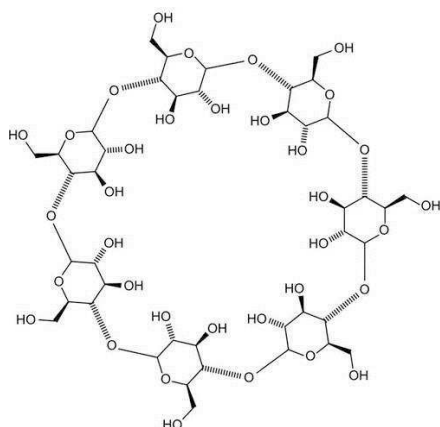


Figure 11: β -Cyclodextrin

Chemical structure of the 7-membered sugar ring molecule of β -Cyclodextrin

Due to their ability to form reversible inclusion complexes with drugs (Martel 2002; Martel et al. 2002) without the alteration of their physical, chemical or biological properties when the incorporated molecule is released from their cavity, cyclodextrins can act as a versatile drug delivery carrier (Blanchemain et al. 2008a). As cyclodextrins have been shown to be biologically inert and are recognized as safe by the Food and Drug Administration (FDA), they can be used as carriers for numerous drug formulations (Chordiya Mayur A 2012). Since conjugates with cyclodextrins seem to have a strong binding potential to hydroxyapatite (which is the main component of the skeleton) and the exhibition of the stimulation of strong local bone anabolic reaction *in vivo* (Liu et al. 2008), β -dextrins can be applied to hydroxyapatite bone substitutes as potential anticancer agent carriers accompanied by bone regenerating impact. Previous studies revealed that cyclodextrins do not exhibit toxic effects on the human epithelial cell line L132 (Blanchemain et al. 2007). The studies of Blanchemain *et al.* or Leprêtre *et al.* reported that cyclodextrins act as effective drug-delivery models for loading with different antibiotics in infection prevention, as a release of drugs and their prolonged bacteriostatic activity were demonstrated (Leprêtre et al. 2009; Blanchemain et al. 2008b). These results are the basis for extending the application of cyclodextrin to chemotherapeutic agents (Figure 12). Moreover, previous data have shown that the application of anticancer agent loaded methyl- β -cyclodextrin exhibited an increased cytotoxic activity in different human parental cancer cell lines (Grosse et al. 1998; Loukas 1997).

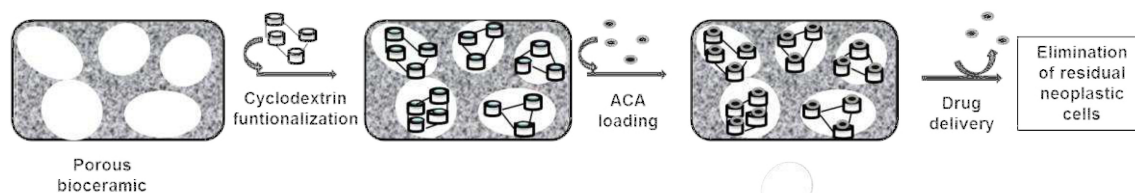


Figure 12: Drug delivery from anticancer agent treated cyclodextrin functionalized hydroxyapatite
Hydroxyapatite, a porous bioceramic, functionalized with poly(CD) and anticancer agent loaded that is released after implantation to kill residual neoplastic cells.

1.4 Aim of the study

Cancer is one of the most life-threatening diseases of humans and is accompanied by severe pain, impairment of the patient's quality of life and often leads to death. Therefore, constant attempts are being made to improve cancer therapy with the goal of achieving full recovery. Several approaches have been adopted during the last decades to advance pre- and post-operative chemotherapy to limit the major side effects the patient has to deal with. A bone graft that combines a drug delivery system with a bone regenerative component as a bone substitute is suggested. Bone grafts in general have to provide certain features, such as biocompatibility, osseointegration and osseointegration. For the successful clinical application of the bone graft, the formation of a functioning vasculature around the implant is a prerequisite for the supply of the newly formed bone with nutrients and oxygen as well as the removal of waste. To improve the process of neovascularization it is proposed to utilize tissue engineered scaffolds which includes the application of endothelial cells and osteoblasts or osteoblast precursors in order to support the natural process of bone regeneration. As it is desirable to achieve an accelerated blood vessel formation in the area of the bone construct *in vivo*, the natural strategy of the human body that induces angiogenesis through inflammation might provide an innovative approach to *in vitro* research.

Nevertheless, patients have to face the major side effects that might occur during cancer therapy. Thus, many chemotherapeutic drugs have an immense cytotoxic impact on proliferating cells, which are for the main part cancer cells but also include primary healthy cells. It is desirable to find a way to protect healthy cells from the cytotoxic effect of anticancer agents and to maintain their natural function to regenerate injured tissue while cancer cells are eliminated.

The focus of the following studies is on the analysis of cytotoxic effects derived from the treatment of various cell types with chemotherapeutic drugs by direct application or by using a biomaterial-based drug delivery component. The effects of anticancer agent

treatment are evaluated on osteosarcoma-derived cancer cells versus primary healthy cells that play a crucial role in bone tissue regeneration in order to investigate strategies to make healthy cells less sensitive towards anticancer drugs and cancer cells more vulnerable for chemotherapy. In a second step an attempt was made to accelerate healing processes during bone tissue regeneration with a focus on the formation of microcapillary-like structures *in vitro* by mimicking the natural function of the human body through the application of an inflammatory stimulus.

2 Materials and methods

2.1 Materials

2.1.1 Instruments

Instrument	Type	Manufacturer
Analytical Balance	A120S	Sartorius, Göttingen
Autoclave		Heraeus, Hanau
Balance	LC42	Sartorius, Göttingen
Centrifuge Megafuge	1.0	Kendro, Langenselbold
Confocal microscope	DM RE	Leica, Wetzlar
Electrophoresis	Mini-Protean	Bio-Rad, München
Flouescence microscope Biorevo	BZ-9000E	Keyence, Neu-Isenburg
Fluorescent Microplate- Reader	GENios plus	TECAN, Crailsheim
Freezer -20°C		Siemens, München
Laminar Flow	KS 12	Kendro, Langenselbold
Liquid nitrogen tank	MVE Cryosystem 6000	German-Cryo, Jüchen
Luerforceps		Aesculap, Tuttlingen
Magnet	MPC-1	Dynal, Hamburg
Magneticstirrer	IKAMAG RET-GS	IKA-Labortechnik, Staufen
NanoDrop	ND-1000	NanoDrop, Wilmington
Neubauer counting chamber		Roth, Karlsruhe
pH meter	InoLab 730	WTW, Weilheim
Roll mixer	Assistent RM5	Assistent, Sondheim
Real Time PCR Cylcer	7300	Applied Biosystems, Foster City
Refridgerator 4°C		Bosch, München
Thumb forceps		Tierärztebedarf J. Lehnecke, Schortens
Vacuum Pump	Vacusaft Comfort	Integra Biosciences, Fernwald
Water bath julabo	SW-20C	Julabo, Seelbach

2.1.2 Consumables

Consumables	Manufacturer
6/24/96-well cell culture plate	TPP, Trasadingen
Cover slips 18x18mm	Menzel, Braunschweig
Cryovials	Nalgene, Rochester
Cellstrainer 40/100µm	BD Falcon, Heidelberg
Cell culture flask (10/25/75cm ²)	Greiner, Frickenhausen
Cell scraper	BD Falcon, Heidelberg
Eppendorf Cups (1,5ml, 2ml)	Eppendorf, Hamburg
Examination gloves, latex	Semper med, Wien
Falcon Tubes (15ml, 50ml)	BD Falcon, Heidelberg
Kolibri examination gloves, nitrile	Igefa, Ahrensfelde OT Blumberg
Laboratoryfilm/Parafilm	Pechiney Plastic Packaging, Chicago
MicroAMP™ Optical 96-well reaction plate	Applied Biosystems, Foster City
Nalgene Syringe Filter 0.2µm	Thermo Fisher Scientific, Bonn
Object slides	Menzel, Braunschweig
Optical adhesive film	Applied Biosystems, Foster City
Pipette Tip (10/100/1000µl)	Greiner, Solingen
Pipette (2/5/10/25ml)	Greiner, Solingen
Scalpels	Braun, Tuttlingen
Terralin Liquid	Pharmacy, Universitätsmedizin Mainz

2.1.3 Chemicals

Name	Manufacturer
40% Acrylamide/Bisacrylamide solution 19:1	Bio-Rad, Hercules
APS	Bio-Rad, Hercules
Aqua dest.	Braun, Melsungen
BSA	Sigma-Aldrich, St. Luis
BSA, Fraction V	Sigma-Aldrich, St. Luis
bFGF (25µg)	Sigma-Aldrich, St. Luis
Calcein AM	Invitrogen, Carlsbad

Ciprobay 200	Bayer, Leverkusen
Cisplatin, Neocorp 1mg/ml	Pharmacy, Universitätsmedizin Mainz
Collagenase type I	Worthington, Lakewood
Crystal violet	Merck, Darmstadt
Doxorubicin, Hexal AG	Pharmacy, Universitätsmedizin Mainz
Dynabeads CD31	Dynal, Hamburg
Dispase	Gibco, Carlsbad
DMSO	Sigma-Aldrich, St. Luis
ECGS 50mg/ml	BD, Franklin Lakes
EDTA	Gibco, Carlsbad
EtOH	AppliChem, Darmstadt
FCS	Sigma-Aldrich, St. Luis
Fungizone	Gibco, Carlsbad
Gelatine	Sigma-Aldrich, St. Luis
GlutaMax™-1 (100X)	Gibco, Carlsbad
Hoechst 33342	Sigma-Aldrich, St. Luis
Methanol	VWR, Darmstadt
<i>n</i>-butanol	Fluka, Basel
PBS	Gibco, Carlsbad
Penicillin/Streptomycin (each 10,000U/ml)	Gibco, Carlsbad
PFA	Merck, Darmstadt
PMA	Sigma-Aldrich, St. Luis
Precision Plus Protein™ WesternC™	Bio-Rad, Hercules
Precision StrepTactin-HRP	Bio-Rad, Hercules
SYBR® Green	Applied Biosystems, Foster City
Sodium heparin	Sigma-Aldrich, St. Luis
TEMED	Bio-Rad, Hercules
Trypsin	Gibco, Carlsbad
0.25% Trypsin-EDTA (1X)	Gibco, Carlsbad
Tween®20	Serva, Heidelberg
Versene	Gibco, Carlsbad

2.1.4 Cell culture media

DMEM	Sigma-Aldrich, St. Luis
FCS	Sigma-Aldrich, St. Luis
Penicillin/Streptomycin	Gibco, Carlsbad
GlutaMax™	Gibco, Carlsbad

The medium consisted of:DMEM + 10% FCS + 1% P/S + 2%GlutaMax™

DMEM/F-12 (1:1) (1X) + GlutaMax™	Gibco, Carlsbad
FCS	Sigma-Aldrich, St. Luis
Penicillin/Streptomycin	Gibco, Carlsbad

The medium consisted of DMEM/F-12 (1:1) (1X) + GlutaMax™ + 20% FCS + 1% P/S

Endothelial Cell Basal Medium MV	PromoCell, Heidelberg
FCS	Sigma-Aldrich, St. Luis
Penicillin/Streptomycin	Gibco, Carlsbad
bFGF	Sigma-Aldrich, St. Luis
Sodium heparin	Sigma-Aldrich, St. Luis

The medium for the cultivation and expansion of HDMEC consisted of Endothelial Cell Basal Medium MV + 15% FCS + 1% P/S + bFGF (2ng/ml) + sodium heparin (10µg/ml)

Endothelial Cell Basal Medium MV	PromoCell, Heidelberg
Penicillin/Streptomycin	Gibco, Carlsbad
PromoCell Supplement Mix	PromoCell, Heidelberg

For the isolation of HDMEC Endothelial Cell Basal Medium MV supplemented with 1% P/S + 5% PromoCell Supplement Mix was used

Endothelial cell basal medium-2	Lonza, Verviers
--	-----------------

For the cultivation and expansion of OEC endothelial cell basal medium-2 supplemented with 35ml FCS and supplements from the kit was used.

Medium 199	Sigma-Aldrich, St. Luis
FCS	Sigma-Aldrich, St. Luis
Penicillin/Streptomycin	Gibco, Carlsbad
GlutaMax™	Gibco, Carlsbad
ECGS	BD, Franklin Lakes
Sodium heparin	Sigma-Aldrich, St. Luis

The medium consisted of Medium 199 + 20% FCS + 1% P/S + 0.34% GlutaMax™ + ECGS (50µg/ml) + sodium heparin (50µg/ml)

RPMI 1640 (1X)	Gibco, Carlsbad
FCS	Sigma-Aldrich, St. Luis
Penicillin/Streptomycin	Gibco, Carlsbad

The medium consists of RPMI 1640 (1X) + 10% FCS + 1% P/S

2.1.5 Buffers

Roti®Load-1 loading buffer Reducing	Roth, Karlsruhe
Lysis buffer #13 1mM EDTA 0.5% Triton X-100 10mM NaF 150mM NaCl 20mM β-Glycerophosphate 1mM DTT 0.1% Protease-Inhibitor-Cocktail	Sigma-Aldrich, St Luis Roth, Karlsruhe Sigma-Aldrich, St. Luis
Rotiphorese® 10x SDS PAGE buffer	Roth, Karlsruhe
PAGE Transfer buffer 100ml Rotiphorese® 10x SDS PAGE buffer 200ml MeOH 700ml aqua dest.	
Buffer RLT 0.01% β-Mercaptoethanol	Qiagen, Hilden
Wash buffer 0.05% Tween®20 in PBS pH 7.2-7.4	Serva, Heidelberg
Buffy Coat Buffer 0,5% FCS 2mM EDTA Adjust to 1l PBS	Sigma-Aldrich, St. Louis Gibco, Carlsbad Gibco, Carlsbad

2.1.6 Antibodies

Antibody	Source	Dilution	Provider
Anti-HIF-1α	Mouse	1:250	BD Biosciences, Franklin Lanes
Anti-ERK-2	Rabbit	1:3000	Santa Cruz Biotechnology
AlexaFlour 488 anti-goat IgG	Donkey	1:1000	Molecular Probes, Carlsbad

Materials and methods

Anti-CD31	Goat	1:50	Santa Cruz Biotechnology
AlexaFlour 546 anti-mouse IgG	Rabbit	1:1000	Molecular Probes, Carlsbad
Anti-CD68	Mouse	1:50	Dako, Glostrup
Anti-CD105	Mouse	1:25	Dako, Glostrup
AlexaFlour 488 anti- Mouse IgG	Rabbit	1:1000	Molecular Probes, Carlsbad

2.1.7 Primers

Primer	Sequence
E-selectin 3'	5'-CCCGTGTTTGGCACTGTGT-3'
E-selectin 5'	5'-GCCATTGAGCGTCCATCCT-3'
HIF-1 α 3'	5'-GCAAGCCCTGAAAGCG-3'
HIF-1 α 5'	5'-GGCTGTCCGACTTTGA-3'
ICAM-1 3'	5'-CGGCTGACGTGTGCAGTAAT-3'
ICAM-1 5'	5'-CACCTCGGTCCCTTCTGAGA-3'
IL-6 3'	5'-AATGAGGAGACTTGCCTGGT-3'
IL-6 5'	5'-TTTCTGCAGGAACTGGATCA-3'
IL-8 3'	5'-TGGCAGCCTTCTGATTTCT-3'
IL-8 5'	5'-TTAGCACTCCTTGGCAAACTG-3'
p21 3'	5'-CCGTTGTCTCTTCGGTCCC-3'
p21 5'	5'-CATGAGCGCATCGCAATC-3'
p53 3'	5'-TAACAGTTCCTGCATGGGCGGC-3'
p53 5'	5'-CGGAGGCCCATCCTCACCATCATCA-3'
RPL13A 3'	5'-CCTGGAGGAGAAGAGGAAAGAGA-3'
RPL13A 5'	5'-TCCGTAGCCTCATGAGCTGTT-3'
TNF- α 3'	5'-CCCCCAGAGGGAAGAGTTCCCCA-3'
TNF- α 5'	5'-CGGCGGTTTCAGCCACTGGAG-3'
VEGF 3'	5'-CGAGGGCCTGGAGTGTGT-3'
VEGF 5'	5'-CCGCATAATCTGCATGGTGAT-3'

Random Primer

New England Biolabs,
Frankfurt/Main

2.1.8 Kits and Assays

MTS CellTiter 96®AQ _{ueous} One Solution Cell Proliferation Assay	Promega, Madison
LDH CytoTox 96® Non-Radio Cytotoxicity Assay	Promega, Madison
alamarBlue®	Invitrogen, Carlsbad
LIVE/DEAD® Viability/Cytotoxicity Kit	Invitrogen Molecular Probes, Eugene
Quant-iT™ PicoGreen® dsDNA Assay Kit	Invitrogen, Carlsbad
NanoOrange® protein quantitation Kit	Molecular Probes, Carlsbad
DuoSet ELISA Human VEGF	R&D Systems, Wiesbaden
DuoSet ELISA p53	R&D Systems, Wiesbaden
DuoSet ELISA p21	R&D Systems, Wiesbaden
RNeasy Micro Kit	Qiagen, Hilden
Omniscript RT Kit	Qiagen, Hilden
AnaeroGen COMPACT kit Anaerobic Indicator	Thermo Fisher Scientific, Bonn Oxoid, Hants, UK

2.1.9 Inhibitors

HIF-1 α -inhibitor	Calbiochem, Darmstadt
YC1-inhibitor	Cayman Europe, Tallinn, Estonia

2.1.10 Biomaterials

Osbone®	Curasan, Kleinostheim
Osbone® poly-Cyclodextrins (poly(CD))	Curasan, Kleinostheim in cooperation with UMET, Lille
Matrigel® Basement Membrane Matrix	BD Biosciences, Franklin Lanes

2.1.11 Cell lines

Table 1: Cell lines

Cell lines	Cell type/Source	Organism	Company
MG-63	adherent Organ: bone Disease: osteosarcoma	Homo sapiens (human)	ATCC
SaOS-2	adherent Organ: bone Disease: osteosarcoma	Homo sapiens (human)	ATCC
Cal-72	adherent Organ: bone Disease: osteosarcoma	Homo sapiens (human)	DSMZ
THP-1	suspension Organ: peripheral blood Disease: acute monocytic leukemia Cell Type: monocyte	Homo sapiens (human)	ATCC
HCMEC/D3	Adherent Organ: brain	Homo sapiens (human)	Department of Biological Sciences, The Open University Walton Hall, Milton Keynes UK

2.2 Methods

2.2.1 Isolation and culture of cells

All cells were obtained from excess tissue and were used in accordance with the principle of informed consent and approved by the responsible Ethics Commission of the State of Rhineland-Palatinate, Germany.

2.2.1.1 Isolation and expansion of human primary osteoblasts

Human primary osteoblasts (pOB) were isolated from human cancellous bone fragments from healthy donors (Dalby et al. 2002; Annaz et al. 2004). The bone fragments were obtained from the Department of Orthopedics of the University Medical Center Mainz.

A vitreous Petri dish was used to clean the bone fragments with sterile phosphate buffered saline (PBS, Gibco, Carlsbad) containing 1% P/S. Small pieces of bone were

cut out of the bone with Luer forceps and stored in a new Petri dish containing sterile PBS. With sterile thumb forceps the pieces were placed in a 50ml Falcon tube and sterile PBS was added. The bone pieces were separated from tissue and blood by shaking the tube vigorously. The supernatant was discarded. This step was repeated until the supernatant was transparent and did not show any tissue or blood residues. Subsequently, the bone specimens were placed in sterile 6-well plates, each well carrying 3 fragments. Each well was filled with 2ml Dulbecco's Modified Eagle's Medium Nutrient Mixture F-12 (DMEM/F-12) containing 1% P/S and 20% fetal calf serum (FCS). The cells were cultured at 37°C in an atmosphere of 95% air and 5% CO₂. The medium was changed daily. The cell proliferation was monitored twice a week. When the cell layer was confluent the cells were trypsinized with trypsin-EDTA for one minute at 37°C until the pOB were fully detached. To stop the digestive effect of trypsin on cells the enzyme activity was stopped with DMEM/F-12 medium containing 20% FCS. The detached cells were pooled in a 50ml tube and separated from the bone residues by using a 40µm strainer and transferred into a 75cm² cell culture flask (4 confluent wells in one 75cm² cell culture flask). After transferring the cells to a cell culture flask the pOB were in passage 1 (P₁). The medium was changed twice a week and the DMEM/F-12 medium was substituted by DMEM medium containing 1% P/S, 10% FCS and 2% GlutaMax™. When the cells were grown to confluence they were ready for experimental purposes or were alternatively stored in the liquid nitrogen tank. Thus, the cells were trypsinized from each cell culture flask, pooled and centrifuged for 5 minutes at 12000rpm. The cell pellet was resuspended in FCS containing 10% DMSO filled in 2ml cryo vials and stored in a -80°C deep freezer for 24h before the cells were kept in the liquid nitrogen tank.

2.2.1.2 Isolation and expansion of human primary endothelial cells

Human dermal microvascular endothelial cells

Human dermal microvascular endothelial cells (HDMEC) were isolated from infantile foreskin, obtained after surgical removal from healthy donors up to 12 years old (Unger et al. 2002). The foreskin was washed twice with PBS and blood and connective tissue were removed and discarded. The foreskin was cut into small pieces and incubated in 5ml of a 2.36U/ml dispase solution over night at 4°C to remove the epidermis. After two wash steps with PBS the dermal parts were removed and the skin was incubated in 5ml 0,48mM versene containing 80µl of a 2.5% trypsin solution in a sterile 50ml Falcon tube for 2h at 37°C in a shaking waterbath to digest the tissue. To

avoid any contamination the cap of the tube was sealed with laboratory film. The trypsin was stopped with 2ml FCS and the Falcon was filled up to 40 ml with PBS. To separate the tissue fragments and debris from cells the tissue was filtered through a 100µm sterile nylon strainer. The obtained cell suspension containing the endothelial cell and non-endothelial cell populations was centrifuged for 5minutes at 12000rpm. The supernatant was discarded and the pellet was resuspended in 11ml PromoCell Endothelial Cell Basal Medium MV supplemented with 5% PromoCell Supplement Mix (Complete medium). The cells were seeded on a 75cm² cell culture flask that was coated with 4ml 0.2% gelatin for 30 minutes at 37°C. The next day the medium with unattached cells and tissue residues was removed and substituted by 11ml fresh medium. The medium was changed every two-three days. After 7-8 days the cells were separated from other cell types by immunomagnetic beads (Dynabeads) conjugated with anti-CD31 antibody. Approximately 11µl of the Dynabeads solution was washed with 5ml PBS containing 0.1% BSA in a 15ml tube and fixed at a magnetic particle concentrator for one minute to allow the beads to bind. After discarding the PBS-BSA, the Dynabeads were resuspended in 5ml PC supplement medium that was taken from the cell culture flask and put on the mixed cell population. By gently shaking, the Dynabeads solution was dispensed over the cells. The beads were incubated with cells for 20min at 37°C. To separate the endothelial cells from non-endothelial cells the mixed population was trypsinized. The suspension was placed on the magnet for 1min and the medium was aspirated. To resuspend the magnetic beads loaded with endothelial cells 5ml PBS containing 0.1% BSA was added and the cells were mixed on a roll mixer for 10 minutes at 4°C. Subsequently, the cells were filtered through a 40µm cell strainer to help to separate the CD31-positive cells from contaminating cells. Following this, the washing step with PBS-0.1% BSA was repeated three times. After the last washing and centrifugation step the cells were resuspended in 11ml PromoCell Endothelial Cell Basal Medium MV supplemented with 5% PromoCell Supplement Mix (Complete medium) and seeded on a gelatine-coated cell culture flask (P₁). The size of the cell culture flask was dependent from the number of cells that were obtained after the separation. The cells were grown to confluence for approximately 4 days to 1 week and then split 1:3 4h before a second CD31 Dynabeads separation, as previously described, was implemented (P₂). When the cells were grown to confluence the medium was changed to PromoCell Endothelial Cell Basal Medium MV supplemented with 15% FCS, 1% P/S, sodium heparin (10µg/ml) and bFGF (2.5ng/ml). 24h later the cells were split 1:3 and could be used for experiments or were alternatively stored in the liquid nitrogen tank as previously described.

Human umbilical vein endothelial cells (HUVEC)

Human umbilical vein endothelial cells (HUVEC) were isolated from umbilical cords which were obtained from the GPR Clinic in Rüsselsheim, Germany (Jaffe et al. 1973). The cord was excised from the placenta soon after birth and placed in a sterile wide-mouth bottle containing cord buffer constituted of 900ml aqua dest., 100ml HEPES (10X), 1% P/S, 1% Ciprobay and 1% fungizone and were kept at 4°C until processing. In a first step, areas with clamp marks were cut off. Subsequently, drain tubes were placed in the vein on both ends to rinse the umbilical cord with 4-(2-hydroxyethyl)-1-piperazineethanesulfonic acid (HEPES). To assure that the vein had no defects, one of the drain tubes was sealed with a combi stopper and HEPES was syringed. Eventually occurring defects were fixed with clamps. After running off the HEPES solution, 5ml collagenase type I (0.1%) was mixed 1:1 (v/v) with HEPES and syringed into the vein. The second drain tube was closed with a combi stopper. The vein was incubated with collagenase type I for 20 minutes at 37°C. To help the HUVEC to detach from the vein the umbilical cord was massaged for one minute. One combi stopper was opened to release the collagenase into a sterile 50ml Falcon tube. The second combi stopper was opened to rinse the vein with 10ml medium 199 which was also collected in the tube and centrifuged for 5 minutes and 1200rpm. The supernatant was discarded and the pellet was resuspended in 5ml medium 199, containing 10% FCS, 1% P/S and 0.34% GlutaMax™, and seeded on a gelatin-coated 25cm² cell culture flask. Endothelial cell growth supplement (ECGS) – sodium heparin solution (each 50µg/ml/1:1000) was added. The cells were cultivated at 37°C in an atmosphere of 95% air and 5% CO₂ and were allowed to grow to confluence (P₀), split 1:3 after a few days and seeded on a gelatin-coated cell culture flask (P₁). After the HUVEC were grown to confluence they were split 1:3 (P₂) or were alternatively stored in the liquid nitrogen tank. The cells were used for experimental purposes in passage 3 but not exceeding passage 4.

Isolation and expansion of human outgrowth endothelial cells (OEC)

Human outgrowth endothelial cells, a subpopulation of endothelial progenitor cells (EPC), were isolated from human peripheral blood buffy coats (Fuchs et al. 2006). Human blood buffy coats were obtained from the transfusion center of the University Medical Center Mainz. The mononuclear cell fraction (75ml), where OEC appear, was isolated by Ficoll® or Histopaque® gradient centrifugation. 25ml of peripheral blood buffy coats were gently mixed in a ratio of 1:1 with phosphate-buffered saline (PBS)

containing 0.5% fetal calf serum (FCS) and 2mM ethylene diaminetetraacetic acid (EDTA) in a 50ml Falcon tube. Sterile 50ml Falcon tubes were filled with 15ml Histopaque® solution. 30ml of the buffy coat PBS/FCS/EDTA solution were pipetted gently on 15ml Histopaque® solution without intermixing the buffy coat with Histopaque® and centrifuged at 400g for 35min without brake. Four different phases appear after centrifugation. The plasma phase was removed and the interphase, containing mononuclear cells, was collected in a fresh sterile 50ml Falcon tube. The mononuclear phase was washed three times with PBS and between each washing step centrifuged at 400g for 10min. Subsequently, the cells were cultivated in endothelial basal medium-2 (EBM-2) supplemented with the BulletKit™ to obtain endothelial cell growth medium (EGM-2). Additional 5% FCS were added to obtain EGM-2 medium with 7% FCS. A total number of 5×10^6 cells per well were seeded on a collagen-coated 24-well plate. Three times per week the medium was discarded and substituted with fresh medium. After four to seven days of cultivation early EPC with a spindle-shaped morphology appeared. After seven days all the cells cultivated on 24-well plates from one donor were trypsinized, pooled and seeded on fibronectin-coated 24-well plates (10µg/ml) in a ratio of 1:2. After three to four weeks of cultivation, cells with a cobblestone-like morphology appeared. These late outgrowth endothelial cells (OEC) exhibited a typical mature endothelial marker profile and a high proliferation capacity. OEC were expanded by splitting over several passages in a ratio of 1:2 and were used for experimental purposes ranging from passage 8 to passage 20.

2.2.1.3 Isolation and expansion of human primary fibroblasts

Human primary fibroblasts were isolated from oral mucosa from healthy infantile donors after cleft lip surgery. The tissue was obtained by the Clinic of Maxillofacial and Plastic Surgery of the Goethe University Frankfurt/Main. After washing twice with PBS to remove residual blood and loose tissue pieces the mucosa was cut into small pieces. The pieces were collected in a 50ml tube. To digest the tissue trypsin-EDTA was added until the pieces were fully covered with the solution and incubated for 30-45 minutes in a 37°C water bath. To stop the trypsinization 5ml DMEM supplemented with 10% FCS, 1% P/S and 2% GlutaMax™ was added. The solution together with the pieces of mucosa were transferred to a 25cm² cell culture flask and kept at 37°C in an atmosphere of 95% air and 5% CO₂. After approximately 7 days the tissue was removed and the cells were washed with PBS. When the cells were confluent they could be used for experimental purposes or were alternatively stored in the liquid nitrogen tank, as previously described.

2.2.1.4 Expansion of THP-1 and differentiation into macrophages

The acute human monocytic leukemia cell line THP-1 was obtained from the ATCC (Manassas, VA). Cells were grown in suspension at 1.2×10^5 cells/ml in RPMI 1640 medium containing 10% FCS (Gibco, Carlsbad) and 1% Penicillin/Streptomycin (Invitrogen, Carlsbad) and maintained at 37°C in an atmosphere of 95% air and 5% CO₂. To fully differentiate the monocytes to macrophages (M ϕ), 5×10^5 THP-1 monocytic cells were seeded on a fibronectin-coated (5 μ g/ml, Milipore, Billerica, MA, USA) 6-well-plate on a growth area of 9.6cm² in 3ml RPMI medium (Gibco, Carlsbad) containing 8nM PMA (Phorbol-12-myristate-13-acetate) (Sigma-Aldrich, St. Luis) for 4 days. Unattached cells were removed by washing with PBS (Dulbeccos's Phosphate Buffered Saline, Gibco, Carlsbad).

2.2.2 Conditions for co- and triple-cultures

OEC and pOB were seeded in a ratio of 1:1.5 in EBM-2 medium as previously published. Co-cultures of outgrowth endothelial cells and primary osteoblasts were grown on fibronectin-coated 24-well plates (1.96cm²), always seeding primary osteoblasts first (300,000/well). After one day OEC were added (200,000/well) together with THP-1 derived macrophages (M ϕ) in a ratio of 30,000 cells per well. After 7 or 14 days of cultivation the co- and triple-cultures were analyzed for inflammatory markers and growth factors by using ELISA or quantitative real-time PCR. For immunofluorescence staining, triple- and co-cultures were seeded in fibronectin-coated petri dishes (9.6cm²) to avoid auto-fluorescence. The triple-cultures as well as control co-cultures were cultivated in EBM-2 medium supplemented with EGM-2 BulletKit (Lonza, Basel), 1% Penicillin/Streptomycin (Invitrogen, Carlsbad) and additional 4% fetal calf serum (FCS, Gibco, Carlsbad) for 7 and 14 days at 37°C in an atmosphere of 5% CO₂ and 95% air.

The osteosarcoma cell line MG-63 was alternatively used in the co- and triple-cultures to induce OEC to form microvessel-like structures. After 7 and 14 days the co- and triple cultures were analyzed in terms of angiogenic activation by the determination of VEGF by using ELISA.

Human dermal endothelial cells (HDMEC) and human primary osteoblasts (pOB) were seeded in endothelial cell basal medium (PromoCell) on a gelatin-coated petri dish (9.6cm² surface area) in a ratio of 4:1 (120,000 HDMEC/30,000 pOB). After 14 days of cultivation, poly(CD)-modified and unmodified hydroxyapatite granules were added to

the co-culture and incubated for 14 days before the cells were analyzed by fluorescence microscopy (Keyence, Neu-Isenburg).

2.2.3 Matrigel® angiogenesis assay

Matrigel® Basement Membrane Matrix (not growth factor depleted) was thawed on ice and diluted with ice-cold EGM-2 cell culture medium in a ratio of 1:1. 50µl of Matrigel®-cell culture medium solution was added air bubble-free to a 96-well plate. To allow the gel to polymerize the cell culture plate was incubated for 30min at 37°C. Subsequently, 50,000 OEC per well were resuspended in 200µl of warm EGM-2 medium and pipetted gently on the top of the solidified Matrigel® membrane. 7,000 THP-1 derived macrophages per well were stained with calcein AM in a dilution of 1:1000 for 5min at 37°C. To leach out the remaining calcein AM macrophages were washed three times with EGM-2 medium before they were added to the Matrigel®. 24h later, the cells were imaged by using a fluorescence microscope.

2.3 Cytotoxicity Assays

2.3.1 Cell viability test: MTS Assay

The MTS assay (CellTiter 96® AQueous One Solution Cell Proliferation Assay) was performed according to the manufacturers' protocol. The MTS assay is a colorimetric method for determining the number of viable cells in the cytotoxicity assay. The tetrazolium component of the assay is enzymatically reduced to the colored insoluble formazan by the dehydrogenases of viable cells. The absorbance of the colored formazan can be quantified by measuring at the wavelength of 492nm by a microplate reader. Before the MTS solution, diluted 1:6 in cell culture medium, was added, the cells were gently washed with 100µl 0.2% HEPES/BSA per well. The MTS solution was incubated at 37°C for 1.5h.

2.3.2 Cytotoxicity test: Release of Lactate dehydrogenase (LDH)

Lactate dehydrogenase, a soluble cytosolic enzyme is present in most eukaryotic cells. Cell death and concomitant damage of the plasma membrane forces the release of LDH into the cell culture medium. The increase of the LDH activity in culture supernatants is proportional to the number of lysed cells.

LDH catalyzes the reduction of NAD⁺ to NADH in the presence of L-lactate. The CytoTox 96® Non-Radio Cytotoxicity Assay quantitatively measures LDH with a 30-minute coupled enzymatic assay, which results in the conversion of a tetrazolium salt (INT) into a red formazan product (Figure 13). The amount of the highly colored and soluble formazan can be measured at 490 nm spectrophotometrically.

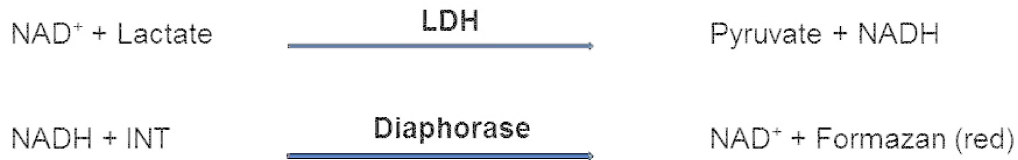


Figure 13: Chemical reaction of CytoTox 96® Non-Radio Cytotoxicity Assay

Lactate is oxidized via LDH to pyruvate while NAD⁺ is reduced to NADH. In a second reaction, NADH is oxidized via diaphorase to NAD⁺ while tetrazolium salt is reduced to highly colored formazan.

2.3.3 Cell viability test: alamarBlue®

The alamarBlue® cell viability assay was performed as described in the manufacturers' protocol. The alamarBlue® assay is a method for determining the number of viable cells in the cytotoxicity assay. The indicator resazurin (blue, non-flourescent) is converted by dehydrogenases of viable cells into the flourescent molecule resorufin (red). Viable cells continuously convert resazurin to resorufin, enabling quantitative measurement of cell viability or cytotoxicity. The ingredients of the assay are nontoxic so that resazurin-treated cells can continue to be cultivated. The alamarBlue® solution was diluted in fresh cell culture medium in a ratio of 1:10 and incubated with cells for 1h at 37°C in the incubator. The medium containing alamarBlue® measured on plastic served as the negative control. After incubation the supernatant was pipetted on a fresh 96-well plate and measured in a microplate reader using 560EX nm/590EM nm filter settings.

2.3.4 LIVE/DEAD® viability/toxicity assay

The LIVE/DEAD® viability/toxicity assay consists of two components to discriminate between viable and dead cells. Calcein AM, a cell permeable dye, is converted into green-flourescent calcein after acetoxymethyl ester hydrolysis by intracellular esterases. Ethidium homodimer-1 exhibits a high affinity for nucleic acids and gives red fluorescence when it binds to DNA as an indication for the loss of plasma

membrane integrity. 20µl of a 2mM ethidium homodimer-1 solution were added together with 5µl of a 4mM calcein AM solution to 10ml serum-free medium. The staining solution contained a final volume of 4µM ethidium homodimer-1 and 2µM calcein AM. 150µl per well were applied to cells on a 48-well plate and incubated for 30min at 37°C, protected from light, before they were analyzed in terms of cell viability in a fluorescence microscope.

2.3.5 DNA Quantification

Using Quant-iT™ PicoGreen® dsDNA Quantitation Reagent from Invitrogen, which is an ultrasensitive fluorescent stain, the quantitation of double-stranded DNA is possible and contains a reference to the cell number. Three wells of each cell type treated identically were detached from the 96-well cell culture plate by using 200µl aqua dest. The cells were scratched from the cell culture plate with a yellow 200µl pipette tip. To rupture the cell membranes the samples were frozen at -20°C and defrosted at 37°C three times. Additionally, the repetitively frozen and defrosted samples were sonicated for 15min to release the DNA. To measure the correct DNA concentration of the samples in a microplate reader, a standard curve ranging from 0.2µg/ml to 3µg/ml was established using a standard stock solution from the kit of 100µg/ml. The fluorescent staining of the DNA by using PicoGreen® could be quantified by measuring at a wavelength of 485nm.

Alternatively, DNA was quantified by using crystal violet staining. Cells were washed with PBS and incubated with 100µl/well of a methanol-ethanol solution in a ratio of 1:2 for 15min. The fixed cells were washed with PBS and stored at 4°C or immediately prepared for the crystal violet staining. The cells were washed three times with a solution of PBS and 0.05% Tween®20. 50µl/well of a 0.1% crystal violet solution was incubated at room temperature for 20min at 175rpm. When crystal violet has bound to the phosphate backbone of the cells' DNA, the unbound stain was washed out with tap water and the plates were thoroughly air-dried. Subsequently, the color crystals were dissolved out with 100µl/well of 33% acetic acid for 15min at 175rpm. Using a microplate reader, the optical density was measured at 600nm. Acetic acid incubated on plastic was used as a blank sample.

2.3.6 Cytotoxic effect of cisplatin and doxorubicin on various cell types

In this study the cytotoxic effects of anticancer agents was studied on human cancer cell lines (MG-63, SaOS-2 and Cal-72) and human primary cells (pOB, HDMEC and fibroblasts). 5000 cells per well were seeded on 96-well plates. For endothelial cell seeding, the wells were coated with gelatin and incubated for 30min at 37°C before the cells were added. The cells were allowed to proliferate for 14 days in cell-specific media. After 14 days of culture the cells were treated with control medium alone or with medium containing cisplatin (0.005;0.5;50µg/ml) or doxorubicin (0.005;0.05;5µg/ml) for an additional 4 day period and the medium was changed every 24h with a fresh dose of chemotherapeutic agents. Cell viability was determined after 4 days of treatment by using the MTS colorimetric assay and LIVE/DEAD® viability/toxicity kit. The MTS assay was analyzed by One-way-ANOVA (GraphPad). As a post test the Dunnett test was chosen to compare the groups of diverse treatments with the control group (not treated).

2.3.7 Determination of median lethal dose (LD₅₀)

The median lethal dose is the concentration of a certain substance which causes 50% of cells to die. In this study the LD₅₀ was determined for cisplatin or doxorubicin on different cell types. HUVEC were seeded on gelatin-coated plates, whereas the plates for OEC and THP-1-derived macrophages were coated with fibronectin. Primary osteoblasts as well as the osteosarcoma cell line MG-63, which represents a cancer cell model, were seeded on plastic without any coating. 5,000 cells per well were seeded on a 96-well plate and allowed to adhere for 24h in cell-specific cell culture medium. Subsequently, the cells were treated with concentrations ranging from 0.001µg/ml up to 100µg/ml cisplatin or doxorubicin using fresh cell culture medium. The untreated control group was cultivated in the same way. After 24h of treatment, the cell culture supernatants were discarded, the cells were washed with a 0.1% HEPES/BSA solution and the MTS assay for cell viability analysis was performed. Following this, the cells were fixed for the crystal violet DNA quantification assay.

2.3.8 Biomaterial

Osbone®, an open porous, slowly resorbable bioceramic from pure-phase hydroxyapatite ($\text{Ca}_{10}(\text{PO}_4)_6(\text{OH})_2$) (HA) was obtained from Curasan (Kleinostheim). The

granules had a size of 2000-3000 μ m and a porosity of approximately 65%. The structural appearance of the material was similar to bone (Figure 14).

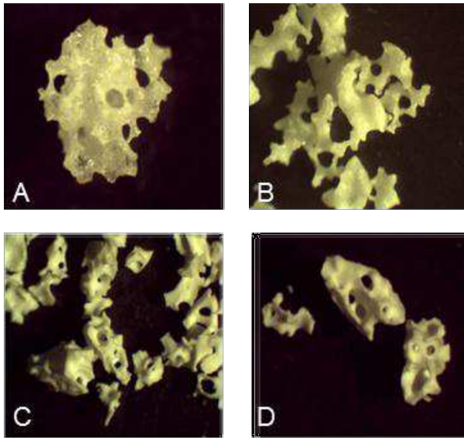


Figure 14: Images of light microscopy
Comparison of Osborne® (A,B) and bone granules (C,D) (Source: Dr. F. Peters, Curasan, 2011)

Osbone® was alternatively modified by Unité Matériaux Et Transformations (UMET) in Lille (France) with poly-cyclodextrins (poly(CD)) in order to load and deliver a certain amount of anticancer agents (ACA). After the modification all the samples were gamma irradiated by Curasan so that the sterility of both types of biomaterial, modified and unmodified, was guaranteed. Unmodified (HA) and poly-cyclodextrin-modified (HACD) granules were used for *in vitro* experiments (Figure 15).



Figure 15: Osbone® hydroxyapatite granules (HA) and cyclodextrin-functionalized hydroxyapatite granules (HACD)

2.3.9 Extraction Assay

The poly(CD)-functionalized (HACD) and non-functionalized (HA) gamma sterilized biomaterial samples were obtained by the Groupe Recherche Biomatériaux in Lille. To load the poly(CD)-functionalized biomaterial with anticancer agents 300mg of the granules (HACD) were placed in a sterile Greiner tissue culture dish with a diameter of 35mm and 10mm height. 5ml of cisplatin (1mg/ml) or 2.5ml of doxorubicin (2mg/ml) were added to the samples. The biomaterial was incubated with the chemotherapeutics for 30 minutes at room temperature and protected from light. Subsequently the anticancer agents were removed and the samples were rinsed 4 times with 5ml aqua dest. for one minute and 80rpm. Following this, the samples were allowed to dry for 4h under sterile conditions in the laminar flow at room temperature and were protected from light. As a control the non-functionalized samples were treated in the same way. 1.5ml of cell culture medium were then added to the cisplatin- and doxorubicin-treated samples. Additionally, 300mg of untreated poly(CD)-functionalized HA and un-functionalized HA were placed in a sterile cell culture dish containing cell culture medium. Treated and un-treated samples were incubated at 37°C for 24h at 80rpm (Figure 16).

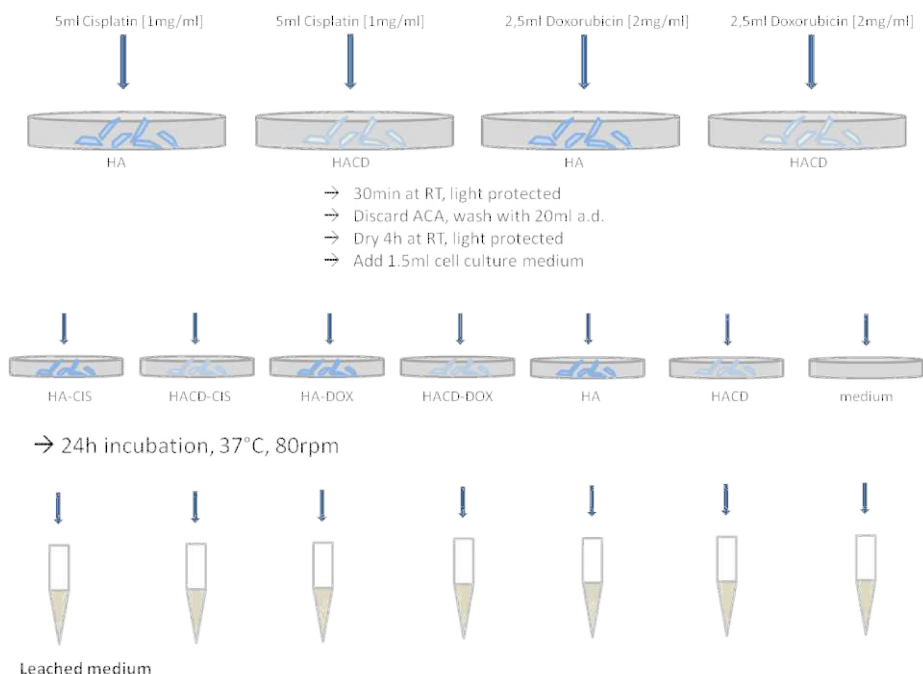


Figure 16: Scheme of extraction assay

300mg of functionalized or non-functionalized HA were treated with 5ml cisplatin (1mg/ml) or 2.5ml of doxorubicin (2mg/ml) for 30 minutes protected from light at room temperature. After washing the drug treated biomaterial with 20ml aqua dest., the granules were allowed to dry while protected from light for 4h. Subsequently, 1.5ml of cell culture medium were applied to the biomaterial to leach the soluble components from the drug treated HA at 37°C, protected from light for 24h while shaking (80rpm).

Materials and methods

To test the cytotoxic effect of poly(CD)-functionalized hydroxyapatite loaded with chemotherapeutic agents like cisplatin or doxorubicin, various cell types (Table 2) were seeded on 96-well cell culture plates. 17,000 cells per well were seeded in cell-specific cell culture medium (Figure 17). Thus, the cells were trypsinized from the cell culture flask (using 0.5ml/1.5ml for a confluent cell layer on a 25cm²/75cm² cell culture flask) for approximately one minute. The enzymatic effect of trypsin was stopped by using cell-specific cell culture medium containing at least 10% FCS. The cells were counted in a Neubauer counting chamber. The amount of cells needed for the experiment was centrifuged for 5 minutes at 1200rpm. Subsequently, the cells were resuspended in cell-specific cell culture medium and seeded as triplets on a 96-well cell culture plate (gelatin-coated if required) and were cultivated for 24h at 37°C in an atmosphere of 95% air and 5% CO₂.

Table 2: List of cells and medium used for extraction assay

Human primary cells were used as models for healthy cells while human osteosarcoma cell lines were used as models for cancer cells

Cell name	Cell type (human)	Cell culture medium	Coating
HUVEC	Primary human umbilical vein endothelial cell	Endothelial Cell Basal Medium MV	Gelatin
HCMEC/D3	Microvascular endothelial cell line	Endothelial Cell Basal Medium MV	Fibronectin
pOB	Primary osteoblast	Dulbecco's modified Eagle's medium	-
SaOS-2	Osteosarcoma cell line	Dulbecco's modified Eagle's medium	-
MG-63	Osteosarcoma cell line	Dulbecco's modified Eagle's medium	-
Fibroblast	Primary fibroblast	Dulbecco's modified Eagle's medium	-

The human primary cells for the extraction assay were isolated and cultured by myself or members of our institute, while the human osteosarcoma cells were obtained from ATCC.

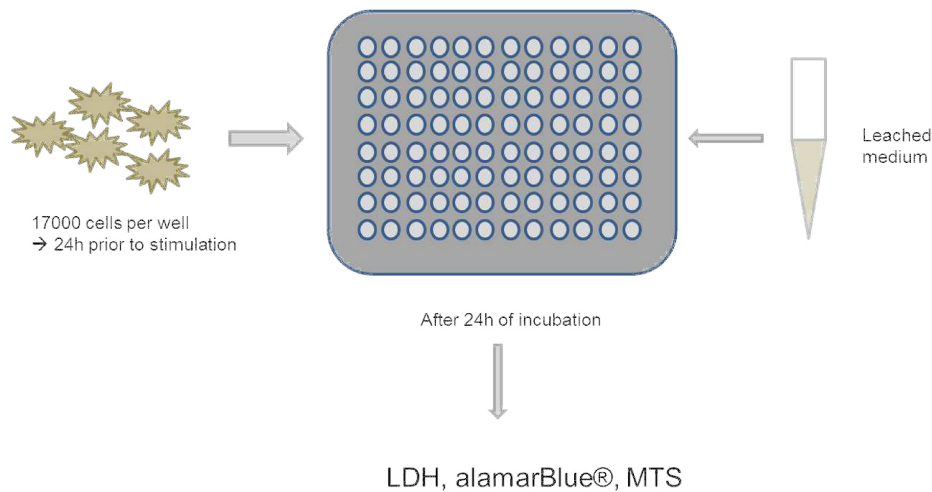


Figure 17: Scheme of extraction assay

17.000 cells were seeded on a 96-well plate 24h prior to treatment with leached medium from the extraction assay. 100µl of each extracted medium was applied to the cells and incubated for 24h at 37°C, 5% CO₂ and 95% air before LDH, alamarBlue® and MTS assay were performed.

To monitor the duration of the release of chemotherapeutic agents and their cytotoxic effect on cells, another 1.5ml of cell culture medium were applied to the granules after 24h to allow the soluble components of the treated and untreated biomaterial to diffuse into the medium. Subsequently, the medium was applied to cells for 24h before cytotoxicity and cell viability assays were performed (Figure 17). This step was repeated again (Figure 18).

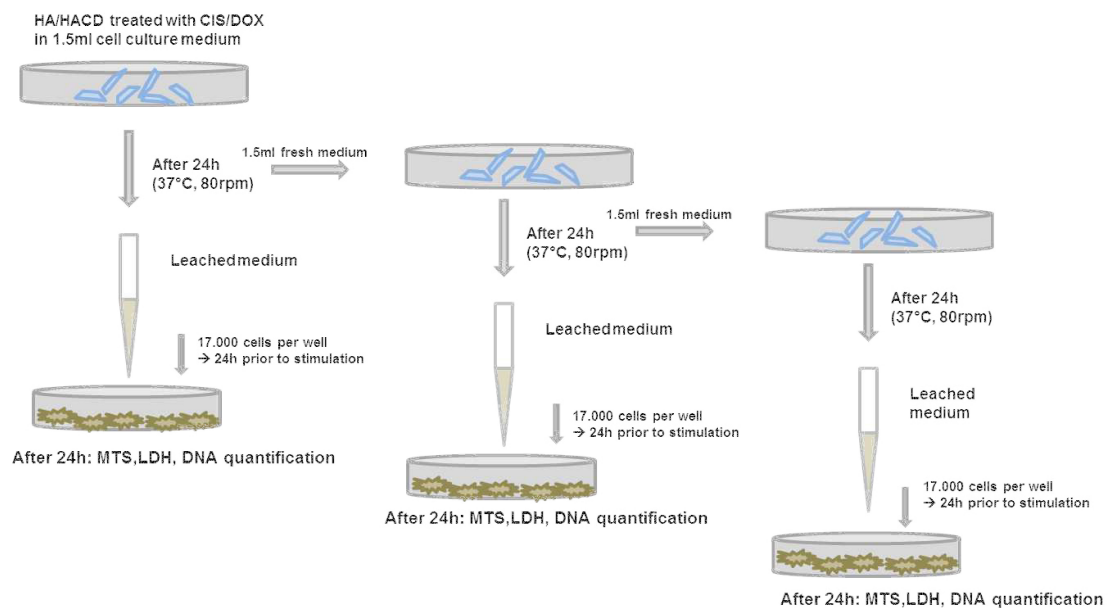


Figure 18: Scheme of extraction assay: 24/48/72h

According to the previously described process of the extraction assay, cell culture medium was applied to the cisplatin- or doxorubicin-treated and untreated granules. After 24h the medium was used as supernatants for cells and another 1.5ml of cell culture medium were added to the biomaterial for another 24h at 37°C with shaking. Subsequently, the medium was removed and applied to cells that were seeded on 96-well plates prior to treatment with leached medium. The process was repeated for the third time. At the end of each treatment, the cells were analyzed for cytotoxicity and cell viability.

2.3.10 Quantification of doxorubicin-release from poly(CD)-functionalized or unfunctionalized hydroxyapatite

The chemical constitution of doxorubicin allows the quantification of its release from polyCD-functionalized and unfunctionalized hydroxyapatite granules by fluorescence measurement. Therefore, doxorubicin was diluted 1:1 in Endothelial Cell Basal Medium MV, supplemented with 15% FCS, 1% P/S, 2ng/ml bFGF and 10µg/ml sodium heparin. By the preparation of a standard curve (doxorubicin: 0.005µg/ml-7.5µg/ml), the concentration of doxorubicin in leached media was determined in triplicates by the measurement of fluorescence using 485nm excitation and 590nm emission filters in a microplate reader.

2.3.11 Cell adhesion and growth on hydroxyapatite granules

To analyze the adhesion and growth of human cancer cells and human primary endothelial cells, 100,000 MG-63 or HUVEC were seeded on poly(CD)-functionalized or non-functionalized hydroxyapatite granules. Before the cells were added to the biomaterial, both types of granules were treated with cisplatin and subsequently washed and dried as described in 2.3.9. Additionally, untreated controls were also tested. Both cell types were added in cell-specific medium to the treated or untreated, modified or unmodified biomaterials. After 48h of cultivation, the cells were stained with calcein AM green-fluorescent dye to make viable cells in the fluorescence microscope visible.

2.3.12 Anoxic culture

Cell culture plates were placed in plastic pouch from the AnaeroGen COMPACT kit together with a paper gas-generating sachet. The paper sachet contains ascorbic acid and activated carbon which reacts on contact with air. Oxygen is rapidly absorbed and carbon dioxide is produced. By using the sachet, the oxygen content in the pouch is reduced to below 1% within 30 minutes. For the indication of an anoxic environment, an anaerobic indicator was added to the pouch, which turned from red into white in an anoxic area. The plastic pouches were sealed with a plastic clip.

2.3.13 Inhibition of HIF-1 α

For the inhibition of HIF-1 α cells were treated with 20 μ M HIF-1 α inhibitor or 75 μ M YC1 inhibitor. After 24h of cultivation in an anoxic environment, the cells were lysed with buffer#13 and subsequently analyzed for p53 and p21 by using ELISA. As a control, untreated or cisplatin- and doxorubicin-treated HUVEC under anoxic conditions were used.

2.4 Gene expression

2.4.1 RNA isolation

Cells of two wells of a 24-well plate were lysed by using 350 μ l RLT buffer from the RNeasy Micro Kit, suitable for purification of up to 45 μ g of total RNA. In a ratio of 1:100, RLT buffer was mixed with β -mercaptoethanol. The lysates were stored at -80°C or directly used for RNA purification according to the manufacturers' protocol. RNA was precipitated with 1 volume of ethanol (70%) and pipetted to a spin column from the kit. After the centrifugation for 15sec at maximum speed (13 000 rpm), the flow-through was discarded. 350 μ l buffer RW1 from the kit was added and the centrifugation was repeated. To eliminate residual DNA from the sample, 80 μ l of DNase (10 μ l DNase Stock: 1500U + 70 μ l RDD buffer \rightarrow 43.6U per sample) was incubated for 15min at room temperature and the previous step with RW1 buffer was repeated. Subsequently, the membrane was washed with 500 μ l RPE buffer, containing 75% ethanol, and 500 μ l ethanol (80%). To dry the membrane completely, the spin columns were centrifuged for 2min at maximum speed in a first step. In a second step the spin columns were centrifuged with open lid for 5min at full speed to evaporate the ethanol. In a last step

the RNA was eluted with 14µl of RNase-free water by centrifugation of the samples for one minute at maximum speed. The concentration of RNA was measured by using a NanoDrop spectrophotometer. The samples were directly used for reverse transcription or stored at -80°C.

2.4.2 Reverse transcription

One µg of the obtained RNA was utilized for the transcription to copy DNA (cDNA) by using the Omniscript Reverse Transcription Kit. One µg of RNA was adjusted to 10µl diluted in RNase-free water if needed. 10µl of master mix (2.5µl RNase-free water, 2µl 10X buffer Reverse Transcription (RT), 2µl dNTP mix containing 5mM of each dNTP, 2µl random primer, 1µl Reverse Transcription Omniscriptenzyme and 0.5µl RNase inhibitor) were added to each sample and gently mixed. The reaction mixture was incubated for one hour at 37°C. The cDNA can be used directly for quantitative real-time reverse transcription-polymerase chain reaction.

2.4.3 Quantitative real-time reverse transcriptase-polymerase chain reaction (Quantitative real-time RT-PCR)

For detection and quantification of a specific DNA sequence, 5ng cDNA per reaction were analyzed by quantitative real-time PCR by using 12.5µl PowerSYBR®Green, a fluorescent DNA binding dye. Together with aqua dest. and 0.2µM of a forward and reverse (3' and 5') primer, the reaction mix was adjusted to 25µl. The reaction was performed in a MicroAmp™optical 96-well reaction plate and carried out in an Applied Biosystems 7300 Real-Time PCR System. Quantitative real-time PCR was conducted in triplicates with the following cycler program: 95°C for 10min for the denaturation step to melt the DNA into single-stranded DNA molecules; 95°C for 15sec for the annealing step to bind the primers at the single-stranded DNA and 60°C for 1min for the elongation step to allow the DNA polymerase to synthesize a new DNA strand complementary to the DNA template strand by adding dNTPs in 5' to 3' direction. 40 cycles were performed. To specify the length of the DNA fragments, a dissociation stage was added to the end of the program by elevating the temperature to 95°C for 15sec, 60°C for 1min, 95°C for 15sec and 60°C for 15sec.

As an endogenous control (housekeeping gene) primers for ribosomal protein 13A (RPL13A) were used and the relative gene expression was determined by the $\Delta\Delta C_t$ method. This normalization procedure allows the comparison of gene expression in

different samples. The data were analyzed with SDS software to receive the cycle threshold (Ct). The Ct value of the endogenous control was subtracted from the Ct value of the samples to obtain Δ Ct value. The Δ Ct value of the control (untreated) sample was subtracted from the Δ Ct value of the experimental (treated) sample to gain the $\Delta\Delta$ Ct value. The n-fold expression was calculated with the $2^{-\Delta\Delta Ct}$.

2.5 Protein expression

2.5.1 Enzyme-linked immunosorbent assay (ELISA)

For the detection of human VEGF in cell culture supernatants which were collected from mono-, co- and triple-cultures, the DuoSet ELISA kit was used according to the manufacturers' protocol. MaxiSorp® flat-bottom 96-well plates were coated with 100 μ l/well capture antibody (mouse, anti-human VEGF) with a working concentration of 1 μ g/ml and incubated over night at room temperature and 50rpm. The next day the plate was washed three times with wash buffer consisting of PBS (pH 7.2-7.4) containing 0.05% Tween®20. To block unspecific binding sites, the plate was incubated with 300 μ l/well reagent diluent consisting of PBS (pH 7.2-7.4) and 1% bovine serum albumin (BSA) fraction V for one hour. Subsequently, the plate was washed three times with wash buffer. The standards were diluted according to the manufacturers' protocol and ranged from 31.25pg/ml up to 2000pg/ml. The supernatants of cell culture samples were diluted in a ratio of 1:5 before they were added to the plate. Samples and standards were diluted in reagent diluent. 100 μ l/well of samples or standards were added as triplicates to the plate to bind to the capture antibody for a period of two hours, followed by a repetition of the washing step. 100 μ l/well of a working concentration of 100ng/ml biotinylated detection antibody (goat, anti-mouse) were incubated on the plate for two hours. After washing the plate for three times with wash buffer, 100 μ l/well of a streptavidin-HRP working solution (1:200) were incubated for 20min. Subsequently, the plate was washed and 100 μ l/well of the substrate solution (a mixture consisting of H₂O₂ and tetramethylbenzidine in a ratio of 1:1) applied to the wells and incubated for another 20min. To stop the enzymatic reaction 50 μ l of a 2N H₂SO₄ solution per well were applied. Using a microplate reader, the optical density was measured at 450nm and the amount of VEGF was calculated according to the standard curve.

For the detection of total human p53 and p21, cell lysates were measured according to the manufacturers' protocol by using the DuoSet ELISA kit. Thus, cells were rinsed

twice with PBS and solubilized with lysis buffer. The lysates were thoroughly scraped from the cell culture surface and kept on ice for 15min. Subsequently, the lysates were centrifuged at 4000g for 5min. The supernatant was stored in a fresh cell culture tube and stored at -20°C or immediately transferred to a capture antibody-coated (working solution for p53: 4µg/ml; for p21: 1µg/ml) MaxiSorp® flat-bottom 96-well plate, followed by adding the detection antibody (working solution for p53: 100ng/ml; for p21: 250ng/ml) and streptavidin-HRP working solution as well as the substrate solution. After stopping the enzymatic reaction with 2N H₂SO₄ solution, the optical density was measured at 450nm. The amount of p53 or p21 was determined from the standard curve.

2.5.2 Sodium dodecyl sulfate polyacrylamide gel electrophoresis - SDS-PAGE

After finishing the experiment, the cells were lysed with 100µl/well Roti®Load-1 (diluted 1:3 in aqua dest.) buffer and gently scraped from the 6-well plate. The samples were stored at -20°C or directly used for SDS-PAGE. The samples were pretreated with sonification (Branson SLPe, Shanghai) and denatured at 95°C for 5min before being stained with 0.5µl of a 1% bromophenol blue solution. Subsequently, the samples were added to a denaturing SDS polyacrylamide gel, where proteins were separated proportionately to their molecular weight. The gel consisted of a 10% resolving gel and a 10% stacking gel. The resolving gel (10% polyacrylamide (PAA), 375mM Tris-HCl pH 8.8, 0.1% SDS, 0.05% APS, 0.005% TEMED) was poured between two glass plates and sealed with n-butanol to allow the gel to polymerize for 1h. The n-butanol was discarded before the stacking gel (5% PAA, 125mM Tris-HCl, pH 6.8, 0.1% SDS, 0.05% APS, 0.005% TEMED) was cast on top of the polymerized resolving gel. A ten-toothed comb was inserted between the glass plates to obtain 10 chambers after approximately 20min of polymerization.

15µl of each sample were loaded into each chamber of the stacking gel. One of 5µl of the chambers was saved for the WesternC™ standard ladder. Electrophoretic separation of proteins was carried out in Rotiphorese® 10x buffer, diluted 1:10 in aqua dest. at 30mA for approximately 80min.

2.5.3 Western Blot

Once the SDS-PAGE was carried out, the proteins were transferred to a nitrocellulose membrane by western blotting. The membrane, six filter papers and two sponges were equilibrated in transfer buffer (10% Rotiphorese® 10x buffer, 20% MeOH, 70% aqua dest.) before the nitrocellulose membrane was clamped on the gel between the sponges and filter papers from each side. Following this, the construct was placed vertically into a holder of PROTEAN Mini transfer chamber so constituted that the membrane was directed to the anode and the gel to the cathode. To prevent the proteins from overheating, a block of ice was added to the chamber. In transfer buffer at 350mA the proteins were blotted for 1h from the gel to the membrane. To control if the proteins had been transferred, the membrane was stained with Ponceau S solution to make the proteins visible. After washing out the residual Ponceau S stain with PBS-0.2% (v/v) Tween 20, the membrane was incubated in 5% degreased milk powder in PBS-0.2% (v/v) Tween 20 for at least one hour to saturate the unspecific protein-binding sides. Overnight, the primary antibody HIF-1 α (mouse) was incubated on the membrane at 4°C and diluted 1:250 in 5% degreased milk powder. After washing the membrane three times for five minutes to remove the unbound antibody, the HRP-linked secondary antibody anti-mouse (sheep), diluted 1:2000 in 5% degreased milk powder was incubated for 1h at room temperature. The membrane was washed three times before 1ml of the SuperSignal® West Dura (500 μ l stable peroxidase buffer mixed with 500 μ l Luminol/Enhancer solution) was added to the membrane and incubated for five minutes to detect the protein of interest by chemiluminescence. As an endogenous control the primary antibody against ERK-2 (rabbit) was used to correct the possible unequal protein concentration in each sample. The antibody was diluted 1:3000 in 5% degreased milk powder and incubated on the membrane for 1h at room temperature. The secondary antibody was diluted 1:3000 and incubated for another hour until the EKR-2 protein was detected by chemiluminiscence. To make the WesternC standard ladder visible Precision StrepTactin-HRP Conjugate was added in a ratio of 1:20000.

2.5.4 NanoOrange® protein quantification

To quantify the total protein content of cell lysates, the NanoOrange® protein quantitation kit was used. The NanoOrange® diluent was diluted in a ratio of 1:10 in aqua dest. to obtain the working solution. The fluorescent component was added to the working solution in a ratio of 1:500 to bind to the proteins. The cell lysates were diluted

in a ratio of 1:1000 in working solution containing the fluorescent dye. To determine the concentration of proteins in the sample, different BSA concentrations were prepared in the same solution for a standard curve. Samples and standards were incubated at 95°C for 10 minutes in the dark and subsequently allowed to cool down at room temperature for 20 minutes in the dark. In a final step, the samples were transferred in a Greiner plate with 200µl per well as duplicates and fluorescence was measured in a microplate reader using 485nm excitation and 590nm emission filters.

2.6 Immunofluorescence staining

To visualize the cells, the culture supernatant was discarded and the cells were washed with PBS. After fixation with 3.7% paraformaldehyde (PFA) for 15min at room temperature, the cells were washed three times with PBS. Subsequently the cells were permeabilized with 0.5% Triton X-100 in PBS for an additional 15min at room temperature. After washing the cells three times with PBS, the primary antibody anti-human CD31 (goat) was incubated at room temperature for 1h in a dilution of 1:50 in 1% PBS/BSA. The washing step was repeated before the secondary anti-goat antibody Alexa 488 (donkey), diluted 1:1000 in PBS/BSA, was incubated for 1h at room temperature in the dark. To visualize the macrophages in triple-cultures, the cells were additionally stained for the macrophage and monocyte marker CD68 (mouse), diluted 1:50 for 1h. After washing the cells, the secondary anti-mouse antibody Alexa 546 (rabbit), diluted 1:1000 in PBS/BSA was incubated for 1h. After the last washing step 1µg/ml Hoechst dye 33342 was incubated for 5min to stain the cell nuclei.

The cells were mounted with Flourosshield and examined using a confocal laser scanning microscope (LeicaTCS-NT, Wetzlar) or a fluorescence microscope (Keyence, Neu-Isenburg).

To differentiate between non-activated and macrophage-activated THP-1, the cells were stained for CD68 (mouse) and CD105 (mouse) diluted 1:25 and PBS/BSA before and after treatment with PMA. With the secondary anti-mouse antibody Alexa 488 (goat), the cells appeared green in the fluorescence microscope. The monocyte and macrophage nuclei were stained with Hoechst dye 33342.

2.6.1 Image quantification

Microvessel-like structures of microscopic immunofluorescence images were semi-automatically quantified by using Fiji, an element of ImageJ. In a first step, the background of the images was corrected by subtracting a corresponding UV-image. An automatic threshold was set and microvessel-like structures were extracted from the remaining background and binaries were obtained. Using Photoshop CS5, the binaries were manually corrected. The resulting images were characterized in terms of vascular area, mean vessel length, mean branching points and the mean number of branches. The mean vessel length was determined by skeletonization, whereas the branching points of the skeleton were measured by locating the pixels with more than two neighbors (Fuchs et al. 2009).

2.7 Statistical analysis

All data are presented as mean values \pm standard error of the mean and all experiments were performed with at least 3 different donors. Statistical significance was evaluated using the paired Student's t-test and was performed with Excel (Microsoft Office; Microsoft, München, Germany). For the co- and triple-cultures the test was chosen to compare M ϕ -treated and untreated co-cultures from the same individuals. Statistical significance was assessed by p-value *p<0.05 or **p<0.03, ***p<0.01 respectively.

For the cytotoxicity assays, as well as for the cell cycle and hypoxia experiments, statistical significance was evaluated by using One-way-ANOVA (GraphPad) and Dunnett's Multiple Comparison Test or Two-way-ANOVA (GraphPad) and Bonferroni post-test. Statistical significance was set at a p-value of *p<0.05; **p<0.01; ***p<0.001 respectively.

3 Results

3.1 Treatment of osteosarcoma cell lines and human primary cells with chemotherapeutic agents

The cytotoxic effect of various cisplatin or doxorubicin concentrations on human osteosarcoma cell lines as well as human primary cells was examined by using the MTS cell viability assay.

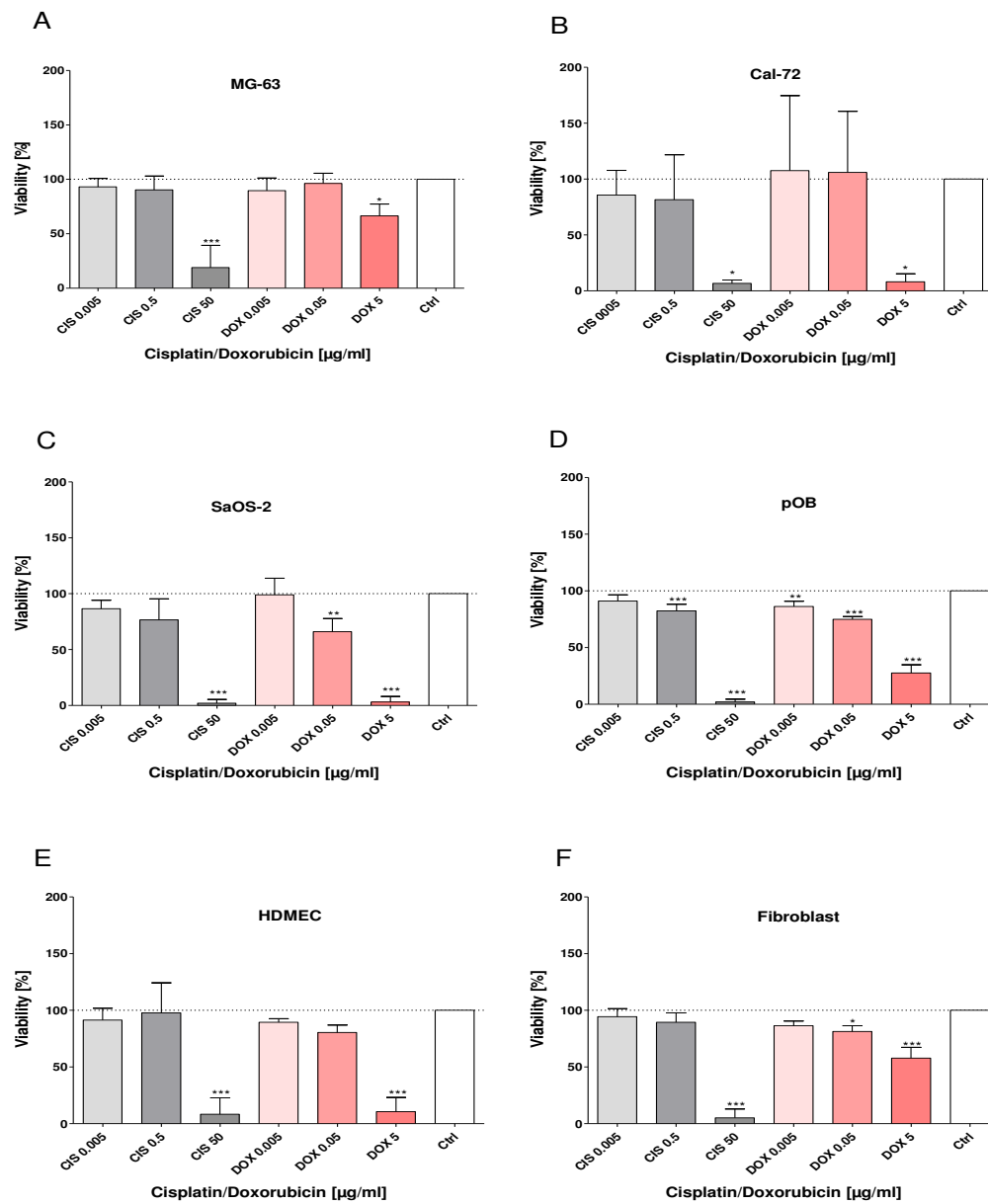


Figure 19: Determination of cell viability of osteosarcoma cell lines and human primary cells by the MTS of cells treated for 4 days with different concentrations of cisplatin or doxorubicin (*p<0.05; **p<0.01; ***p<0.001) (n=3)

Figure 19 shows the viability of various osteosarcoma cell lines and human primary cell types treated for 4 days with cisplatin or doxorubicin, as analyzed using the MTS cell viability assay. Figure 19A, B and C shows the effect of varying anticancer agent concentrations on three different osteosarcoma cell lines. The treatment of MG-63 in A resulted in a highly significant decrease of viability when 50 μ g/ml cisplatin were applied. A significant decline of about 50% of cell growth was also detected when MG-63 were treated with 5 μ g/ml doxorubicin. With lower anticancer drug concentrations, the cells remained viable, compared to the untreated control. The results of cisplatin or doxorubicin-treated Cal-72 are depicted in B. The cells are significantly inhibited when high concentrations of both anticancer drugs were applied. There was also a slight decrease of cell viability when low and medium cisplatin concentrations were used, but the effects were not significant. The decline of SaOS-2 viability is shown in C. A significant mitochondrial interference was measured when the cells were treated with high cisplatin or medium and high doxorubicin concentrations. A decline in cell viability was also detectable when 0.5 μ g/ml cisplatin were applied, but the effect was not significant. Cisplatin and doxorubicin thus exhibited different cytotoxic impacts on various osteosarcoma cell lines.

Figure 19D, E and F show the effect of both anticancer drugs on human primary cells, isolated from different tissue. When cells were treated for 4 days with various concentrations of cisplatin and doxorubicin, the viability of human primary osteoblasts (pOB) was measured via MTS assay, as depicted in D. There was a strong decrease of viability when high concentrations of cisplatin or doxorubicin were applied to the cells. After the treatment with 50 μ g/ml cisplatin there was a more than 95% decline in cell viability observed. In contrast, the application of 5 μ g/ml doxorubicin resulted in a decrease of mitochondrial activity of almost 70%. There was also a significant but less marked impairment of viability measurable, when medium cisplatin or low and medium doxorubicin concentrations were used. The cytotoxic effects of the chemotherapeutic agents on human endothelial cells, HDMEC, are depicted in E. A highly significant decrease in cell viability was detectable after the treatment with high concentrations of cisplatin or doxorubicin. Both agents evoked a decline of viability of about 90%. Human fibroblasts, isolated from oral mucosa, exhibited a reduction of mitochondrial activity when treated with high concentrations of antitumor drugs, as depicted in F. The application of 50 μ g/ml cisplatin effected a reduction of viability of about 95%, compared to the untreated control. After the incubation of 5 μ g/ml doxorubicin for 4 days, the cells exhibited a decrease in viability of about 43%. There was also a significant decline in mitochondrial activity after treatment with 0.05 μ g/ml doxorubicin, resulting in a reduction of viability of about 20% compared to the untreated control. Low and medium

Results

cisplatin as well as low doxorubicin concentrations seemed to have no significant inhibitory effect on the viability of fibroblasts. The analyses of the effect of cisplatin and doxorubicin on various cancer cell lines and human primary cells resulted in different intensities of impairment of viability, depending on cell type.

To visualize the effect of various cisplatin or doxorubicin concentrations, the cells were stained by using the live/dead staining kit. Calcein AM was used to mark viable cells, seen by a green-fluorescent staining. Ethidium homodimer-1, as an indicator for the loss of an intact plasma membrane, bound to DNA and exhibited a red fluorescence.

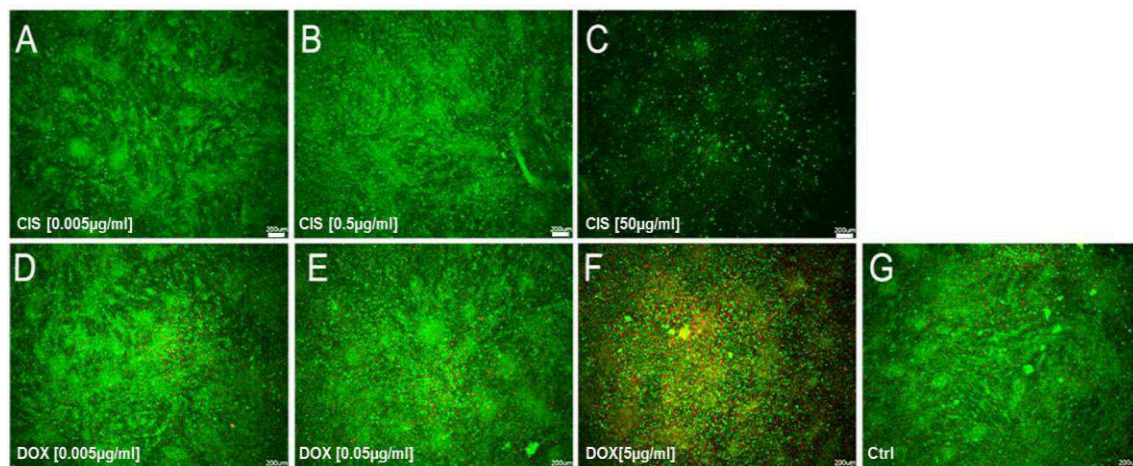


Figure 20: LIVE/DEAD® assay of MG-63 after 4 days of treatment with therapeutic agents

5 000 MG-63 were cultured on 96-well plates for 14 days until they were treated with cisplatin: 0.005 µg/ml (A), 0.5 µg/ml (B), 50 µg/ml (C) or doxorubicin: 0.005 µg/ml (D), 0.05 µg/ml (E), 5 µg/ml (F) for 4 days. The untreated control group (G) was cultured similarly. On day 19 the LIVE/DEAD® assay was performed. Scale bars 200 µm.

After 4 days of cisplatin and doxorubicin treatment, MG-63 were analyzed in terms of viability by using LIVE/DEAD® viability/toxicity kit. The results are shown in figure 20A-G. Compared to the untreated control, depicted in G, MG-63 remained viable when treated with low and medium concentrations of cisplatin (A/B) or doxorubicin (D/E). When 50 µg/ml cisplatin were applied, most of the cells died, as imaged in C. The highest administered concentration of doxorubicin (F) exhibited a toxic effect on MG-63, although some viable cells were detectable. The results from the live/dead staining confirm to the findings of the MTS assay, depicted in figure 19A.

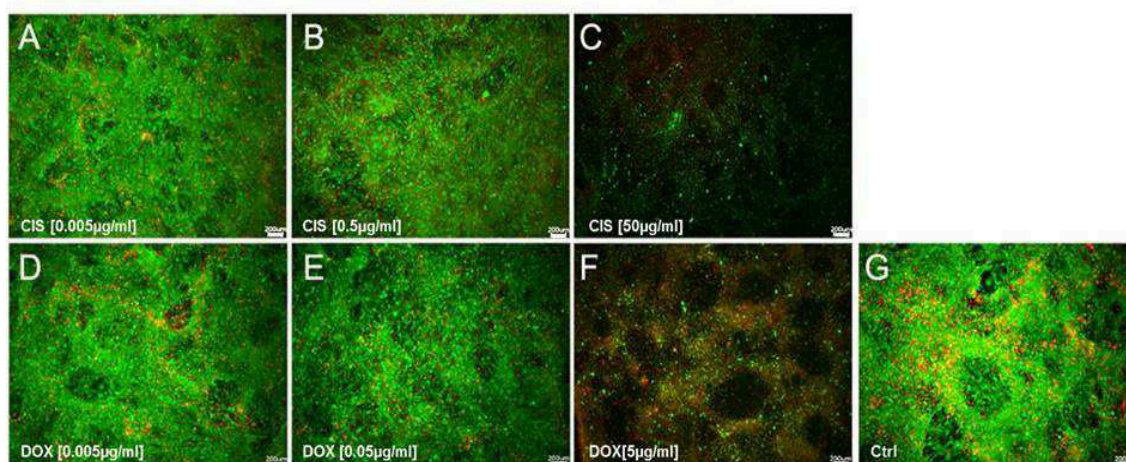


Figure 21: LIVE/DEAD® assay of Cal-72 after 4 days of treatment with therapeutic agents

5 000 Cal-72 were cultured on 96-well plates for 14 days until they were treated with cisplatin: 0.005 µg/ml (A), 0.5 µg/ml (B), 50 µg/ml (C) or doxorubicin: 0.005 µg/ml (D), 0.05 µg/ml (E), 5 µg/ml (F) for 4 days. The untreated control group (G) was cultured similarly. On day 19 the LIVE/DEAD® assay was performed. Scale bars 200 µm.

Cal-72 were treated in the same manner as MG-63 and then stained with the LIVE/DEAD kit (Figure 21A-G). Compared to the untreated control (G), the cells remained viable, when low or medium concentrations of cisplatin (A/B) or doxorubicin (D/E) were applied. The administration of high concentrations of cisplatin (C) or doxorubicin (F) resulted in a high degree of cell death, demonstrated by a global red-fluorescent signal. These results agree with the results from the MTS assay, depicted in figure 19B.

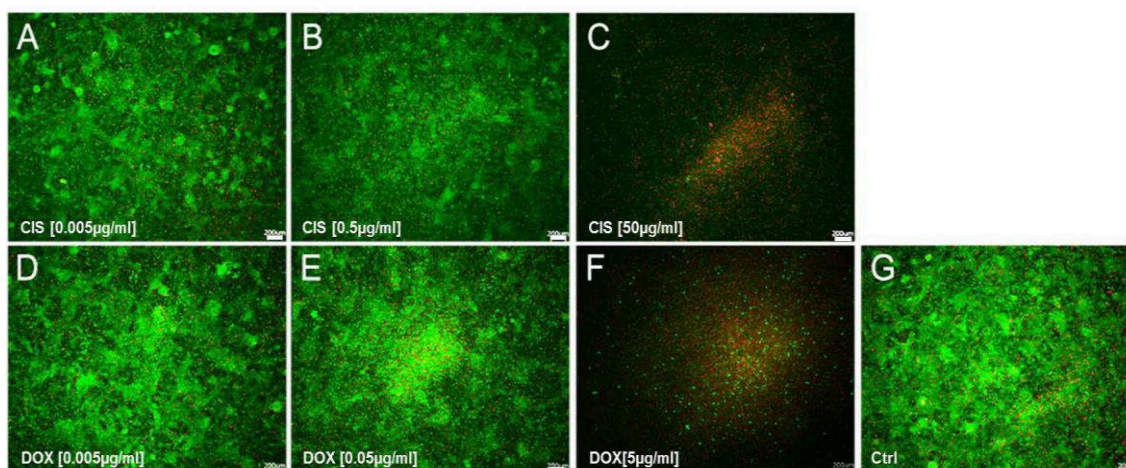


Figure 22: LIVE/DEAD® assay of SaOS-2 after 4 days of treatment with therapeutic agents

5 000 SaOS-2 were cultured on 96-well plates for 14 days until they were treated with cisplatin: 0.005 µg/ml (A), 0.5 µg/ml (B), 50 µg/ml (C) or doxorubicin: 0.005 µg/ml (D), 0.05 µg/ml (E), 5 µg/ml (F) for 4 days. The untreated control group (G) was cultured similarly. On day 19 the LIVE/DEAD® assay was performed. Scale bars 200 µm.

Results

SaOS-2 were stained using the LIVE/DEAD® kit after the treatment with various concentrations of chemotherapeutic agents. The images in figure 22 show that the osteosarcoma cell line exhibited no visually detectable decrease of viability when low or medium concentrations of cisplatin (A/B) or doxorubicin (D/E) were applied compared to the untreated control (G). However, a strong inhibiting effect on cell viability was detectable when SaOS-2 were treated with 50µg/ml cisplatin (C) or 5µg/ml doxorubicin (F) in relation to untreated cells (G).

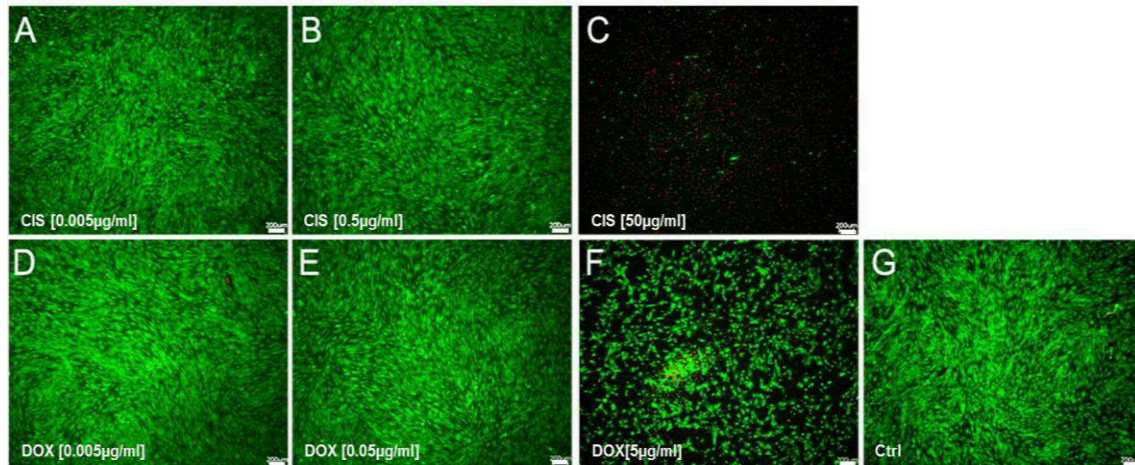


Figure 23: LIVE/DEAD® assay of primary osteoblasts after 4 days of treatment with therapeutic agents

5 000 pOB were cultured on 96-well plates for 14 days until they were treated with cisplatin: 0.005µg/ml (A), 0.5µg/ml (B), 50µg/ml (C) or doxorubicin: 0.005 µg/ml (D), 0.05µg/ml (E), 5µg/ml (F) for 4 days. The untreated control group (G) was cultured similarly. On day 19 the LIVE/DEAD® assay was performed. Scale bars 200µm.

Following the 4-days treatment of cells with anticancer drugs, human primary osteoblasts were analyzed in terms of viability by using the LIVE/DEAD® staining kit, and the results are depicted in figure 23, A-G. No inhibition of cell growth was detectable, when low and mid-level concentrations of cisplatin (A/B) or doxorubicin (D/E) were present. Compared to untreated cells (G), the application of 50µg/ml cisplatin resulted in complete cell death (C). When 5µg/ml doxorubicin (F) was used, pOB exhibited less viability in relation to the untreated control. Nevertheless, a sizeable number of cells remained viable.

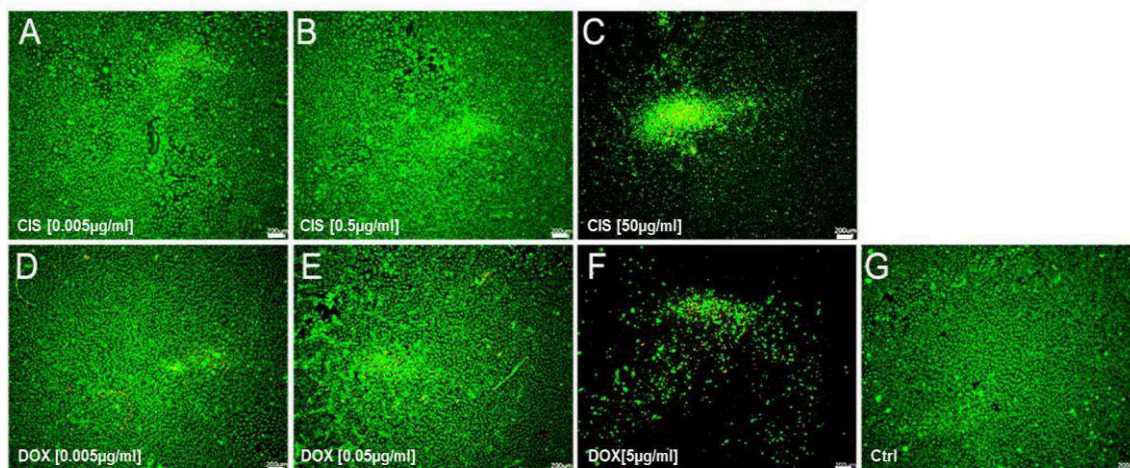


Figure 24: LIVE/DEAD® assay of HDMEC after 4 days of treatment with therapeutic agents

5 000 HDMEC were cultured on 96-well plates for 14 days until they were treated with cisplatin: 0.005 µg/ml (A), 0.5 µg/ml (B), 50 µg/ml (C) or doxorubicin: 0.005 µg/ml (D), 0.05 µg/ml (E), 5 µg/ml (F) for 4 days. The untreated control group (G) was cultured similarly. On day 19 the LIVE/DEAD® assay was performed. Scale bars 200 µm.

Figure 24 shows live/dead staining images of human endothelial cells (HDMEC) after 4 days of treatment with chemotherapeutic drugs. Compared to the untreated control (G), the application of low and mid-level concentrations of cisplatin and 0.005 µg/ml doxorubicin, resulted in no inhibition of cell growth. A slight decrease of viability was observable when HDMEC were treated with 0.05 µg/ml doxorubicin (E). The administration of high cisplatin (C) or doxorubicin (F) concentrations resulted in cell death.

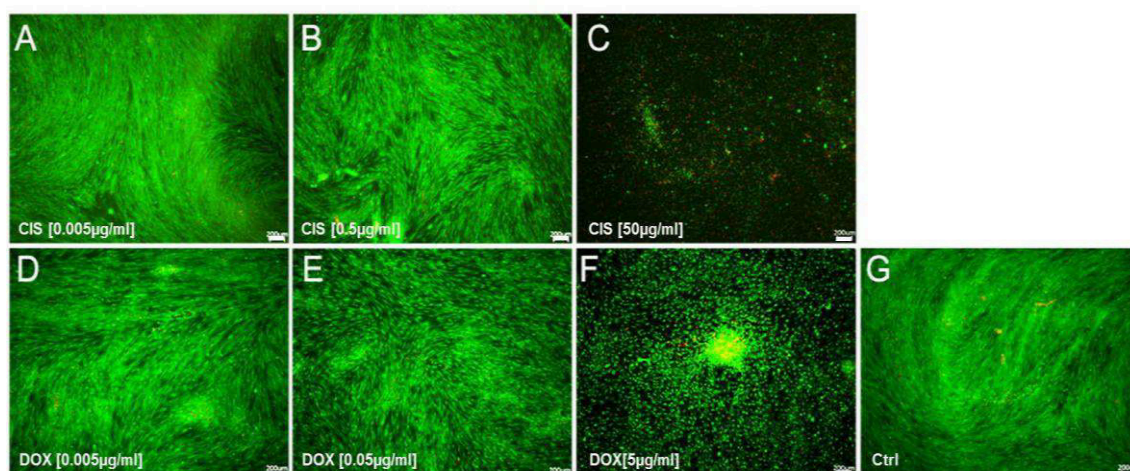


Figure 25: LIVE/DEAD® assay of fibroblast after 4 days of treatment with therapeutic agents

5 000 fibroblasts were cultured on 96-well plates for 14 days until they were treated with cisplatin: 0.005 µg/ml (A), 0.5 µg/ml (B), 50 µg/ml (C) or doxorubicin: 0.005 µg/ml (D), 0.05 µg/ml (E), 5 µg/ml (F) for 4 days. The untreated control group (G) was cultured similarly. On day 19 the LIVE/DEAD® assay was performed. Scale bars 200 µm.

Results

After 4 days of cisplatin and doxorubicin treatment, human fibroblasts were analyzed with the LIVE/DEAD® viability/toxicity kit. Although the cells were treated with 0.05µg/ml and 0.5µg/ml cisplatin (A/B) or 0.005µg/ml doxorubicin (D), fibroblasts exhibited no reduction of viability compared to untreated cells (G). The administration of 0.05µg/ml doxorubicin resulted in a slight decrease of viability (E). When high concentrations of cisplatin were applied to human primary fibroblasts, after 4 days of treatment, no viable cells remained (C). The use of high doxorubicin concentrations resulted in the inhibition of cell growth but a good number of fibroblasts remained vital (F).

In summary, the sensitivity of cells towards both anticancer agents varied depending on the concentrations the cells were exposed to and differences among cancer cell lines as well as among human primary cells were seen. Similar differences were observed in the MTS assay by primary cells compared to cell lines.

The median lethal dose (LD_{50}) of anticancer agents is the dose that is required to kill 50% of the treated cells. The median lethal dose varies among populations and is not representative for one individual and can differ among cells. For the following studies, the LD_{50} value was used as a guideline in the selection of the concentration range of cisplatin or doxorubicin. To determine the median lethal dose for cisplatin or doxorubicin in different cells, various cell types were treated with a range of drug concentrations for 24h. Subsequently, the cells were analyzed for mitochondrial activity using MTS cell viability test and crystal violet DNA quantification assay (The lethal median dose was calculated by GraphPad Prism 5).

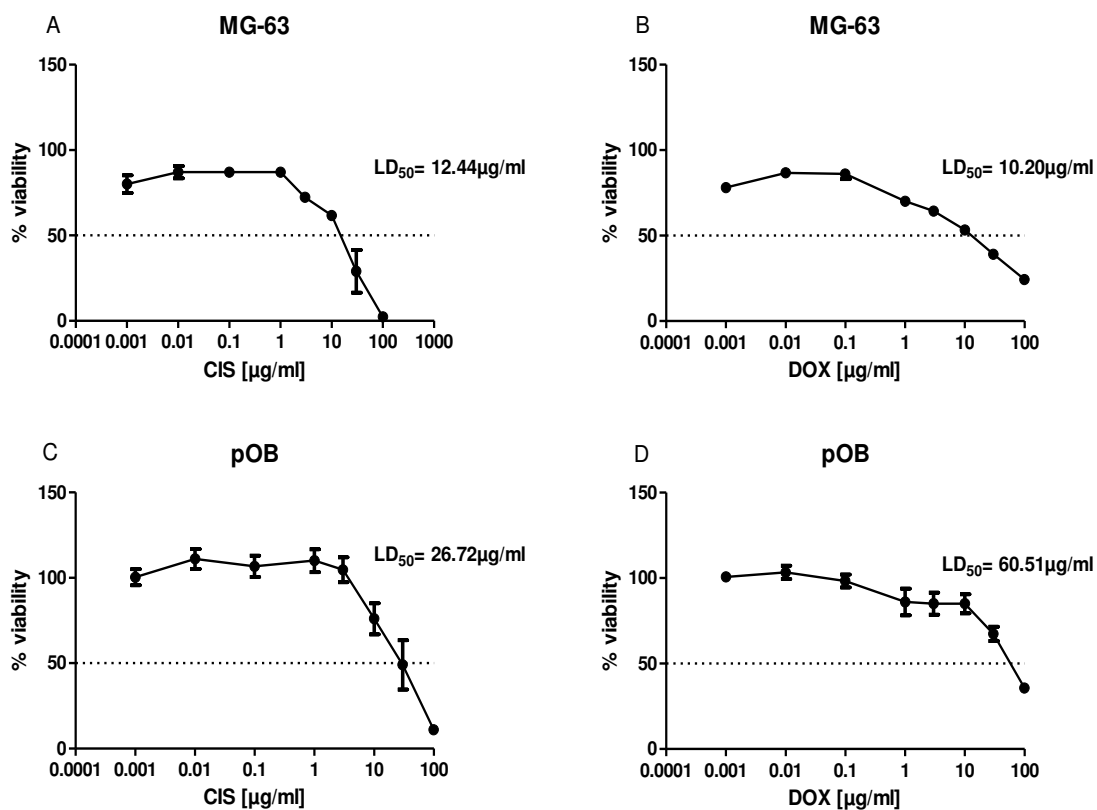


Figure 26: Determination of LD_{50}

MG-63 and pOB were treated with various concentration of cisplatin or doxorubicin, ranging from 0.001 $\mu\text{g/ml}$ to 100 $\mu\text{g/ml}$. After 24h the viability of cells was analyzed using the MTS assay. All data are presented as mean values \pm standard error of the mean and all experiments were performed with $n=3$.

In figure 26 the median lethal dose for cisplatin and doxorubicin in the osteosarcoma cell line MG-63 (A/B) and human primary osteoblasts (C/D) is shown. The LD_{50} value for cisplatin in MG-63 is 12.44 $\mu\text{g/ml}$ (A), whereas the pOB show a higher resistance to the toxic effect, indicated by a median lethality of 26.72 $\mu\text{g/ml}$ cisplatin. A higher variability in the cytotoxic effect of doxorubicin for different cell types is depicted in B and C. The LD_{50} value for doxorubicin was 10.20 $\mu\text{g/ml}$ for MG-63, while the value for pOB was much higher (60.51 $\mu\text{g/ml}$).

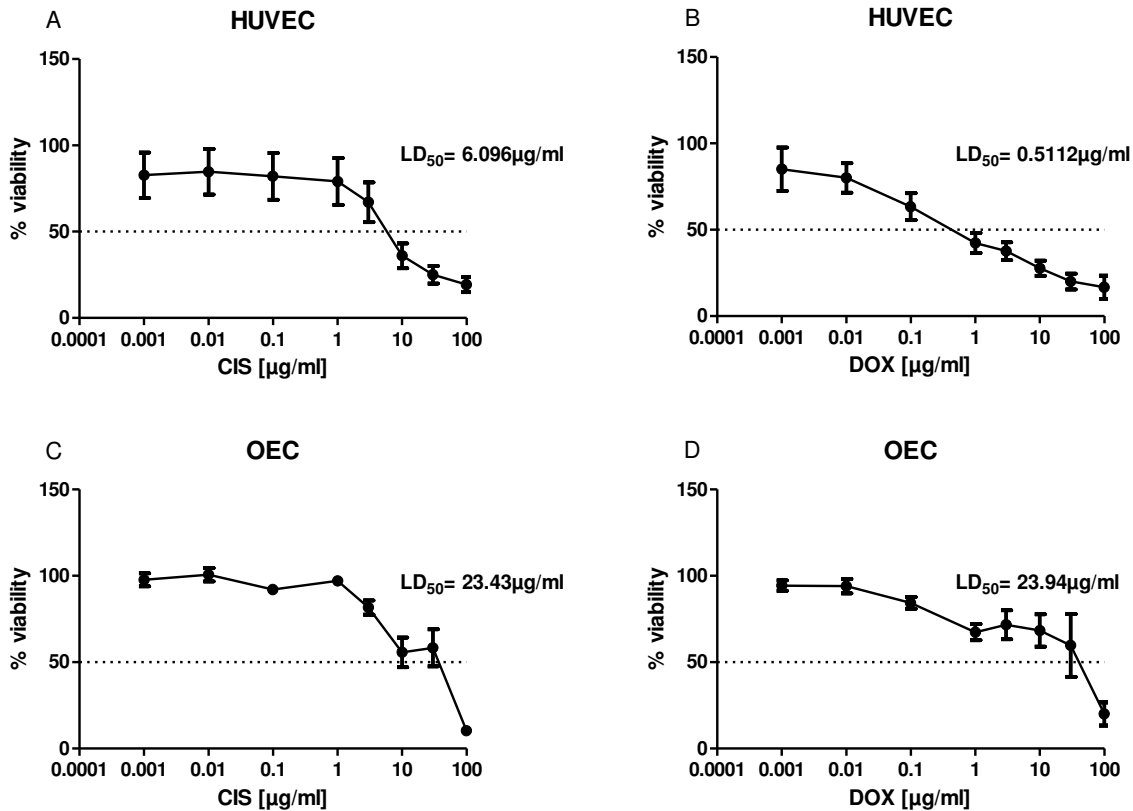


Figure 27: Determination of LD_{50}

The human primary endothelial cells HUVEC and OEC were treated with various concentration of cisplatin or doxorubicin, ranging from 0.001 $\mu\text{g/ml}$ to 100 $\mu\text{g/ml}$. After 24h the viability of cells was analyzed by MTS assay. All data are presented as mean values \pm standard error of the mean and all experiments were performed with $n=3$.

Figure 27 shows the median lethal dose for cisplatin and doxorubicin for endothelial cells. HUVEC exhibited a high sensitivity for cisplatin (A) and doxorubicin (B) indicated by a LD_{50} value for cisplatin of 6.096 $\mu\text{g/ml}$ and 0.5112 $\mu\text{g/ml}$ for doxorubicin. While cisplatin and doxorubicin seem to exert a distinct cytotoxic effect on HUVEC, human outgrowth endothelial cells (OEC) are less sensitive as indicated by a concentration of 23 $\mu\text{g/ml}$ of either compound to cause 50% death of the cells.

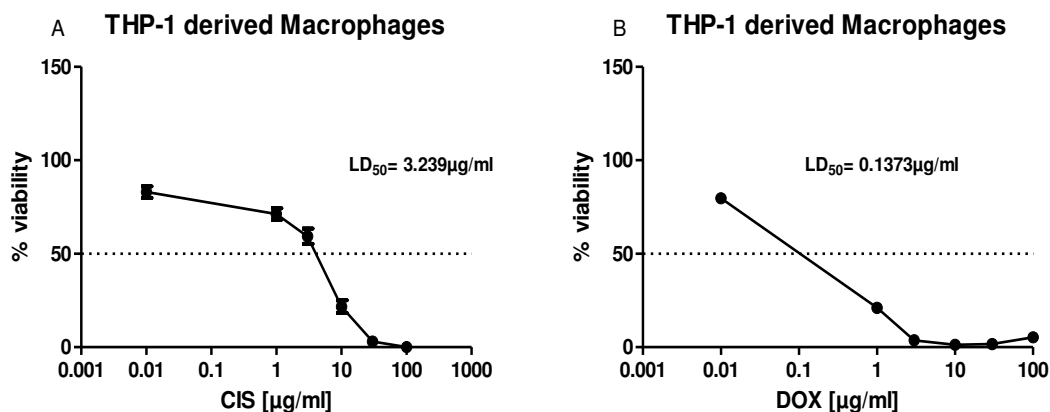


Figure 28: Determination of LD₅₀

THP-1 derived macrophages were treated with various concentrations of cisplatin or doxorubicin, ranging from 0.001 µg/ml to 100 µg/ml. After 24h the viability of cells was analyzed by MTS assay. All data are presented as mean values \pm standard error of the mean and all experiments were performed with n=3.

As depicted in figure 28, THP-1 derived macrophages were treated with a range of cisplatin or doxorubicin concentrations. These macrophages appear to be highly sensitive to doxorubicin, reflected by the low median lethal dose (B). Much higher concentrations of cisplatin (3 µg/ml) were required for 50% lethality.

In summary, the most sensitive cells to the anticancer agents cisplatin and doxorubicin, determined by MTS assay, are HUVEC and THP-1 derived macrophages. The cytotoxic effect on various cell types differed considerably, and was independent of cell type whether cancer cells or human primary cells.

The crystal violet DNA quantification assay was also determined under the same conditions to evaluate the LD₅₀ value for cisplatin and doxorubicin for the different cell types.

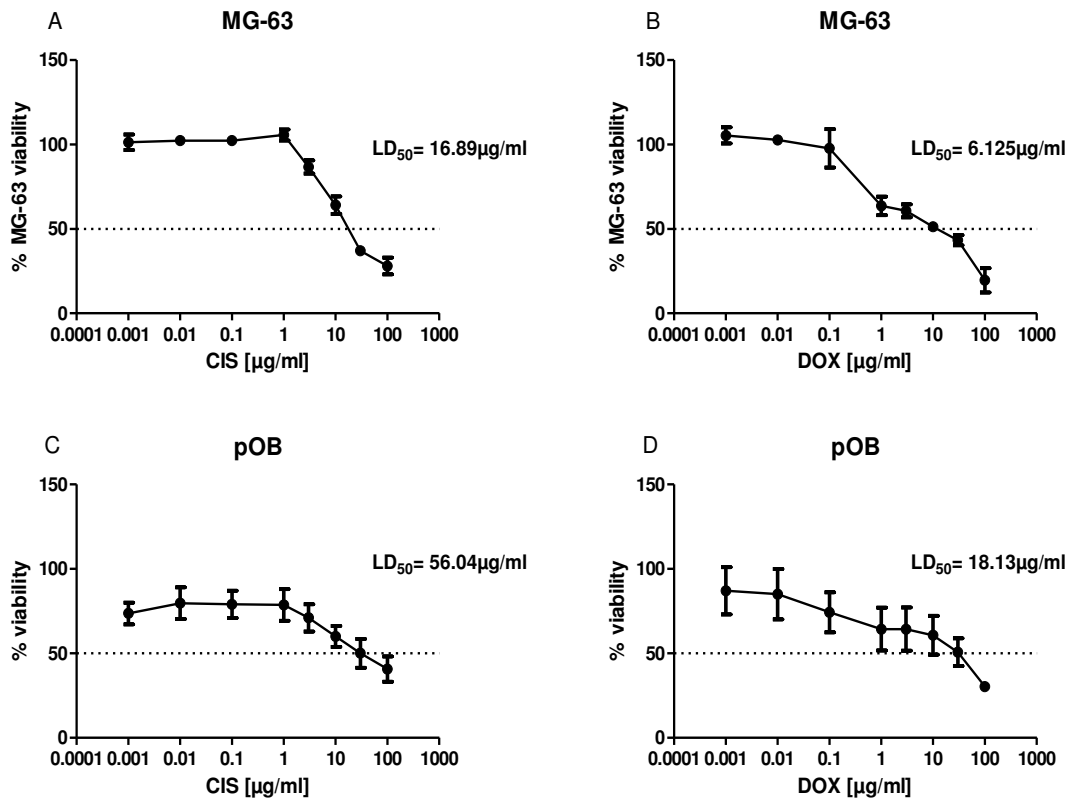


Figure 29: Determination of LD₅₀

MG-63 and pOB were treated with various concentrations of cisplatin or doxorubicin, ranging from 0.001µg/ml to 100µg/ml. After 24h the DNA content was determined by crystal violet DNA quantification. All data are presented as mean values ± standard error of the mean and all experiments were performed with n=3.

Figure 29 depicts the results from the DNA quantification after the treatment of cells with a wide range of cisplatin or doxorubicin concentrations. The median lethal dose was calculated as described in Materials and Methods using GraphPad Prism 5. In A and B the curve for the determination of the LD₅₀ value of cisplatin and doxorubicin by quantification of the DNA of MG-63 is shown. While the data for MG-63 are similar to the MTS assay, the results for primary osteoblasts show an opposite result (C/D/Table 3). Under the same conditions, a cisplatin concentration of 56.04µg/ml was required to decrease the DNA of pOB to 50%, whereas the LD₅₀ for doxorubicin was 18.13µg/ml.

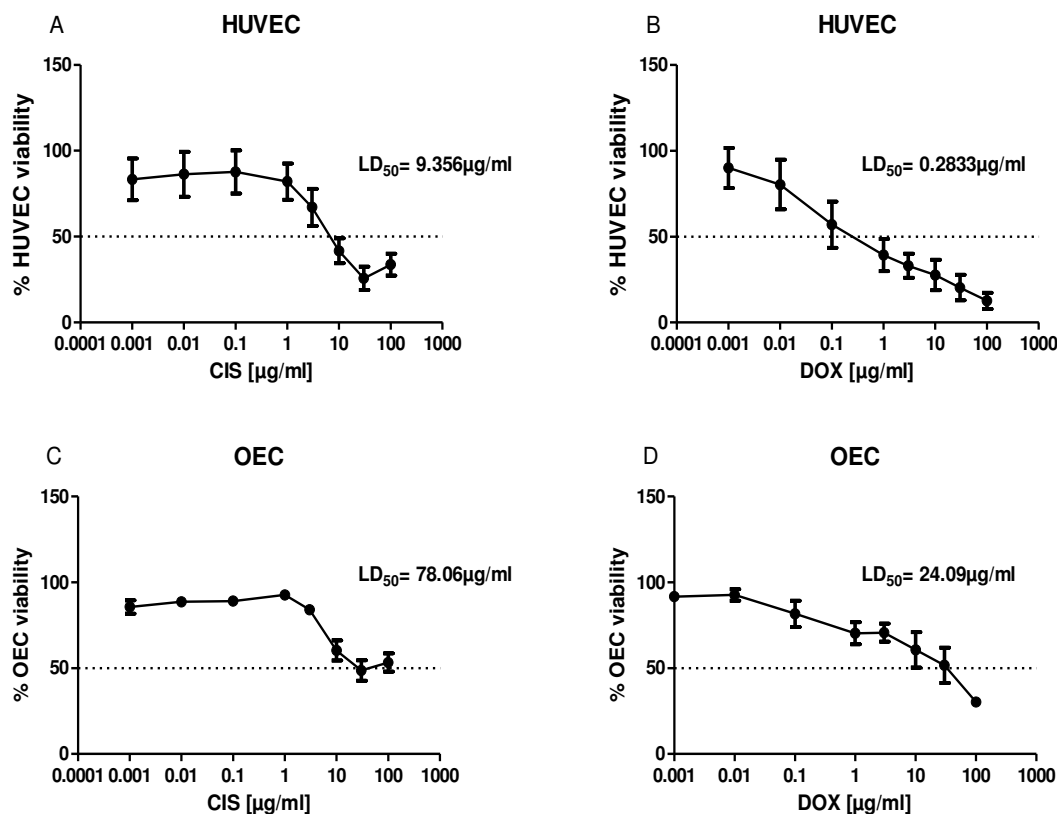


Figure 30: Determination of LD_{50}

HUVEC and OEC were treated with various concentrations of cisplatin or doxorubicin, ranging from 0.001 $\mu\text{g/ml}$ to 100 $\mu\text{g/ml}$. After 24h the DNA content was determined by crystal violet DNA quantification. All data are presented as mean values \pm standard error of the mean and all experiments were performed with $n=3$.

Similar results were observed for HUVEC using the MTS and the crystal violet assay (Figure 27A/B and Figure 30A/B, respectively).

OEC exhibited a difference in sensitivity to cisplatin (C) in the DNA assay compared to the results observed in the MTS assay (Figure 27C/D). In the crystal violet assay the LD_{50} of 78.06 $\mu\text{g/ml}$ was observed for cisplatin (Figure 30C) compared to an LD_{50} of 23.43 $\mu\text{g/ml}$ observed in the MTS assay (Figure 27C). The LD_{50} value for doxorubicin for OEC reflects what was observed in the MTS test (Table 3).

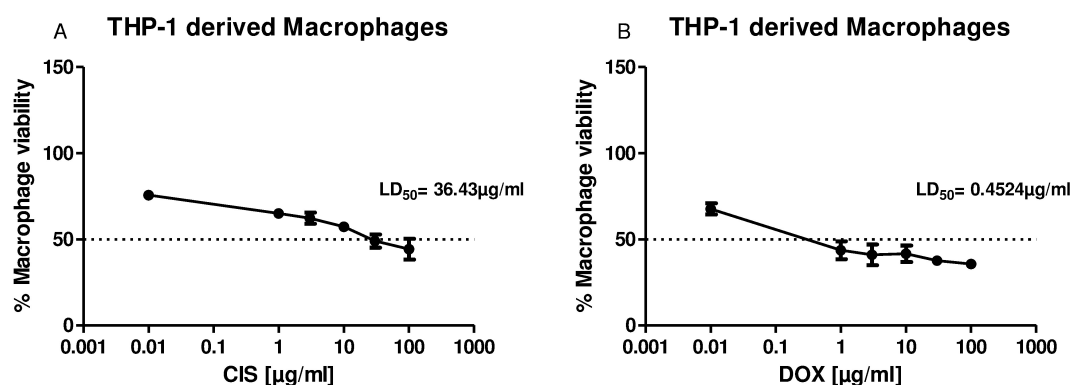


Figure 31: Determination of LD₅₀

THP-1 derived macrophages were treated with various concentrations of cisplatin or doxorubicin, ranging from 0.001µg/ml to 100µg/ml. After 24h the DNA content was determined by crystal violet DNA quantification. All data are presented as mean values \pm standard error of the mean and all experiments were performed with n=3.

THP-1-induced macrophages appear to exhibit less sensitivity to cisplatin, indicated by a median lethal dose of 36.43µg/ml (Figure 31A) compared to the data obtained from the MTS assay (3.239µg/ml, Figure 28A). The data for the LD₅₀ value for doxorubicin, depicted in B, supported the results observed in the MTS assay (Figure 28B). A concentration of 0.4524µg/ml doxorubicin reduced the DNA of the macrophage population to 50%.

Table 3: LD₅₀ values for cisplatin or doxorubicin of various cell types, determined by MTS cell viability assay or crystal violet DNA quantification

LD ₅₀ values [µg/ml]	MTS		crystal violet	
	CIS	DOX	CIS	DOX
MG-63	12.44	10.20	16.89	6.13
pOB	26.72	60.51	56.04	18.13
HUVEC	6.1	0.51	9.36	0.28
OEC	23.43	23.94	78.06	24.09
THP-1 Mφ	3.24	0.14	36.43	0.45

Table 3 summarizes the LD₅₀ values for each of the cell types in each of the assays (MTS, crystal violet).

3.2 Cytotoxic effect of chemotherapeutically treated biomaterials on human primary cells and human cancer cells

To analyze the effects of the release of chemotherapeutic drugs from unmodified and poly(CD)-modified hydroxyapatite granules on different types of cells, an extraction assay was performed. This type of evaluation offers the possibility to analyze the effects of the hydroxyapatite granules, obtained from Curasan and poly-cyclodextrin-modified hydroxyapatite granules from UMET, for their effects on the various cell types. Prior to the extraction assay, some of the granules were also treated with cisplatin or doxorubicin as described in the Materials and Methods. Briefly, after the incubation of non-functionalized and poly(CD)-functionalized hydroxyapatite granules with anticancer agents, the biomaterials were washed thoroughly with sterile water as recommended by UMET. Chemotherapeutic agent-loaded or -unloaded granules were treated similarly. All biomaterials were then placed in media and after 24, 48, and 72 hours supernatant was collected and tested for the effects on the various cell types. These supernatants were added to human primary cells that were isolated from healthy donors on the one hand and for cancer cells on the other hand, similar to the assays described for the chemotherapeutic compounds alone in the sections above. MTS and DNA assays were carried out after 24h.

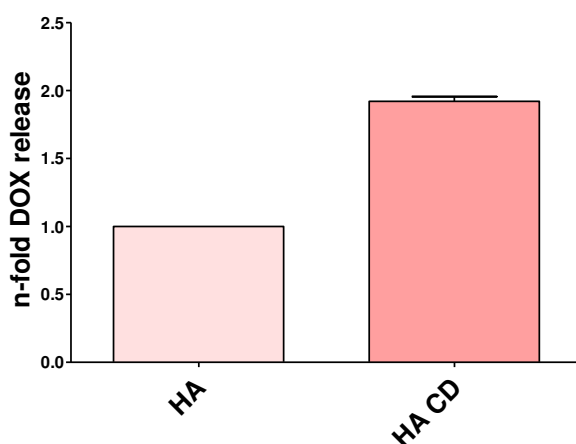


Figure 32: Release of doxorubicin from doxorubicin-treated unmodified (HA) and poly(CD)-modified hydroxyapatite (HACD) after 24h. (n=3).

Measuring the leached media of doxorubicin- treated poly(CD)-functionalized and unfunctionalized hydroxyapatite granules by fluorescence measurement resulted in a higher release of doxorubicin from functionalized hydroxyapatite compared to the release from non-functionalized biomaterial (Figure 32).

Results

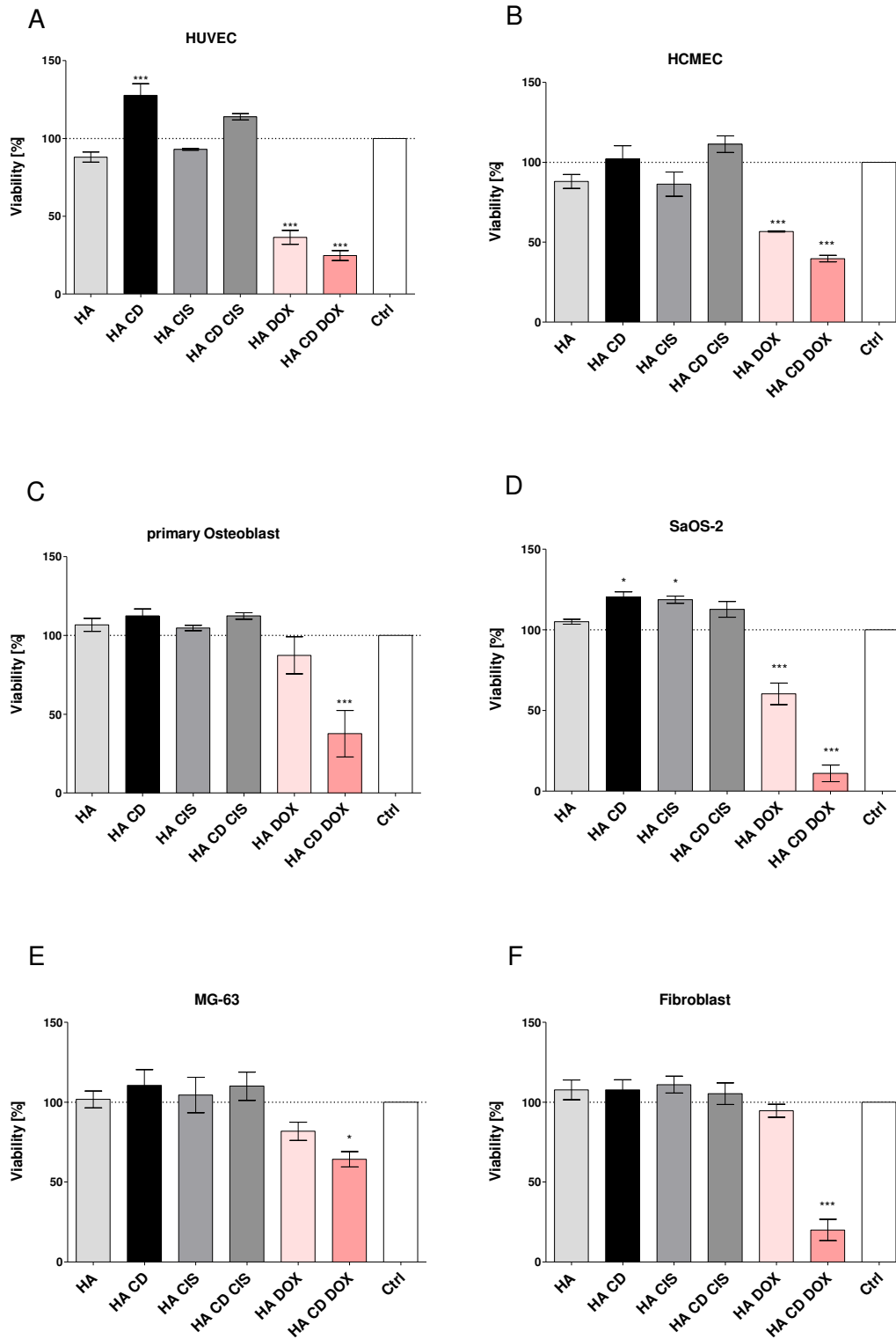


Figure 33: Extraction assay: Cell viability test: MTS assay

Different human primary cells, as models for human healthy cells, and human osteosarcoma cell lines, as models for cancer cells, were used to analyze the extracts obtained from the various treated materials using MTS cell viability assay. (*p<0.05; ***p<0.001) (n=3).

The cell viability was analyzed after cells were exposed to the extracted supernatants obtained from materials after 24 hrs. A MTS cell proliferation assay was then performed as described in Materials and Methods. The supernatants of untreated and cisplatin or doxorubicin-treated poly(CD)-functionalized or non-functionalized hydroxyapatite revealed different effects on the various cell types. While human endothelial cells exhibited a high sensitivity to doxorubicin-treated biomaterial extracts as shown by a significant decrease of cell viability, there was no loss of viability detectable when the supernatants of cisplatin-treated HA was examined (Figure 33A/B). The toxic effect was even more pronounced when leached cell culture medium from poly(CD) was used. Human primary osteoblasts, as well as the human osteosarcoma cell line MG-63, exhibited only a significant decrease of cell viability when the cells were treated with leached medium from doxorubicin-treated poly(CD) HA (Figure 33C/E). MG-63 exhibited a less significant decrease in cell viability compared to pOB. In contrast to MG-63, the human osteosarcoma cell line SaOS-2, was highly sensitive to supernatants of doxorubicin-treated functionalized and non-functionalized biomaterial (Figure 33D). A highly significant decrease in cell viability was observed in both cases and this was even more pronounced when supernatants of doxorubicin-treated poly(CD) HA were examined. Human primary fibroblasts only exhibited a significant decline in viability when the cells were treated with supernatants of doxorubicin-treated poly(CD)-functionalized biomaterial (Figure 33E). There was no significant decrease in fibroblast viability when extracted cell culture medium of cisplatin-treated or doxorubicin-treated non-functionalized HA was used. In general, no differences or inhibition of cell viability was measured when either poly(CD)-functionalized or non-functionalized HA was treated with cisplatin or remained untreated.

Lactate dehydrogenase, a soluble cytosolic enzyme, is released as a result of damage to the plasma membrane of eukaryotic cells and is an indicator for cell death. The amount of LDH released into the cell culture supernatants was measured after cells were exposed for 24h to the biomaterial-extracted media using the LDH cytotoxicity assay.

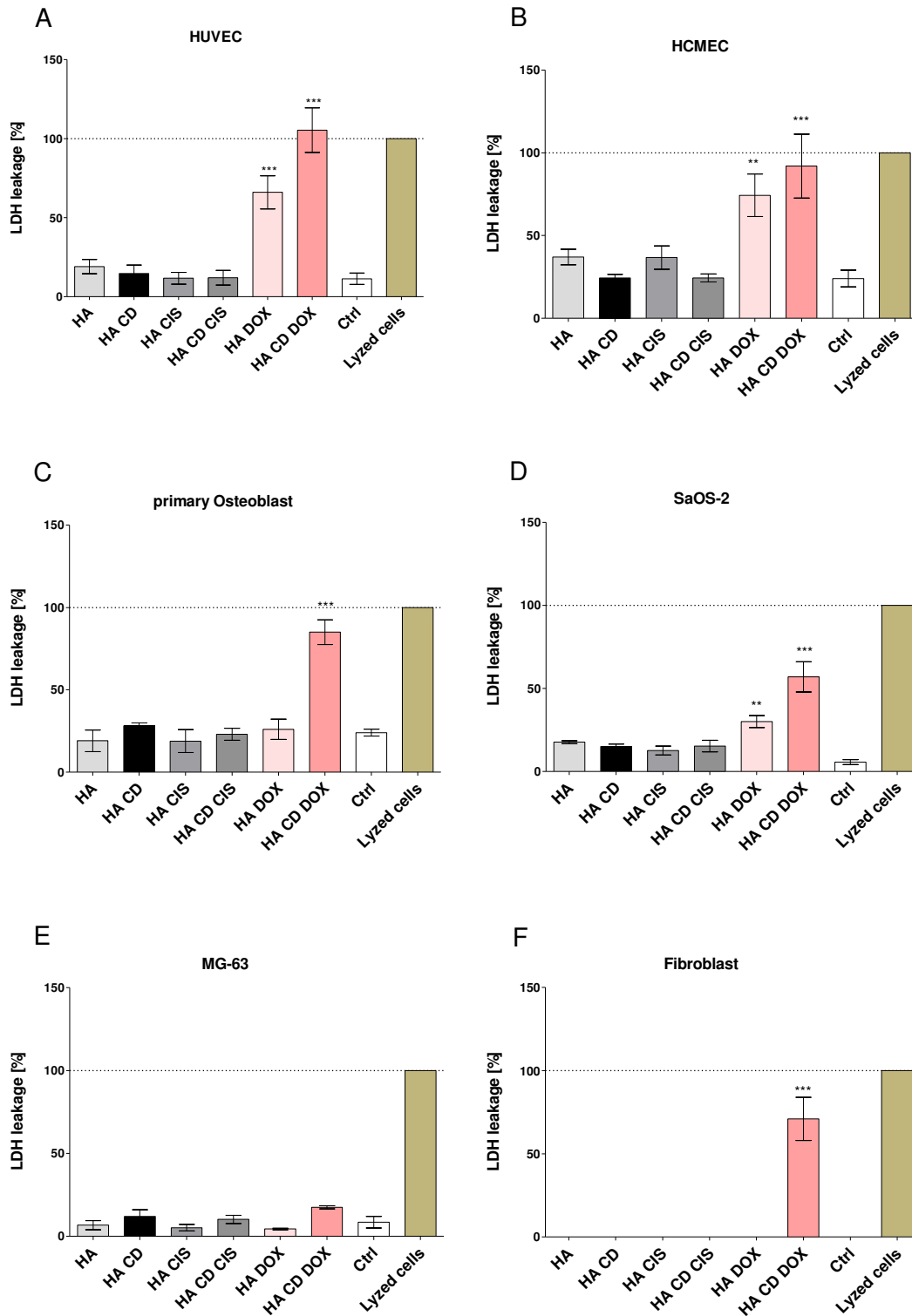


Figure 34: Cytotoxicity test: release of LDH

Different human primary cells, as models for human healthy cells, and human osteosarcoma cell lines, as models for cancer cells, were used to analyze the extracts obtained from the various treated materials using LDH cytotoxicity assay. (* $p < 0.05$; *** $p < 0.001$) (n=3).

Human primary endothelial cells, as well as the endothelial cell line HCMEC exhibited a highly significant release of LDH when the cells were cultivated in the leached cell

culture medium from doxorubicin-treated biomaterial (Figure 34A/B). More LDH was detected when the cell culture medium from doxorubicin-treated poly(CD)-functionalized HA was used. Human primary osteoblasts and human primary fibroblasts showed a significantly elevated concentration of LDH in the cell culture supernatant after 24h of treatment with leached medium of doxorubicin-treated poly(CD)-functionalized biomaterial (Figure 34C/F). The human sarcoma cell lines SaOS-2 and MG-63, exhibited differences in LDH release patterns (Figure 34D/E). SaOS-2 exhibited a significant release of LDH when the cells were treated with leached medium of doxorubicin-treated biomaterial and significantly higher levels when cells were exposed to medium from leached doxorubicin-treated poly(CD)-functionalized HA. In contrast, no LDH was measurable in supernatants of MG-63 treated from any of the medium obtained from the extraction assay (Figure 34E). No LDH was measured in any of the cells types when these were exposed to leached media from the extraction assay of cisplatin-treated or untreated HA or HACD.

In addition to the MTS cell viability test and LDH cytotoxicity assay, the cells in the wells were also analyzed for cell viability by using alamarBlue®.

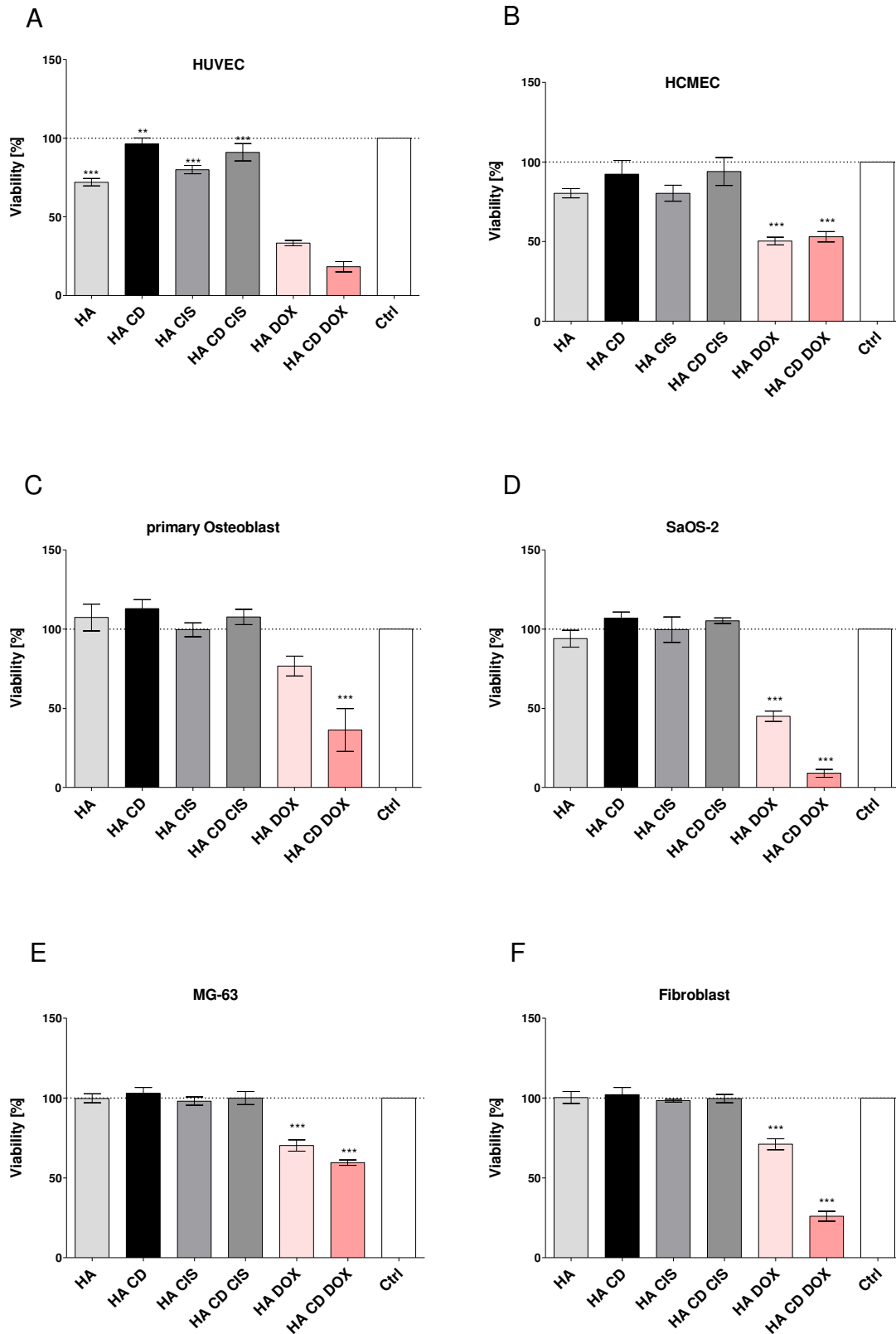


Figure 35: Cell viability test: alamarBlue®

Different human primary cells, as models for human healthy cells, and human osteosarcoma cell lines, as models for cancer cells, were used to analyze the extracts obtained from the various treated materials using alamarBlue® assay. (* $p < 0.05$; *** $p < 0.001$) (n=3).

Results from the MTS assay showed that endothelial cells exhibited a very significant decrease in cell viability when treated with leached medium from the doxorubicin-treated poly(CD)-functionalized and non-functionalized HA. The effect on HUVEC was even greater when supernatants of functionalized biomaterial were applied, whereas HCMEC did not show a difference in reduction of viability regardless of whether extractions from modified or non-modified HA were used (Figure 35A/B). HUVEC exhibited a slight decrease in viability when leached medium from HA or cisplatin-treated HA were analyzed in the MTS assay. The same results were observed with the alamarBlue® assay. Primary osteoblasts exhibited similar results in the MTS assay as shown by a highly significant reduction of cell viability when cells were treated with leached medium from the doxorubicin-treated functionalized biomaterial (Figure 35C). Both human osteosarcoma cell lines exhibited a reduction of viability when supernatants of doxorubicin-treated HA or poly(CD)-modified HA were examined (Figure 35D/E). MG-63 exhibited only a slight reduction of cell viability (30%) while SaOS-2 cells exhibited a reduction of cell viability of about 45% compared to the untreated control of the extracted medium of doxorubicin-treated unmodified biomaterial. When leached medium of doxorubicin-treated poly(CD)-functionalized HA was applied to both cell types, MG-63 exhibited a moderate decrease in viability (40%) while SaOS-2 decreased significantly (90%). The toxic effect on both cell lines was highly significant, although MG-63 cells were more resistant to the toxic effect of doxorubicin. According to the MTS assay human primary fibroblasts exhibited a highly significant decrease in viability when cell culture medium of doxorubicin-treated functionalized HA was applied (Figure 35F/Figure 33 F). Results for the MTS test showed there was no significant decrease (about 5%) of viability detected in supernatants from unmodified biomaterial treated with doxorubicin. The results from the alamarBlue® assay indicated a significant inhibition of cell growth (around 30%) for the same sample. Table 4 gives an overview of the cytotoxic effects of diverse leached media on various cell types.

Results

Table 4: Effect of leached medium from extraction assay after 24h

The table was generated based on the results of the MTS cell viability assay:

+ = less than 20% inhibition

++ = 30% - 50% inhibition

+++ = more than 60% inhibition

- = no inhibitory effect

	HA	HA CD	HA CIS	HA CD CIS	HA DOX	HA CD DOX
HUVEC	-	-	-	-	+++	+++
HCMEC	-	-	-	-	++	+++
pOB	-	-	-	-	+	+++
SaOS-2	-	-	-	-	++	+++
MG-63	-	-	-	-	+	++
Fibroblasts	-	-	-	-	-	+++

In summary, the cytotoxicity assays and cell viability assay exhibit similar results, reproducibility and patterns and provide a useful means to obtain a toxicity profile of a drug on specific cell types.

To demonstrate that the treated biomaterials release a specific chemotherapeutic agent with time and to determine if these released compounds exhibited a cytotoxic effect on various cell types, the leached medium was collected from the biomaterial after various time points. The supernatant media in which the loaded biomaterial was incubated was collected after 24h, 48h and 72h of leaching. These media were added to various cell types and the effects on cells were analyzed by the MTS cell viability, the LDH cytotoxicity assay and by DNA quantification after 24h of treatment.

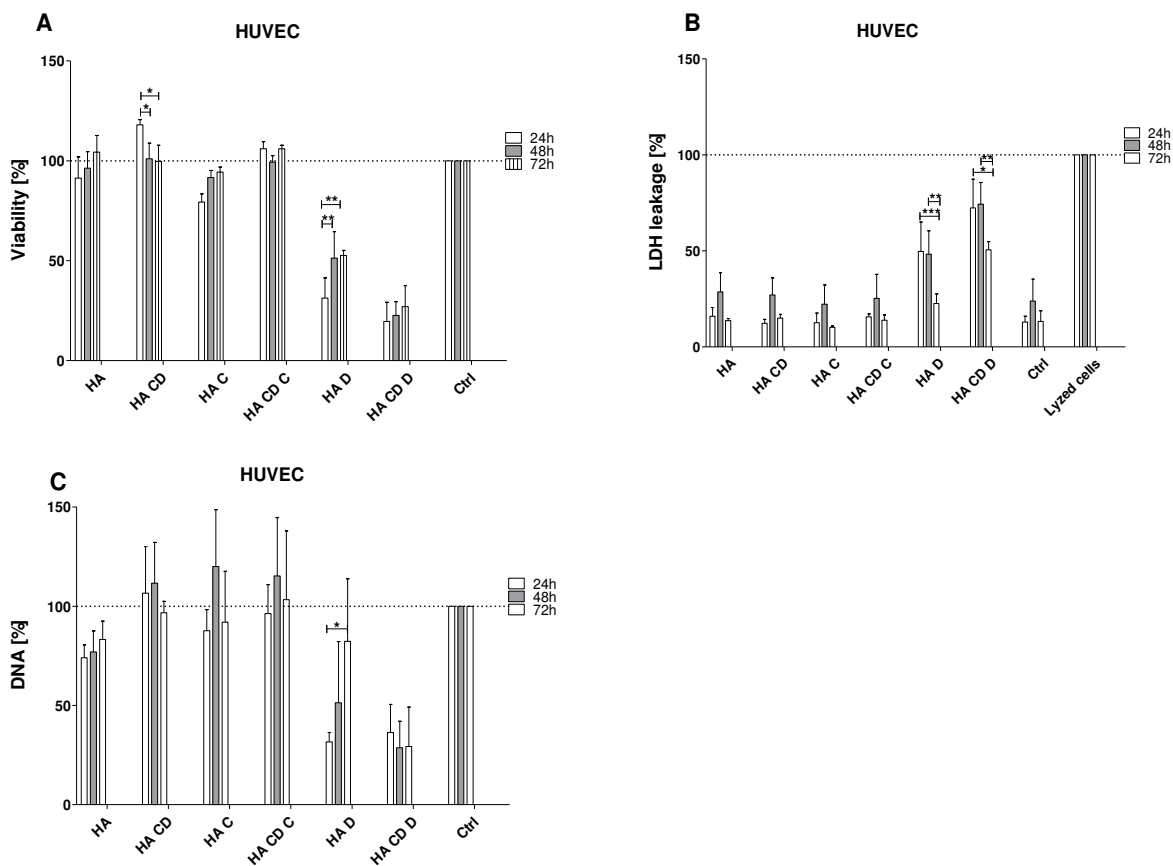


Figure 36: Effect of leached medium on HUVEC after 24h, 48h and 72h analyzed by MTS cell viability assay, LDH cytotoxicity assay and crystal violet DNA quantification

The cisplatin- or doxorubicin-treated and non-treated poly(CD)-functionalized and non-functionalized hydroxyapatite granules were incubated in endothelial cell medium for 24h, 48h and 72h. These media were added to endothelial cells and after 24h of incubation the viability of HUVEC was measured by using the MTS assay.

The viability of cells was compared for the three time points at which the leached medium was collected. Ctrl: cell culture medium.

(* $p < 0.05$; ** $p < 0.01$; *** $p < 0.001$) ($n = 3$).

Figure 36A shows the results of the MTS assay of HUVEC exposed to the leached medium collected at various time points from doxorubicin- or cisplatin-treated and non-treated poly(CD)-functionalized and non-functionalized HA. HUVEC cultivated for 24h with leached medium collected at various time points from the doxorubicin-treated non-functionalized HA granules showed significant decreases in cell viability in cells incubated in medium collected after 48h or 72h of leaching. A higher decrease in viability was observed when the cells were cultivated in leached medium from doxorubicin-treated poly(CD)-functionalized biomaterial. No significant increase of viability of HUVEC was detectable over time in medium collected after 72h of leaching since at this time point there was a reduction of cell survival of more than 70%.

The release of LDH from HUVEC that were treated with leached medium from the extraction assays is depicted in figure 36A/B. As a control, untreated cells were lysed

with a lysis buffer to gain a 100% release of LDH. In figure 36B the LDH release after 24h until 72h is compared. There was no significant change of LDH measurable when the cells were cultured in leached medium from cisplatin-treated and non-treated poly(CD)-functionalized and non-functionalized HA. HUVEC exhibited a higher release of LDH when cultivated in leached medium from doxorubicin-treated biomaterial. The detection of LDH was higher when the cells were cultured in medium of doxorubicin-treated, poly(CD)-functionalized HA. The treatment of HUVEC after 24h and 48h resulted in a significantly higher measurable concentration of LDH in the supernatant compared to those observed after 72h. This was also observed with non-functionalized HA.

The DNA content of HUVEC was also quantified by using crystal violet assay after each treatment. In figure 36C the amount of DNA after the cultivation of cells with leached medium from poly(CD)-modified and un-modified, cisplatin or doxorubicin-treated or untreated hydroxyapatite is shown. The images show the effects on cells after the different time points at which the medium was collected. Only the medium collected between 24h and 72h of doxorubicin-treated, non-functionalized HA granules exhibited a significant increase in DNA quantity. In general, the inhibition of HUVEC only occurred when the cells were cultivated in leached medium of doxorubicin-treated, poly(CD)-modified HA. The effect did not change over the time periods of leaching up to 72h. The DNA quantification assay showed a reduction of the DNA content when the cells were cultivated in medium collected at various time points from untreated hydroxyapatite, but the effect was not significant. The amount of DNA did not show any decrease when HUVEC were cultured in medium collected from untreated or cisplatin-treated functionalized or cisplatin-treated non-modified HA granules. On the contrary, there was a slight but not significant increase of DNA detectable after 48h of leaching.

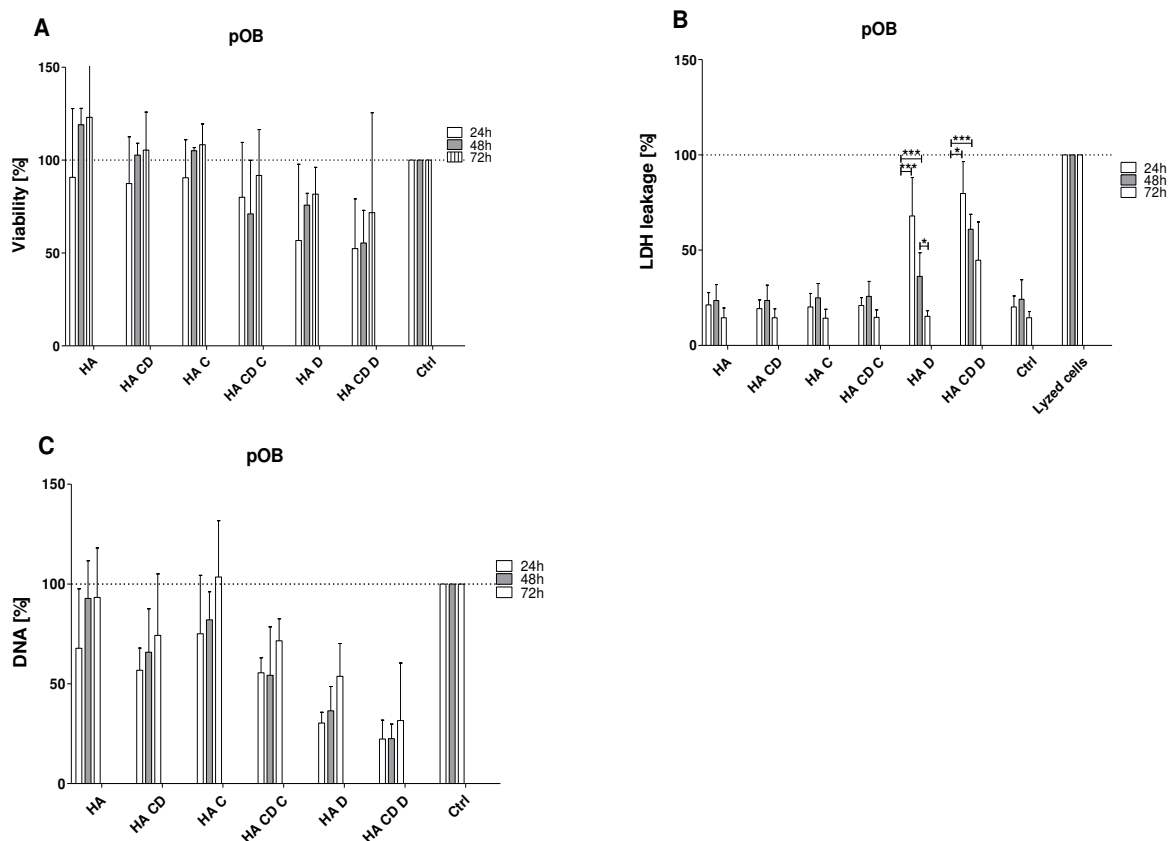


Figure 37: Effect of leached medium on pOB after 24h, 48h and 72h analyzed by MTS cell viability assay, LDH cytotoxicity assay and crystal violet DNA quantification

The cisplatin- or doxorubicin-treated and non-treated poly(CD)-functionalized and non-functionalized hydroxyapatite granules were incubated in endothelial cell medium for 24h, 48h and 72h. These media were added to primary osteoblasts and after 24h of incubation the viability of pOB was measured using the MTS assay. The viability of cells was compared for the three time points at which the leached medium was collected. Ctrl: cell culture medium.

(* $p < 0.05$; ** $p < 0.01$; *** $p < 0.001$) ($n = 3$).

The viability of human primary osteoblasts after the treatment with medium, obtained from the extraction assay, is depicted in figure 37. The mitochondrial activity was measured by using MTS cell viability test.

Figure 37A shows the comparison of viability of pOB after treatment with leached medium obtained from the extraction assay collected after 24h, 48h and 72h. There was no significant change in the effect on viability in samples collected after 24h up to 72h. The strongest inhibition of viability was measurable when pOB were cultivated in medium collected from doxorubicin-treated poly(CD)-modified HA. In figure 37B, the LDH concentration in supernatants of pOB after the treatment with leached medium from different collection time points is compared. There was no change in the concentration of LDH detectable when cells were cultivated in medium collected from untreated or cisplatin-treated poly(CD)-functionalized or non-functionalized biomaterial. In supernatants from pOB cultivated in leached medium from doxorubicin-treated,

Results

poly(CD)-modified or unmodified HA granules, there was a significant decrease of LDH over time. The content of DNA after the treatment of pOB with leached media at the various time points is observed in figure 37C. There was a decrease of DNA content detectable, when the cells were cultivated in leached medium from cisplatin- or doxorubicin-treated or untreated, modified or unmodified biomaterial that was collected after 24h. The DNA of pOB was strongly affected when medium from doxorubicin-treated biomaterial was used for cell culture. The amount of DNA increased slightly but not significantly with the treatment of pOB medium collected after 48h and 72h of leaching compared to medium that was collected after 24h.

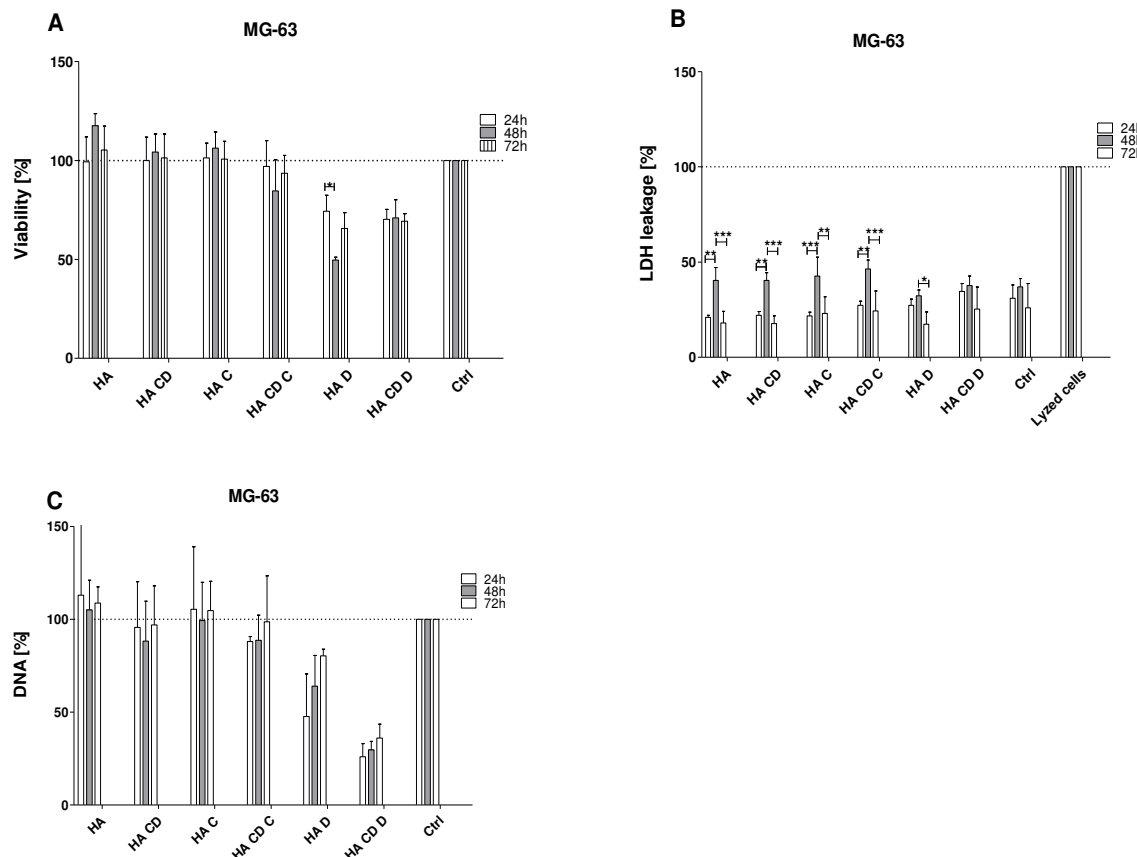


Figure 38: Effect of leached medium on MG-63 after 24h, 48h and 72h analyzed by MTS cell viability assay, LDH cytotoxicity assay and crystal violet DNA quantification

The cisplatin- or doxorubicin-treated and non-treated poly(CD)-functionalized and non-functionalized hydroxyapatite granules were incubated in endothelial cell medium for 24h, 48h and 72h. These media were added to MG-63 and after 24h of incubation the viability of MG-63 was measured using the MTS assay.

The viability of cells was compared for the three time points at which the leached medium was collected. Ctrl: cell culture medium. (* $p < 0.05$; ** $p < 0.01$; *** $p < 0.001$) ($n=3$).

Figure 38 shows the results obtained in the MTS, LDH and DNA assays with MG-63 exposed to media collected as described above at 24h, 48h and 72h. No significant differences in cell viability from 24h to 72h were observed for medium of untreated or cisplatin-treated poly(CD)-functionalized or non-functionalized leached medium. The viability of MG-63 decreased about 30% when cultured in extracts from doxorubicin-treated modified and unmodified hydroxyapatite. The concentration of LDH in supernatants from MG-63 after the culture in medium collected at different time points is compared. Media from untreated or cisplatin-treated modified or unmodified as well as medium from doxorubicin-treated HA granules, collected after 48h of leaching resulted in a significant increase of LDH in the supernatants of MG-63. Medium collected after 72h resulted in the same or a lower release of LDH into the cell supernatants compared to the untreated control. When the effect on MG-63 from various time points of medium collection was compared, no significant difference between 24h to 72h was detectable. Finally, in figure 38C it can be seen that the DNA content of cells decreased when the MG-63 was cultivated in washed-out medium of doxorubicin-treated, poly(CD)-modified and unmodified biomaterial. The inhibitory effect was most prevalent when the medium from functionalized granules was used. The quantity of DNA rose from the first day of medium collection to the third day of collection, indicating a decrease of cytotoxicity due to less doxorubicin over time.

Results

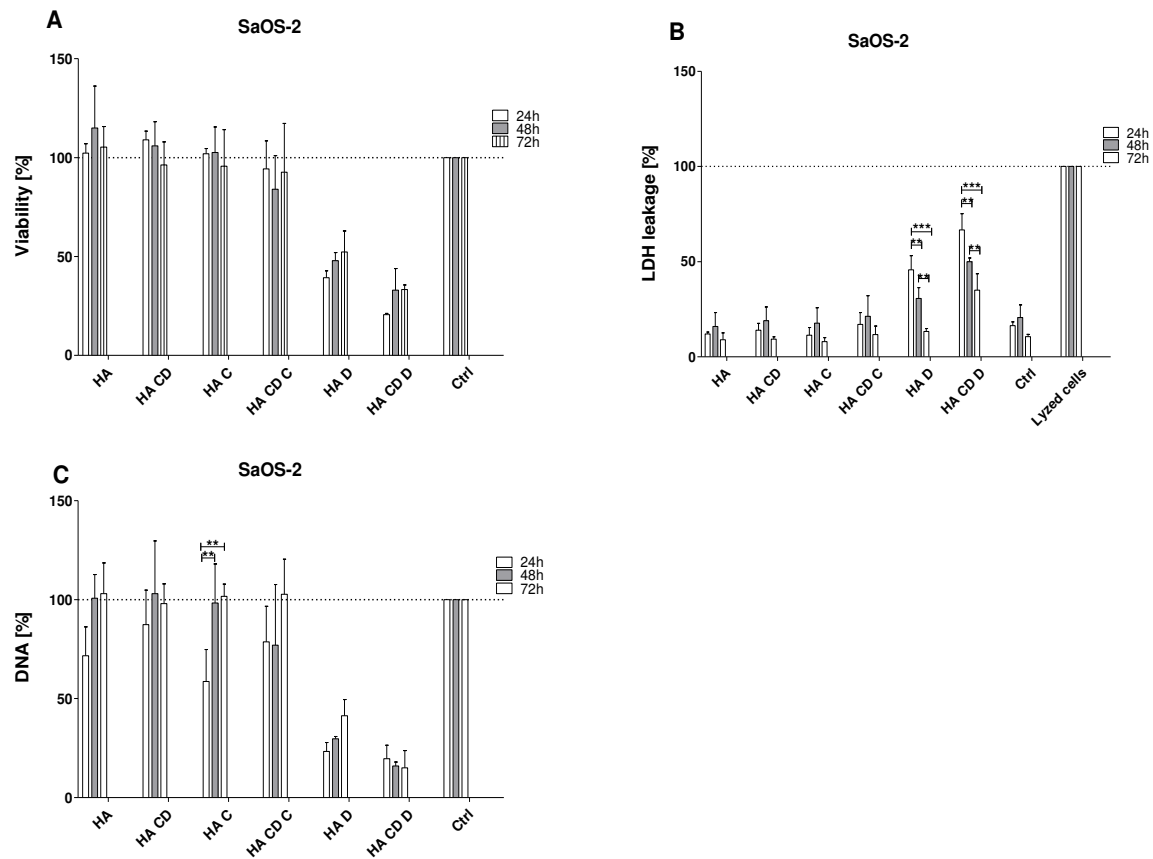


Figure 39: Effect of leached medium on SaOS-2 after 24h, 48h and 72h analyzed by MTS cell viability assay, LDH cytotoxicity assay and crystal violet DNA quantification

The cisplatin- or doxorubicin-treated and non-treated poly(CD)-functionalized and non-functionalized hydroxyapatite granules were incubated in endothelial cell medium for 24h, 48h and 72h. These media were added to SaOS-2 and after 24h for incubation the viability of SaOS-2 was measured using the MTS assay.

The viability of cells was compared of the three time points at which the leached medium was collected. Ctrl: cell culture medium.

(* $p < 0.05$; ** $p < 0.01$; *** $p < 0.001$) (n=3).

Figure 39A shows the comparison of viability of SaOS-2 after the treatment with leached medium from the extraction assay that was collected after 24h, 48h and 72h. Within each group there was no significant difference in terms of the effect on cell viability at any of the three time points. In figure 39B the concentration of LDH in supernatants of SaOS-2 after the treatment with leached medium of the extraction assay with different collection time points is compared. The use of media from untreated or cisplatin-treated modified or unmodified granules collected at the various time points resulted in no increase in LDH in the supernatants of SaOS-2. The use of leached medium from the doxorubicin-treated HA or poly(CD)-functionalized hydroxyapatite, resulted in an increase of LDH in the cell supernatants after 24h of cultivation. The LDH content decreased significantly when the cells were treated with leached medium collected at 48h or 72h. The quantity of LDH was higher in

supernatants of SaOS-2 cultivated in medium from doxorubicin-treated cyclodextrin-modified biomaterial. The influence of leached media on the DNA content is depicted in figure 39C. A significant difference was observed in between the time points in medium collected from cisplatin-treated unmodified HA with the SaOS-2 cells. The use medium that was collected after 24h resulted in a highly significant decrease of the DNA content in relation to the effect of media that were collected after 48h or 72h of leaching. Table 5 gives an overview of the cytotoxic effects of the media collected at the various time points on the various cell types.

Table 5: Effect of leached medium from extraction assay after 24/48/72h of medium collection

The table was generated based on the results of the MTS cell viability assay:

- + = less than 30% inhibition
- ++ = 30% - 50% inhibition
- +++ = more than 60% inhibition
- = no inhibitory effect

	Collection Time point	HA	HA CD	HA CIS	HA CD CIS	HA DOX	HA CD DOX
HUVEC	24h	-	-	-	-	+++	+++
	48h	-	-	-	-	++	+++
	72h	-	-	-	-	++	+++
pOB	24h	-	-	-	-	++	++
	48h	-	-	-	-	+	++
	72h	-	-	-	-	+	+
MG-63	24h	-	-	-	-	+	++
	48h	-	-	-	-	++	++
	72h	-	-	-	-	++	++
SaOS-2	24h	-	-	-	-	+++	+++
	48h	-	-	-	-	++	+++
	72h	-	-	-	-	++	+++

The data from the extraction assay show that the release of cisplatin or doxorubicin from the treated modified or poly(CD)-modified hydroxyapatite granules resulted in distinct cytotoxic effects on various cell types. The media recovered from the untreated or cisplatin-treated functionalized and non-functionalized biomaterials, exhibited no significant cytotoxic effect on cells. Leached medium from doxorubicin-treated hydroxyapatite resulted in a marked decline of cell viability of HUVEC and SaOS-2. The viability of pOB and MG-63 was also reduced but these cells appeared to be less sensitive compared to endothelial cells or the SaOS-2 cells.

3.3 Cell growth on the biomaterials

To investigate the cell growth on the surface of unmodified or poly(CD)-modified cisplatin-treated or untreated hydroxyapatite, the attachment of MG-63 and human endothelial cells was followed. The modified and unmodified hydroxyapatite remained untreated or was treated with cisplatin for 30min. After washing the granules thoroughly, they were dried for 4h before the MG-63 was seeded on the biomaterial. After 48h, the cells were stained with calcein AM and morphologically studied by using a confocal fluorescence microscope. The results of MG-63 cultivation after 48h on unmodified (A) and poly(CD)-modified (B) HA granules and cisplatin-treated non-functionalized biomaterial (C) and cisplatin-treated cyclodextrin-functionalized HA (D), are depicted in figure 40.

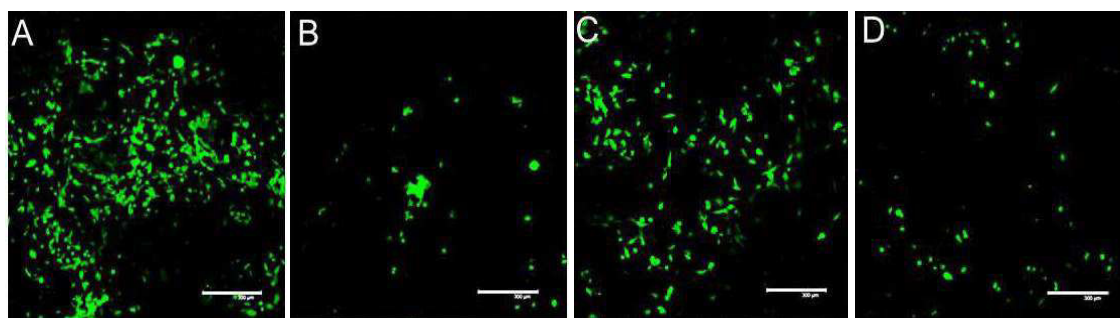


Figure 40: MG-63 on functionalized and non-functionalized hydroxyapatite

MG-63 osteosarcoma cells were seeded on non-functionalized hydroxyapatite granules (A) and on cyclodextrin-functionalized hydroxyapatite granules (B). In (C) and (D) MG-63 were seeded on cisplatin-treated biomaterial. After 48h of cultivation, the cells were stained with calcein AM. Scale bars 300µm.

MG-63 exhibited the best adhesion and cell growth, when cultivated on unmodified hydroxyapatite (A). There was less cell growth detectable when cisplatin-treated biomaterial was used (C). The adhesion and growth was reduced when MG-63 was seeded on untreated (B) or cisplatin-treated (D) poly(CD)-functionalized hydroxyapatite.

HUVEC were cultured on the same materials and analyzed after 48 h. The results from the analysis of adhesion and cell growth of human endothelial cells on unmodified (A) and poly(CD)-modified HA granules (B) as well as on cisplatin-treated virgin (C) and cisplatin-treated cyclodextrin-functionalized biomaterial (D) are depicted in figure 41.

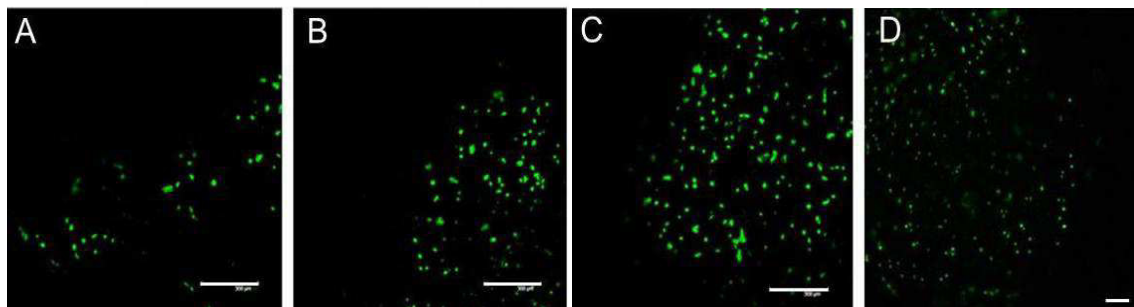


Figure 41: HUVEC on functionalized and non-functionalized hydroxyapatite

Human endothelial cells were seeded on non-functionalized hydroxyapatite granules (A) and on cyclodextrin-functionalized hydroxyapatite granules (B). In (C) and (D) HUVEC were seeded on cisplatin-treated biomaterial. After 48h of cultivation, the cells were stained with calcein AM. Scale bars A-C: 300µm; D: 200µm.

HUVEC adhered and grew poorly on both cisplatin-treated or untreated biomaterials. Little or no attachment or growth was observed for HUVEC on cisplatin-treated hydroxyapatite granules (D). Cells exhibited a spheroidal morphology and only a few cells were detectable by calcein AM staining. In C, HUVEC adhered to cisplatin-treated HA.

In summary, MG-63 exhibited a better adherence and cell growth on the untreated, unmodified HA compared to primary endothelial cells. Both cell types exhibited very poor adherence and proliferation on the biomaterials that were functionalized with poly(CD).

In order to evaluate the survival and angiogenic potential of endothelial cells on the biomaterials, a previously developed co-culture model of primary human osteoblasts and microvascular endothelial cells was used. When human endothelial cells (HDMEC) were co-cultivated with human primary osteoblasts on normal cell culture plastic the endothelial cells exhibited microvessel-like structure formation after 14 days (Figure 42).

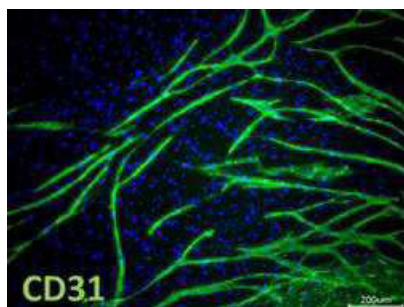


Figure 42: Co-cultivation of HDMEC together with pOB after 14d

HDMEC exhibited microvessel-like structures induced by pOB after 14 days of co-cultivation. To visualize the endothelial cells, the co-culture was stained using immunofluorescence for the specific endothelial cell marker CD31.

Results

Similar studies were carried out with unmodified and poly(CD)-modified hydroxyapatite granules. Both types of granules were added to a co-culture model and incubated for another 14 days and analyzed by immunofluorescence staining for CD31.

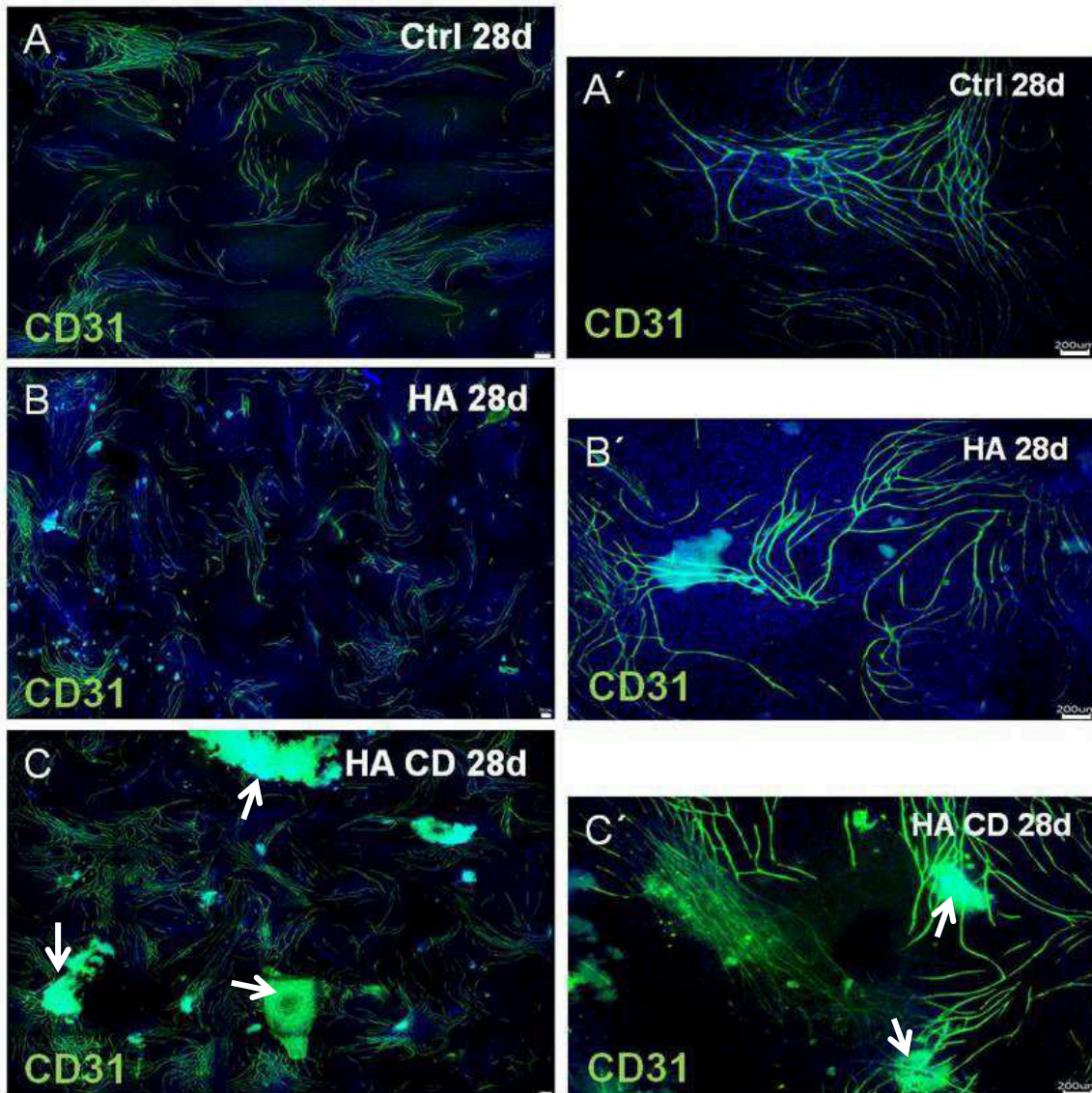


Figure 43: Microvessel-like structures formed by HDMEC, induced by human primary osteoblasts after 4 weeks of co-cultivation. A and A' show microvessel-like structures, formed by HDMEC in co-culture with pOB after 28 days of co-cultivation (control). HA(B/B') or poly(CD)-modified (C/C') hydroxyapatite granules were added to the co-culture after 14 days and the co-culture was cultivated for another 14 days. Scale bars 200 μ m.

As can be seen in figure 43A and A', the co-cultivation of HDMEC and pOB resulted in the development of microvessel-like structures formed by endothelial cells after 28 days. B and B' show angiogenic structures of the co-culture after 28 days of cultivation, when unmodified hydroxyapatite granules were added to the co-culture at day 14 and incubated for an additional 14 days. Similar microvessel-like structures were observed in the cells cultured with the granules C and C' compared to the control co-culture in A

or A'. In this case, at day 14 of the co-culture, poly(CD)-functionalized granules were added and incubated for an additional 14 days. In this case also, the microvessel-like structures remained during the incubation period with the poly(CD)-modified biomaterial. Thus, the cyclodextrin-treated material did not appear to have any negative effects compared to the biomaterial that was not treated with cyclodextrin on the angiogenic effects of the endothelial cells.

3.4 Effect of anoxia on anticancer drug-treated cells

Hypoxic conditions often predominate in tumor regions *in vivo*. Therefore, the cytotoxic effects of cisplatin and doxorubicin on human primary osteoblasts and endothelial cells isolated from healthy donors, as well as on human osteosarcoma cell lines were investigated under anoxic settings (lower than 1% O₂) *in vitro* using AnaeroGen COMPACT kit. An indicator was used to monitor anoxic settings.

To compare the effect of anticancer agents in normoxia or anoxia, HUVEC cells were treated with a range of cisplatin or doxorubicin concentrations and incubated in an atmosphere with no or normal (atmospheric) oxygen supply. After 24 hours the cells were analyzed for the effects on cell viability by MTS assay (Figure 44A/B) or crystal violet DNA quantification (C/D).

Results

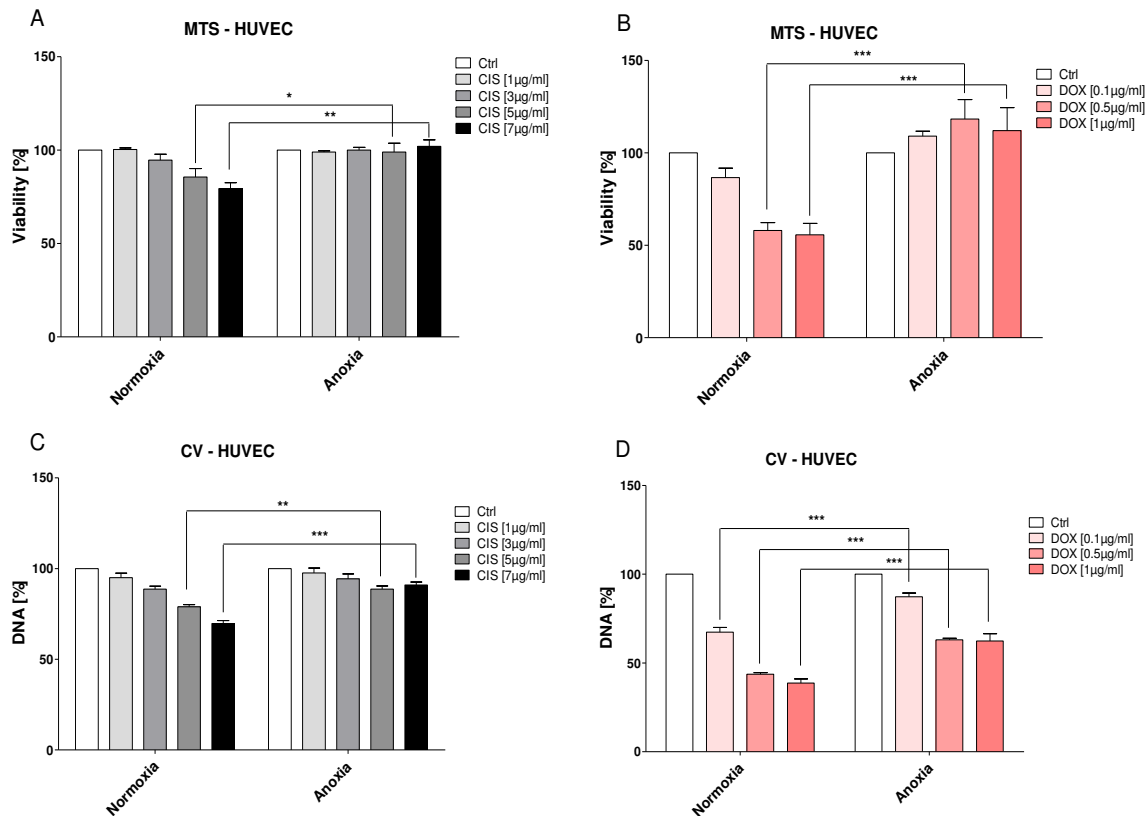


Figure 44: Cell viability of cisplatin- or doxorubicin-treated HUVEC in normoxia or anoxia after 24h
 A and B show the results of the MTS assay of HUVEC treated with cisplatin (A) or doxorubicin (B) in a normoxia as well as in anoxia. C and D depict the results from the DNA quantification of cisplatin- (C) or doxorubicin- (D) treated HUVEC under anoxic or normoxic conditions. (* $p < 0.05$; ** $p < 0.01$; *** $p < 0.001$) (n=3).

In figure 44A, the viability of cisplatin-treated HUVEC is shown under normoxic conditions as well as under anoxic conditions. In normoxia the cells exhibited a decrease in viability with increasing concentrations of cisplatin. Under anoxia conditions, HUVEC remained viable even with increasing drug concentrations. Figure 44B the effect of doxorubicin on HUVEC under normoxic or anoxic conditions is depicted. While cell viability declines constantly in normoxia with increasing doxorubicin concentrations, HUVEC under anoxic conditions exhibited a higher viability compared to the control. This protective effect observed during anoxia was also observed when analyzing the cells for DNA concentration (Figure 44C/D).

To determine if the cultivation of HUVEC under anoxic conditions resulted in a cell-protecting effect against the cytotoxicity of chemotherapeutic drugs observed under normoxia and to determine if this effect might be maintained when normoxic conditions were re-established, the anoxia- and drug-treated cells were incubated for an additional 24h period under normoxic conditions after anoxic conditions and then analyzed by MTS and for DNA content (Figure 45).

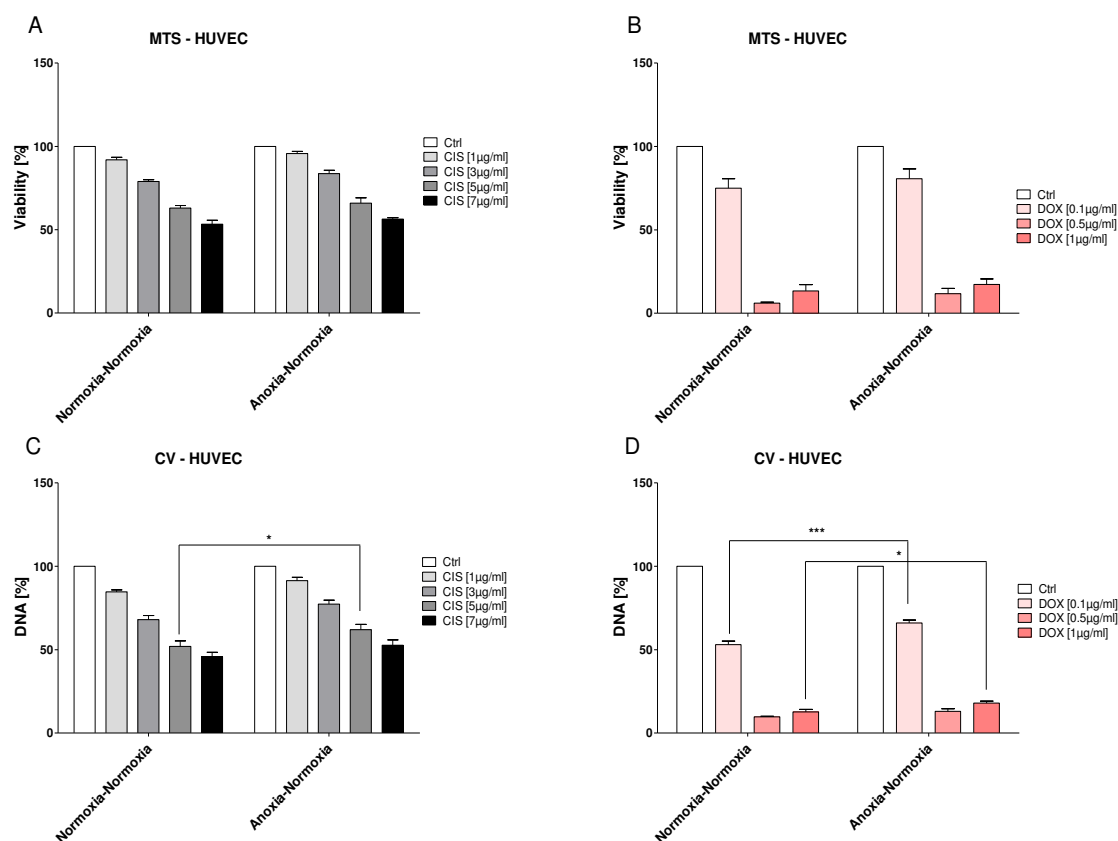


Figure 45: Cell viability of cisplatin- or doxorubicin-treated HUVEC in normoxia or anoxia after 48h
After 24 hours of cultivation in anoxia or normoxia, HUVEC were cultivated for additional 24h in normoxia. A and B show the results of the MTS assay of HUVEC treated with cisplatin (A) or doxorubicin (B). C and D depict the results from the DNA quantification of cisplatin- (C) or doxorubicin- (D) treated HUVEC. (* $p < 0.05$; *** $p < 0.001$) (n=3).

Cisplatin and doxorubicin treatment after 48h resulted in a higher inhibitory effect on HUVEC under normoxic conditions compared to the effect after 24h of treatment. When the conditions of cultivation of HUVEC were changed from anoxia to normoxia after 24h, the cell viability decreased with rising concentrations of cisplatin or doxorubicin, which was observed in the MTS cell viability assay (A/B) and was supported by the DNA quantification (C/D).

During hypoxia various physiological reactions are activated in cells, mostly mediated by the transcription factor hypoxia-inducible factor 1 (HIF-1). HIF-1 α is the subunit of the heterodimer that initiates the adaptive responses when hypoxia occurs such as

Results

angiogenesis or metabolic reprogramming, in addition to other factors. As an oxygen sensor in cells, the main target of HIF-1 α is the regulation of the oxygen requirement. To determine if HIF-1 α might be activated in HUVEC as a response to hypoxia when anticancer therapeutics were applied, the cells were cultivated under anoxic or normoxic conditions. In addition, cobalt chloride (CoCl₂) was added to induce HIF-1 α . Addition of CoCl₂ to cell culture media has been shown to mimic the effects observed by hypoxia. The induction of HIF-1 α in HUVEC was analyzed by western blot, as depicted in figure 46.

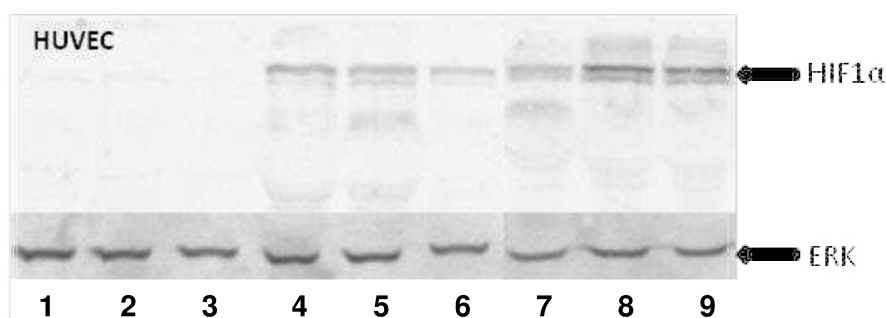


Figure 46: Results from western blot analysis for HIF-1 α protein after the treatment of HUVEC with anoxia, CoCl₂ and anticancer agents

HIF-1 α was induced when HUVEC were grown in an anoxic environment. No induction took place when cells were cultivated in normoxia.

1: Ctrl; 2: cisplatin [3 μ g/ml]; 3: doxorubicin [1 μ g/ml]; 4: Ctrl and CoCl₂; 5: cisplatin [3 μ g/ml] and CoCl₂; 6: doxorubicin [1 μ g/ml] and CoCl₂; 7: doxorubicin [1 μ g/ml] and anoxia; 8: cisplatin [3 μ g/ml] and anoxia; 9: Ctrl and anoxia.

Under normoxic conditions, no induction of HIF-1 α was detectable in HUVEC in the presence or absence of anticancer agents. When CoCl₂ was applied to the cells, HIF-1 α induction was detectable in cells. This induction was not influenced by the addition of chemotherapeutic agents. However, it appears that HIF-1 α induction decreased slightly when doxorubicin-treated HUVEC were analyzed. The same effect was detectable for cells that were cultivated with or without drug treatment under anoxia conditions.

For the analysis of the effects of anticancer agents on pOB during normoxia or anoxia, a range of cisplatin or doxorubicin concentrations were evaluated. The drug-treated cells were incubated for 24h under normoxic or anoxic conditions before they were analyzed for their effects on cell viability. In figure 47 the effect of cisplatin (A) and doxorubicin (B) on the cell viability of human primary osteoblasts under normoxic or anoxic conditions, by using MTS cell viability assay or crystal violet DNA quantification (C/D), is depicted.

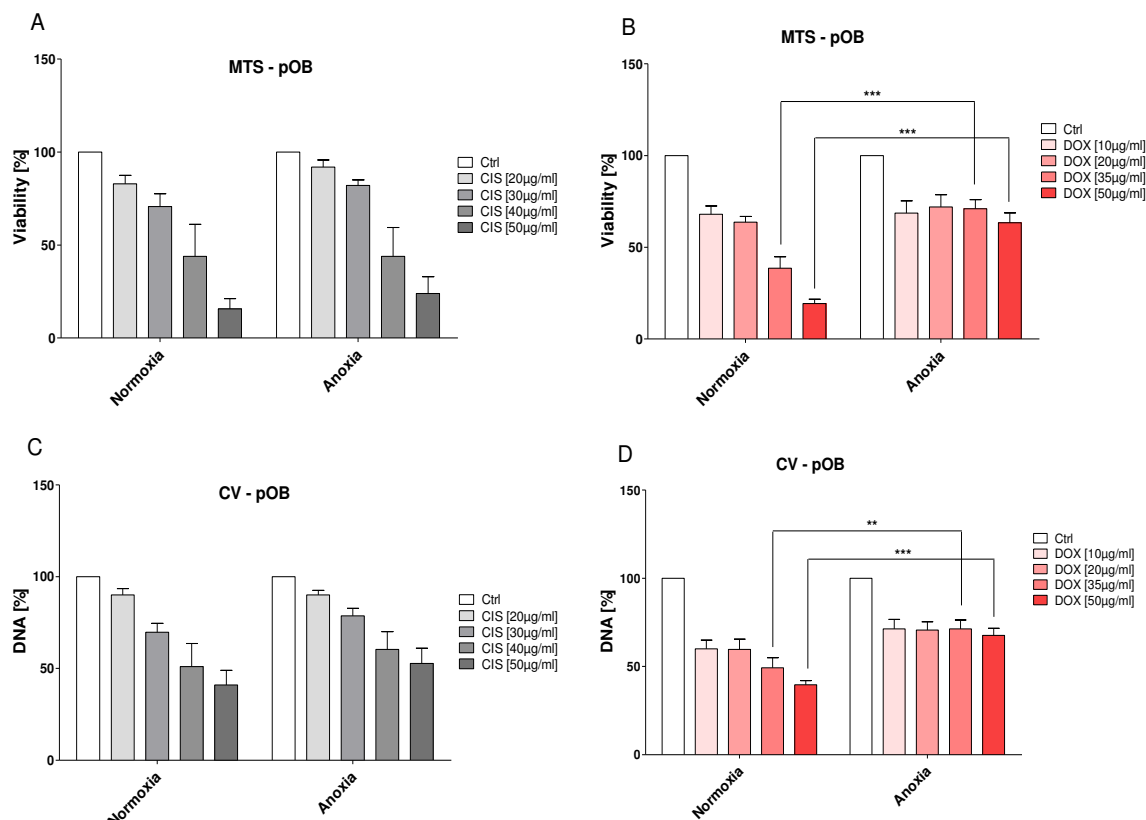


Figure 47: Cell viability of cisplatin- or doxorubicin-treated pOB in normoxia or anoxia after 24h
 A and B show the results of the MTS assay of pOB treated with cisplatin (A) or doxorubicin (B) in normoxia as well as in anoxia. C and D depict the results from the DNA quantification of cisplatin- (C) or doxorubicin- (D) treated pOB under anoxic or normoxic conditions. ** $p < 0.01$; *** $p < 0.001$) ($n = 3$).

Figure 47A shows the effect of cisplatin on pOB under normoxic and anoxic conditions. The inhibitory effect increased with increasing concentrations of cisplatin. The effect was detectable in normoxia as well as under anoxia conditions. The treatment of pOB with doxorubicin resulted in a decline of cell viability with increasing concentrations in a normoxic environment. The cultivation under anoxic conditions resulted in little to no effects on viability when pOB were treated with doxorubicin. Most notably, this protective effect was detectable when a concentration as high as 50µg/ml doxorubicin was applied. In figure 47C and D the results from the DNA quantification are depicted. The amount of DNA that was measured corresponds to the results from the MTS assay.

To determine if anoxic conditions were responsible for the protective effect to chemotherapeutic drugs compared to toxic effects under normoxic conditions, the cells cultured under anoxic conditions were switched to normoxic conditions after 24h. The viability of cells was then analyzed using the MTS assay and a DNA determination was made (Figure 48).

Results

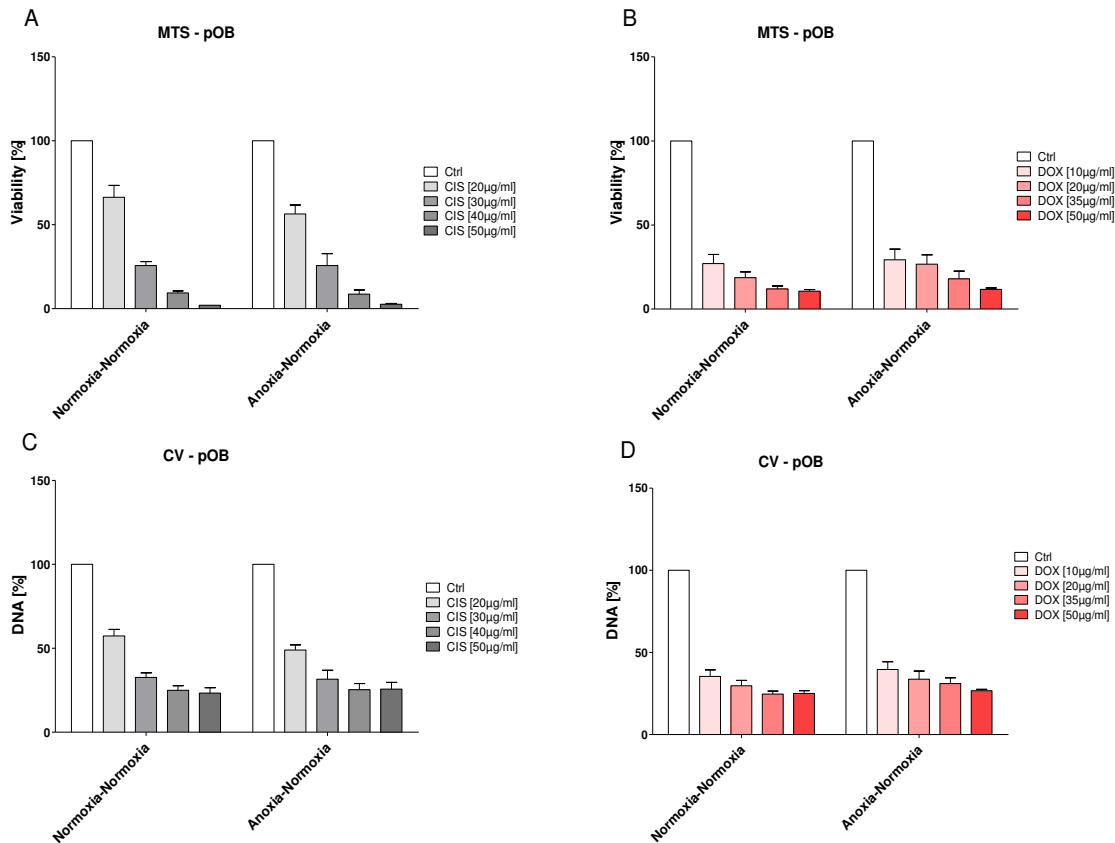
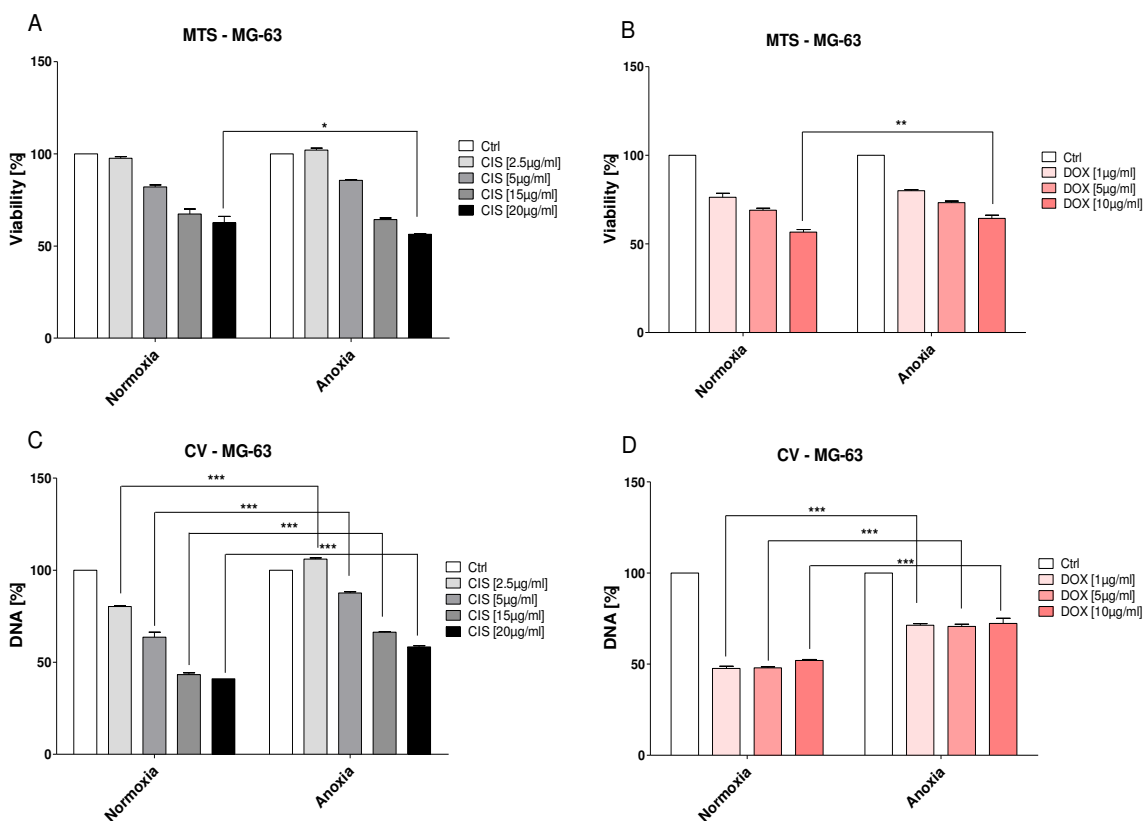


Figure 48: Cell viability of cisplatin- or doxorubicin-treated pOB in normoxia or anoxia after 48h

After 24 hours of cultivation in anoxia or normoxia, pOB were cultivated for additional 24h in normoxia. A and B show the results of the MTS assay of pOB treated with cisplatin (A) or doxorubicin (B). C and D depict the results from the DNA quantification of cisplatin- (C) or doxorubicin- (D) treated pOB. (n=3).

The inhibitory effect of cisplatin (Figure 48A) on cell growth increased after switching to normoxic conditions compared to 24h of treatment. Concerning the viability of pOB, there was no difference between the cultivation in normoxia and anoxia measurable. When cells, treated with doxorubicin, were changed from the anoxic environment to normoxic conditions, the protective effect disappeared. There were no marked differences in terms of cell viability between pOB cultured in normoxia for 48h or cells compared to those that were grown in an anoxic environment for the first 24h. The results were supported by the DNA quantification assay, depicted in figure 48, C and D, respectively.

Figure 49 shows the effect of cisplatin (A) and doxorubicin (B) on the cell viability of human osteosarcoma cell line MG-63 under normoxic or anoxic conditions, as evaluated by using MTS cell viability assay or crystal violet DNA quantification (C/D)



under similar conditions described for pOB above.

Figure 49: Cell viability of cisplatin- or doxorubicin-treated MG-63 in normoxia or anoxia after 24h

A and B show the results of the MTS assay of MG-63 treated with cisplatin (A) or doxorubicin (B) in normoxia as well as in anoxia. C and D depict the results from the DNA quantification of cisplatin- (C) or doxorubicin- (D) treated MG-63 under anoxic or normoxic conditions. (* $p < 0.05$; ** $p < 0.01$; *** $p < 0.001$) (n=3).

The viability of MG-63 decreased with increasing concentrations of cisplatin or doxorubicin (Figure 49A and B). There was a slight but not a marked difference in the viability detectable if the cells were treated with cisplatin. At low or medium concentrations of doxorubicin there was no significant difference detectable in viability of cells cultivated in normoxia or anoxia. In figure 49C and D, the DNA content was significantly increased when cisplatin- or doxorubicin-treated MG-63 were cultivated in anoxia. Based on the cell viability assay, there was no protective effect detectable for MG-63 when treated with low or medium anticancer agent concentrations.

To analyze if the cytotoxic effect of anticancer agents maintained over time changed during longer incubation periods, drug-treated MG-63 cultivated in normoxia and

Results

anoxia for 24h, were incubated for additional 24h under normoxic conditions and were then analyzed by MTS and for DNA content, as depicted in figure 50.

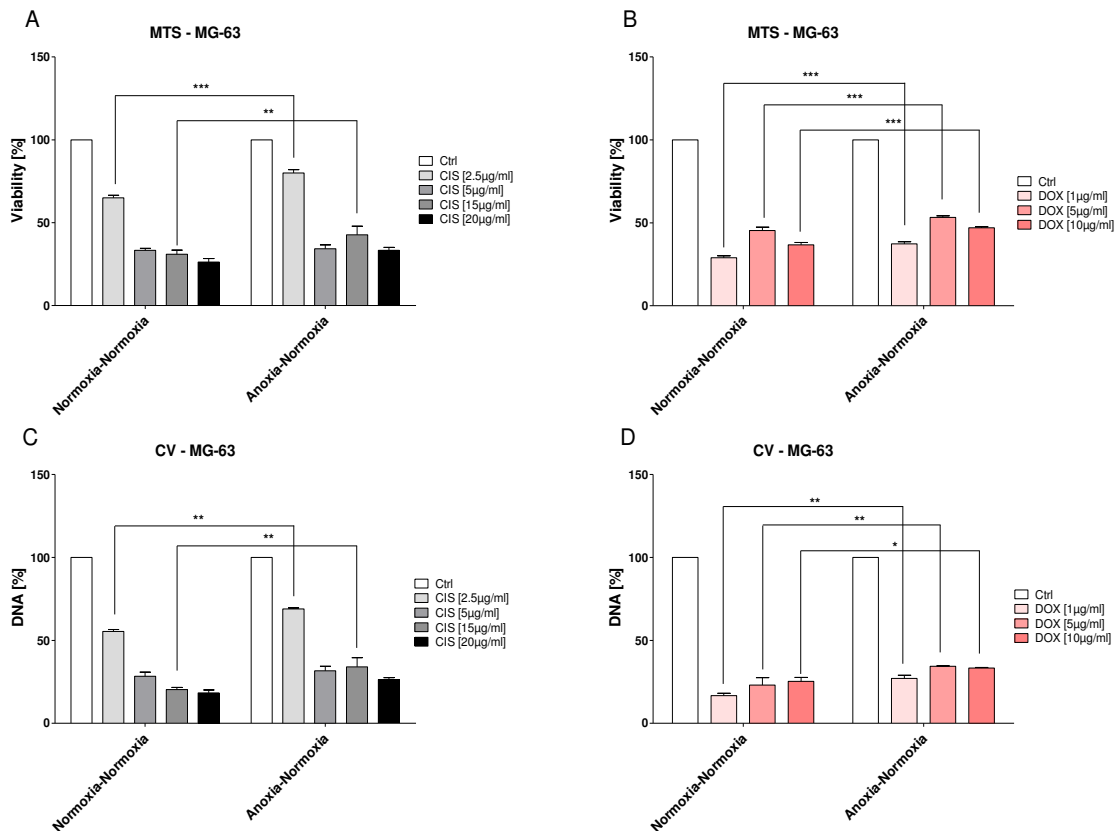


Figure 50: Cell viability of cisplatin- or doxorubicin-treated MG-63 in normoxia or anoxia after 48h

After 24 hours of cultivation in anoxia or normoxia, MG-63 were cultivated for additional 24h in normoxia. A and B show the results of the MTS assay of MG-63 treated with cisplatin (A) or doxorubicin (B). C and D depict the results from the DNA quantification of cisplatin- (C) or doxorubicin- (D) treated HUVEC. (*p<0.05; **p<0.01; ***p<0.001) (n=3).

Both the MTS assay and the DNA quantification showed that the inhibitory effect of both anticancer drugs was enhanced over time (A-D). After 48h the viability of the cancer cell line was considerably decreased, although drug-treated cells exhibited increased cell viability and DNA content when cultivated 24h in anoxia and additional 24h in normoxia.

In summary, the cultivation of HUVEC under anoxic conditions exhibited a protective effect against the cytotoxic agents cisplatin and doxorubicin, compared to the effects of cells grown under normoxic conditions. When MG-63 were grown in an anoxic environment, there was a slight protective effect detectable, which was much less marked compared to the anoxic effect on HUVEC. Human primary osteoblasts exhibited a decrease of cell viability and proliferation, when treated with cisplatin, independent of the oxygen concentration in the surrounding environment. The

treatment of pOB with doxorubicin under anoxic conditions resulted in an increase in viability in contrast to the cultivation in normoxia. In general, the cytotoxic effect of cisplatin and doxorubicin decreased after 48h of treatment, independent of the oxygen concentration that was provided during the first 24h of cultivation.

3.5 Analysis of the cell cycle in anticancer drug-treated cells

The primary target for chemotherapeutic agents like cisplatin and doxorubicin is DNA. Both agents bind to DNA and cause damage in cells. The most sensitive phase is during the S-phase of the cell cycle. In general, both anticancer agents affect highly proliferating cells. Among others, the tumor suppressor protein p53 is one of the crucial factors in preventing cancer due to its ability to affect genes that induce cell cycle arrest or apoptosis. The protein p21, a CDK inhibitor, is directly targeted by p53. p53 alone, or by the induction of p21, leads to DNA repair, the inhibition of the cell cycle or directs the affected cell into apoptosis. To study the cell cycle of human cancer cells and human primary cells from healthy donors, primary endothelial cells, primary osteoblasts and the osteosarcoma cell line MG-63 were analyzed in terms of p53 or p21 up regulation by using ELISA or quantitative real-time PCR in the presence and absence of cisplatin and doxorubicin.

As can be seen in figure 51, HUVEC treated with a range of cisplatin and doxorubicin concentrations for 24h exhibited an up regulation of the transcription factor p53 as determined by ELISA (Figure 51).

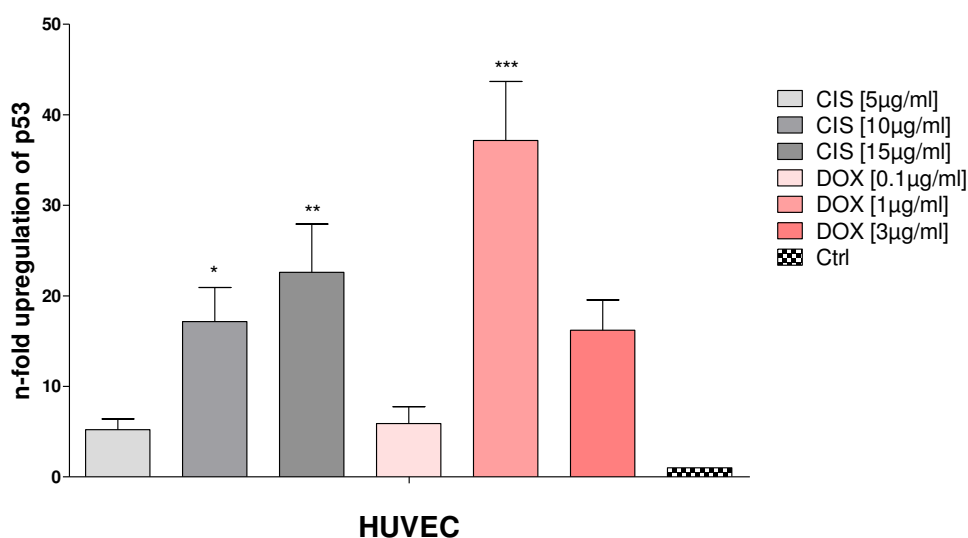


Figure 51: ELISA of cell cycle protein p53 in cisplatin- or doxorubicin-treated HUVEC after 24h
Treatment of HUVEC with various cisplatin or doxorubicin concentrations.
(*p<0.05; **p<0.01; ***p<0.001) (n=3)

Results

After 24h of treatment with cisplatin, there was a significant increase of p53, corresponding to increasing concentrations of the anticancer agent. Compared to the untreated control, the higher concentration of p53 was highly significant when HUVEC were treated with 1 μ g/ml doxorubicin. Due to the high toxicity, there was a slight but not significant up regulation of the transcription factor measurable, when higher concentrations of doxorubicin were applied.

Figure 52 shows the results from the determination of the gene expression of p53 in cells treated with cisplatin or doxorubicin as determined by quantitative real-time PCR.

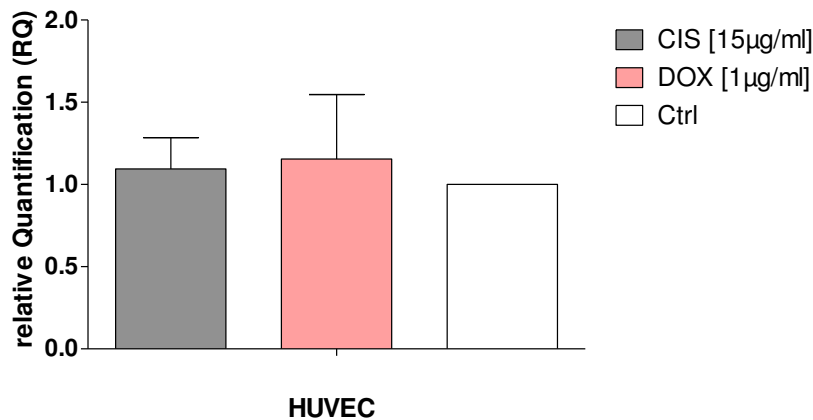


Figure 52: Quantitative real-time PCR of the cell cycle protein p53 after 24h in HUVEC

Analysis of the gene expression of the tumor suppressor protein p53 in HUVEC exposed to different concentrations of cisplatin and doxorubicin.

The drug concentrations selected were based on the results from the ELISA analysis (Figure 51), where the highest amounts of p53 were detectable. On the basis of gene expression for p53, there was no increase of the tumor suppressor over the 24h period studied, in comparison to the untreated control (Figure 52).

The regulation of p53 in human primary osteoblasts exposed to different concentrations of cisplatin or doxorubicin as determined by using ELISA, is depicted in figure 53.

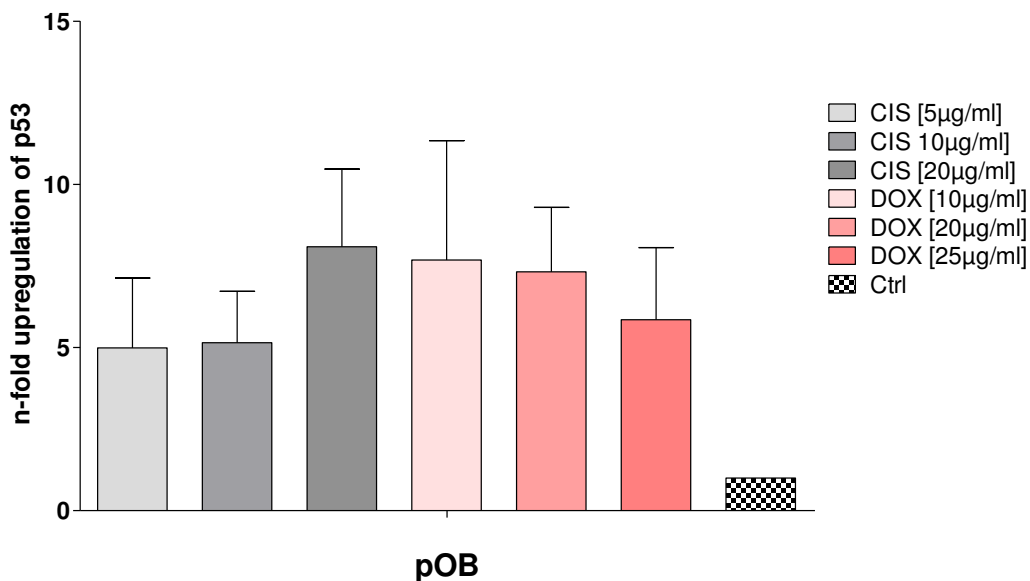


Figure 53: ELISA of cell cycle protein p53 in cisplatin- or doxorubicin-treated pOB after 24h
The treatment of pOB with various cisplatin or doxorubicin concentrations.

After 24h of treatment with cisplatin or doxorubicin, there was an increase of p53 measurable in the cells compared to the untreated control. The highest up-regulation of p53 could be observed, when 20µg/ml cisplatin or 10/20µg/ml doxorubicin were applied.

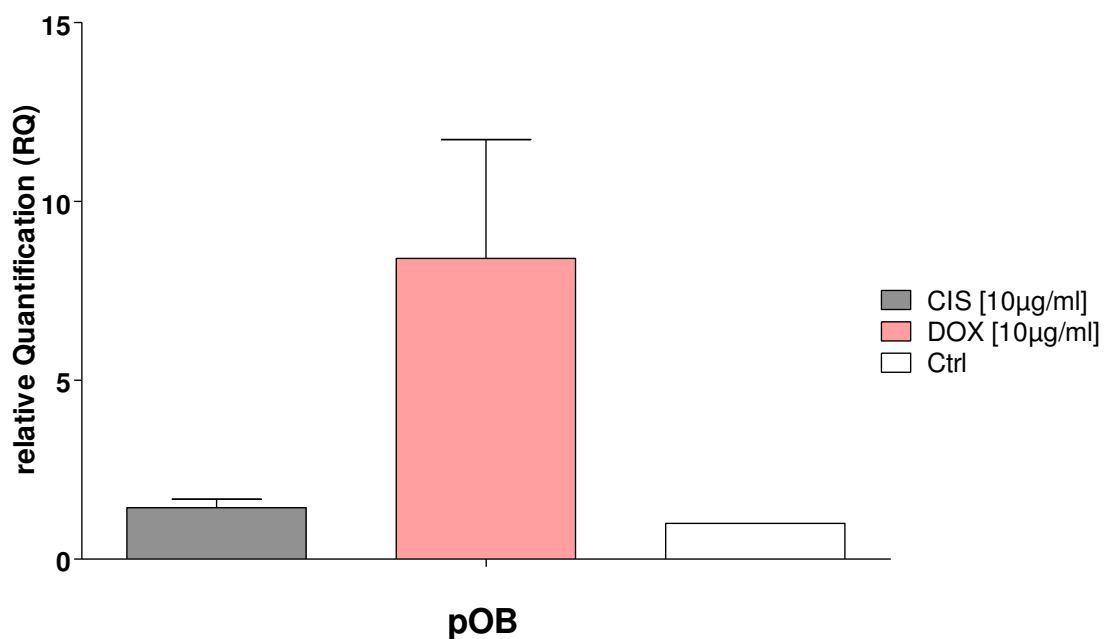


Figure 54: Quantitative real-time PCR of cell cycle protein p53 after 24h in pOB
The analysis of the gene expression of the tumor suppressor protein p53 in pOB exposed to cisplatin and doxorubicin for 24h.

Results

The treatment of human primary osteoblasts with 10 μ g/ml doxorubicin resulted in an up-regulation of the gene expression of p53. No increase of the tumor suppressor was detectable when the cells were treated with 10 μ g/ml cisplatin compared to the untreated control (Figure 54).

The analysis of the tumor suppressing protein p53 in MG-63 resulted in the absence of the transcription factor as no expression could be detected by using ELISA and quantitative real-time PCR.

A stabilization of p53 could result in an increase in p21-concentration. p21, also known as cyclin-dependent kinase (CDK) inhibitor 1, binds and inhibits the activity of CDK complexes. As a result, the transition of the cell from the G1-phase of the cell cycle to the S-phase is blocked and the cell arrests in the G0-phase in order to prevent genome mutation and give the cell time to repair damaged DNA. To determine if this was the case in HUVEC, cells were treated with various cisplatin or doxorubicin concentrations and incubated for 24h before they were analyzed for the expression of p21 by ELISA or quantitative real-time PCR.

Figure 55 shows the regulation of the cell cycle protein p21 after the treatment of primary endothelial cells with chemotherapeutic agents, analyzed by ELISA.

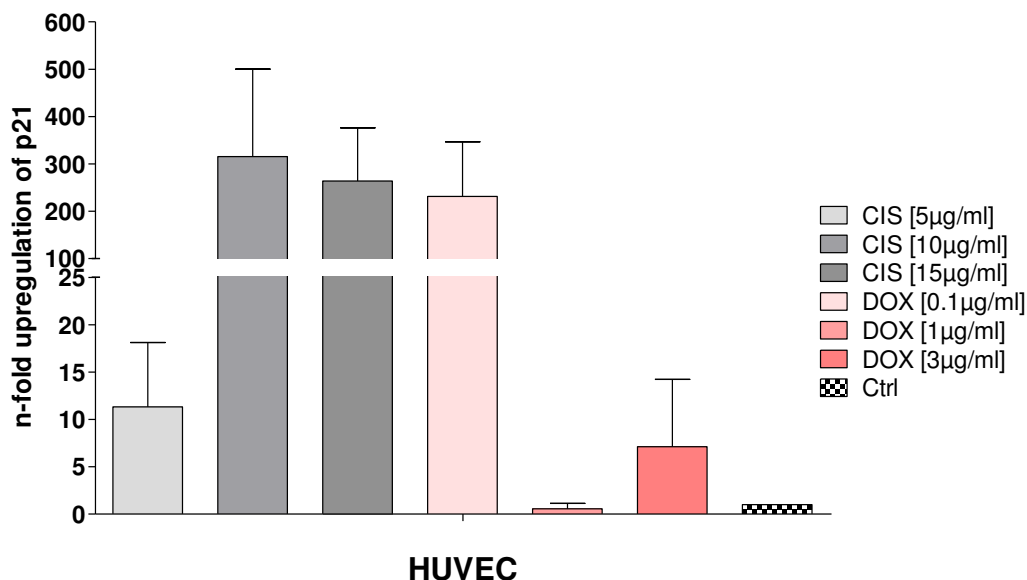


Figure 55: ELISA of cell cycle protein p21 in cisplatin- or doxorubicin-treated HUVEC after 24h
The analysis of p21 in HUVEC treated with various cisplatin or doxorubicin concentrations.

The application of cisplatin concentrations of 10-15 μ g/ml as well as 0.1 μ g/ml doxorubicin resulted in an increase of p21 compared to the untreated control after 24h.

Quantitative real-time PCR evaluated the gene expression of the p21 protein after the treatment with cisplatin or doxorubicin as depicted in figure 56.

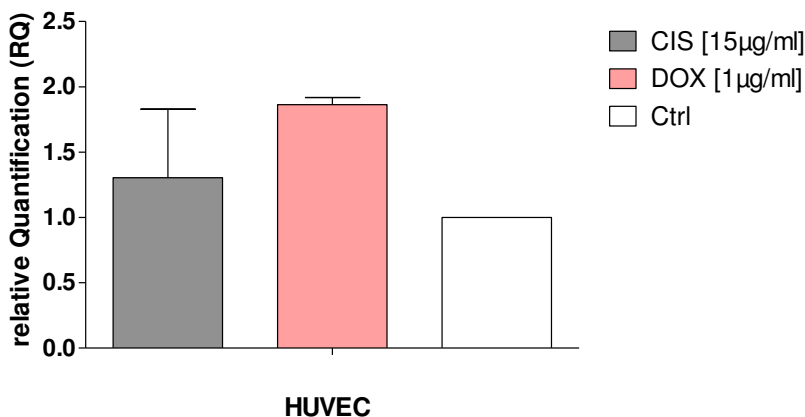


Figure 56: Quantitative real-time PCR of cell cycle protein p21

The analysis of the gene expression of the tumor suppressor protein p21 in HUVEC after treatment with cisplatin and doxorubicin.

Compared to the untreated control, there was no significant up regulation of the gene expression for p21 after the treatment of HUVEC with cisplatin or doxorubicin detectable.

The regulation of p21 was analyzed in cisplatin- and doxorubicin-treated MG-63. After 24h of the incubation of drugs, the cells were analyzed for the protein p21 by ELISA (Figure 57)

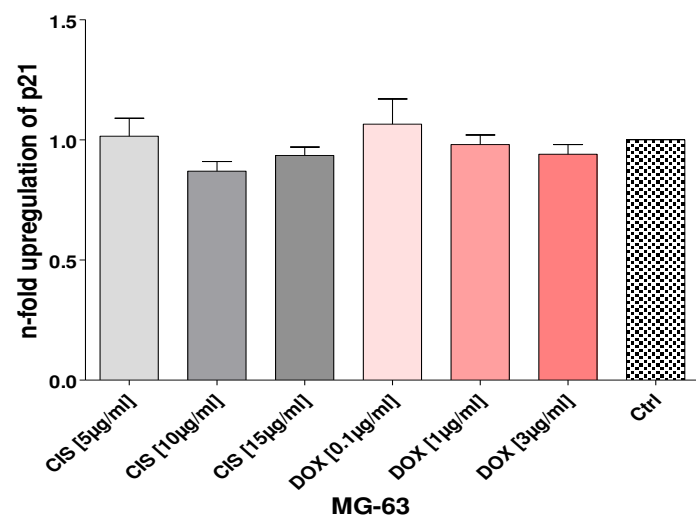


Figure 57: ELISA of cell cycle protein p21 in cisplatin- or doxorubicin-treated MG-63 after 24h.

The analysis of p21 in MG-63 treated with various cisplatin or doxorubicin concentrations.

The screening of MG-63 for the cell cycle protein p21 resulted in no changes in the regulation when treated with different anticancer drug concentrations compared to the untreated control as evaluated by ELISA. An up-regulation for p21 was observed in HUVEC after exposure to cisplatin or doxorubicin, however, no changes were observed in the osteosarcoma cell line MG-63. Surprisingly, no p21 was detected in pOB.

3.6 Analysis of cell cycle under hypoxic conditions

HIF-1 α was up-regulated in HUVEC under hypoxic conditions (Figure 46). To determine whether there was a link between the induction of HIF-1 α and the up-regulation of tumor suppressor genes during exposure to the anticancer agents, HUVEC were analyzed for p53 and p21 expression after the application of varying cisplatin and doxorubicin concentrations under anoxic conditions and under conditions inhibiting the transcription of HIF-1 α (Figure 58).

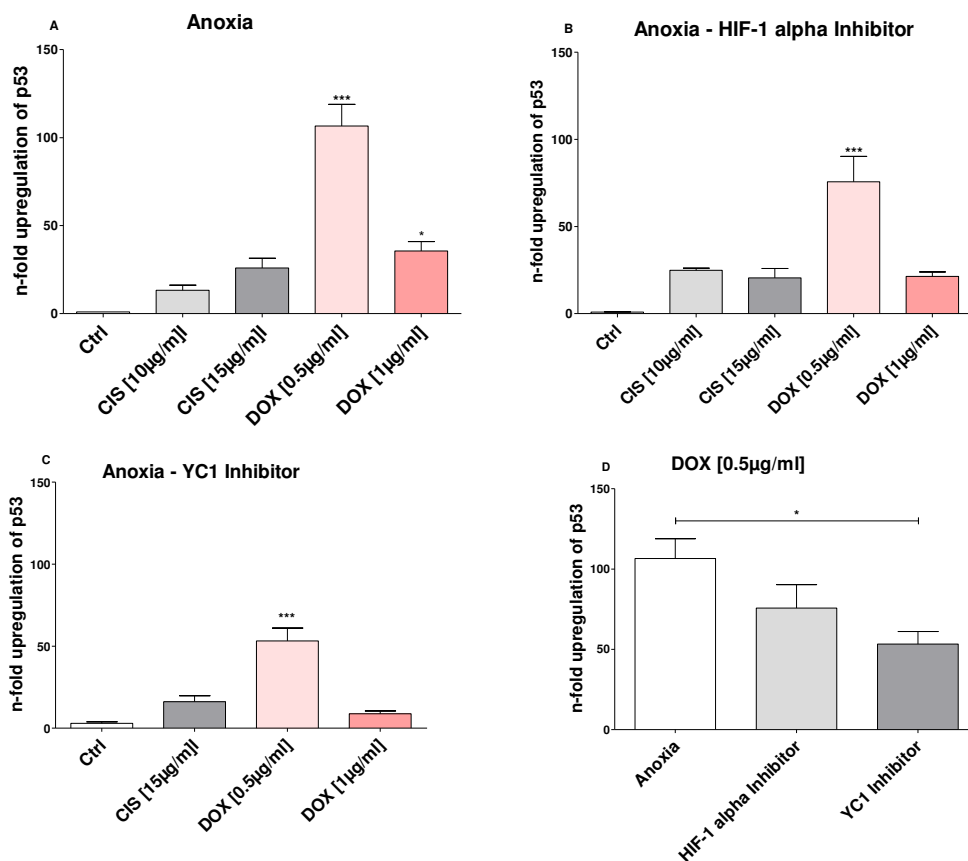


Figure 58: Regulation of p53 on protein level in cisplatin- or doxorubicin-treated HIF-1 α -inhibited HUVEC under anoxic conditions after 24h using ELISA

HUVEC were treated with various cisplatin or doxorubicin concentrations for 24h under anoxic conditions (A). In addition, the cells were also treated with inhibitors of the transcription factor HIF-1 α . In B HIF-1 α inhibitor was used and in C YC1 inhibitor was administered. D shows the effects on the p53 regulation when HIF-1 α inhibitors were used, compared to HIF-1 α -uninhibited doxorubicin (0.5 μ g/ml)-treated HUVEC. The results from B and C were compared to the untreated control in A. (*p<0.05; **p<0.01; ***p<0.001) (n=3)

Figure 58A shows the expression of p53 24h after treatment with different concentrations of cisplatin and doxorubicin under anoxic conditions. The treatment of endothelial cells with various anticancer agent concentrations resulted in an up-regulation of the transcription factor p53 compared to the untreated control. The application of 0.5µg/ml doxorubicin resulted in a highly significant, more than 100-fold, up-regulation of the tumor suppressor protein. In B, the induction of hypoxia-inducible factor 1 α (HIF-1 α) by the treatment with anoxia was inhibited by the application of 20µM HIF-1 α -inhibitor. The treatment with the same cisplatin or doxorubicin concentrations as used before, resulted in a highly significant up-regulation of p53, when 0.5µg/ml doxorubicin were applied to the cells. As depicted in figure 58C, 75µM YC1 inhibitor was used to inhibit the HIF-1 α expression. The treatment of HUVEC with cisplatin or doxorubicin resulted in an up-regulation of p53 compared to the untreated control. The cells exhibited a highly significant increase of p53 after the treatment with 0.5µg/ml doxorubicin for 24h. These results were observed when HUVEC were cultured with or without the application of HIF-1 α inhibitors in an anoxic atmosphere. Figure 58D shows the up-regulation of p53 when HUVEC were treated with 0.5µg/ml doxorubicin with and without the application of HIF-1 α inhibitors. The expression of p53 was markedly increased in an anoxic environment when the transcription factor HIF-1 α was not inhibited. The treatment with both inhibitors resulted in a lower amount of p53 in HUVEC compared to the uninhibited cells. After the treatment with the YC1 inhibitor the cells exhibited a significantly less up-regulation of p53 compared to uninhibited HUVEC.

Results

The regulation of p21 in anticancer drug-treated and HIF-1 α -inhibited HUVEC under anoxic conditions after 24h of incubation is depicted in figure 59.

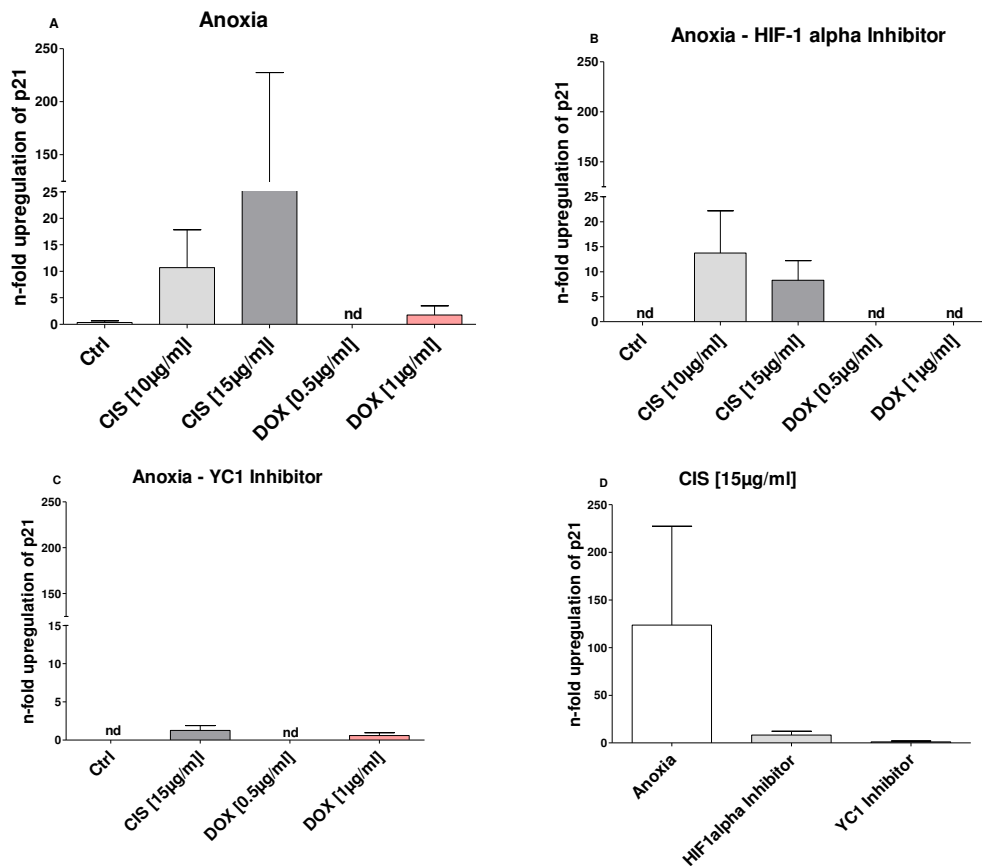


Figure 59: Regulation of p21 on protein level in cisplatin- or doxorubicin- treated HIF-1 α -inhibited HUVEC under anoxic conditions after 24h using ELISA

HUVEC were treated with various cisplatin or doxorubicin concentrations for 24h under anoxic conditions (A). In addition, the cells were also treated with inhibitors of the transcription factor HIF-1 α . In B HIF-1 α inhibitor was used and in C YC1 inhibitor was administered. D shows the effects on the p21 regulation when HIF-1 α inhibitors were used, compared to HIF-1 α -uninhibited doxorubicin (0.5 μ g/ml)-treated HUVEC. The results from B and C were compared to the untreated control in A. (* p <0.05; ** p <0.01; *** p <0.001) (n=3)

Figure 59A shows the up-regulation of p21 when 10 μ g/ml or 15 μ g/ml cisplatin were administered to the HIF-1 α uninhibited cells. In an anoxic environment, there was no p21 detectable when HUVEC were treated with 0.5 μ g/ml doxorubicin. Compared to the untreated control, there was a slight increase of p21 detectable, when 1 μ g/ml doxorubicin was applied to the cells. In B, HIF-1 α was down-regulated by the application of HIF-1 α inhibitor. p21 expression was only measurable when cisplatin was administered at concentrations of 10 μ g/ml or 15 μ g/ml. HUVEC that were not treated with anticancer agents or doxorubicin-treated cells did not exhibit the p21 protein. In figure 59C the YC1 inhibitor was used to down-regulate the expression of HIF-1 α . As a result, only a slight up-regulation of p21 was detectable when cells were

treated with 15µg/ml cisplatin or 1µg/ml doxorubicin. p21 was not detectable in HUVEC that were not treated with chemotherapeutic drugs or with 0.5µg/ml doxorubicin. Figure 59D depicts the different effects on p21 regulation when HIF-1α inhibitors were used, compared to HIF-1α-uninhibited cisplatin (15µg/ml) treated HUVEC. When HUVEC were treated with different anticancer agent concentrations under anoxic conditions, p21 was more than 100-fold up-regulated when 15µg/ml cisplatin were added to the cells. D shows that this effect disappeared when HIF-1α was inhibited.

The up-regulation of p53 under anoxic conditions in cisplatin-treated HUVEC is previously described. The application of 15µg/ml cisplatin resulted in a 25-fold increase of p53. When HIF-1α inhibitors were added to the cells, the up-regulation declined to 20.5-fold or 16.2-fold increase of the tumor suppressor. For the cell cycle arrest, p53 induces p21, which is depicted in figure 59. The administration of 0.5µg/ml doxorubicin resulted in a more than 100-fold up-regulation of p53 in anoxic conditions. When HUVEC were incubated with HIF-1α inhibitors, the regulation decreased to a 75-fold or 53-fold up-regulation. Regarding the regulation of p21, the protein was not detectable at all when 0.5µg/ml doxorubicin was administered. The samples were normalized to the total protein content.

3.7 Angiogenic activation of OEC in co-culture with pOB

Studies with autologous cells would be optimal in a therapeutic application in the field of bone tissue engineering focusing on the formation of new blood vessels. Outgrowth endothelial cells (OEC), isolated from human peripheral blood can serve as a potential cell source for the process of neovascularization in tissue engineering. The induction of OEC to form angiogenic structures in a co-cultivation setting with human primary osteoblasts, isolated from human bone, is well established (Fuchs et al. 2007). An acceleration of the formation of microvessel-like structures would improve the beneficial effect of the co-culture with regard to a clinical application. Therefore, mimicking the natural response of the human body might be a possibility to improve the co-culture system in terms of neovascularization. Under physiological conditions, angiogenesis is mainly induced by hypoxia and inflammation. During the inflammation process, monocytes are recruited at the site of action and differentiate into macrophages. Pro-inflammatory cytokines are then secreted. The interaction of macrophages with endothelial cells is mediated through adhesion molecules like E-selectin or ICAM-1. In addition, they secrete pro-angiogenic factors like VEGF, which finally leads to the formation of new blood vessels. In order to determine the effects of

Results

monocytes on the above described co-culture system, the human monocytic leukemia cell line THP-1 was differentiated into the macrophage phenotype and added to the co-culture. After 7 and 14 days of cultivation, the co- and triple-cultures were analyzed for angiogenic activation, pro-inflammatory signals, adhesion molecules and pro-angiogenic factors.

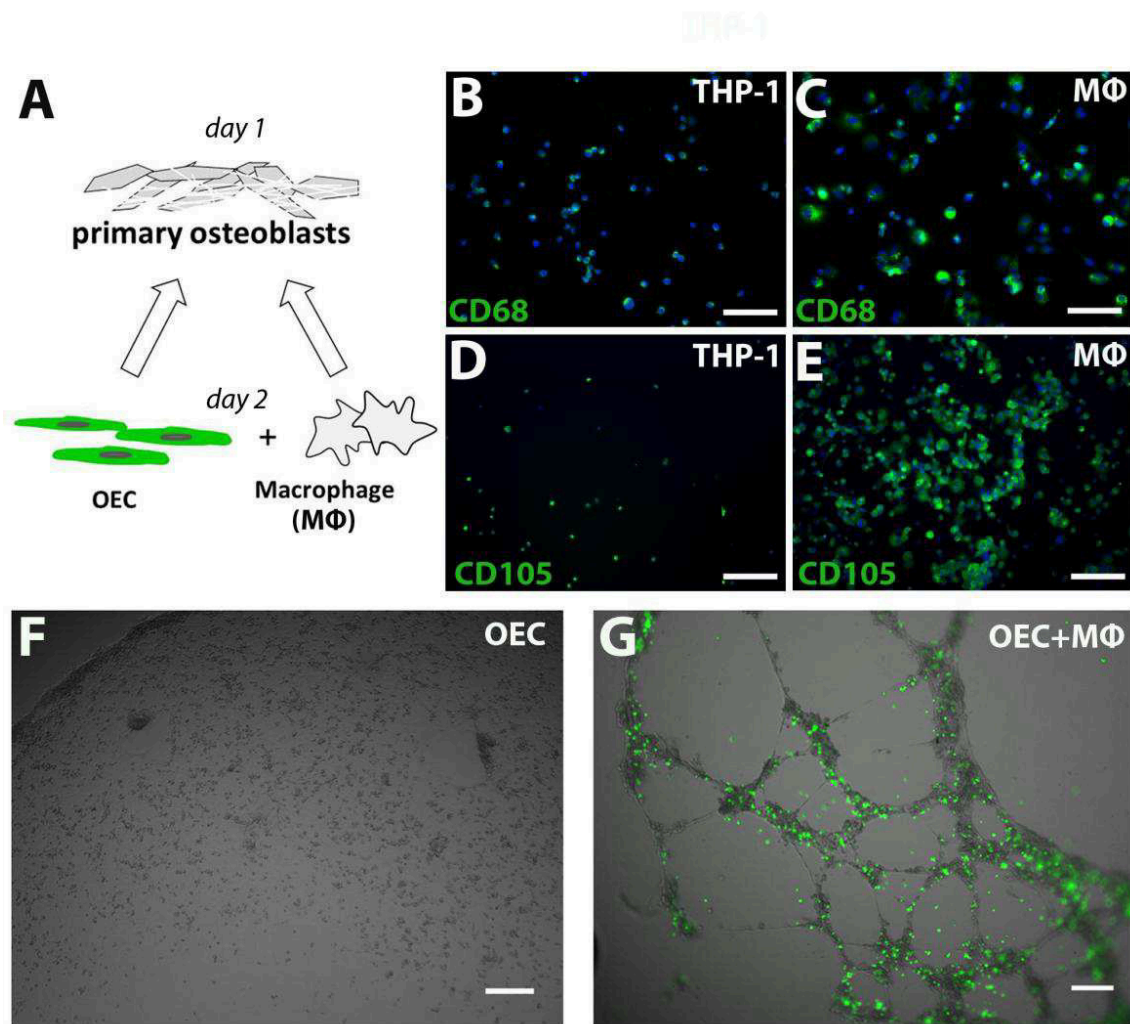


Figure 60: Culture conditions for triple-culture.

(A) Human primary osteoblasts were seeded on day one in a ratio of 300 000 cells per well of a 24-well plate. On day two, 200 000 OEC and 30 000 macrophage induced THP-1 (MΦ) were added. Co- and triple-cultures were cultivated for 7 and 14 days. (B/D) THP-1 monocytic cells stained negatively for the macrophage marker CD68 and CD105 (scale bar 100µm). When cells were treated with 8nm PMA for 4 days, they exhibited the typical macrophage phenotype and stained positively for CD68 and CD105 (C/E, scale bar 100µm). (F/G) OEC mono-culture (F) as well as OEC together with macrophage-induced THP-1 (G) (Calcein AM-labeled; green fluorescence) were seeded on Matrigel basement membrane matrix and cultivated for 14 hours (n=4). Scale bars 200µm.

The THP-1 cell line resembles primary monocytes in their morphology as well as in their differentiation capacity and marker profile (Figure 60B/C/D/E). Non-activated THP-1 cells stained negatively for the macrophage marker CD68 and CD105 (Figure 60B/D). When THP-1 cells were treated with PMA, they began to adhere and changed their monocytic phenotype to a macrophage phenotype, indicated by a positive staining for CD68 and CD105 (Figure 60C/E). It has been shown that co-cultivation of pOB and OEC leads to the formation of angiogenic structures by OEC in long term cultures and under different culture conditions dependent on growth factor treatment. This model system can be used as a tool to study important processes essential for bone repair, especially the inflammation-induced angiogenic activation. In a first step, the effects of macrophage-induced THP-1 on the angiogenic activation of OEC mono-cultures seeded on Matrigel® basement membrane matrix were analyzed (Figure 60F/G). This angiogenesis assay clearly demonstrates the arrangement of OEC into microvessel-like structures in response to the addition of THP-1 which accumulate at the sites of angiogenic structures formed by OEC (Figure 60G).

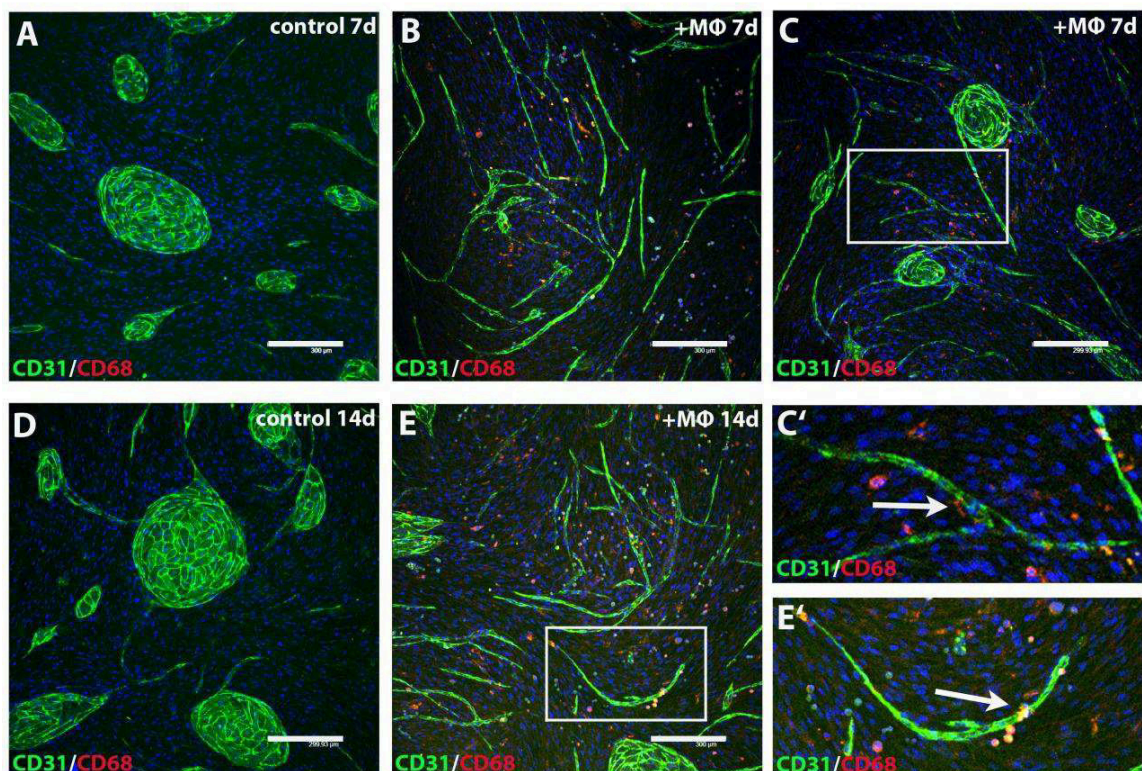


Figure 61: Immunofluorescence staining of co- and triple-cultures.

Co-cultures consisting of pOB and OEC as well as triple-cultures of pOB, OEC and macrophage-induced THP-1 (MΦ) were cultivated for 7d (A/B/C) and 14 days (D/E) and stained for the endothelial marker CD31 (green) and for the macrophage marker CD68 (red). The formation of angiogenic structures can be detected in 7d triple-cultures (B/C) as well as after 14d of triple-cultivation (E) as seen by positive staining of microvessel-like structures for CD31 compared to co-cultures of pOB and OEC alone (A/D) (n=7). Higher magnification shows aggregation of macrophage-induced THP-1 in areas of vessel-like structures formed by OEC (arrows C'/E'). Scale bars 150μm.

Results

Based on these results, macrophage-induced THP-1 ($M\phi$) were added to the co-cultures of pOB and OEC, were triple-cultured for 7 and 14 days and analyzed for the angiogenic activation of OEC in the triple-culture. Interestingly, treatment of co-cultures consisting of pOB and OEC with macrophage-induced THP-1 ($M\phi$) results in an increase of the formation of microvessel-like structures after both time periods of triple-cultivation as indicated by immunofluorescence staining for the endothelial marker CD31 (Figure 61B/C/E, $n=7$). Furthermore, CD68-positive cells representing macrophage-induced THP-1 can be detected in microvessel-surrounding areas (Figure 61C'/E', arrows). In contrast, untreated control co-cultures (Figure 61A/D) stained for CD31 exhibit a lower amount of angiogenic structures after 7 and 14 days of co-cultivation, indicating a delayed onset of angiogenic activation in the absence of macrophages.

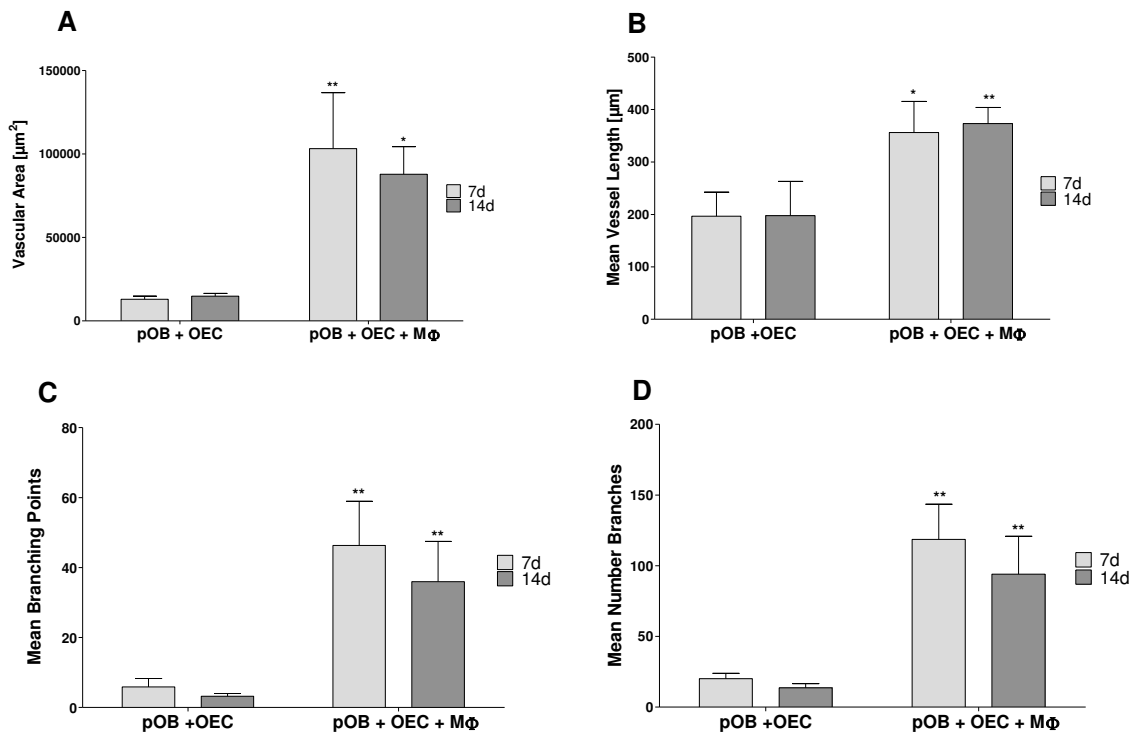


Figure 62: Angiogenic structures were quantified by comparing vascular area (A), the mean of vessel length (B), the mean of branching points (C) as well as the mean number of branches (D) of macrophage-treated cultures and co-cultures after 7 and 14 days of THP-1 exposure ($M\phi$). ($n=3$). Statistical significance was established (* $p < 0.05$ and ** $p < 0.03$).

Quantification of the vascular area, as well as the mean of branch points, vessel length and branches in co- and triple-cultures for both treatment time points are shown in figure 62A-D. In general, a significantly higher amount of microvessel-like structures can be observed in triple-cultures of pOB, OEC and M ϕ compared to the double co-cultures, i.e. without M ϕ .

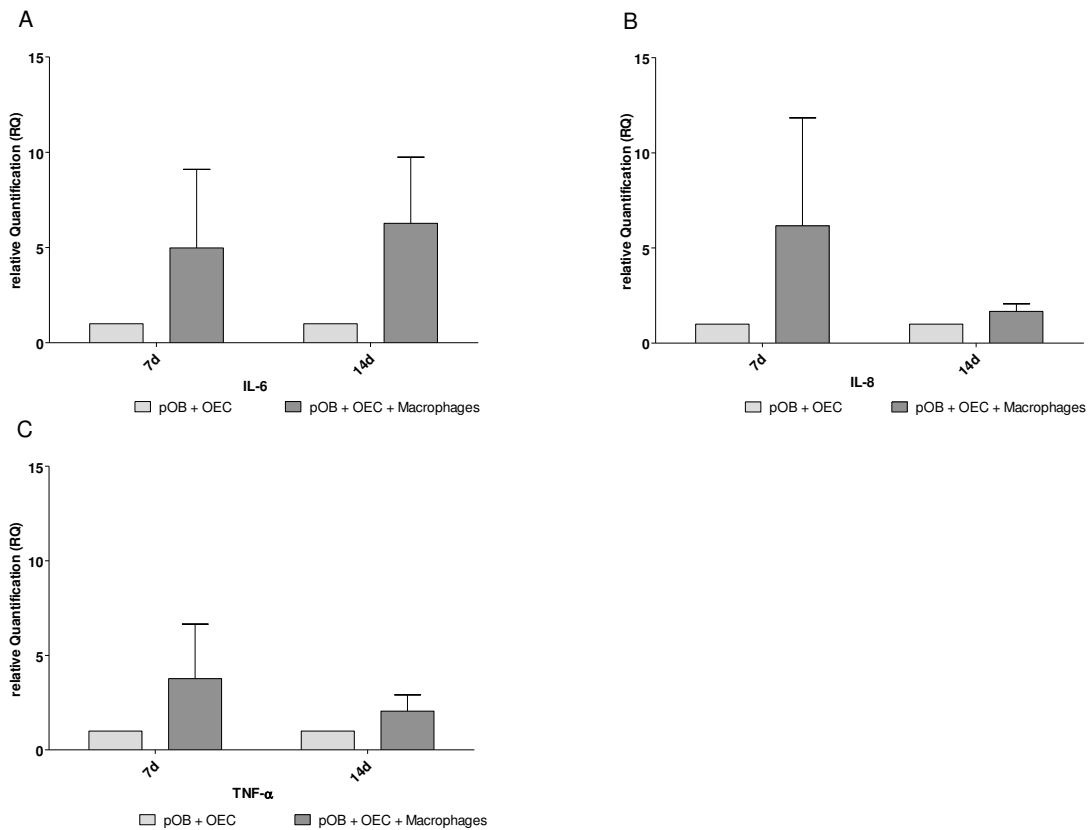


Figure 63: Proinflammatory effect of macrophage treatment on the co-culture consisting of pOB and OEC.

Inflammatory cytokines Interleukin-6 (A), Interleukin-8 (B) and TNF- α (C) are upregulated in the co-culture system in response to treatment with macrophage-induced THP-1 (M ϕ) after 7d as well as after 14d of triple-culturing evaluated using quantitative real time PCR analysis (A/B/C). (n=3)

In order to analyze if treatment of co-cultures of pOB and OEC with THP-1 (M ϕ) results in an inflammatory-like response that could lead to the angiogenic activation of OEC in the co-culture system, the expression of different proinflammatory cytokines like interleukin 6 (IL-6), interleukin 8 (IL-8) and tumor necrosis factor alpha (TNF- α) was evaluated at the mRNA level using quantitative real-time RT-PCR (Figure 63A-C; n=4). IL-6 and TNF- α are the major proinflammatory cytokines that are responsible for the early inflammatory response, whereas IL-8 is also essentially involved in acute inflammation, where it induces trafficking of neutrophils along the vessel wall. In response to treatment of co-cultures with macrophage-induced THP-1 (M ϕ), the expression of IL-6, IL-8 and TNF- α was up-regulated after

7 days as well as after 14 days of triple-cultivation.

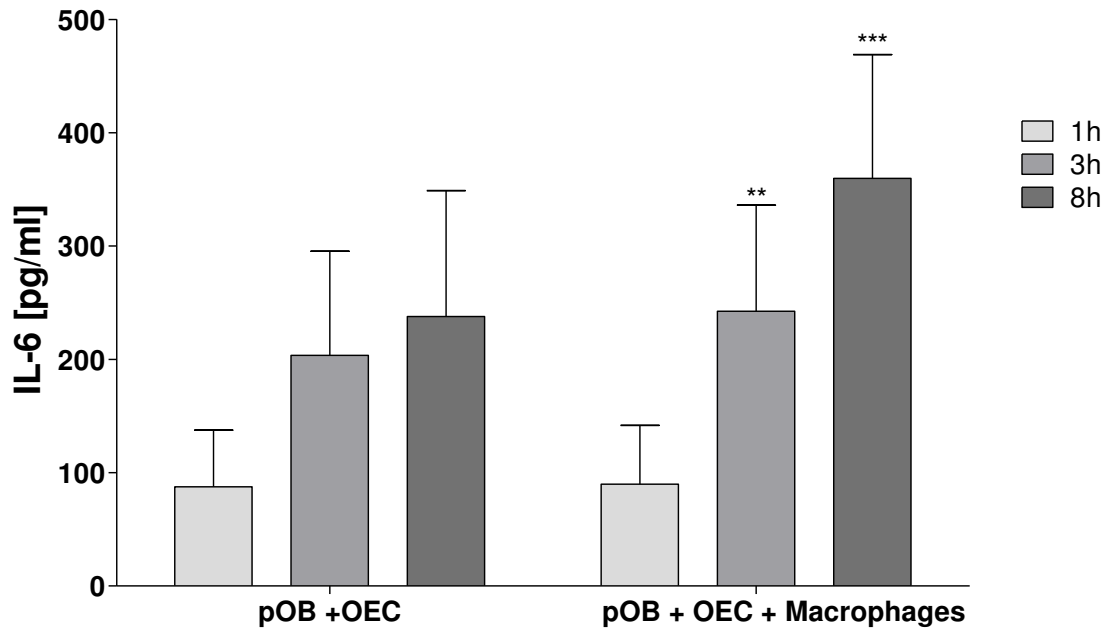


Figure 64: IL-6 ELISA

The results from the ELISA exhibited the significant up-regulation of IL-6 when pOB and OEC were cultivated together with THP-1-derived macrophages (MΦ) after 3h. The increase of IL-6 was highly significant in triple-cultures after 8h of cultivation. (**p<0.03; ***p<0.01) (n=3).

Furthermore, the pro-inflammatory cytokine IL-6 was analyzed by ELISA, after 1 hour, 3 hours and 8 hours of cultivation (Figure 64). Compared to the co-culture, the triple-culture with THP-1-derived macrophages exhibited a marked increase of IL-6 after 3h and 8h of cultivation. Statistical significance was established for IL-6 expression after 3h and 8h of cultivation together with macrophages compared to the expression of IL-6 in the double co-culture.

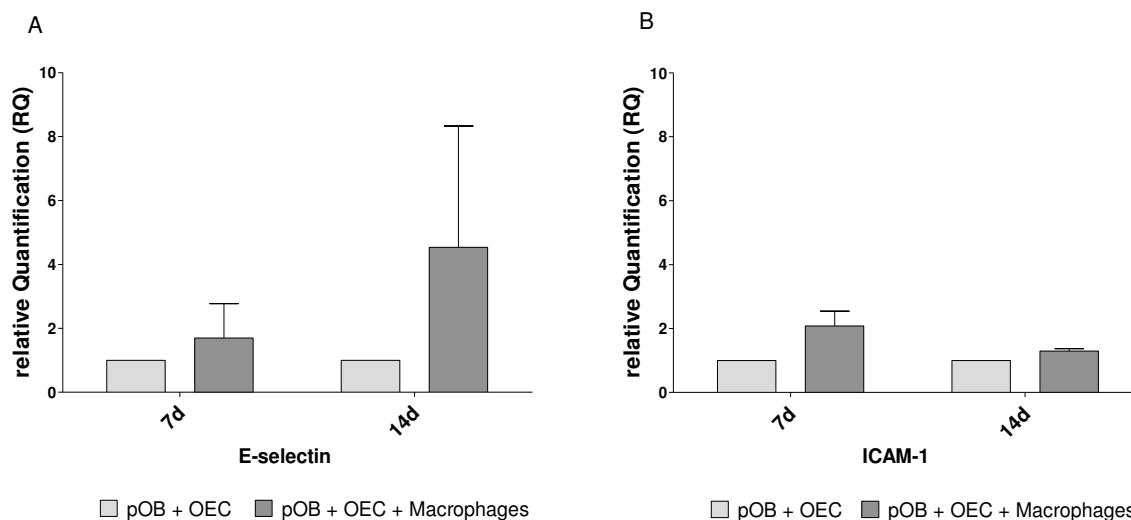


Figure 65: Effect of macrophage-induced THP-1 on the expression of the adhesion molecules E-selectin (A) and ICAM-1 (B), involved in inflammation.

Treatment of co-cultures with M Φ leads to an increase in the expression of ICAM-1 and E-selectin on the mRNA level evaluated using quantitative real time RT-PCR compared to the co-culture consisting of pOB and OEC (A/B). (n=3)

The expression of different adhesion molecules that are strongly involved in the interaction of endothelial cells and leucocytes, in particular macrophages, during the process of inflammation was also assessed at the mRNA level using quantitative real time PCR (Figure 65A/B, n=4). During inflammation, the adhesion of macrophages to endothelial cells starts with leucocyte rolling, which is mainly mediated through E-selectin, followed by more stable adhesion mediated through ICAM-1. The expression of E-selectin (Figure 65A) and ICAM-1 (Figure 65B) is up-regulated when co-cultures were treated with macrophage-induced THP-1 (M Φ) compared to the double co-cultures alone, documenting an ongoing proinflammatory stimulus in the triple-culture consisting of pOB, OEC and M Φ .

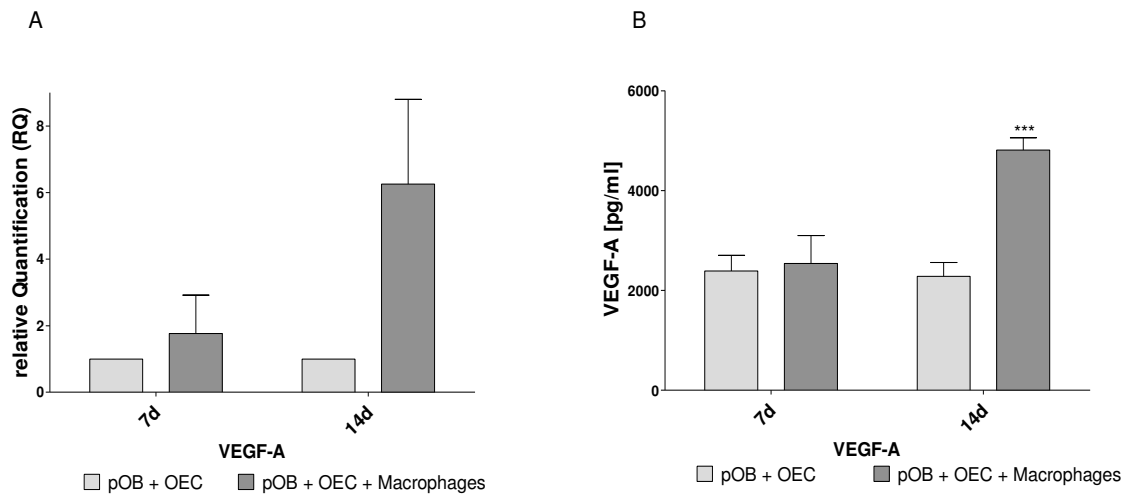


Figure 66: Effect of macrophage-induced THP-1 on the expression of the pro-angiogenic growth factor VEGF at the mRNA (A) as well as at the protein level (B). In response to M Φ exposure, the expression of VEGF mRNA increased after 7d as well as after 14d in triple-culture. Protein concentration of VEGF in supernatants of M Φ -treated cultures was statistically significantly increased after 14d of treatment, as evaluated by enzyme-linked immunosorbent assay (ELISA) (B, *** $p < 0.01$). (n=3).

Following the process of acute inflammation, vascular endothelial growth factor (VEGF), a well-known pro-angiogenic factor, is secreted by macrophages and fibroblastic cells, which leads to higher vessel permeability, endothelial migration and new blood vessel formation. The expression of VEGF was analyzed in triple-cultures of pOB, OEC and macrophage-induced THP-1 (M ϕ) at the mRNA level using quantitative real time PCR (qRT-PCR) (Figure 66A) as well as at the protein level evaluated using ELISA (Figure 66B) and was compared to the untreated co-cultures (Figure 66; n=6). The relative expression of VEGF at the mRNA level is up-regulated after 7 and 14 days of triple-cultivation compared to the control cultures, being especially marked after 14 days of cultivation. The higher expression of VEGF mRNA in response to THP-1 treatment in co-cultures was confirmed at the protein level as well. A significantly higher concentration of VEGF in cell culture supernatants of triple-cultures after 14 days of cultivation was observed using ELISA (Figure 66B; *** $p < 0.01$). After 7 days of triple-culture, no differences in the concentration of VEGF in cell culture supernatants were found compared to the co-culture alone (Figure 66B).

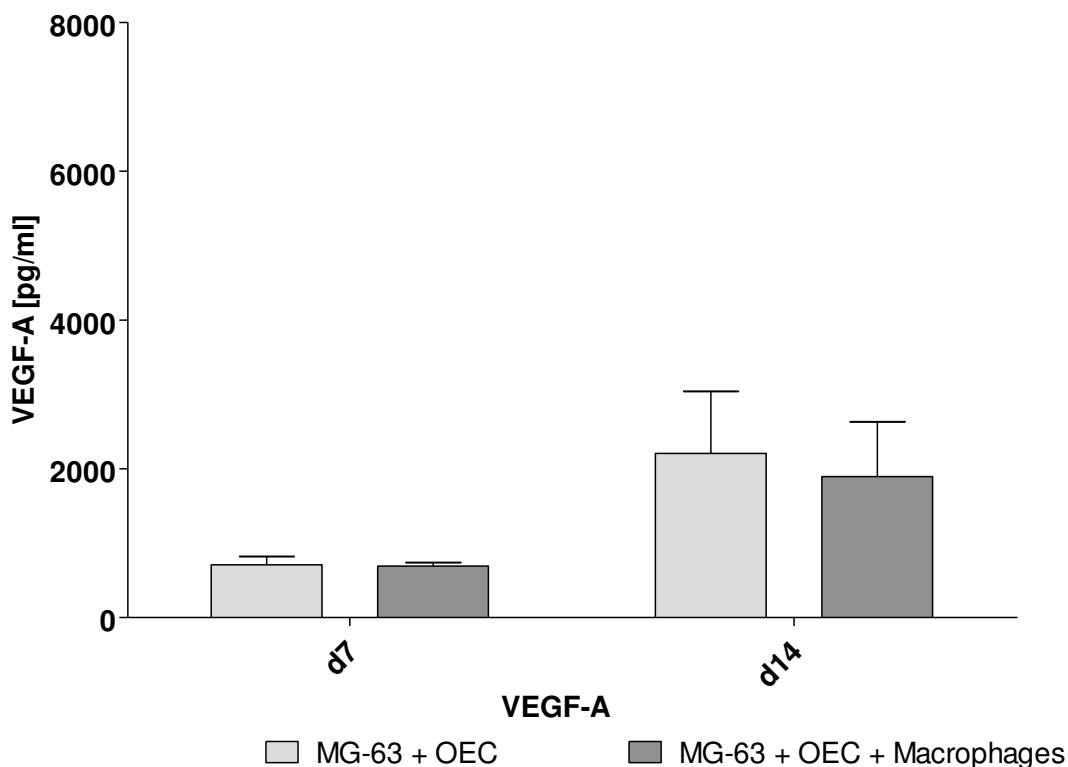


Figure 67: Effect of macrophage-induced THP-1 on the expression of the proangiogenic growth factor VEGF at the protein level. In response to M Φ exposure, there was no increase in the protein concentration of VEGF in the supernatants after 7d or 14d of triple-culture detectable when the osteosarcoma cell line MG-63 was used. (n=3)

The co-cultivation of OEC and primary osteoblasts together with THP-1-derived macrophages, resulted in a significant up-regulation of the pro-angiogenic growth factor VEGF after 14 days of culture, compared to the double co-culture alone (Figure 66). To determine if the effect can be induced by using a different co-culture model, MG-63 (osteosarcoma cell line) were substituted for the pOB. Previous studies have already shown that in co-cultures MG-63 behave similar to primary osteoblasts in terms of induction of endothelial cells to form microvessel-like structures. MG-63 and OEC were cultivated together with macrophages for 7 and 14 days. The supernatants were analyzed for VEGF by using ELISA, as depicted in figure 67. There was no up-regulation of VEGF at any time point detectable in the triple-culture compared to the double co-culture.

4 Discussion

4.1 Drug delivery systems for osteosarcoma

Cancer is one of the main causes of death worldwide. The world health organization (WHO) documented a mortality rate of cancer accounting for about 7.6 million deaths in the year 2008 (Daher 2012). In the coming years, the WHO predicts a continuing mortality rising to 13.1 million deaths by the year 2030 (WHO 2013). 20% of all primary bone cancers are osteosarcoma. In juvenile patients osteosarcomas are the eighth most common occurring type of cancer (Ottaviani and Jaffe 2009). The treatment of osteosarcoma by using pre- and post-operative chemo- and radiotherapy is associated with major side effects (Longhi et al. 2012) that limit the patient's quality of life considerably. In addition, a recurrence of cancer often occurs (Bielack et al. 2002). Therefore, a new strategy with the goal of killing residual cancer cells by locally administered chemotherapy combined with a bone graft to substitute the lost bone is needed. In the present study, hydroxyapatite granules were used as bone substitutes. It is already known that hydroxyapatite satisfies the criteria as a bone graft as it has been shown to be crystallographically similar to bone (Ducheyne and Groot 1981). In addition, hydroxyapatite has characteristics of good biocompatibility, as the material is known not to interfere with host metabolism (Rathbone et al. 2013). Due to its osteoconductive nature, the biomaterial acts as a scaffold. By supporting the adherence and growth of osteoblasts and their precursors and finally the formation of bone hydroxyapatite it is able to promote osseointegration (Liljensten et al. 2003). Poly(cyclodextrin) (poly(CD)) was suggested for the incorporation of chemotherapeutic drugs, as it can serve as a "host" component incorporating a "guest" molecule without forming covalent bonds. Cyclodextrins are cyclic oligosaccharides with a hydrophilic surface and a hydrophobic core and can be used in numerous areas of laboratory research and industry (Wolfram Saenger 1980; Del Valle 2004). For a pharmaceutical application it can be loaded with additional molecules such as chemotherapeutic agents. Several studies already indicate that pharmaceutical agents can be incorporated into cyclodextrins and be released over a period of time (Tiwari et al. 2010). Cisplatin and doxorubicin are suitable agents for the treatment of osteosarcoma. Major side effects arise during the systemically administered application of chemotherapy. The attempt to combine a bone graft substitute with a localized drug delivery system, in which the release of anticancer agents is sustained, might provide an advantage for the patient's quality of life.

The aim of the study was to investigate cytotoxic effects of chemotherapeutic drugs on cells that are involved in bone tissue regeneration after tumor resection. Human osteosarcoma cell lines were used as models for cancer cells and human primary cells were used as models for healthy cells. A benefit of this study was the possibility to compare directly the cytotoxic effect of chemotherapeutic drugs on cancer cells versus their impact on healthy human primary cells. Anticancer drugs are generally used in cancer therapy (Winkler et al. 1988). Chemotherapeutic agents like cisplatin or doxorubicin are widely applied for the treatment of sarcoma and carcinoma and several other cancer types. Cisplatin binds to DNA targets and causes intrastrand and interstrand crosslinks (Monnet and Kozelka 2012; Poklar et al. 1996). Doxorubicin is an intercalating drug, generating single- and doublestrand breaks and inhibits the topoisomerase II (Swift et al. 2006; Haidle and McKinney 1986). Both agents affect the cells mostly during the S-phase of the cell cycle (Wagner and Karnitz 2009), which makes highly proliferating cells vulnerable. Immortalized cancer cell lines exhibit a high and unlimited proliferation rate (Hayflick limit). Human primary endothelial cells, such as HUVEC or HDMEC, as well as human primary osteoblasts exhibit contact inhibition, which lowers the proliferation rate when cells grow to confluence (Suzuki et al. 2000).

The studies carried out in this project investigated the effect of anticancer agents (cisplatin and doxorubicin) on human cancer cell lines on the one hand and their effect on healthy cells on the other hand. The MTS cell viability assay gives information about mitochondrial activity in cells and reflects the number of viable cells. In addition, the use of LIVE/DEAD® viability/toxicity assay that discriminates between viable and dead cells gave some indication of the cytotoxic effect of chemotherapeutic drugs on different cells types. After 4 days of treatment with different cisplatin or doxorubicin concentrations, the MTS assay as well as the LIVE/DEAD® assay revealed that among the tested osteosarcoma cell lines, MG-63 exhibited the highest resistance to cisplatin and doxorubicin. There was a strong and highly significant cytotoxic effect of high dose application of cisplatin on MG-63, while the treatment with a high dose of doxorubicin resulted in a lower decrease of viability compared to the high-dose treatment with cisplatin. Compared to the cytotoxic effect of cisplatin and doxorubicin on MG-63, the cell lines Cal-72 and SaOS-2 featured a stronger decrease of cell viability when treated with the highest applied dose of cisplatin or doxorubicin. Both Cal-72 and SaOS-2 in the MTS assay as well as the staining of live and dead cells, exhibited only a low survival rate after the treatment with 50µg/ml cisplatin or 5µg/ml doxorubicin. The comparison of the results of drug-treatment of three osteosarcoma cell lines revealed that the cytotoxic impact varied considerably among cancer cells. The effect of drug resistance among cancer cells is a far reaching problem in clinical practice (Godwin et

al. 1992; Baas et al. 1990). High levels of cisplatin resulted in a highly significant and strong inhibitory effect on human primary osteoblasts (pOB), comparable to the decrease of cell viability of SaOS-2 treated with a high dose of cisplatin. Regarding the effect of doxorubicin on human pOB, there was a decreasing impact on the cell viability with rising doxorubicin concentrations steadily. Nevertheless, the highest applied doxorubicin concentrations affected Cal-72 or SaOS-2 much more than pOB as there were still some viable cells remaining. Human osteoblasts were more sensitive to both agents compared to the cell line MG-63 but less sensitive than SaOS-2. Previous studies have already shown that the use of different chemotherapeutic agents might have less inhibitory effect on human primary osteoblasts compared to osteosarcoma cell lines (Davies et al. 2002), indicating that the primary cells exhibit a certain resistance to anticancer agents in terms of viability. Nevertheless, drug-treatment can have adverse effects on the cell function of pOB (Davies et al. 2003). Human primary endothelial cells exhibited a strong and highly significant decrease of cell viability when treated with the highest concentration of cisplatin or doxorubicin that was used in these experiments. Although human primary endothelial cells seem to be very sensitive towards cisplatin and doxorubicin, several studies are underway way to investigate the role of molecules that can serve as chemoprotectants for endothelial cells, such as VEGF (Tran et al. 2002). Human primary fibroblasts, that are also present in the surrounding tissue of bone, exhibited a high sensitivity to high doses of cisplatin, whereas the highest applied concentrations of doxorubicin affected the fibroblasts significantly, although more than 50% of the treated cells remained viable. Previous studies with doxorubicin revealed similar results for normal human dermal fibroblasts (NHDF), which exhibited a higher resistance to doxorubicin-treatment as compared to e.g. human umbilical vein endothelial cells (HUVEC) (Bocci et al. 2002).

For the evaluation of the sensitivity of various cell types towards anticancer drugs, the lethal median dose (LD_{50}), which represents the drug dose that is required to kill 50% of the treated cells, was evaluated. As this value might vary in different cell types, it was determined for cancer cell lines as well as for primary human healthy cells that play a crucial role in bone regeneration. Therefore, endothelial cells, primary osteoblasts, the osteosarcoma cell line MG-63 and macrophages were treated with a range of cisplatin or doxorubicin concentrations for 24h before they were analyzed in terms of cytotoxicity by using the MTS cell viability assay and crystal violet DNA quantification. The results showed that MG-63 exhibited a mid-level sensitivity for both agents. In contrast to the osteosarcoma cell line, the primary osteoblasts, isolated from different bone fragments, exhibited a higher tolerance for cisplatin as more than a twofold higher concentration of the drug was needed to kill 50% of the healthy human

pOB. The treatment of pOB with doxorubicin resulted in an even greater difference in viability compared to MG-63, as the LD₅₀ for doxorubicin was about six-fold higher for pOB than that for the cell line. These first results appear to be promising regarding the goal of bone tissue regeneration after tumor resection, accompanied with a chemotherapeutic treatment with the aim of eliminating residual neoplastic cells in the soft tissue. The successful regeneration of bone tissue requires the formation of new blood vessels that are needed to supply the newly formed tissue with nutrients and oxygen. The localized post-operative treatment with chemotherapy needs to allow endothelial cells to invade, proliferate and form capillaries. The treatment of HUVEC, isolated from human umbilical cord, with a range of cisplatin and doxorubicin concentrations, resulted in a low LD₅₀ for both agents. Particularly, the application of very low doxorubicin levels resulted in a decrease of viability of 50%. To prove if the sensitivity of endothelial cells isolated from different tissues might vary the median lethal dose for cisplatin and doxorubicin was also determined for outgrowth endothelial cells (OEC), isolated from peripheral blood from human donors. As a result, the dose of cisplatin or doxorubicin that is required to affect HUVEC was markedly lower than the concentrations that were needed to kill OEC. An about fourfold higher level of cisplatin was needed to inhibit the half of the drug-treated OEC. The effect when OEC were treated with doxorubicin was shown to be even more dramatic, as the LD₅₀ value for doxorubicin for OEC exposed to be about 47 times higher than for HUVEC. This indicates that the origin of endothelial cells matters with regard to their sensitivity towards anticancer agents. Since macrophages play an important role during the formation of new blood vessels (Sunderkötter et al. 1994) and in bone formation processes (Yannas 2005), the median lethal dose for cisplatin and doxorubicin for THP-1-derived macrophages was also analyzed. The results show that THP-1-derived macrophages exhibited a strong sensitivity towards cisplatin and doxorubicin. Tsan *et al.* demonstrated similar results as the leukemia cell lines seemed to be sensitive to the treatment with resveratrol (Tsan et al. 2000).

Cyclodextrin-functionalized hydroxyapatite (HA) has been suggested as a bone substitute combined with a drug delivery system. During this study drug delivery was analyzed using an extraction assay. Cyclodextrin (poly(CD))-functionalized and non-functionalized biomaterials were treated with cisplatin or doxorubicin or remained untreated. After the incubation with both agents, the bone graft materials were washed and dried for four hours before cell-specific cell culture medium was added to the hydroxyapatite granules to allow the incorporated anticancer drugs to diffuse out. Biomaterials without drug loading were treated in the same way to evaluate any cytotoxic effects potentially coming from the unmodified or poly(CD)-modified granules.

Leached media were added to cells that are potential targets *in vivo*, that is cancer cells on the one hand and human primary healthy cells on the other hand. Since the goal is to eliminate malignant cells, human osteosarcoma cell lines which represent cancer cells, were analyzed in terms of viability after the treatment with leached medium from the extraction assay. As it is already known that healthy cells are also affected by cisplatin and doxorubicin, the effect of washed-out media was also tested on healthy cells that play a crucial role in bone repair, such as human primary endothelial cells (HUVEC), human primary osteoblasts and human fibroblasts. After 24 hours of treatment, all cell types were analyzed in terms of toxicity or viability by the MTS test or alamarBlue® assay and LDH cytotoxicity assay. In addition, the release of cisplatin or doxorubicin from uncoated or poly(CD)-coated hydroxyapatite was analyzed over a period of time, by adding medium to the cells that was removed from the granules after 24h, 48h or 72h.

The treatment of primary endothelial cells with doxorubicin-treated poly(CD)-functionalized hydroxyapatite resulted in a significant decrease in cell viability that remained over time. A similar but less cytotoxic effect was shown when leached medium of doxorubicin-treated unmodified granules was used. The cytotoxic effect of doxorubicin-treated biomaterials was stronger on HUVEC compared to the endothelial cell line, as HCMEC exhibited less decrease in cell viability, indicating that primary endothelial cells exhibit a higher sensitivity towards cytotoxic agents that are used during chemotherapy. The application of leached medium from doxorubicin-treated biomaterial to osteosarcoma cell lines resulted in a decrease of cell viability for MG-63 and SaOS-2 after 24 hours. Most notably, the cytotoxic effect ensuing from doxorubicin-loaded poly(CD)-modified hydroxyapatite exerted a stronger cell growth inhibiting effect on SaOS-2 and MG-63 than the extracted medium from non-functionalized biomaterial. The cytotoxic effect on SaOS-2 was much higher than on MG-63, supporting the results from the initial drug-treatment experiments. Furthermore, the cytotoxic effect as a result of the treatment of MG-63 with extracted medium of doxorubicin-loaded poly(CD)-modified biomaterial, remained over 72h. As the tumor cell line MG-63 seemed to be more drug resistant than SaOS-2, it was interesting to know what effect the leached media might have on human pOB. In comparison to both cell lines, pOB and MG-63 exhibited similar results. There was a slight but not significant decrease of cell viability detectable when the cells were cultured in leached medium of doxorubicin-treated unmodified HA. A stronger cytotoxic effect on the cells was evaluated when washed-out medium of doxorubicin-treated functionalized biomaterial was used for the cultivation of pOB. It seemed that more doxorubicin was incorporated and delivered from the cyclic oligosaccharides that were added to HA and

the effect remained over time. Human fibroblasts exhibited a strong and highly significant decrease of cell viability when treated with medium of doxorubicin-loaded poly(CD)-functionalized HA granules. According to the results from the MTS test and the LDH cytotoxicity assay, there was no inhibiting effect detectable when the pure granules without modification were used for the extraction medium.

Cisplatin-treated biomaterials did not exhibit any significant cytotoxic effect on any cell type that was treated with leached media. The addition of cyclodextrins to the biomaterial did not show a cytotoxic effect, indicating that no or not enough cisplatin was released to inhibit any treated cell type. As opposed to a cell-inhibiting effect, there was an increase in proliferation detectable, particularly for HUVEC when they were cultured in medium of untreated or cisplatin-treated poly(CD)-functionalized biomaterial. As β -cyclodextrin molecules consist of seven glucose molecules, it could be postulated that the cyclodextrin dissolved to some degree during the time period when functionalized hydroxyapatite granules were washed for 24 hours in cell culture medium. This may have been subsequently metabolized by cells, as seen by an increased mitochondrial activity or proliferation.

The importance of a functional bone substitution lies in the necessity of a stabilizing component that permits new autologous bone to form at the site where the bone loss occurred (Rao and Stegemann 2013). Without this, in many cases the healing process is prevented or delayed and is accompanied by severe pain and impairment of the patient's quality of life. The successful integration of a bone graft substitute is strongly dependent on the formation of blood vessels after implantation, as it is necessary to guarantee the supply to the bone and the surrounding tissue with nutrients and oxygen. Different types of substitutes such as the transplantation of autografts (tissue from different part of the patient's own body), xenografts (tissue from different species) or allografts (tissue from human donor) have been examined but have a number of disadvantages. While the use of autografts is often associated with pain and donor-site morbidity as additional surgery is needed, the use of allografts or xenografts is accompanied by a risk of disease transmission and immunological response (Khan et al. 2008; Schroeder and Mosheiff 2011). Another possibility might be the implantation of a "biomaterial" such as tricalcium phosphate or hydroxyapatite. Generally, a synthetic material such as hydroxyapatite does not have any cytotoxicity or show inflammation or a foreign body response (Jarcho 1981). Since synthetic hydroxyapatite is crystallographically similar to naturally occurring bone hydroxyapatite, the interest in using this material as a bone graft substitute has grown in the last decade. Numerous studies have shown that hydroxyapatite acts as a suitable bone substitute material, as

it exhibited a high rate of osteoconductivity with compact newly formed bone around the hydroxyapatite in a bone defect area after implantation (Klein et al. 1983).

The application of a bone substitute for the replacement of lost bone due to trauma or tumor resection must satisfy various criteria. A major prerequisite is to not interfere with the host's vasculature and at the same time provide a graft on which osteoblasts can adhere and form new bone. The newly grown bone around the implantation area needs to be supplied with oxygen and nutrients. In addition, waste removal must be guaranteed (Zhou et al. 2009). Therefore, it is absolutely essential that in the presence of the biomaterial capillary structures can form via angiogenesis and move into the biomaterial. In the case of a tumor resection, the patient's vasculature is disrupted, leading to a wound healing process after bone loss. The new implant is then part of the healing cascade as it must be included in the process of bone formation and sustenance. Inflammatory cells, fibroblasts and stem cells are recruited to the site of tumor resection and implantation area to promote angiogenic activation and participate in wound healing (Carano, Richard A D and Filvaroff 2003).

To determine if the cyclodextrin-modified hydroxyapatite or the biomaterial alone exhibited any inhibiting effect on angiogenic structures *in vitro*, single granules of each sample were added to pre-existing microvessel-like structures. *In vitro* studies from Santos *et al.* and Unger *et al.* have already shown that human dermal microvascular endothelial cells (HDMEC) are able to form capillary-like structures induced by human pOB (Unger et al. 2011; Santos et al. 2009). When angiogenic structures were formed, poly(CD)-functionalized or non-functionalized hydroxyapatite granules were added to the co-cultures consisting of HDMEC and pOB and incubated for 14 days before they were stained for CD31 and analyzed by fluorescence microscopy. No differences were seen in the angiogenic structures formed after 14 days of exposure to hydroxyapatite granules with or without cyclodextrin. Cyclodextrin-modified biomaterial exhibited some degradation, generating fine-grained particles. Studies from Laschke *et al.* demonstrate that using nanocrystalline hydroxyapatite paste as a bone substitute resulted in angiogenic sprouting at the border zone of the biomaterial after 3 days of implantation. 14 days later the tissue around the implantation site exhibited vascularized granulation tissue which had begun to invade the bone substitute (Laschke et al. 2007). The formation of new blood vessels is a crucial step, as the presence of endothelial cells enhances the differentiation of osteoblast precursors into osteoblasts by the expression of IGF-1 and endothelin-1, thus stimulating the formation of bone (Rubanyi and Polokoff 1994). On the other hand, osteoblasts support the vascularization process by the secretion of VEGF leading to

proliferation and differentiation of endothelial cells (Deckers et al. 2000). It becomes clear that it is imperative that an implanted material must function in concert with natural processes in the human body and must support the healing procedure after trauma.

4.2 Enhancement of angiogenesis in bone tissue regeneration

After the resection of tumor and cancerous bone tissue and the implantation of a bone substitute the patient's quality of life is severely impaired, as the process of wound healing takes a long time. Therefore, different approaches have been taken over the last decade to provide a rapid connection of tissue engineered bone grafts with the host vasculature and ensure that the formation of new bone and its sufficient supply with nutrients and oxygen occur. It is already known that VEGF promotes the process of vascularization and in addition enhances osteoblast differentiation (Deckers et al. 2000). Street *et al.* indicated that exogenous VEGF enhanced the vascularization process and the formation of new bone in mouse femur fractures (Street et al. 2002). During the last years, drug delivery systems are under investigation that can be loaded with pro-angiogenic growth factors, to be released over time. Gu *et al.* introduced calcium alginate beads that encapsulate VEGF and released the drug over time (Gu et al. 2004). However, the application of VEGF leads to the undesirable formation of leaky vessels (Carmeliet and Jain 2000). Another strategy to improve the vascularization process and wound healing constitutes the generation of prevascularized constructs or tissues by the use of microvascular (Schanz et al. 2010) or macrovascular endothelial cells (Rouwkema et al. 2006) or endothelial precursor cells (Rivron, N.C., et al. 2008). Nevertheless, it has been shown that the seeding of endothelial cells on bone substitute constructs alone does not induce the formation of capillary-like structures *in vitro* (Unger et al. 2007). Therefore, co-culture systems consisting of different cell types have been shown to improve the vascularization process (Kaigler et al. 2003; Rouwkema et al. 2006; Wenger et al. 2004). Previous studies show that endothelial cells that were co-cultured with human osteoblasts form microvessel-like structures (Unger et al. 2011; Fuchs et al. 2007). Nevertheless, the strategies in bone regeneration regarding the formation of blood vessels have to be accelerated to enhance the healing process and thus the quality of life. In the studies by Dohle *et al.* the application of morphogens, such as sonic hedgehog, a protein that plays a crucial role in vertebrate organogenesis, to a co-culture consisting of pOB and outgrowth endothelial cells, resulted in a markedly higher amount of capillary-like structures already after 24 hours of incubation (Dohle et al. 2011). Nevertheless, the application

of morphogens is always associated with side effects due to their multifunctionality. Therefore, it would be useful to take advantage of the natural response of the human body.

Under physiological conditions, angiogenesis is induced either by hypoxia or by inflammation. During inflammation the first cells that are recruited to the site of action are neutrophils and monocytes. At the site of inflammation monocytes differentiate into macrophages which play a significant role in the induction of new blood vessels. Macrophages and monocytes have been shown to be essential and to be the dominant cells during the process of wound healing, as they secrete various factors that are crucial for angiogenesis. Macrophages release pro-inflammatory cytokines, like TNF- α , several growth factors such as VEGF and interleukins such as IL-6 or IL-8 (Werner and Grose 2003) *in vivo*. Nevertheless, the role of macrophages in the regulation of angiogenesis seems to be very complex and incompletely understood. Recently, it has been shown that tissue macrophages act as chaperones for vascular anastomosis and can stimulate tissue vascularization (Fantin et al. 2010).

The first stage of the healing process is the formation of a provisional wound matrix, called "lag-phase" (Robson et al. 2001). The first cells that are recruited at the site of inflammation are the platelets of the fibrin clot, that trigger vasoconstriction and the formation of a coagulum to prevent blood loss and automatically initiate the inflammatory response (Reinke and Sorg 2012). The wound matrix consists of a mesh of fibrinogen-derived crosslinked fibrin fibers, plasma fibronectin, vitronectin and thrombospondin, providing a range of cytokines and growth factors, released by platelets. Thus, leukocytes such as neutrophils and monocytes are attracted from the circulating blood through chemotactic signals in response to molecular changes at the surface of injured blood vessels. The interaction of leukocytes with endothelial cells is mediated by selectins that are expressed on the surface of endothelial cells (Palabrica et al. 1992). Monocytes undergo a loose adhesion to E-selectin or P-selectin through integrins (Springer 1994). Once monocytes are at wound sites, they differentiate into macrophages. Beside the phagocytosis of pathogens and damaged tissue, macrophages play a key role in wound debridement (Leibovich and Ross 1975). TNF- α , a secretory product of macrophages, is known to mimic the tumor necrotic effect of endotoxins. Studies by Carswell *et al.* demonstrated that TNF- α caused necrosis of sarcoma and mediates the suppression of mutated cells (Carswell et al. 1975). Regarding the process of new vessel formation, TNF- α is thought to induce vessel growth (Seiler et al. 2001). Based on *in vivo* studies, Leibovich *et al.* reported that TNF- α promoted the formation of capillary-like structures in rat cornea and the

developing chick chorioallantoic membrane. *In vitro* experiments demonstrated that TNF- α stimulated chemotaxis of bovine adrenal capillary endothelial cells and their induction to form tube-like structures (Leibovich et al. 1987). Together with TNF- α , interleukins such as IL-1- β or IL-6 are secreted by macrophages to amplify the inflammatory response (Eming et al. 2007). *In vivo* studies from Gallucci et al. indicated that IL-6 plays a significant role in wound healing, as IL-6-deficient mice exhibited a markedly delayed cutaneous wound healing (Gallucci et al. 2000). IL-8 is another macrophage-derived mediator of angiogenesis. Previous work demonstrated its role during the process of inflammation and wound healing, as IL-8 was shown to be pro-angiogenic when implanted in rat cornea (Koch et al. 1992).

The human monocytic leukemia cell line THP-1 was first established thirty years ago by Tsuchiya *et al.* and proved to be one of the most useful cell line to analyze the function of macrophages or monocytes *in vitro* (Tsuchiya et al. 1980). Previous work showed that THP-1 can be successfully differentiated into macrophages by the application of phorbol 12-myristate 13-acetate (PMA) (Park et al. 2007). It is already known that pro-inflammatory cytokines can be released from differently treated THP-1 cells and can induce an inflammatory response. Studies by He *et al.* showed that lipopolysaccharide (LPS)-activated THP-1 released high levels of TNF- α or IL-1 β (He et al. 2012). Insulin-treated, THP-1-derived macrophages were shown to secrete significantly high concentrations of TNF- α (Iida et al. 2001). Previous studies by Zhang *et al.* and Li *et al.* already reported interactions between the mononuclear THP-1 cell line and endothelial cells (Zhang et al. 2008; Li et al. 2006). However, there is less known about the inflammatory effect of macrophage-induced THP-1 (M ϕ) in combination with co-culture systems in general. Therefore, the human leukemia cell line THP-1 was added to the co-culture consisting of OEC and pOB. After seven and 14 days of incubation the co- and triple-cultures were analyzed in terms of pro-inflammatory signals. In response to the treatment of co-cultures with macrophages, the expression of IL-6, IL-8 and TNF- α was up-regulated on the mRNA level after both stimulation time points in the triple-cultures in comparison to the double co-culture. The results demonstrated that the combination of THP-1-derived macrophages with the established co-culture system of pOB and OEC leads to an up-regulation of the pro-inflammatory cytokines IL-6, IL-8 and TNF- α and provide a first hint that this combination alone seems to induce an inflammatory response *in vitro*. In addition, the protein expression of IL-6 was significantly increased in triple-cultures at early time points (3h/8h), indicating that the secretion of IL-6 by macrophages is promptly induced when co-cultivated with pOB and OEC, resulting in a rapid inflammatory response.

During the process of inflammation, endothelial cells induce adhesion molecules such as E-selectin or ICAM-1 on their surface in order to mediate the interaction between activated macrophages and endothelial cells (Hwang et al. 1997). The initial loose adhesion of macrophages to endothelial cells is mediated by integrins, located on the surface of macrophages and E-selectin or P-selectin which are expressed on the surface of endothelial cells (Doré et al. 1993; Gaboury and Kubes 1994; Abbassi et al. 1993). This process is named leukocyte rolling. In a next step, the weak adhesion is replaced by a stronger binding to intercellular adhesion molecule 1 (ICAM-1) or vascular cell adhesion molecule 1 (VCAM-1) before macrophages transmigrate and initiate the proliferative phase of wound healing which finally leads to new blood vessel formation (Libby et al. 2002; Fernandez-Borja et al. 2010; Leeuwenberg et al. 1992). The expression of E-selectin and ICAM-1 were found to be up-regulated at the mRNA level in triple-cultures of pOB, OEC and macrophages compared to the mRNA expression of these molecules in the double co-cultures at both time points. These results demonstrated an ongoing pro-inflammatory stimulus in the co-culture when co-cultivated with macrophages. Research by Subramaniam *et al.* showed the crucial role of the expression of selectins during wound healing. Their analysis of cutaneous wound repair in mice lacking either P-selectin or E-selectin, elicited a mild reduction of neutrophil recruitment, while mice, deficient for both types of selectins, showed a significantly reduced macrophage recruitment resulting in a marked interference of wound closure (Subramaniam et al. 1997). Similar results were obtained by Nagaoka *et al.*, as mice lacking ICAM-1 showed a reduced wound healing, indicating the important role for adhesion molecules during inflammation (Nagaoka et al. 2000).

During the proliferative phase of wound healing activated wound macrophages secrete platelet-derived growth factor (PDGF) and transforming growth factor beta (TGF- β), which attract fibroblasts to the site of inflammation. Fibroblasts proliferate and form a new extracellular matrix consisting of cross-linked collagen, thus providing the granulation tissue (Greiling and Clark 1997). As high metabolic activity dominates the site of wound healing, nutrients and oxygen are required for the formation of angiogenic structures (Diegelmann and Evans 2004; Eming et al. 2007). As the proliferative phase proceeds, fibroblasts and macrophages secrete pro-angiogenic growth factors, such as basic fibroblast growth factor (bFGF) or VEGF (Gurtner et al. 2008). VEGF production, in turn, leads to an increase in vessel permeability, endothelial migration and finally to new blood vessel formation (Werner and Grose 2003). VEGFA is known to be a crucial regulator during the process of vessel formation (Napoleone Ferrara 2003). Howdieshell *et al.* demonstrated by using a ventral hernia model in pigs the important role of VEGF during wound healing. After the

- 120 -

subcutaneous application of an anti-VEGF antibody, the wound exhibited a lower thickness of the granulation tissue and wound fluid volume. In addition, wound vessel count and evaluation of the vascular surface area revealed a lower vasculature development compared to the controls (Howdieshell et al. 2001). Tjiu *et al.* has shown that THP-1-derived macrophages were able to induce the formation of angiogenic structures via VEGF and bFGF up-regulation in different settings (Tjiu et al. 2009). In the present study, the co-cultivation of pOB and OEC together with THP-1-derived macrophages resulted after 7 and 14 days in an up-regulation of VEGF at the gene expression and protein level. Most notably, the VEGF amount increased after 14 days of cultivation and exhibited a highly significant up-regulation at the protein level. In addition, fluorescence microscopic analysis of co- and triple-cultures in which OEC were stained for their specific cell marker CD31, revealed a distinct increased formation of microcapillary-like structures after both time points compared to the double co-culture. Parameters such as vascular area, mean vessel length, mean branching points as well as the number of branches exhibited a highly significant increase in relation to the co-culture without macrophages. Based on these results, it is possible that activated macrophages play an important role in the regulation of angiogenesis by the production and secretion of different growth factors and cytokines, primarily VEGF (Ferrara 2000; McLaren et al. 1996), IL-6, IL-8 and TNF- α (Ono et al. 1999; Sunderkötter et al. 1994) and this was confirmed during the *in vitro* studies that examined the effect of THP-1-derived macrophages on human primary cells.

Numerous studies in the field of tissue engineering involve experiments in which cell lines were used in *in vitro* experiments. The osteosarcoma cell line MG-63 is known to induce the formation of angiogenic structures when co-cultivated with human primary endothelial cells (Unger et al. 2007). To examine if the pro-angiogenic effect that THP-1-derived macrophages seem to have on the co-culture consisting of primary cells might be also transferred to cell lines, MG-63 were substituted for pOB in similar studies. After 7 or 14 days of cultivation the co- and triple-cultures were analyzed by the determination of VEGF at the protein expression level. There were no differences in the expression of VEGF, indicating that the effects of THP-1-derived macrophages on osteoblasts and endothelial cells are based on interactions between cells of primary origin.

The use of an *in vitro* co-culture model to investigate different processes during bone repair was undertaken to understand mechanisms of new vessel formation in the co-culture model in relation to inflammation-induced angiogenic activation. This acceleration of angiogenic structures in response to the addition of macrophages was

the result of a higher secretion of the pro-angiogenic factor VEGF. It might be assumed that up-regulation of VEGF was initiated through the up-regulation of pro-inflammatory cytokines such as TNF- α , IL-6 or IL-8 and adhesion molecules like E-selectin and ICAM-1, indicating an ongoing inflammatory process in the triple-culture consisting of pOB, OEC and THP-1-derived macrophages. The substitution of primary osteoblasts by the osteosarcoma cell line MG-63 indicates that primary cells cannot be replaced in such model systems by permanent cell lines with osteoblast phenotype. However, additional studies are needed to analyse the underlying mechanisms and the basic control machinery during bone repair process with regard to inflammation-induced angiogenesis. Beyond this, the use of primary cells might be extended to the application of human blood monocyte-derived macrophages.

4.3 Effect of hypoxia and drug-treatment on the cell cycle

Hypoxia pre-dominates the cancer environment, as there is generally insufficient vascularization around the tumor area. The blood vessels that enclose the tumor are leaky and aberrant, leading to a low oxygen supply in cancerous tissue (Harris 2002). Tumor hypoxia is known to promote cancer invasion and metastasis, thus promoting the spread of cancer cells. In addition, systemically administered chemotherapy has difficulty in reaching the cancer cells, as the tumor area is surrounded by fragile blood vessels (Arsenault et al. 2012). In a system in which anticancer drugs can be applied directly to the tumor environment, it is important to understand the cytotoxic effects on cancer cells on the one hand and on healthy cells on the other.

Studies were carried out to determine the effects of anticancer drugs on cells specifically associated with bone cancer. These included human primary cell types such as endothelial cells and osteoblasts. The tumor-derived osteosarcoma cell line MG-63 was utilized as a representative for bone cancer cells. All cell types were exposed to hypoxia and simultaneously treated with a range of cisplatin or doxorubicin concentrations. Increased cell viability was observed in drug-treated endothelial cells under hypoxia in contrast to the cultivation under normoxic conditions. Mitochondrial activity was even stronger when compared to the untreated control. After cultivation under hypoxia, the cells were exposed to normoxia, resulting in a decrease of cell viability, indicating that the low oxygen tension might be responsible for the cell protective effect during drug-treatment. A similar but weaker effect was detectable for doxorubicin-treated pOB. The application of cisplatin resulted in a constantly

decreasing cell viability with increasing drug concentrations under normoxic and hypoxic conditions. The drug-treatment of MG-63 resulted in an increasing cytotoxic effect with rising concentrations of cisplatin and doxorubicin under both normoxia and hypoxia, indicating that a low oxygen supply does not exert a marked protective effect on the osteosarcoma cell line. Based on these results, it might be promising to implant bone substitutes that combine a bone substitute with a drug delivery system. After the removal of cancer-affected bone, the vasculature has to regenerate during the healing process. As the blood vessels were disrupted by the invasive procedure of surgery, new vessel formation has to take place. Hypoxic conditions that dominate at the site of implantation promote the vascularization process. The results of the *in vitro* studies indicate that a drug delivery system that locally inhibits the growth of cancer cells while not interfering with the viability and proliferation of healthy cells such as endothelial cells and osteoblasts in a hypoxic environment might be promising in cancer therapy.

During hypoxia, a number of processes are activated to balance the oxygen level in the cell. The transcription factor, hypoxia inducible factor-1 α (HIF-1 α), is one of the molecules that is activated when low oxygen concentrations dominate in the cell (Berra et al. 2003). The present *in vitro* studies showed that cisplatin-treated or untreated HUVEC expressed HIF-1 α when cells were cultivated under hypoxia or were treated with CoCl₂, mimicking the hypoxic response. In normoxia, there was no detectable expression of the protein. Interestingly, doxorubicin-treated HUVEC grown under hypoxia or alternatively treated with CoCl₂, expressed decreasing levels of HIF-1 α . Under normoxic conditions, HIF-1 α is constantly hydroxylated by prolyl hydroxylases and ubiquitinated by the van Hippel-Lindau tumor suppressor protein (VHL), resulting in proteasomal degradation (Jaakkola et al. 2001). When the oxygen tension drops, the activation of prolyl hydroxylases is decreased and HIF-1 α is post-translationally stabilized and thus accumulates (Berra et al. 2003). Together with HIF-1 β it dimerizes and forms a complex with the transcriptional co-activators p300/CBP that target genes responsible for O₂-regulation in the cell (Semenza 2003). Adaptive responses such as erythropoiesis, metabolic reprogramming, ROS scavenging or angiogenesis are induced to balance the oxygen supply (Miyata et al. 2011). It is already known that in renal carcinoma cells the VHL protein is non-functional. Therefore, HIF-1 α is not sensitive to ubiquitination and proteasomal degradation, resulting in an increase of HIF-1 α in a non-hypoxic environment (Maxwell et al. 1999; Harris 2002). Studies by Zhong *et al.* revealed that HIF-1 α is over-expressed in many malignant and metastatic cancer types and results in tumor growth as various factors that take part in tumor progression such as vascular endothelial growth factor (VEGF), glucose transporters, glycolytic enzymes, IGF-2 or IGF-binding protein (IGFBP)-2 and IGFBP- 3, are induced by the

transcription factor (Zhong et al. 1999; Feldser et al. 1999). For cancer treatment, it might be useful to introduce anticancer agents that control or down-regulate the expression and stabilization of HIF-1 α .

When DNA damage occurs by the application of chemotherapeutic agents or hypoxia, several mechanisms are initiated to suppress the proliferation of cells with abnormal DNA to prevent dissemination of aberrant genetic material. The tumor suppressor protein p53 is one such factor. After stabilization and accumulation, it acts as a transcription factor for the induction of an adaptive response to prevent genome mutation. In normal healthy cells the activity of p53 is regulated by the murine double minute 2 homolog (Mdm2). After ubiquitination, the tumor suppressor protein is translocated from the nucleus to the cytosol where p53 is subjected to proteasomal degradation (Ryan et al. 2001). In case of interference of DNA, p53 is structurally modified resulting in the inability of Mdm2 to target p53 (Bond et al. 2005). As a result, p53 accumulates and undergoes further protein modifications. Together with cofactors, p53 can then target genes that are involved in mechanisms to protect the organism from the spread of aberrant cells which might give rise to carcinogenesis. Thus, p53 is intimately involved in DNA repair, cell cycle arrest or apoptosis (Prives and Hall 1999; Riley et al. 2008).

To determine how and if the regulation of p53 is affected in chemotherapy, human endothelial cells and human osteoblasts isolated from healthy donors and the cancer cell line MG-63 were treated with a range of cisplatin or doxorubicin concentrations. At the protein expression level, the transcription factor was up-regulated in anticancer agent-treated HUVEC. The highest amounts of p53 were detectable when a dose of doxorubicin was applied to the cells that was slightly higher than the LD₅₀. However, at the gene expression level, p53 was not up-regulated compared to the untreated control. The application of both anticancer drugs to pOB resulted in an increasing concentration of p53 compared to the untreated control. In addition, at the gene expression level a marked up-regulation of p53 was observed after the treatment with doxorubicin. It is widely known that human tumors, including osteosarcoma, contain a mutation or deletion in the p53 gene (Bischoff et al. 1996). The origin for those mutations varies among different types of cancer (Hollstein et al. 1991). Studies from Toguchida *et al.* revealed that rearrangements of the p53 gene are common in osteosarcoma, including point mutations, small deletions and insertions (Toguchida et al. 1992). The short arm of chromosome 17 is the gene locus where the p53 gene is located (Isobe et al. 1986) and is frequently mutated by deletions. The analysis of MG-63 regulation of p53 after cisplatin or doxorubicin-treatment resulted in no protein

expression of the transcription factor. Research by Diller *et al.* showed that 9 of 10 examined osteosarcoma cell lines exhibited aberrant p53 genes and a reduced or abnormal protein amount, among them SaOS-2 and MG-63 (Diller *et al.* 1990). The resistance of cancer cells, such as the tumor-inducing cell line MG-63, to anticancer agents increases through mutations that interfere with apoptosis. Cancer cells can thus proliferate and spread finally leading to metastasis (Lowe *et al.* 1993).

The cell cycle regulator cyclin-dependent kinase inhibitor protein (CKI) or p21 is directly transcriptionally targeted by p53 (Gartel and Radhakrishnan 2005). p21 inhibits the cyclin-dependent kinase (CDK)-2 or CDK-4 (Wade Harper 1993). In healthy cells, CDK is activated by binding cyclin or by phosphorylation. By direct interactions of p21 or other CKI with CDK, their phosphorylation is prevented and thus the protein is inhibited (Morgan 1995; Aprelikova *et al.* 1995). CDKs are responsible for transition of the cell from the G1-phase of the cell cycle to the S-phase (Elledge 1996). The induction of p21 leads to the prevention of the normal cell cycle pathway, as the transition is inhibited and the cells remain in the G0-phase of the cell cycle. Thus, the replication of DNA is inhibited and the cell cycle comes to an arrest in order to prevent the passing on of aberrant DNA (Cazzalini *et al.* 2010).

To determine whether p21 expression is changed in primary cells compared to the cancer cell line, cisplatin and doxorubicin-treated endothelial cells, primary osteoblasts and MG-63 were analyzed for the regulation of p21. At the protein expression level, HUVEC exhibited a distinct up-regulation of p21 when treated with a range of cisplatin concentrations. Similar results were obtained for low doxorubicin concentrations. However, the incubation of the doxorubicin dose that resulted in a strong and highly significant increase of p53 compared to the untreated control, resulted in no change in the expression of p21. Studies from Chen *et al.* indicated that low levels of p53 resulted in cell cycle arrest by the induction of p21, whereas high quantities move the cells to apoptosis (Chen *et al.* 1996). In case of irreversible damage, p53 promotes the Apaf-1/caspase 9 apoptosis pathway. Bcl-2 associated X (BAX) is one of the p53 target genes as it contains a p53 binding site. When p53 targets the BAX gene, the pro-apoptotic protein is accumulated and promotes the release of mitochondrial cytochrome c (Schuler *et al.* 2000). It is expected that diverse other factors that are targeted by p53 are involved in the process leading to the release of cytochrome c (Benchimol 2001). In addition, p53 induces Apaf-1, which oligomerizes as a cofactor with caspase 9 in the presence of cytochrome c and results in activation of a caspase cascade which finally causes cell death (Soengas *et al.* 1999). The outcomes of the p53 and p21 analysis of doxorubicin-treated HUVEC appear to indicate that the cells

entered the apoptosis pathway when p53 was detectable at high levels, whereas p21 did not exhibit an up-regulation. Lower concentrations of doxorubicin or cisplatin resulted in an up-regulation of p21, indicating that the adaptive response of the cells to the drug-treatment might result in cell cycle arrest. The analysis of drug-treated MG-63 for regulation of p21 showed that none of the applied doses of cisplatin or doxorubicin resulted in an increase of the cell cycle regulating protein compared to the untreated control. Nevertheless, the presence of p21 in all samples, among them the untreated control, indicated that there must be a p53-independent induction of p21. Zenmyo *et al.* reported that the induction of p21 in p53-deficient MG-63 can be triggered by vitamin D₃ or K₂, indicating that the expression of p21 can be initiated independently of p53 (Zenmyo *et al.* 2001). Other investigations show that the application of TNF- α increases the expression of p21 and thus decreases proliferation, supporting the idea of a p53-independent pathway for the regulation of p21 (Merli *et al.* 1999). After the treatment of primary osteoblasts with cisplatin or doxorubicin the cells were analyzed for p21 by using ELISA, in the same way as for HUVEC or MG-63. No p21 was detectable. Studies by Bellosta *et al.* show that p21 is strongly down-regulated in primary mouse osteoblasts during cell differentiation and the application of fibroblast growth factor (FGF) resulted in an up-regulation of p21 (Bellosta *et al.* 2003). One possibility is that if the osteoblast cells were in the process of differentiating during drugtreatment, this might be a situation in which p21 was present in very low concentrations and was therefore not detectable.

The accumulation of p53 is induced by DNA damage. Hypoxic stress is an additional factor that leads to the stabilization of p53. At low oxygen concentrations, HIF-1 α is stabilized to maintain the O₂ balance of the cell. Studies by Fels *et al.* documented an interaction between HIF-1 α and p53 which was reported by An *et al.* (An *et al.* 1998; Fels and Koumenis 2005). Previous studies also indicated an interaction through the binding of p53 to a HIF/p300 complex, resulting in the inhibition of HIF activity (Blagosklonny *et al.* 1998). Other research shows the direct interaction between HIF and p53 via mdm2, which acts as a link between both transcription factors (Chen *et al.* 2003). The group of Sánchez-Puig *et al.* suggested that the interactions between HIF-1 α and p53 are based on the oxygen-dependent degradation (ODD) domain which in normoxia is the prolyl hydroxylase-binding domain, providing an additional binding area for p53. Under hypoxic conditions, p53 can bind to the ODD domain, which might result in a decrease of p53 activity and the abolition of adaptive responses such as apoptosis or cell cycle arrest (Sánchez-Puig *et al.* 2005).

To study the effect of anticancer agent treatment and anoxia on the regulation of p53, HUVEC were treated with two concentrations of cisplatin or doxorubicin. In addition, a HIF-1 α inhibitor and YC-1, which inactivates the COOH-terminal transactivation domain (CAD) of HIF-1 α (Li et al. 2008), were applied separately to the cells and subsequently analyzed for p53 and p21 expression. The cells were incubated for 24 hours. Anoxia alone did not trigger the increase of p53 in the cells. Combined with cisplatin and most notably with doxorubicin, p53 increased markedly, indicating that anoxia did not have an impact over the period of time on the stabilization process of p53. Under anoxic conditions, HIF-1 α is stabilized in order to balance the oxygen level in the cell. When HIF-1 α was blocked by a HIF-1 α inhibitor, a lower amount of p53 was detectable in the cells that were treated with doxorubicin or a high dose of cisplatin. This effect was potentiated when the YC-1 inhibitor was applied to the cells. When the cells were exposed to a low doxorubicin dose combined with the YC-1 inhibitor under anoxic conditions, there was a decrease of p53 to a level of about 50% compared to cells with stabilized HIF-1 α . The treatment of HUVEC with anoxia and anticancer agents resulted in an up-regulation of p21 in cisplatin-treated cells. In contrast, low or no levels of p21 were detectable after the treatment with doxorubicin under anoxia. The additional treatment of endothelial cells with HIF-1 α inhibitor resulted in a much lower amount of p21 when cells were treated with 15 μ g/ml cisplatin. There was no p21 detectable in doxorubicin-treated cells or in the untreated control. The effect was amplified in YC-1 inhibitor-treated HUVEC. There was almost no p21 detectable in differently treated cells. With the highest applied concentration of cisplatin under different conditions, it is remarkable that the cultivation of cells under anoxia resulted in an up-regulation of p21 of more than 100% compared to the untreated anoxic control. The application of both inhibitors resulted in a dramatic decrease of p21. In general, the application of doxorubicin resulted in high levels of p53, while p21 was not induced. The treatment with cisplatin resulted in a moderate stabilization of the tumor suppressor protein. The analysis of p21 revealed that higher levels were induced by low levels of p53. The presence of HIF-1 α seemed to stabilize p53 and p21 in drug-treated endothelial cells cultivated under anoxic conditions. Based on this information, it is concluded that there might be an interaction between the molecules intended to protect the cells from passing possible genome mutations to daughter cells. The presence of HIF-1 α appears not to inhibit the activation of p53 by binding the tumor suppressor to its ODD binding domain, as the inhibition of HIF-1 α resulted in a lower level of p53 and p21 compared to the situation when HIF-1 α is stabilized.

Overall, this study has to be considered as fundamental research and additional studies have to be performed to analyze the interactions of underlying mechanisms. Regarding the inflammation-induced angiogenesis which resulted in a significant enhancement of angiogenic formation through the use of macrophages, it might be of interest to combine the triple-culture with a three-dimensional scaffold such as hydroxyapatite to analyze the induction of an accelerated formation of angiogenic structures in a pre-treated system before implantation. In a second step a three-dimensional system might be used with the goal of an accelerated vascularization process and thus improved integration at site of a bone defect combined with a drug-delivery component to eliminate residual cancer cells in the soft tissue after cancer resection.

With regard to the marked protective effect of anoxia on drug-treated primary endothelial cells, which was not found to be distinct in the osteosarcoma cell line, it would be interesting to analyze this effect at the molecular level to investigate the interactions of the transcription factors p53 and HIF-1 α which might play an important role during cancer treatment. These future experiments might give an insight into the interplay of different factors and offer the opportunity to improve the situation for cancer patients. This might lead to greater chances of recovery and improvement of the patient's quality of life.

5 Summary

Patients diagnosed with osteosarcoma are currently treated with intravenous injections of anticancer agents after tumor resection, this being often associated with severe side effects and delayed bone healing processes. Moreover, due to remaining neoplastic cells at the site of tumor removal, cancer recurrence often occurs. Successful bone regeneration combined with the control of residual cancer cells presents a challenge for tissue engineering after bone loss due to tumor surgery. In this regard the use of hydroxyapatite as a bone graft substitute combined with cyclodextrin molecules that can serve as drug carriers seems promising. Chemotherapeutic drugs such as doxorubicin can be loaded on to the biomaterials and released over a period of time directly at the original tumor site to eliminate any residual neoplastic cells that could be responsible for cancer recurrence. Locally applied chemotherapy has several advantages, including the protection of the drug from metabolism, its direct cytotoxic impact on local cells and above all, the reduction of severe adverse side effects that occur during intravenous injection. Therefore, this study was undertaken to evaluate the feasibility of such drug delivery systems and to investigate tissue engineering strategies to promote bone healing and especially vascularization.

The results show that not only cancer cells are affected by chemotherapeutic treatment. Different cell types exhibited different sensitivities towards drug treatment. Primary endothelial cells such as HUVEC were shown to be highly sensitive to cisplatin or doxorubicin. Both agents triggered a tumor-suppressing response in primary endothelial cells by the up-regulation of p53 and p21. Importantly, hypoxia appears to have a cancer-therapeutic impact, as the treatment of drug-sensitive primary endothelial cells with hypoxia protected the cells from this cytotoxicity. The chemoprotective effect seemed to be far less prominent for tumor-inducing cancer cell lines. These findings might implicate a possible chemotherapeutic strategy to enhance the drug-targeting effect on tumor cells with the protection of more sensitive healthy cells. A successful integration of a drug delivery component, combined with a scaffold that offers the opportunity to stabilize the tissue around the removed bone in order to promote regeneration, might allow healthy endothelial cells to proliferate and form blood vessels to supply newly formed bone with nutrients, whilst eliminating residual neoplastic cells.

As the process of bone remodeling is always accompanied by a strong impairment of the patient's quality of life, it is one of the goals in tissue engineering to accelerate the healing process after surgery. The use of implantable materials represents one such approach. Hydroxyapatite that was used in this study was shown not to interfere with

microvessel-like structures *in vitro*, this being important as hydroxyapatite is a suitable material for the replacement and regeneration of bone. The formation of blood vessels to ensure tissue supply of nutrients and oxygen is a *conditio sine qua non* for the successful integration of a bone graft into the host's tissue. Thus, an extensively formed vasculature could accelerate bone regeneration and is desirable for an improved healing process in clinical applications.

In the past, the use of co-cultures consisting of human primary osteoblasts and human primary endothelial cells has proved to be successful regarding the formation of stable microvessel-like structures *in vitro*, which can be efficiently integrated into microvascular system *in vivo*. This approach might be used to produce pre-vascularized scaffolds to promote bone healing after implantation. In addition, co-culture systems represent an excellent *in vitro* model to analyze and identify factors that are strongly involved in the process of bone healing, including angiogenesis. Macrophages are known to play a significant role in the formation of new blood vessels in inflammation-induced angiogenesis. In this context, the present study highlights the positive influence of macrophages in co-culture with osteoblasts and human primary endothelial cells. The findings showed that mimicking the natural cell response by using THP-1-derived macrophages as an inflammatory stimulus in the established co-culture system consisting of pOB and OEC has led to a pro-angiogenic activation of endothelial cells, resulting in a significantly increased formation of microvessel-like structures *in vitro*. In addition, the analysis of factors that play an important role during inflammation-induced angiogenesis, revealed a marked up-regulation of VEGF, inflammatory cytokines and adhesion molecules that ultimately contribute to an increased vascularization. These findings can be attributed to macrophage treatment and might be used in the future in a tissue engineering context to accelerate healing mechanisms and thus improve the clinical situation of patients. Moreover, combination of a co-culture based approach for bone tissue engineering with a scaffold-based drug delivery system might result in a complex clinical setup, which could simultaneously eliminate remaining cancer cells, while promoting bone regeneration.

6 Zusammenfassung

Patienten, die an Osteosarkom leiden werden derzeit mit intravenös applizierten krebstherapeutischen Mitteln nach Tumorresektion behandelt, was oftmals mit schweren Nebenwirkungen und einem verzögerten Knochenheilungsprozess einhergeht. Darüber hinaus treten vermehrt Rezidive aufgrund von verbleibenden neoplastischen Zellen an der Tumorresektionsstelle auf. Erfolgreiche Knochenregeneration und die Kontrolle von den im Gewebe verbleibenden Krebszellen stellt eine Herausforderung für das Tissue Engineering nach Knochenverlust durch Tumorentfernung dar. In dieser Hinsicht scheint der Einsatz von Hydroxyapatit als Knochenersatzmaterial in Kombination mit Cyclodextrin als Medikamententräger, vielversprechend. Chemotherapeutika können an Biomaterial gebunden und direkt am Tumorbett über einen längeren Zeitraum freigesetzt werden, um verbliebene neoplastische Zellen zu eliminieren. Lokal applizierte Chemotherapie hat diverse Vorteile, einschließlich der direkten zytotoxischen Auswirkung auf lokale Zellen, sowie die Reduzierung schwerer Nebenwirkungen. Diese Studie wurde durchgeführt, um die Funktionsfähigkeit eines solchen Arzneimittelabgabesystems zu bewerten und um Strategien im Bereich des Tissue Engineerings zu entwickeln, die den Knochenheilungsprozess und im speziellen die Vaskularisierung fördern sollen. Die Ergebnisse zeigen, dass nicht nur Krebszellen von der chemotherapeutischen Behandlung betroffen sind. Primäre Endothelzellen wie zum Beispiel HUVEC zeigten eine hohe Sensibilität Cisplatin und Doxorubicin gegenüber. Beide Medikamente lösten in HUVEC ein tumor-unterdrückendes Signal durch die Hochregulation von p53 und p21 aus. Zudem scheint Hypoxie einen krebstherapeutischen Einfluss zu haben, da die Behandlung sensitiver HUVEC mit Hypoxie die Zellen vor Zytotoxizität schützte. Der chemo-protective Effekt schien deutlich weniger auf Krebszelllinien zu wirken. Diese Resultate könnten eine mögliche chemotherapeutische Strategie darstellen, um den Effekt eines zielgerichteten Medikamenteneinsatzes auf Krebszellen zu verbessern unter gleichzeitiger Schonung gesunder Zellen. Eine erfolgreiche Integration eines Systems, das Arzneimittel abgibt, kombiniert mit einem Biomaterial zur Stabilisierung und Regeneration, könnte gesunden Endothelzellen die Möglichkeit bieten zu proliferieren und Blutgefäße zu bilden, während verbleibende Krebszellen eliminiert werden. Da der Prozess der Knochengeweberemodellierung mit einer starken Beeinträchtigung der Lebensqualität des Patienten einhergeht, ist die Beschleunigung des postoperativen Heilungsprozesses eines der Ziele des Tissue Engineerings. Die Bildung von Blutgefäßen ist unabdingbar für eine erfolgreiche Integration eines Knochentransplantats in das Gewebe. Daher ist ein umfangreich ausgebildetes Blutgefäßsystem für einen verbesserten Heilungsprozess während der klinischen

Anwendung wünschenswert. Frühere Experimente zeigen, dass sich die Anwendung von Ko-Kulturen aus humanen primären Osteoblasten (pOB) und humanen outgrowth endothelial cells (OEC) im Hinblick auf die Bildung stabiler gefäßähnlicher Strukturen *in vitro*, die auch effizient in das mikrovaskuläre System *in vivo* integriert werden konnten, als erfolgreich erweisen. Dieser Ansatz könnte genutzt werden, um prä-vaskularisierte Konstrukte herzustellen, die den Knochenheilungsprozess nach der Implantation fördern. Zusätzlich repräsentiert das Ko-Kultursystem ein exzellentes *in vitro* Model, um Faktoren, welche stark in den Prozess der Knochenheilung und Angiogenese eingebunden sind, zu identifizieren und zu analysieren. Es ist bekannt, dass Makrophagen eine maßgebliche Rolle in der inflammatorisch-induzierten Angiogenese spielen. In diesem Zusammenhang hebt diese Studie den positiven Einfluss THP-1 abgeleiteter Makrophagen in Ko-Kultur mit pOB und OEC hervor. Die Ergebnisse zeigten, dass die Anwendung von Makrophagen als inflammatorischer Stimulus im bereits etablierten Ko-Kultursystem zu einer pro-angiogenen Aktivierung der OEC führte, was in einer signifikant erhöhten Bildung blutgefäßähnlicher Strukturen *in vitro* resultierte. Außerdem zeigte die Analyse von Faktoren, die in der durch Entzündung hervorgerufenen Angiogenese eine wichtige Rolle spielen, eine deutliche Hochregulation von VEGF, inflammatorischer Zytokine und Adhäsionsmoleküle, die letztlich zu einer verstärkten Vaskularisierung beitragen. Diese Resultate werden dem Einfluss von Makrophagen zugeschrieben und könnten zukünftig im Tissue Engineering eingesetzt werden, um den Heilungsprozess zu beschleunigen und damit die klinische Situation von Patienten zu verbessern. Darüber hinaus könnte die Kombination der auf Ko-Kulturen basierenden Ansätze für das Knochen Tissue Engineering mit einem biomaterial-basierenden Arzneimittelabgabesystem zum klinischen Einsatz kommen, der die Eliminierung verbliebener Krebszellen mit der Förderung der Knochenregeneration verbindet.

7 References

- Abbassi, O.; Kishimoto, T. K.; McIntire, L. V.; Anderson, D. C.; Smith, C. W. (1993): E-selectin supports neutrophil rolling in vitro under conditions of flow. In: *J. Clin. Invest.* 92 (6), S. 2719–2730. DOI: 10.1172/JCI116889.
- Adams, Ralf H.; Alitalo, Kari (2007): Molecular regulation of angiogenesis and lymphangiogenesis. In: *Nat. Rev. Mol. Cell Biol.* 8 (6), S. 464–478. DOI: 10.1038/nrm2183.
- Adimoolam, Shanthi; Ford, James M. (2003): p53 and regulation of DNA damage recognition during nucleotide excision repair. In: *DNA Repair (Amst.)* 2 (9), S. 947–954.
- Albrektsson, T.; Johansson, C. (2001): Osteoinduction, osteoconduction and osseointegration. In: *Eur Spine J* 10 Suppl 2, S. S96-101. DOI: 10.1007/s005860100282.
- Allen, Theresa M.; Cullis, Pieter R. (2004): Drug delivery systems: entering the Mainstream. In: *Science (Science (New York, N.Y.))* 303 (5665), S. 1818–1822.
- An, W. G.; Kanekal, M.; Simon, M. C.; Maltepe, E.; Blagosklonny, M. V.; Neckers, L. M. (1998): Stabilization of wild-type p53 by hypoxia-inducible factor 1alpha. In: *Nature* 392 (6674), S. 405–408. DOI: 10.1038/32925.
- Annaz, B.; Hing, K. A.; Kayser, M.; Buckland, T.; Di Silvio, L. (2004): Porosity variation in hydroxyapatite and osteoblast morphology: a scanning electron microscopy study. In: *J Microsc* 215 (Pt 1), S. 100–110. DOI: 10.1111/j.0022-2720.2004.01354.x.
- Aprelikova, O.; Xiong, Y.; Liu, E. T. (1995): Both p16 and p21 families of cyclin-dependent kinase (CDK) inhibitors block the phosphorylation of cyclin-dependent kinases by the CDK-activating kinase. In: *J. Biol. Chem.* 270 (31), S. 18195–18197.
- Aragonés, Julián; Schneider, Martin; van Geyte, Katie; Fraisl, Peter; Dresselaers, Tom; Mazzone, Massimiliano et al. (2008): Deficiency or inhibition of oxygen sensor Phd1 induces hypoxia tolerance by reprogramming basal metabolism. In: *Nat. Genet.* 40 (2), S. 170–180. DOI: 10.1038/ng.2007.62.
- Arras, M.; Ito, W. D.; Scholz, D.; Winkler, B.; Schaper, J.; Schaper, W. (1998): Monocyte activation in angiogenesis and collateral growth in the rabbit hindlimb. In: *J. Clin. Invest.* 101 (1), S. 40–50. DOI: 10.1172/JCI119877.
- Arsenault, Dominique; Lucien, Fabrice; Dubois, Claire M. (2012): Hypoxia enhances cancer cell invasion through relocalization of the proprotein convertase furin from the trans-Golgi network to the cell surface. In: *J. Cell. Physiol.* 227 (2), S. 789–800. DOI: 10.1002/jcp.22792.
- Auguste, Patrick; Lemièrre, Sylvie; Larrièu-Lahargue, Frédéric; Bikfalvi, Andreas (2005): Molecular mechanisms of tumor vascularization. In: *Crit. Rev. Oncol. Hematol.* 54 (1), S. 53–61. DOI: 10.1016/j.critrevonc.2004.11.006.
- Baas, F.; Jongasma, A. P.; Broxterman, H. J.; Arceci, R. J.; Housman, D.; Scheffer, G. L. et al. (1990): Non-P-glycoprotein mediated mechanism for multidrug resistance precedes P-glycoprotein expression during in vitro selection for doxorubicin resistance in a human lung cancer cell line. In: *Cancer Res.* 50 (17), S. 5392–5398.
- Babensee, J. E.; McIntire, L. V.; Mikos, A. G. (2000): Growth factor delivery for tissue engineering. In: *Pharm. Res.* 17 (5), S. 497–504.
- Bachur, N. R.; Gordon, S. L.; Gee, M. V. (1977): Anthracycline antibiotic augmentation of microsomal electron transport and free radical formation. In: *Mol. Pharmacol.* 13 (5), S. 901–910.

References

- Bachur, N. R.; Gordon, S. L.; Gee, M. V. (1978): A general mechanism for microsomal activation of quinone anticancer agents to free radicals. In: *Cancer Res.* 38 (6), S. 1745–1750.
- Baggiolini, M.; Walz, A.; Kunkel, S. L. (1989): Neutrophil-activating peptide-1/interleukin 8, a novel cytokine that activates neutrophils. In: *J. Clin. Invest.* 84 (4), S. 1045–1049. DOI: 10.1172/JCI114265.
- Baradari, Hiba; Damia, Chantal; Dutreih-Colas, Maggy; Champion, Eric; Chulia, Dominique; Viana, Marylène (2011): β -TCP porous pellets as an orthopaedic drug delivery system: ibuprofen/carrier physicochemical interactions. In: *Sci. Technol. Adv. Mater.* 12 (5), S. 55008. DOI: 10.1088/1468-6996/12/5/055008.
- Bassett, Ekaterina; King, Nicole M.; Bryant, Miriam F.; Hector, Suzanne; Pendyala, Lakshmi; Chaney, Stephen G.; Cordeiro-Stone, Marila (2004): The role of DNA polymerase eta in translesion synthesis past platinum-DNA adducts in human fibroblasts. In: *Cancer Res.* 64 (18), S. 6469–6475. DOI: 10.1158/0008-5472.CAN-04-1328.
- Bellosta, Paola; Masramon, Laia; Mansukhani, Alka; Basilico, Claudio (2003): p21(WAF1/CIP1) acts as a brake in osteoblast differentiation. In: *J. Bone Miner. Res.* 18 (5), S. 818–826. DOI: 10.1359/jbmr.2003.18.5.818.
- Benchimol, S. (2001): p53-dependent pathways of apoptosis. In: *Cell Death Differ.* 8 (11), S. 1049–1051. DOI: 10.1038/sj.cdd.4400918.
- Bernhardt, Anne; Lode, Anja; Peters, Fabian; Gelinsky, Michael (2011): Novel ceramic bone replacement material Osbone® in a comparative in vitro study with osteoblasts. In: *Clinical Oral Implants Research* 22 (6), S. 651–657. DOI: 10.1111/j.1600-0501.2010.02015.x.
- Berra, Edurne; Benizri, Emmanuel; Ginouvès, Amandine; Volmat, Véronique; Roux, Danièle; Pouysségur, Jacques (2003): HIF prolyl-hydroxylase 2 is the key oxygen sensor setting low steady-state levels of HIF-1alpha in normoxia. In: *EMBO J.* 22 (16), S. 4082–4090. DOI: 10.1093/emboj/cdg392.
- Bielack, Stefan S.; Kempf-Bielack, Beate; Delling, Günter; Exner, G. Ulrich; Flege, Silke; Helmke, Knut et al. (2002): Prognostic factors in high-grade osteosarcoma of the extremities or trunk: an analysis of 1,702 patients treated on neoadjuvant cooperative osteosarcoma study group protocols. In: *J. Clin. Oncol.* 20 (3), S. 776–790.
- Bischoff, J. R.; Kirn, D. H.; Williams, A.; Heise, C.; Horn, S.; Muna, M. et al. (1996): An adenovirus mutant that replicates selectively in p53-deficient human tumor cells. In: *Science* 274 (5286), S. 373–376.
- Blagosklonny, M. V.; An, W. G.; Romanova, L. Y.; Trepel, J.; Fojo, T.; Neckers, L. (1998): p53 inhibits hypoxia-inducible factor-stimulated transcription. In: *J. Biol. Chem.* 273 (20), S. 11995–11998.
- Blanchemain, N.; Chai, F.; Haulon, S.; Krump-Konvalinkova, V.; Traisnel, M.; Morcellet, M. et al. (2008a): Biological behaviour of an endothelial cell line (HPMEC) on vascular prostheses grafted with hydroxypropylgamma-cyclodextrine (HPgamma-CD) and hydroxypropylbeta-cyclodextrine (HPbeta-CD). In: *J Mater Sci Mater Med* 19 (6), S. 2515–2523. DOI: 10.1007/s10856-008-3388-3.
- Blanchemain, N.; Haulon, S.; Boschini, F.; Traisnel, M.; Morcellet, M.; Martel, B.; Hildebrand, H. F. (2007): Vascular prostheses with controlled release of antibiotics Part 2. In vitro biological evaluation of vascular prostheses treated by cyclodextrins. In: *Biomol. Eng.* 24 (1), S. 143–148. DOI: 10.1016/j.bioeng.2006.05.011.
- Blanchemain, Nicolas; Laurent, Thomas; Chai, Feng; Neut, Christel; Haulon, Stéphan; Krump-Konvalinkova, Vera et al. (2008b): Polyester vascular prostheses coated with a

- cyclodextrin polymer and activated with antibiotics: cytotoxicity and microbiological evaluation. In: *Acta Biomater* 4 (6), S. 1725–1733. DOI: 10.1016/j.actbio.2008.07.001.
- Bocci, Guido; Nicolaou, K. C.; Kerbel, Robert S. (2002): Protracted low-dose effects on human endothelial cell proliferation and survival in vitro reveal a selective antiangiogenic window for various chemotherapeutic drugs. In: *Cancer Res.* 62 (23), S. 6938–6943.
- Bond, Gareth L.; Hu, Wenwei; Levine, Arnold J. (2005): MDM2 is a central node in the p53 pathway: 12 years and counting. In: *Curr Cancer Drug Targets* 5 (1), S. 3–8.
- Boyle, Robert George; Travers, Stuart (2006): Hypoxia: targeting the tumour. In: *Anticancer Agents Med Chem* 6 (4), S. 281–286.
- Boyle, MD,Edward M; Pohlman, MD,Timothy H; Johnson, MD,Marion C; Verrier, MD,Edward D (1997): Endothelial Cell Injury in Cardiovascular Surgery: The Systemic Inflammatory Response. Edward D. Verrier, MD. In: *The Annals of Thoracic Surgery* 63 (1), S. 277–284. DOI: 10.1016/S0003-4975(96)01061-2.
- Brandi, Maria Luisa; Collin-Osdoby, Patricia (2006): Vascular biology and the skeleton. In: *J. Bone Miner. Res.* 21 (2), S. 183–192. DOI: 10.1359/JBMR.050917.
- Brennan, J. A.; Mao, L.; Hruban, R. H.; Boyle, J. O.; Eby, Y. J.; Koch, W. M. et al. (1995): Molecular assessment of histopathological staging in squamous-cell carcinoma of the head and neck. In: *N. Engl. J. Med.* 332 (7), S. 429–435. DOI: 10.1056/NEJM199502163320704.
- Bristow, M. R.; Billingham, M. E.; Mason, J. W.; Daniels, J. R. (1978): Clinical spectrum of anthracycline antibiotic cardiotoxicity. In: *Cancer Treat Rep* 62 (6), S. 873–879.
- Brugarolas, J.; Moberg, K.; Boyd, S. D.; Taya, Y.; Jacks, T.; Lees, J. A. (1999): Inhibition of cyclin-dependent kinase 2 by p21 is necessary for retinoblastoma protein-mediated G1 arrest after gamma-irradiation. In: *Proc. Natl. Acad. Sci. U.S.A.* 96 (3), S. 1002–1007.
- Bunz, F.; Dutriaux, A.; Lengauer, C.; Waldman, T.; Zhou, S.; Brown, J. P. et al. (1998): Requirement for p53 and p21 to sustain G2 arrest after DNA damage. In: *Science* 282 (5393), S. 1497–1501.
- Caetano-Lopes, Joana; Canhão, Helena; Fonseca, João Eurico (2007): Osteoblasts and bone formation. In: *Acta Reumatol Port* 32 (2), S. 103–110.
- Carano, Richard A D; Filvaroff, Ellen H. (2003): Angiogenesis and bone repair. In: *Drug Discov. Today* 8 (21), S. 980–989.
- Carmeliet, P.; Jain, R. K. (2000): Angiogenesis in cancer and other diseases. In: *Nature* 407 (6801), S. 249–257. DOI: 10.1038/35025220.
- Carswell, E. A.; Old, L. J.; Kassel, R. L.; Green, S.; Fiore, N.; Williamson, B. (1975): An endotoxin-induced serum factor that causes necrosis of tumors. In: *Proc. Natl. Acad. Sci. U.S.A.* 72 (9), S. 3666–3670.
- Cazzalini, Ornella; Scovassi, A. Ivana; Savio, Monica; Stivala, Lucia A.; Prosperi, Ennio (2010): Multiple roles of the cell cycle inhibitor p21(CDKN1A) in the DNA damage response. In: *Mutat. Res.* 704 (1-3), S. 12–20. DOI: 10.1016/j.mrrev.2010.01.009.
- Chai, F.; Hornez, J-C; Blanchemain, N.; Neut, C.; Descamps, M.; Hildebrand, H. F. (2007): Antibacterial activation of hydroxyapatite (HA) with controlled porosity by different antibiotics. In: *Biomol. Eng.* 24 (5), S. 510–514. DOI: 10.1016/j.bioeng.2007.08.001.
- Chen, Delin; Li, Muyang; Luo, Jianyuan; Gu, Wei (2003): Direct interactions between HIF-1 alpha and Mdm2 modulate p53 function. In: *J. Biol. Chem.* 278 (16), S. 13595–13598. DOI: 10.1074/jbc.C200694200.

References

- Chen, X.; Ko, L. J.; Jayaraman, L.; Prives, C. (1996): p53 levels, functional domains, and DNA damage determine the extent of the apoptotic response of tumor cells. In: *Genes Dev.* 10 (19), S. 2438–2451.
- Chipuk, Jerry E.; Kuwana, Tomomi; Bouchier-Hayes, Lisa; Droin, Nathalie M.; Newmeyer, Donald D.; Schuler, Martin; Green, Douglas R. (2004): Direct activation of Bax by p53 mediates mitochondrial membrane permeabilization and apoptosis. In: *Science* 303 (5660), S. 1010–1014. DOI: 10.1126/science.1092734.
- Chordiya Mayur A (2012): CYCLODEXTRIN: A DRUG CARRIER SYSTEMS.
- Clauss, M. (2000): Molecular biology of the VEGF and the VEGF receptor family. In: *Semin. Thromb. Hemost.* 26 (5), S. 561–569. DOI: 10.1055/s-2000-13213.
- Collin-Osdoby, P. (1994): Role of vascular endothelial cells in bone biology. In: *J. Cell. Biochem.* 55 (3), S. 304–309. DOI: 10.1002/jcb.240550306.
- Colombo, Paolo (1993): Swelling-controlled release in hydrogel matrices for oral route. In: *Advanced Drug Delivery Reviews* 11 (1-2), S. 37–57. DOI: 10.1016/0169-409X(93)90026-Z.
- Cypher, T. J.; Grossman, J. P. (1996): Biological principles of bone graft healing. In: *J Foot Ankle Surg* 35 (5), S. 413–417.
- Daher, M. (2012): Cultural beliefs and values in cancer patients. In: *Ann. Oncol.* 23 Suppl 3, S. 66–69. DOI: 10.1093/annonc/mds091.
- Dalby, M. J.; Di Silvio, L.; Harper, E. J.; Bonfield, W. (2002): Increasing hydroxyapatite incorporation into poly(methylmethacrylate) cement increases osteoblast adhesion and response. In: *Biomaterials* 23 (2), S. 569–576.
- Davies, J. H.; Evans, B A J; Jenney, M E M; Gregory, J. W. (2002): In vitro effects of chemotherapeutic agents on human osteoblast-like cells. In: *Calcif. Tissue Int.* 70 (5), S. 408–415. DOI: 10.1007/s002230020039.
- Davies, J. H.; Evans, B A J; Jenney, M E M; Gregory, J. W. (2003): Effects of chemotherapeutic agents on the function of primary human osteoblast-like cells derived from children. In: *J. Clin. Endocrinol. Metab.* 88 (12), S. 6088–6097.
- Deckers, M. M.; Karperien, M.; van der Bent, C; Yamashita, T.; Papapoulos, S. E.; Löwik, C. W. (2000): Expression of vascular endothelial growth factors and their receptors during osteoblast differentiation. In: *Endocrinology* 141 (5), S. 1667–1674.
- Deckers, Martine M L; van Bezooijen, Rutger L; van der Horst, Geertje; Hoogendam, Jakomijn; van Der Bent, Chris; Papapoulos, Socrates E.; Löwik, Clemens W G M (2002): Bone morphogenetic proteins stimulate angiogenesis through osteoblast-derived vascular endothelial growth factor A. In: *Endocrinology* 143 (4), S. 1545–1553.
- Del Valle, E.M.Martin (2004): Cyclodextrins and their uses: a review. In: *Process Biochemistry* 39 (9), S. 1033–1046. DOI: 10.1016/S0032-9592(03)00258-9.
- Diegelmann, Robert F.; Evans, Melissa C. (2004): Wound healing: an overview of acute, fibrotic and delayed healing. In: *Front. Biosci.* 9, S. 283–289.
- Diller, L.; Kassel, J.; Nelson, C. E.; Gryka, M. A.; Litwak, G.; Gebhardt, M. et al. (1990): p53 functions as a cell cycle control protein in osteosarcomas. In: *Mol. Cell. Biol.* 10 (11), S. 5772–5781.
- Dirckx, Naomi; van Hul, Matthias; Maes, Christa (2013): Osteoblast recruitment to sites of bone formation in skeletal development, homeostasis, and regeneration. In: *Birth Defects Res. C Embryo Today* 99 (3), S. 170–191. DOI: 10.1002/bdrc.21047.

- Dohle, E.; Fuchs, S.; Kolbe, M.; Hofmann, A.; Schmidt, H.; Kirkpatrick, C. J. (2011): Comparative study assessing effects of sonic hedgehog and VEGF in a human co-culture model for bone vascularisation strategies. In: *Eur Cell Mater* 21, S. 144–156.
- Dohle, Eva; Fuchs, Sabine; Kolbe, Marlen; Hofmann, Alexander; Schmidt, Harald; Kirkpatrick, Charles James (2010): Sonic hedgehog promotes angiogenesis and osteogenesis in a coculture system consisting of primary osteoblasts and outgrowth endothelial cells. In: *Tissue Eng Part A* 16 (4), S. 1235–1237. DOI: 10.1089/ten.TEA.2009.0493.
- Doré, M.; Korthuis, R. J.; Granger, D. N.; Entman, M. L.; Smith, C. W. (1993): P-selectin mediates spontaneous leukocyte rolling in vivo. In: *Blood* 82 (4), S. 1308–1316.
- Ducheyne, P.; Groot, K. de (1981): In vivo surface activity of a hydroxyapatite alveolar bone substitute. In: *J. Biomed. Mater. Res.* 15 (3), S. 441–445. DOI: 10.1002/jbm.820150315.
- Ehrbar, Martin; Djonov, Valentin G.; Schnell, Christian; Tschanz, Stefan A.; Martiny-Baron, Georg; Schenk, Ursula et al. (2004): Cell-demanded liberation of VEGF121 from fibrin implants induces local and controlled blood vessel growth. In: *Circ. Res.* 94 (8), S. 1124–1132. DOI: 10.1161/01.RES.0000126411.29641.08.
- Ehrhart, N.; Dernell, W. S.; Ehrhart, E. J.; Hutchison, J. M.; Douple, E. B.; Brekke, J. H. et al. (1999): Effects of a controlled-release cisplatin delivery system used after resection of mammary carcinoma in mice. In: *Am. J. Vet. Res.* 60 (11), S. 1347–1351.
- Eleniste, Pierre P.; Huang, Su; Wayakanon, Kornchanok; Largura, Heather W.; Bruzzaniti, Angela (2014): Osteoblast differentiation and migration are regulated by dynamin GTPase activity. In: *Int. J. Biochem. Cell Biol.* 46, S. 9–18. DOI: 10.1016/j.biocel.2013.10.008.
- Elledge, S. J. (1996): Cell cycle checkpoints: preventing an identity crisis. In: *Science* 274 (5293), S. 1664–1672.
- Eming, Sabine A.; Krieg, Thomas; Davidson, Jeffrey M. (2007): Inflammation in wound repair: molecular and cellular mechanisms. In: *J. Invest. Dermatol.* 127 (3), S. 514–525. DOI: 10.1038/sj.jid.5700701.
- Fantin, Alessandro; Vieira, Joaquim M.; Gestri, Gaia; Denti, Laura; Schwarz, Quentin; Prykhozhiy, Sergey et al. (2010): Tissue macrophages act as cellular chaperones for vascular anastomosis downstream of VEGF-mediated endothelial tip cell induction. In: *Blood* 116 (5), S. 829–840. DOI: 10.1182/blood-2009-12-257832.
- Feldser, D.; Agani, F.; Iyer, N. V.; Pak, B.; Ferreira, G.; Semenza, G. L. (1999): Reciprocal positive regulation of hypoxia-inducible factor 1alpha and insulin-like growth factor 2. In: *Cancer Res.* 59 (16), S. 3915–3918.
- Fels, Diane R.; Koumenis, Constantinos (2005): HIF-1alpha and p53: the ODD couple? In: *Trends Biochem. Sci.* 30 (8), S. 426–429. DOI: 10.1016/j.tibs.2005.06.009.
- Ferlay, Jacques; Shin, Hai-Rim; Bray, Freddie; Forman, David; Mathers, Colin; Parkin, Donald Maxwell (2010): Estimates of worldwide burden of cancer in 2008: GLOBOCAN 2008. In: *Int. J. Cancer* 127 (12), S. 2893–2917. DOI: 10.1002/ijc.25516.
- Fernandez-Borja, Mar; van Buul, Jaap D; Hordijk, Peter L. (2010): The regulation of leucocyte transendothelial migration by endothelial signalling events. In: *Cardiovasc. Res.* 86 (2), S. 202–210. DOI: 10.1093/cvr/cvq003.
- Ferrara, N. (2000): Vascular endothelial growth factor and the regulation of angiogenesis. In: *Recent Prog. Horm. Res.* 55, S. 15-35; discussion 35-6.

References

Ferrara, Napoleone; Kerbel, Robert S. (2005): Angiogenesis as a therapeutic target. In: *Nature* 438 (7070), S. 967–974. DOI: 10.1038/nature04483.

Fratino, Lucia; Rupolo, Maurizio; Mazzucato, Mario; Berretta, Massimiliano; Lleshi, Arben; Tirelli, Umberto; Michieli, Mariagrazia (2013): Autologous Stem Cell Transplantation As A Care Option In Elderly Patients. A Review. In: *Anticancer Agents Med Chem*.

Fuchs, Sabine; Hermanns, Maria Iris; Kirkpatrick, Charles James (2006): Retention of a differentiated endothelial phenotype by outgrowth endothelial cells isolated from human peripheral blood and expanded in long-term cultures. In: *Cell Tissue Res*. 326 (1), S. 79–92. DOI: 10.1007/s00441-006-0222-4.

Fuchs, Sabine; Hofmann, Alexander; Kirkpatrick, C. James (2007): Microvessel-like structures from outgrowth endothelial cells from human peripheral blood in 2-dimensional and 3-dimensional co-cultures with osteoblastic lineage cells. In: *Tissue Eng*. 13 (10), S. 2577–2588. DOI: 10.1089/ten.2007.0022.

Fuchs, Sabine; Jiang, Xin; Schmidt, Harald; Dohle, Eva; Ghanaati, Shahram; Orth, Carina et al. (2009): Dynamic processes involved in the pre-vascularization of silk fibroin constructs for bone regeneration using outgrowth endothelial cells. In: *Biomaterials* 30 (7), S. 1329–1338. DOI: 10.1016/j.biomaterials.2008.11.028.

Gaboury, J. P.; Kubes, P. (1994): Reductions in physiologic shear rates lead to CD11/CD18-dependent, selectin-independent leukocyte rolling in vivo. In: *Blood* 83 (2), S. 345–350.

Gallucci, R. M.; Simeonova, P. P.; Matheson, J. M.; Kommineni, C.; Guriel, J. L.; Sugawara, T.; Luster, M. I. (2000): Impaired cutaneous wound healing in interleukin-6-deficient and immunosuppressed mice. In: *FASEB J*. 14 (15), S. 2525–2531. DOI: 10.1096/fj.00-0073com.

Galluzzi, L.; Senovilla, L.; Vitale, I.; Michels, J.; Martins, I.; Kepp, O. et al. (2012): Molecular mechanisms of cisplatin resistance. In: *Oncogene* 31 (15), S. 1869–1883. DOI: 10.1038/onc.2011.384.

Gartel, Andrei L.; Radhakrishnan, Senthil K. (2005): Lost in transcription: p21 repression, mechanisms, and consequences. In: *Cancer Res*. 65 (10), S. 3980–3985. DOI: 10.1158/0008-5472.CAN-04-3995.

Garzón-Alvarado, Diego A.; González, Andres; Gutiérrez, Maria Lucia (2013): Growth of the flat bones of the membranous neurocranium: A computational model. In: *Comput Methods Programs Biomed*. DOI: 10.1016/j.cmpb.2013.07.027.

Gewirtz, D. A. (1999): A critical evaluation of the mechanisms of action proposed for the antitumor effects of the anthracycline antibiotics adriamycin and daunorubicin. In: *Biochem. Pharmacol*. 57 (7), S. 727–741.

Giaccia, Amato; Siim, Bronwyn G.; Johnson, Randall S. (2003): HIF-1 as a target for drug development. In: *Nat Rev Drug Discov* 2 (10), S. 803–811. DOI: 10.1038/nrd1199.

Giacinta Del Bino, and Zbigniew Darzynkiewicz (1991): Camptothecin, Teniposide, or 4'-(9-Acridinylamino)-3-methanesulfon-m-anisidide, but not Mitoxantrone or Doxorubicin, Induces Degradation of Nuclear DNA in the S Phase of HL-60 Cells. In: *Cancer Res*. (51), S. 1165–1169.

Giannoudis, Peter V.; Dinopoulos, Haralambos; Tsiridis, Eleftherios (2005): Bone substitutes: an update. In: *Injury* 36 Suppl 3, S. S20-7. DOI: 10.1016/j.injury.2005.07.029.

Girling, J. E.; Rogers, P. A. W. (2009): Regulation of endometrial vascular remodelling: role of the vascular endothelial growth factor family and the angiopoietin-TIE signalling system. In: *Reproduction* 138 (6), S. 883–893. DOI: 10.1530/REP-09-0147.

- Gitelis, Steven; Saiz, Paul (2002): What's new in orthopaedic surgery. In: *J. Am. Coll. Surg.* 194 (6), S. 788–791.
- Godwin, A. K.; Meister, A.; O'Dwyer, P. J.; Huang, C. S.; Hamilton, T. C.; Anderson, M. E. (1992): High resistance to cisplatin in human ovarian cancer cell lines is associated with marked increase of glutathione synthesis. In: *Proc. Natl. Acad. Sci. U.S.A.* 89 (7), S. 3070–3074.
- Gotay, C. C.; Korn, E. L.; McCabe, M. S.; Moore, T. D.; Cheson, B. D. (1992): Quality-of-life assessment in cancer treatment protocols: research issues in protocol development. In: *J. Natl. Cancer Inst.* 84 (8), S. 575–579.
- Goumans, Marie-Jose; Lebrin, Franck; Valdimarsdottir, Gudrun (2003): Controlling the angiogenic switch: a balance between two distinct TGF- β receptor signaling pathways. In: *Trends Cardiovasc. Med.* 13 (7), S. 301–307.
- Greenhalgh, D. G. (1998): The role of apoptosis in wound healing. In: *Int. J. Biochem. Cell Biol.* 30 (9), S. 1019–1030.
- Greiling, D.; Clark, R. A. (1997): Fibronectin provides a conduit for fibroblast transmigration from collagenous stroma into fibrin clot provisional matrix. In: *J. Cell. Sci.* 110 (Pt 7), S. 861–870.
- Grosse, P. Y.; Bressolle, F.; Pinguet, F. (1998): In vitro modulation of doxorubicin and docetaxel antitumoral activity by methyl- β -cyclodextrin. In: *Eur. J. Cancer* 34 (1), S. 168–174.
- Gu, Frank; Amsden, Brian; Neufeld, Ronald (2004): Sustained delivery of vascular endothelial growth factor with alginate beads. In: *J Control Release* 96 (3), S. 463–472. DOI: 10.1016/j.jconrel.2004.02.021.
- Gunay, Melih (Hg.) (2013): *Eco-Friendly Textile Dyeing and Finishing: InTech.*
- Gurtner, Geoffrey C.; Werner, Sabine; Barrandon, Yann; Longaker, Michael T. (2008): Wound repair and regeneration. In: *Nature* 453 (7193), S. 314–321. DOI: 10.1038/nature07039.
- Haidle, C. W.; McKinney, S. H. (1986): Adriamycin-mediated introduction of a limited number of single-strand breaks into supercoiled DNA. In: *Cancer Biochem. Biophys.* 8 (4), S. 327–335.
- Hainaut, P.; Soussi, T.; Shomer, B.; Hollstein, M.; Greenblatt, M.; Hovig, E. et al. (1997): Database of p53 gene somatic mutations in human tumors and cell lines: updated compilation and future prospects. In: *Nucleic Acids Res.* 25 (1), S. 151–157.
- Hannan, Ross D.; Drygin, Denis; Pearson, Richard B. (2013): Targeting RNA polymerase I transcription and the nucleolus for cancer therapy. In: *Expert Opin. Ther. Targets* 17 (8), S. 873–878. DOI: 10.1517/14728222.2013.818658.
- Harris, Adrian L. (2002): Hypoxia--a key regulatory factor in tumour growth. In: *Nat. Rev. Cancer* 2 (1), S. 38–47. DOI: 10.1038/nrc704.
- He, Guangan; Siddik, Zahid H.; Huang, Zaifeng; Wang, Ruoning; Koomen, John; Kobayashi, Ryuji et al. (2005): Induction of p21 by p53 following DNA damage inhibits both Cdk4 and Cdk2 activities. In: *Oncogene* 24 (18), S. 2929–2943. DOI: 10.1038/sj.onc.1208474.
- He, Xiaojuan; Shu, Jun; Xu, Li; Lu, Cheng; Lu, Aiping (2012): Inhibitory effect of Astragalus polysaccharides on lipopolysaccharide-induced TNF- α and IL-1 β production in THP-1 cells. In: *Molecules* 17 (3), S. 3155–3164. DOI: 10.3390/molecules17033155.
- Hellström, M.; Kalén, M.; Lindahl, P.; Abramsson, A.; Betsholtz, C. (1999): Role of PDGF-B and PDGFR- β in recruitment of vascular smooth muscle cells and

References

- pericytes during embryonic blood vessel formation in the mouse. In: *Development* 126 (14), S. 3047–3055.
- Hines, Daniel J.; Kaplan, David L. (2013): Poly(lactic-co-glycolic) acid-controlled-release systems: experimental and modeling insights. In: *Crit Rev Ther Drug Carrier Syst* 30 (3), S. 257–276.
- Hollstein, M.; Sidransky, D.; Vogelstein, B.; Harris, C. C. (1991): p53 mutations in human cancers. In: *Science* 253 (5015), S. 49–53.
- Hou, Xi-Miao; Zhang, Xing-Hua; Wei, Kong-Ji; Ji, Chao; Dou, Shuo-Xing; Wang, Wei-Chi et al. (2009): Cisplatin induces loop structures and condensation of single DNA molecules. In: *Nucleic Acids Res.* 37 (5), S. 1400–1410. DOI: 10.1093/nar/gkn933.
- Howard D. Dorfman (1995): Bone cancers. In: *CANCER Supplement* 1995 (1), S. 203–210.
- Howdieshell, T. R.; Callaway, D.; Webb, W. L.; Gaines, M. D.; Procter, C. D.; Sathyanarayana et al. (2001): Antibody neutralization of vascular endothelial growth factor inhibits wound granulation tissue formation. In: *J. Surg. Res.* 96 (2), S. 173–182. DOI: 10.1006/jsre.2001.6089.
- Hu, Bin; Du, Hui-Juan; Yan, Guo-Ping; Zhuo, Ren-Xi; Wu, Yuan; Fan, Chang-Lie (2013): Magnetic polycarbonate microspheres for tumor-targeted delivery of tumor necrosis factor. In: *Drug Deliv.* DOI: 10.3109/10717544.2013.843609.
- Huber, A. R.; Kunkel, S. L.; Todd, R. F.; Weiss, S. J. (1991): Regulation of transendothelial neutrophil migration by endogenous interleukin-8. In: *Science* 254 (5028), S. 99–102.
- Hutmacher, D. W. (2000): Scaffolds in tissue engineering bone and cartilage. In: *Biomaterials* 21 (24), S. 2529–2543.
- Hwang, S. J.; Ballantyne, C. M.; Sharrett, A. R.; Smith, L. C.; Davis, C. E.; Gotto, A. M.; Boerwinkle, E. (1997): Circulating adhesion molecules VCAM-1, ICAM-1, and E-selectin in carotid atherosclerosis and incident coronary heart disease cases: the Atherosclerosis Risk In Communities (ARIC) study. In: *Circulation* 96 (12), S. 4219–4225.
- Iida, K. T.; Shimano, H.; Kawakami, Y.; Sone, H.; Toyoshima, H.; Suzuki, S. et al. (2001): Insulin up-regulates tumor necrosis factor- α production in macrophages through an extracellular-regulated kinase-dependent pathway. In: *J. Biol. Chem.* 276 (35), S. 32531–32537. DOI: 10.1074/jbc.M009894200.
- Isobe, M.; Emanuel, B. S.; Givol, D.; Oren, M.; Croce, C. M. (1986): Localization of gene for human p53 tumour antigen to band 17p13. In: *Nature* 320 (6057), S. 84–85. DOI: 10.1038/320084a0.
- Iyer, L.; Ratain, M. J. (1998): Pharmacogenetics and cancer chemotherapy. In: *Eur. J. Cancer* 34 (10), S. 1493–1499.
- Jaakkola, P.; Mole, D. R.; Tian, Y. M.; Wilson, M. I.; Gielbert, J.; Gaskell, S. J. et al. (2001): Targeting of HIF- α to the von Hippel-Lindau ubiquitylation complex by O₂-regulated prolyl hydroxylation. In: *Science* 292 (5516), S. 468–472. DOI: 10.1126/science.1059796.
- Jaffe, E. A.; Nachman, R. L.; Becker, C. G.; Minick, C. R. (1973): Culture of human endothelial cells derived from umbilical veins. Identification by morphologic and immunologic criteria. In: *J. Clin. Invest.* 52 (11), S. 2745–2756. DOI: 10.1172/JCI107470.
- JAFFE, H. L.; SELIN, G. (1951): Tumors of bones and joints. In: *Bull N Y Acad Med* 27 (3), S. 165–174.

- Jain, Rakesh K. (2003): Molecular regulation of vessel maturation. In: *Nat. Med.* 9 (6), S. 685–693. DOI: 10.1038/nm0603-685.
- Jamieson, Elizabeth R.; Lippard, Stephen J. (1999): Structure, Recognition, and Processing of Cisplatin–DNA Adducts. In: *Chem. Rev.* 99 (9), S. 2467–2498. DOI: 10.1021/cr980421n.
- Jarcho, M. (1981): Calcium phosphate ceramics as hard tissue prosthetics. In: *Clin. Orthop. Relat. Res.* (157), S. 259–278.
- Jemal, Ahmedin; Bray, Freddie; Center, Melissa M.; Ferlay, Jacques; Ward, Elizabeth; Forman, David (2011): Global cancer statistics. In: *CA Cancer J Clin* 61 (2), S. 69–90. DOI: 10.3322/caac.20107.
- Jemal, Ahmedin; Siegel, Rebecca; Ward, Elizabeth; Hao, Yongping; Xu, Jiaquan; Murray, Taylor; Thun, Michael J. (2008): Cancer statistics, 2008. In: *CA Cancer J Clin* 58 (2), S. 71–96. DOI: 10.3322/CA.2007.0010.
- Jeong, B.; Choi, Y. K.; Bae, Y. H.; Zentner, G.; Kim, S. W. (1999): New biodegradable polymers for injectable drug delivery systems. In: *J Control Release* 62 (1-2), S. 109–114.
- Jung, Yongwon; Lippard, Stephen J. (2003): Multiple states of stalled T7 RNA polymerase at DNA lesions generated by platinum anticancer agents. In: *J. Biol. Chem.* 278 (52), S. 52084–52092. DOI: 10.1074/jbc.M310120200.
- Kaigler, Darnell; Krebsbach, Paul H.; Poverini, Peter J.; Mooney, David J. (2003): Role of vascular endothelial growth factor in bone marrow stromal cell modulation of endothelial cells. In: *Tissue Eng.* 9 (1), S. 95–103. DOI: 10.1089/107632703762687573.
- Kelland, Lloyd (2007): The resurgence of platinum-based cancer chemotherapy. In: *Nat. Rev. Cancer* 7 (8), S. 573–584. DOI: 10.1038/nrc2167.
- Khan, Yusuf; Yaszemski, Michael J.; Mikos, Antonios G.; Laurencin, Cato T. (2008): Tissue engineering of bone: material and matrix considerations. In: *J Bone Joint Surg Am* 90 Suppl 1, S. 36–42. DOI: 10.2106/JBJS.G.01260.
- Klein, C. P.; Driessen, A. A.; Groot, K. de; van den Hooff, A (1983): Biodegradation behavior of various calcium phosphate materials in bone tissue. In: *J. Biomed. Mater. Res.* 17 (5), S. 769–784. DOI: 10.1002/jbm.820170505.
- Klein, Michael J.; Siegal, Gene P. (2006): Osteosarcoma: anatomic and histologic variants. In: *Am. J. Clin. Pathol.* 125 (4), S. 555–581. DOI: 10.1309/UC6K-QHLD-9LV2-KENN.
- Kneser, Ulrich; Polykandriotis, Elias; Ohnolz, Jan; Heidner, Kristina; Grabinger, Lucia; Euler, Simon et al. (2006): Engineering of vascularized transplantable bone tissues: induction of axial vascularization in an osteoconductive matrix using an arteriovenous loop. In: *Tissue Eng.* 12 (7), S. 1721–1731. DOI: 10.1089/ten.2006.12.1721.
- Koblizek, T. I.; Weiss, C.; Yancopoulos, G. D.; Deutsch, U.; Risau, W. (1998): Angiopoietin-1 induces sprouting angiogenesis in vitro. In: *Curr. Biol.* 8 (9), S. 529–532.
- Koch, A. E.; Poverini, P. J.; Kunkel, S. L.; Harlow, L. A.; DiPietro, L. A.; Elner, V. M. et al. (1992): Interleukin-8 as a macrophage-derived mediator of angiogenesis. In: *Science* 258 (5089), S. 1798–1801.
- Kronenberg, Henry M. (2003): Developmental regulation of the growth plate. In: *Nature* 423 (6937), S. 332–336. DOI: 10.1038/nature01657.
- Lalan, S.; Pomerantseva, I.; Vacanti, J. P. (2001): Tissue engineering and its potential impact on surgery. In: *World J Surg* 25 (11), S. 1458–1466.

References

- Lamoureux, François; Trichet, Valérie; Chipoy, Céline; Blanchard, Frédéric; Gouin, François; Redini, Françoise (2007): Recent advances in the management of osteosarcoma and forthcoming therapeutic strategies. In: *Expert Rev Anticancer Ther* 7 (2), S. 169–181. DOI: 10.1586/14737140.7.2.169.
- Laschke, Matthias W.; Witt, Kristina; Pohlemann, Tim; Menger, Michael D. (2007): Injectable nanocrystalline hydroxyapatite paste for bone substitution: in vivo analysis of biocompatibility and vascularization. In: *J. Biomed. Mater. Res. Part B Appl. Biomater.* 82 (2), S. 494–505. DOI: 10.1002/jbm.b.30755.
- Lavertu, P.; Adelstein, D. J.; Saxton, J. P.; Secic, M.; Wanamaker, J. R.; Eliachar, I. et al. (1997): Management of the neck in a randomized trial comparing concurrent chemotherapy and radiotherapy with radiotherapy alone in resectable stage III and IV squamous cell head and neck cancer. In: *Head Neck* 19 (7), S. 559–566.
- Lee, D. D.; Tofighi, A.; Aiolova, M.; Chakravarthy, P.; Catalano, A.; Majahad, A.; Knaack, D. (1999): alpha-BSM: a biomimetic bone substitute and drug delivery vehicle. In: *Clin. Orthop. Relat. Res.* (367 Suppl), S. S396-405.
- Leeuwenberg, J. F.; Smeets, E. F.; Neefjes, J. J.; Shaffer, M. A.; Cinek, T.; Jeunhomme, T. M. et al. (1992): E-selectin and intercellular adhesion molecule-1 are released by activated human endothelial cells in vitro. In: *Immunology* 77 (4), S. 543–549.
- Leibovich, S. J.; Polverini, P. J.; Shepard, H. M.; Wiseman, D. M.; Shively, V.; Nuseir, N. (1987): Macrophage-induced angiogenesis is mediated by tumour necrosis factor-alpha. In: *Nature* 329 (6140), S. 630–632. DOI: 10.1038/329630a0.
- Leibovich, S. J.; Ross, R. (1975): The role of the macrophage in wound repair. A study with hydrocortisone and antimacrophage serum. In: *Am. J. Pathol.* 78 (1), S. 71–100.
- Leite de Oliveira, Rodrigo; Deschoemaeker, Sofie; Henze, Anne-Theres; Debackere, Koen; Finisguerra, Veronica; Takeda, Yukiji et al. (2012): Gene-targeting of Phd2 improves tumor response to chemotherapy and prevents side-toxicity. In: *Cancer Cell* 22 (2), S. 263–277. DOI: 10.1016/j.ccr.2012.06.028.
- Leprêtre, Stéphane; Chai, Feng; Hornez, Jean-Christophe; Vermet, Guillaume; Neut, Christel; Descamps, Michel et al. (2009): Prolonged local antibiotics delivery from hydroxyapatite functionalised with cyclodextrin polymers. In: *Biomaterials* 30 (30), S. 6086–6093. DOI: 10.1016/j.biomaterials.2009.07.045.
- Levenberg, Shulamit; Rouwkema, Jeroen; Macdonald, Mara; Garfein, Evan S.; Kohane, Daniel S.; Darland, Diane C. et al. (2005): Engineering vascularized skeletal muscle tissue. In: *Nat. Biotechnol.* 23 (7), S. 879–884. DOI: 10.1038/nbt1109.
- Ley, Klaus; Laudanna, Carlo; Cybulsky, Myron I.; Nourshargh, Sussan (2007): Getting to the site of inflammation: the leukocyte adhesion cascade updated. In: *Nat. Rev. Immunol.* 7 (9), S. 678–689. DOI: 10.1038/nri2156.
- Li, Aihua; Dubey, Seema; Varney, Michelle L.; Dave, Bhavana J.; Singh, Rakesh K. (2003): IL-8 directly enhanced endothelial cell survival, proliferation, and matrix metalloproteinases production and regulated angiogenesis. In: *J. Immunol.* 170 (6), S. 3369–3376.
- Li, Rongsong; Mouillesseaux, Kevin P.; Montoya, Dennis; Cruz, Daniel; Gharavi, Navid; Dun, Martin et al. (2006): Identification of prostaglandin E2 receptor subtype 2 as a receptor activated by OxPAPC. In: *Circ. Res.* 98 (5), S. 642–650. DOI: 10.1161/01.RES.0000207394.39249.fc.
- Li, Shan Hua; Shin, Dong Hoon; Chun, Yang-Sook; Lee, Myung Kyu; Kim, Myung-Suk; Park, Jong-Wan (2008): A novel mode of action of YC-1 in HIF inhibition: stimulation of

- FIH-dependent p300 dissociation from HIF-1{alpha}. In: *Mol. Cancer Ther.* 7 (12), S. 3729–3738. DOI: 10.1158/1535-7163.MCT-08-0074.
- Libby, Peter; Ridker, Paul M.; Maseri, Attilio (2002): Inflammation and atherosclerosis. In: *Circulation* 105 (9), S. 1135–1143.
- Liljensten, Elisabeth; Adolfsson, Erik; Strid, Karl-Gustav; Thomsen, Peter (2003): Resorbable and nonresorbable hydroxyapatite granules as bone graft substitutes in rabbit cortical defects. In: *Clin Implant Dent Relat Res* 5 (2), S. 95–101.
- Lin, Shan-Yang; Kawashima, Yoshiaki (2012): Current status and approaches to developing press-coated chronodelivery drug systems. In: *J Control Release* 157 (3), S. 331–353. DOI: 10.1016/j.jconrel.2011.09.065.
- Lindahl, P.; Hellström, M.; Kalén, M.; Karlsson, L.; Pekny, M.; Pekna, M. et al. (1998): Paracrine PDGF-B/PDGF-Rbeta signaling controls mesangial cell development in kidney glomeruli. In: *Development* 125 (17), S. 3313–3322.
- Liu, Qian; Liang, Yun; Zou, Ping; Ni, Wei-Xin; Li, Yu-Guang; Chen, Song-Ming (2013): Hypoxia-inducible factor-1 α polymorphisms link to coronary artery collateral development and clinical presentation of coronary artery disease. In: *Biomed Pap Med Fac Univ Palacky Olomouc Czech Repub.* DOI: 10.5507/bp.2013.061.
- Liu, Xin-Ming; Wiswall, Andrew T.; Rutledge, John E.; Akhter, Mohammed P.; Cullen, Diane M.; Reinhardt, Richard A.; Wang, Dong (2008): Osteotropic beta-cyclodextrin for local bone regeneration. In: *Biomaterials* 29 (11), S. 1686–1692. DOI: 10.1016/j.biomaterials.2007.12.023.
- Longhi, Alessandra; Ferrari, Stefano; Tamburini, Angela; Luksch, Roberto; Fagioli, Franca; Bacci, Gaetano; Ferrari, Cristina (2012): Late effects of chemotherapy and radiotherapy in osteosarcoma and Ewing sarcoma patients: the Italian Sarcoma Group Experience (1983-2006). In: *Cancer* 118 (20), S. 5050–5059. DOI: 10.1002/cncr.27493.
- Loree, T. R.; Strong, E. W. (1990): Significance of positive margins in oral cavity squamous carcinoma. In: *Am. J. Surg.* 160 (4), S. 410–414.
- Loukas, Y. L. (1997): Evaluation of the methods for the determination of the stability constant of cyclodextrin-chlorambucil inclusion complexes. In: *J Pharm Biomed Anal* 16 (2), S. 275–280.
- Love, R. R.; Leventhal, H.; Easterling, D. V.; Nerenz, D. R. (1989): Side effects and emotional distress during cancer chemotherapy. In: *Cancer* 63 (3), S. 604–612.
- Lowe, S. W.; Ruley, H. E.; Jacks, T.; Housman, D. E. (1993): p53-dependent apoptosis modulates the cytotoxicity of anticancer agents. In: *Cell* 74 (6), S. 957–967.
- Maclaine, Nicola J.; Hupp, Ted R. (2009): The regulation of p53 by phosphorylation: a model for how distinct signals integrate into the p53 pathway. In: *Aging (Albany NY)* 1 (5), S. 490–502.
- Malawer et al. (2008): Sarcomas of Bone 2008.
- Malda, J.; Woodfield, T B F; van der Vloodt, F; Kooy, F. K.; Martens, D. E.; Tramper, J. et al. (2004): The effect of PEGT/PBT scaffold architecture on oxygen gradients in tissue engineered cartilaginous constructs. In: *Biomaterials* 25 (26), S. 5773–5780. DOI: 10.1016/j.biomaterials.2004.01.028.
- Malhotra, Vikas; Perry, Michael C. (2003): Classical chemotherapy: mechanisms, toxicities and the therapeutic window. In: *Cancer Biol. Ther.* 2 (4 Suppl 1), S. S2-4.
- Martel, B. (2002): Finishing of Polyester Fabrics with Cyclodextrins and Polycarboxylic Acids as Crosslinking Agents.

References

- Martel, B.; Weltrowski, M.; Ruffin, D.; Morcellet, M. (2002): Polycarboxylic acids as crosslinking agents for grafting cyclodextrins onto cotton and wool fabrics: Study of the process parameters. In: *J. Appl. Polym. Sci.* 83 (7), S. 1449–1456. DOI: 10.1002/app.2306.
- Martin, Paul; Leibovich, S. Joseph (2005): Inflammatory cells during wound repair: the good, the bad and the ugly. In: *Trends Cell Biol.* 15 (11), S. 599–607. DOI: 10.1016/j.tcb.2005.09.002.
- Masatsugu, Toshihiro; Yamamoto, Ken (2009): Multiple lysine methylation of PCAF by Set9 methyltransferase. In: *Biochem. Biophys. Res. Commun.* 381 (1), S. 22–26. DOI: 10.1016/j.bbrc.2009.01.185.
- Maxwell, P. H.; Wiesener, M. S.; Chang, G. W.; Clifford, S. C.; Vaux, E. C.; Cockman, M. E. et al. (1999): The tumour suppressor protein VHL targets hypoxia-inducible factors for oxygen-dependent proteolysis. In: *Nature* 399 (6733), S. 271–275. DOI: 10.1038/20459.
- McLaren, J.; Prentice, A.; Charnock-Jones, D. S.; Millican, S. A.; Müller, K. H.; Sharkey, A. M.; Smith, S. K. (1996): Vascular endothelial growth factor is produced by peritoneal fluid macrophages in endometriosis and is regulated by ovarian steroids. In: *J. Clin. Invest.* 98 (2), S. 482–489. DOI: 10.1172/JCI118815.
- Meijer, Gert J.; de Bruijn, Joost D; Koole, Ron; Van Blitterswijk, Clemens A (2007): Cell-based bone tissue engineering. In: *PLoS Med.* 4 (2), S. e9. DOI: 10.1371/journal.pmed.0040009.
- Mercatali, Laura; Ibrahim, Toni; Sacanna, Emanuele; Flamini, Emanuela; Scarpi, Emanuela; Calistri, Daniele et al. (2011): Bone metastases detection by circulating biomarkers: OPG and RANK-L. In: *Int. J. Oncol.* 39 (1), S. 255–261. DOI: 10.3892/ijo.2011.1001.
- Merli, M.; Benassi, M. S.; Gamberi, G.; Ragazzini, P.; Sollazzo, M. R.; Molendini, L. et al. (1999): Expression of G1 phase regulators in MG-63 osteosarcoma cell line. In: *Int. J. Oncol.* 14 (6), S. 1117–1121.
- Miyata, Toshio; Takizawa, Shunya; van Ypersele de Strihou, Charles (2011): Hypoxia. 1. Intracellular sensors for oxygen and oxidative stress: novel therapeutic targets. In: *Am. J. Physiol., Cell Physiol.* 300 (2), S. C226-31. DOI: 10.1152/ajpcell.00430.2010.
- Mohamed, Khaled M.; Le, Anh; Duong, Hai; Wu, Yidi; Zhang, Qunzhou; Messadi, Diana V. (2004): Correlation between VEGF and HIF-1alpha expression in human oral squamous cell carcinoma. In: *Exp. Mol. Pathol.* 76 (2), S. 143–152. DOI: 10.1016/j.yexmp.2003.10.005.
- Monnet, Jordan; Kozelka, Jiří (2012): Cisplatin GG-crosslinks within single-stranded DNA: origin of the preference for left-handed helicity. In: *J. Inorg. Biochem.* 115, S. 106–112. DOI: 10.1016/j.jinorgbio.2012.05.015.
- Moore, A. S.; Kirk, C.; Cardona, A. (1991): Intracavitary cisplatin chemotherapy experience with six dogs. In: *J. Vet. Intern. Med.* 5 (4), S. 227–231.
- Morgan, D. O. (1995): Principles of CDK regulation. In: *Nature* 374 (6518), S. 131–134. DOI: 10.1038/374131a0.
- Motro, B.; Itin, A.; Sachs, L.; Keshet, E. (1990): Pattern of interleukin 6 gene expression in vivo suggests a role for this cytokine in angiogenesis. In: *Proc. Natl. Acad. Sci. U.S.A.* 87 (8), S. 3092–3096.
- Nagaoka, T.; Kaburagi, Y.; Hamaguchi, Y.; Hasegawa, M.; Takehara, K.; Steeber, D. A. et al. (2000): Delayed wound healing in the absence of intercellular adhesion molecule-1 or L-selectin expression. In: *Am. J. Pathol.* 157 (1), S. 237–247. DOI: 10.1016/S0002-9440(10)64534-8.

- Napoleone Ferrara (2003): The role of VEGF and its receptors. In: *Nature Medicine* 2003 (Volume Number 6), S. 669–676.
- Nerem, R. M.; Sambanis, A. (1995): Tissue engineering: from biology to biological substitutes. In: *Tissue Eng.* 1 (1), S. 3–13. DOI: 10.1089/ten.1995.1.3.
- Nissen, N. N.; Polverini, P. J.; Koch, A. E.; Volin, M. V.; Gamelli, R. L.; DiPietro, L. A. (1998): Vascular endothelial growth factor mediates angiogenic activity during the proliferative phase of wound healing. In: *Am. J. Pathol.* 152 (6), S. 1445–1452.
- Ogose, Akira; Hotta, Tetsuo; Kawashima, Hiroyuki; Kondo, Naoki; Gu, Wenguang; Kamura, Takeshi; Endo, Naoto (2005): Comparison of hydroxyapatite and beta tricalcium phosphate as bone substitutes after excision of bone tumors. In: *J. Biomed. Mater. Res. Part B Appl. Biomater.* 72 (1), S. 94–101. DOI: 10.1002/jbm.b.30136.
- Oh, S. P.; Seki, T.; Goss, K. A.; Imamura, T.; Yi, Y.; Donahoe, P. K. et al. (2000): Activin receptor-like kinase 1 modulates transforming growth factor-beta 1 signaling in the regulation of angiogenesis. In: *Proc. Natl. Acad. Sci. U.S.A.* 97 (6), S. 2626–2631.
- Ono, M.; Torisu, H.; Fukushi, J.; Nishie, A.; Kuwano, M. (1999): Biological implications of macrophage infiltration in human tumor angiogenesis. In: *Cancer Chemother. Pharmacol.* 43 Suppl, S. S69-71.
- Ottaviani, Giulia; Jaffe, Norman (2009): The epidemiology of osteosarcoma. In: *Cancer Treat. Res.* 152, S. 3–13. DOI: 10.1007/978-1-4419-0284-9_1.
- Palabrica, T.; Lobb, R.; Furie, B. C.; Aronovitz, M.; Benjamin, C.; Hsu, Y. M. et al. (1992): Leukocyte accumulation promoting fibrin deposition is mediated in vivo by P-selectin on adherent platelets. In: *Nature* 359 (6398), S. 848–851. DOI: 10.1038/359848a0.
- Park, E. K.; Jung, H. S.; Yang, H. I.; Yoo, M. C.; Kim, C.; Kim, K. S. (2007): Optimized THP-1 differentiation is required for the detection of responses to weak stimuli. In: *Inflamm. Res.* 56 (1), S. 45–50. DOI: 10.1007/s00011-007-6115-5.
- Parkin, D. Max; Bray, Freddie; Ferlay, J.; Pisani, Paola (2005): Global cancer statistics, 2002. In: *CA Cancer J Clin* 55 (2), S. 74–108.
- Partridge, M.; Li, S. R.; Pateromichelakis, S.; Francis, R.; Phillips, E.; Huang, X. H. et al. (2000): Detection of minimal residual cancer to investigate why oral tumors recur despite seemingly adequate treatment. In: *Clin. Cancer Res.* 6 (7), S. 2718–2725.
- Pepper, M. S. (1997): Manipulating angiogenesis. From basic science to the bedside. In: *Arterioscler. Thromb. Vasc. Biol.* 17 (4), S. 605–619.
- Pepper, M. S. (2001): Role of the matrix metalloproteinase and plasminogen activator-plasmin systems in angiogenesis. In: *Arterioscler. Thromb. Vasc. Biol.* 21 (7), S. 1104–1117.
- Peters, Kirsten; Unger, Ronald E.; Brunner, Joachim; Kirkpatrick, C. James (2003): Molecular basis of endothelial dysfunction in sepsis. In: *Cardiovasc. Res.* 60 (1), S. 49–57.
- Poklar, N.; Pilch, D. S.; Lippard, S. J.; Redding, E. A.; Dunham, S. U.; Breslauer, K. J. (1996): Influence of cisplatin intrastrand crosslinking on the conformation, thermal stability, and energetics of a 20-mer DNA duplex. In: *Proc. Natl. Acad. Sci. U.S.A.* 93 (15), S. 7606–7611.
- Prestayko, A. W.; D'Aoust, J. C.; Issell, B. F.; Crooke, S. T. (1979): Cisplatin (cis-diamminedichloroplatinum II). In: *Cancer Treat. Rev.* 6 (1), S. 17–39.
- Price, Peter M.; Safirstein, Robert L.; Megyesi, Judit (2004): Protection of renal cells from cisplatin toxicity by cell cycle inhibitors. In: *Am. J. Physiol. Renal Physiol.* 286 (2), S. F378-84. DOI: 10.1152/ajprenal.00192.2003.

References

- Prives, C.; Hall, P. A. (1999): The p53 pathway. In: *J. Pathol.* 187 (1), S. 112–126. DOI: 10.1002/(SICI)1096-9896(199901)187:1<112::AID-PATH250>3.0.CO;2-3.
- Pujol, J. L.; Carestia, L.; Daurès, J. P. (2000): Is there a case for cisplatin in the treatment of small-cell lung cancer? A meta-analysis of randomized trials of a cisplatin-containing regimen versus a regimen without this alkylating agent. In: *Br. J. Cancer* 83 (1), S. 8–15. DOI: 10.1054/bjoc.2000.1164.
- Rajani Ravi et al.: Regulation of tumor angiogenesis by p53-induced degradation of hypoxia-inducible factor 1a 1999.
- Rao, Rameshwar R.; Stegemann, Jan P. (2013): Cell-based approaches to the engineering of vascularized bone tissue. In: *Cytotherapy* 15 (11), S. 1309–1322. DOI: 10.1016/j.jcyt.2013.06.005.
- Rathbone, C. R.; Guda, T.; Singleton, B. M.; Oh, D. S.; Appleford, M. R.; Ong, J. L.; Wenke, J. C. (2013): Effect of cell-seeded hydroxyapatite scaffolds on rabbit radius bone regeneration. In: *J Biomed Mater Res A*. DOI: 10.1002/jbm.a.34834.
- Reinke, J. M.; Sorg, H. (2012): Wound repair and regeneration. In: *Eur Surg Res* 49 (1), S. 35–43. DOI: 10.1159/000339613.
- Renbin Zhao,¹ Kurt Gish,³ Maureen Murphy,^{2,6} Yuxin Yin,^{4,6} Daniel Notterman,^{1,6} (2000): Analysis of p53-regulated gene expression patterns using oligonucleotide arrays: Cold Spring Harbor Laboratory Press.
- Riley, Todd; Sontag, Eduardo; Chen, Patricia; Levine, Arnold (2008): Transcriptional control of human p53-regulated genes. In: *Nat. Rev. Mol. Cell Biol.* 9 (5), S. 402–412. DOI: 10.1038/nrm2395.
- Rivron, N.C., et al. (2008): Engineering vascularised tissues in vitro: AO Foundation.
- Robson, M. C.; Steed, D. L.; Franz, M. G. (2001): Wound healing: biologic features and approaches to maximize healing trajectories. In: *Curr Probl Surg* 38 (2), S. 72–140. DOI: 10.1067/msg.2001.111167.
- Rose, Felicity R A J; Oreffo, Richard O C (2002): Bone tissue engineering: hope vs hype. In: *Biochem. Biophys. Res. Commun.* 292 (1), S. 1–7. DOI: 10.1006/bbrc.2002.6519.
- Rouwkema, Jeroen; Boer, Jan de; Van Blitterswijk, Clemens A (2006): Endothelial cells assemble into a 3-dimensional prevascular network in a bone tissue engineering construct. In: *Tissue Eng.* 12 (9), S. 2685–2693. DOI: 10.1089/ten.2006.12.2685.
- Rouwkema, Jeroen; Rivron, Nicolas C.; Van Blitterswijk, Clemens A (2008): Vascularization in tissue engineering. In: *Trends Biotechnol.* 26 (8), S. 434–441. DOI: 10.1016/j.tibtech.2008.04.009.
- Rubanyi, G. M.; Polokoff, M. A. (1994): Endothelins: molecular biology, biochemistry, pharmacology, physiology, and pathophysiology. In: *Pharmacol. Rev.* 46 (3), S. 325–415.
- Ryan, K. M.; Phillips, A. C.; Vousden, K. H. (2001): Regulation and function of the p53 tumor suppressor protein. In: *Curr. Opin. Cell Biol.* 13 (3), S. 332–337.
- Sánchez-Puig, Nuria; Veprintsev, Dmitry B.; Fersht, Alan R. (2005): Binding of natively unfolded HIF-1 α ODD domain to p53. In: *Mol. Cell* 17 (1), S. 11–21. DOI: 10.1016/j.molcel.2004.11.019.
- Santos, Marina I.; Unger, Ronald E.; Sousa, Rui A.; Reis, Rui L.; Kirkpatrick, C. James (2009): Crosstalk between osteoblasts and endothelial cells co-cultured on a polycaprolactone–starch scaffold and the in vitro development of vascularization. In: *Biomaterials* 30 (26), S. 4407–4415. DOI: 10.1016/j.biomaterials.2009.05.004.

- Schanz, Johanna; Pusch, Jacqueline; Hansmann, Jan; Walles, Heike (2010): Vascularised human tissue models: a new approach for the refinement of biomedical research. In: *J. Biotechnol.* 148 (1), S. 56–63. DOI: 10.1016/j.jbiotec.2010.03.015.
- Schroeder, Josh E.; Mosheiff, Rami (2011): Tissue engineering approaches for bone repair: concepts and evidence. In: *Injury* 42 (6), S. 609–613. DOI: 10.1016/j.injury.2011.03.029.
- Schuler, M.; Bossy-Wetzel, E.; Goldstein, J. C.; Fitzgerald, P.; Green, D. R. (2000): p53 induces apoptosis by caspase activation through mitochondrial cytochrome c release. In: *J. Biol. Chem.* 275 (10), S. 7337–7342.
- Seiler, C.; Pohl, T.; Wustmann, K.; Hutter, D.; Nicolet, P. A.; Windecker, S. et al. (2001): Promotion of collateral growth by granulocyte-macrophage colony-stimulating factor in patients with coronary artery disease: a randomized, double-blind, placebo-controlled study. In: *Circulation* 104 (17), S. 2012–2017.
- Semenza, Gregg L. (2003): Targeting HIF-1 for cancer therapy. In: *Nat. Rev. Cancer* 3 (10), S. 721–732. DOI: 10.1038/nrc1187.
- Shah, Jatin P.; Gil, Ziv (2009): Current concepts in management of oral cancer--surgery. In: *Oral Oncol.* 45 (4-5), S. 394–401. DOI: 10.1016/j.oraloncology.2008.05.017.
- Shen, Y.; White, E. (2001): p53-dependent apoptosis pathways. In: *Adv. Cancer Res.* 82, S. 55–84.
- Shibuya, Masabumi (2006): Differential roles of vascular endothelial growth factor receptor-1 and receptor-2 in angiogenesis. In: *J. Biochem. Mol. Biol.* 39 (5), S. 469–478.
- Shum, Lillian; Coleman, Cynthia M.; Hatakeyama, Yuji; Tuan, Rocky S. (2003): Morphogenesis and dysmorphogenesis of the appendicular skeleton. In: *Birth Defects Res. C Embryo Today* 69 (2), S. 102–122. DOI: 10.1002/bdrc.10012.
- Simunovic, F.; Steiner, D.; Pfeifer, D.; Stark, G. B.; Finkenzeller, Günter; Lampert, F. (2013): Increased extracellular matrix and proangiogenic factor transcription in endothelial cells after cocultivation with primary human osteoblasts. In: *J. Cell. Biochem.* 114 (7), S. 1584–1594. DOI: 10.1002/jcb.24500.
- Sinha, V. R.; Singla, A. K.; Wadhawan, S.; Kaushik, R.; Kumria, R.; Bansal, K.; Dhawan, S. (2004): Chitosan microspheres as a potential carrier for drugs. In: *Int J Pharm* 274 (1-2), S. 1–33. DOI: 10.1016/j.ijpharm.2003.12.026.
- Soengas, M. S.; Alarcón, R. M.; Yoshida, H.; Giaccia, A. J.; Hakem, R.; Mak, T. W.; Lowe, S. W. (1999): Apaf-1 and caspase-9 in p53-dependent apoptosis and tumor inhibition. In: *Science* 284 (5411), S. 156–159.
- Sorenson, C. M.; Eastman, A. (1988): Mechanism of cis-diamminedichloroplatinum(II)-induced cytotoxicity: role of G2 arrest and DNA double-strand breaks. In: *Cancer Res.* 48 (16), S. 4484–4488.
- Springer, T. A. (1994): Traffic signals for lymphocyte recirculation and leukocyte emigration: the multistep paradigm. In: *Cell* 76 (2), S. 301–314.
- Steel, D. M.; Whitehead, A. S. (1994): The major acute phase reactants: C-reactive protein, serum amyloid P component and serum amyloid A protein. In: *Immunol. Today* 15 (2), S. 81–88. DOI: 10.1016/0167-5699(94)90138-4.
- Steensberg, Adam; Fischer, Christian P.; Keller, Charlotte; Møller, Kirsten; Pedersen, Bente Klarlund (2003): IL-6 enhances plasma IL-1ra, IL-10, and cortisol in humans. In: *Am. J. Physiol. Endocrinol. Metab.* 285 (2), S. E433-7. DOI: 10.1152/ajpendo.00074.2003.

References

- Stetler-Stevenson, W. G. (1999): Matrix metalloproteinases in angiogenesis: a moving target for therapeutic intervention. In: *J. Clin. Invest.* 103 (9), S. 1237–1241. DOI: 10.1172/JCI6870.
- Street, John; Bao, Min; deGuzman, Leo; Bunting, Stuart; Peale, Franklin V.; Ferrara, Napoleone et al. (2002): Vascular endothelial growth factor stimulates bone repair by promoting angiogenesis and bone turnover. In: *Proc. Natl. Acad. Sci. U.S.A.* 99 (15), S. 9656–9661. DOI: 10.1073/pnas.152324099.
- Subramaniam, M.; Saffaripour, S.; Van De Water, L.; Frenette, P. S.; Mayadas, T. N.; Hynes, R. O.; Wagner, D. D. (1997): Role of endothelial selectins in wound repair. In: *Am. J. Pathol.* 150 (5), S. 1701–1709.
- Sundberg, Christian; Kowanetz, Marcin; Brown, Lawrence F.; Detmar, Michael; Dvorak, Harold F. (2002): Stable expression of angiopoietin-1 and other markers by cultured pericytes: phenotypic similarities to a subpopulation of cells in maturing vessels during later stages of angiogenesis in vivo. In: *Lab. Invest.* 82 (4), S. 387–401.
- Sunderkötter, C.; Steinbrink, K.; Goebeler, M.; Bhardwaj, R.; Sorg, C. (1994): Macrophages and angiogenesis. In: *J. Leukoc. Biol.* 55 (3), S. 410–422.
- Suzuki, E.; Nagata, D.; Yoshizumi, M.; Kakoki, M.; Goto, A.; Omata, M.; Hirata, Y. (2000): Reentry into the cell cycle of contact-inhibited vascular endothelial cells by a phosphatase inhibitor. Possible involvement of extracellular signal-regulated kinase and phosphatidylinositol 3-kinase. In: *J. Biol. Chem.* 275 (5), S. 3637–3644.
- Swift, Lonnie P.; Rephaeli, Ada; Nudelman, Abraham; Phillips, Don R.; Cutts, Suzanne M. (2006): Doxorubicin-DNA adducts induce a non-topoisomerase II-mediated form of cell death. In: *Cancer Res.* 66 (9), S. 4863–4871. DOI: 10.1158/0008-5472.CAN-05-3410.
- Tewey, K. M.; Rowe, T. C.; Yang, L.; Halligan, B. D.; Liu, L. F. (1984): Adriamycin-induced DNA damage mediated by mammalian DNA topoisomerase II. In: *Science* 226 (4673), S. 466–468.
- Thabet, M. H.; Talaat, M.; Rizk, A. M. (2000): Pitfalls in the surgical management of cancer of the larynx and hypopharynx. In: *Otolaryngol Head Neck Surg* 123 (4), S. 482–487. DOI: 10.1067/mhn.2000.105062.
- Thorn, Caroline F.; Oshiro, Connie; Marsh, Sharon; Hernandez-Boussard, Tina; McLeod, Howard; Klein, Teri E.; Altman, Russ B. (2011): Doxorubicin pathways. In: *Pharmacogenetics and Genomics* 21 (7), S. 440–446. DOI: 10.1097/FPC.0b013e32833ffb56.
- Thurston, Gavin; Daly, Christopher (2012): The complex role of angiopoietin-2 in the angiopoietin-tie signaling pathway. In: *Cold Spring Harb Perspect Med* 2 (9), S. a006550. DOI: 10.1101/cshperspect.a006550.
- Tiwari, Gaurav; Tiwari, Ruchi; Rai, Awani K. (2010): Cyclodextrins in delivery systems: Applications. In: *J Pharm Bioallied Sci* 2 (2), S. 72–79. DOI: 10.4103/0975-7406.67003.
- Tjiu, Jeng-Wei; Chen, Jau-Shiuh; Shun, Chia-Tung; Lin, Sung-Jan; Liao, Yi-Hua; Chu, Chia-Yu et al. (2009): Tumor-associated macrophage-induced invasion and angiogenesis of human basal cell carcinoma cells by cyclooxygenase-2 induction. In: *J. Invest. Dermatol.* 129 (4), S. 1016–1025. DOI: 10.1038/jid.2008.310.
- Toguchida, J.; Yamaguchi, T.; Ritchie, B.; Beauchamp, R. L.; Dayton, S. H.; Herrera, G. E. et al. (1992): Mutation spectrum of the p53 gene in bone and soft tissue sarcomas. In: *Cancer Res.* 52 (22), S. 6194–6199.
- Topley, N.; Jörres, A.; Luttmann, W.; Petersen, M. M.; Lang, M. J.; Thierauch, K. H. et al. (1993): Human peritoneal mesothelial cells synthesize interleukin-6: induction by IL-1 beta and TNF alpha. In: *Kidney Int.* 43 (1), S. 226–233.

- Tran, Jennifer; Master, Zubin; Yu, Joanne L.; Rak, Janusz; Dumont, Daniel J.; Kerbel, Robert S. (2002): A role for survivin in chemoresistance of endothelial cells mediated by VEGF. In: *Proc. Natl. Acad. Sci. U.S.A.* 99 (7), S. 4349–4354. DOI: 10.1073/pnas.072586399.
- Tsaryk et al. (2007): The effects of metal implants on inflammatory and healing processes. In: *Int. J. Mat. Res.* 2007.
- Tsan, M.F., White, J.E., Maheshwari, J. G.; Bremner, T. A.; Sacco, J.: Resveratrol induces Fas signalling-independent apoptosis in THP-1 human monocytic leukaemia. In: *Br. J. Haematol. (British journal of haematology)*. 2000. 109 (2), S. 405-412
- Tsuchiya, S.; Yamabe, M.; Yamaguchi, Y.; Kobayashi, Y.; Konno, T.; Tada, K. (1980): Establishment and characterization of a human acute monocytic leukemia cell line (THP-1). In: *Int. J. Cancer* 26 (2), S. 171–176.
- Uekama, Kaneto; Hirayama, Fumitoshi; Irie, Tetsumi (1998): Cyclodextrin Drug Carrier Systems. In: *Chem. Rev. (Chemical Reviews)* 98 (5), S. 2045–2076
- Unger, Ronald E.; Halstenberg, Sven; Sartoris, Anne; Kirkpatrick, C. James (2011): Human endothelial and osteoblast co-cultures on 3D biomaterials. In: *Methods Mol. Biol.* 695, S. 229–241. DOI: 10.1007/978-1-60761-984-0_15.
- Unger, Ronald E.; Krump-Konvalinkova, Vera; Peters, Kirsten; Kirkpatrick, C. James (2002): In vitro expression of the endothelial phenotype: comparative study of primary isolated cells and cell lines, including the novel cell line HPMEC-ST1.6R. In: *Microvasc. Res.* 64 (3), S. 384–397.
- Unger, Ronald E.; Sartoris, Anne; Peters, Kirsten; Motta, Antonella; Migliaresi, Claudio; Kunkel, Martin et al. (2007): Tissue-like self-assembly in cocultures of endothelial cells and osteoblasts and the formation of microcapillary-like structures on three-dimensional porous biomaterials. In: *Biomaterials* 28 (27), S. 3965–3976. DOI: 10.1016/j.biomaterials.2007.05.032.
- Upile, T.; Fisher, C.; Jerjes, W.; El Maaytah, M.; Searle, A.; Archer, D. et al. (2007): The uncertainty of the surgical margin in the treatment of head and neck cancer. In: *Oral Oncol.* 43 (4), S. 321–326. DOI: 10.1016/j.oraloncology.2006.08.002.
- Vacanti, J. P.; Langer, R. (1999): Tissue engineering: the design and fabrication of living replacement devices for surgical reconstruction and transplantation. In: *Lancet* 354 Suppl 1, S. S132-4.
- Vallet-Regí, María; Colilla, Montserrat; González, Blanca (2011): Medical applications of organic-inorganic hybrid materials within the field of silica-based bioceramics. In: *Chem Soc Rev* 40 (2), S. 596–607. DOI: 10.1039/c0cs00025f.
- Vassalli, P. (1992): The pathophysiology of tumor necrosis factors. In: *Annu. Rev. Immunol.* 10, S. 411–452. DOI: 10.1146/annurev.iy.10.040192.002211.
- Venitt, S. (1996): Mechanisms of spontaneous human cancers. In: *Environ. Health Perspect.* 104 Suppl 3, S. 633–637.
- Villars, F.; Bordenave, L.; Bareille, R.; Amédée, J. (2000): Effect of human endothelial cells on human bone marrow stromal cell phenotype: role of VEGF? In: *J. Cell. Biochem.* 79 (4), S. 672–685.
- Villars, F.; Guillotin, B.; Amédée, T.; Dutoya, S.; Bordenave, L.; Bareille, R.; Amédée, J. (2002): Effect of HUVEC on human osteoprogenitor cell differentiation needs heterotypic gap junction communication. In: *Am. J. Physiol., Cell Physiol.* 282 (4), S. C775-85. DOI: 10.1152/ajpcell.00310.2001.
- Visconti, Richard P.; Richardson, Charlene D.; Sato, Thomas N. (2002): Orchestration of angiogenesis and arteriovenous contribution by angiopoietins and vascular

References

- endothelial growth factor (VEGF). In: *Proc. Natl. Acad. Sci. U.S.A.* 99 (12), S. 8219–8224. DOI: 10.1073/pnas.122109599.
- Wade Harper, J. (1993): The p21 Cdk-interacting protein Cip1 is a potent inhibitor of G1 cyclin-dependent kinases. In: *Cell* 75 (4), S. 805–816. DOI: 10.1016/0092-8674(93)90499-G.
- Wagner, Jill M.; Karnitz, Larry M. (2009): Cisplatin-induced DNA damage activates replication checkpoint signaling components that differentially affect tumor cell survival. In: *Mol. Pharmacol.* 76 (1), S. 208–214. DOI: 10.1124/mol.109.055178.
- Weiss, R. B. (1992): The anthracyclines: will we ever find a better doxorubicin? In: *Semin. Oncol.* 19 (6), S. 670–686.
- Wenger, A.; Stahl, A.; Weber, H.; Finkenzeller, G.; Augustin, H. G.; Stark, G. B.; Kneser, U. (2004): Modulation of in vitro angiogenesis in a three-dimensional spheroidal coculture model for bone tissue engineering. In: *Tissue Eng.* 10 (9-10), S. 1536–1547. DOI: 10.1089/ten.2004.10.1536.
- Werner, Sabine; Grose, Richard (2003): Regulation of wound healing by growth factors and cytokines. In: *Physiol. Rev.* 83 (3), S. 835–870. DOI: 10.1152/physrev.00031.2002.
- WHO (2013): Cancer. Hg. v. World Health Organization. World Health Organization. Online verfügbar unter <http://www.who.int/mediacentre/factsheets/fs297/en/>, zuletzt aktualisiert am January 2013.
- Winkler, K.; Beron, G.; Delling, G.; Heise, U.; Kabisch, H.; Purfürst, C. et al. (1988): Neoadjuvant chemotherapy of osteosarcoma: results of a randomized cooperative trial (COSS-82) with salvage chemotherapy based on histological tumor response. In: *J. Clin. Oncol.* 6 (2), S. 329–337.
- Wolfram Saenger (1980): Cyclodextrin Inclusion Compounds in Research and Industry. In: *Angewandte Chemie International Edition in English* 1980 (19, Issue 5), S. 344–362.
- Woods, D. B.; Vousden, K. H. (2001): Regulation of p53 function. In: *Exp. Cell Res.* 264 (1), S. 56–66. DOI: 10.1006/excr.2000.5141.
- Yamamoto, T.; Onga, T.; Marui, T.; Mizuno, K. (2000): Use of hydroxyapatite to fill cavities after excision of benign bone tumours. Clinical results. In: *J Bone Joint Surg Br* 82 (8), S. 1117–1120.
- Yannas, Ioannis V. (Hg.) (2005): Regenerative Medicine II. Berlin, Heidelberg: Springer Berlin Heidelberg (Advances in Biochemical Engineering/Biotechnology).
- Yarmish, G.; Klein, M. J.; Landa, J.; Lefkowitz, R. A.; Hwang, S. (2010): Imaging Characteristics of Primary Osteosarcoma: Nonconventional Subtypes. In: *Radiographics* 30 (6), S. 1653–1672. DOI: 10.1148/rg.306105524.
- Young, R. C.; Ozols, R. F.; Myers, C. E. (1981): The anthracycline antineoplastic drugs. In: *N. Engl. J. Med.* 305 (3), S. 139–153. DOI: 10.1056/NEJM198107163050305.
- Yue, X.; Tomanek, R. J. (2001): Effects of VEGF(165) and VEGF(121) on vasculogenesis and angiogenesis in cultured embryonic quail hearts. In: *Am. J. Physiol. Heart Circ. Physiol.* 280 (5), S. H2240-7.
- Zenmyo, M.; Komiya, S.; Hamada, T.; Hiraoka, K.; Kato, S.; Fujii, T. et al. (2001): Transcriptional activation of p21 by vitamin D(3) or vitamin K(2) leads to differentiation of p53-deficient MG-63 osteosarcoma cells. In: *Hum. Pathol.* 32 (4), S. 410–416. DOI: 10.1053/hupa.2001.23524.
- Zhang, Xiaohong; Qi, Rong; Xian, Xunde; Yang, Fei; Blackstein, Michael; Deng, Xuming et al. (2008): Spontaneous atherosclerosis in aged lipoprotein lipase-deficient

mice with severe hypertriglyceridemia on a normal chow diet. In: *Circ. Res.* 102 (2), S. 250–256. DOI: 10.1161/CIRCRESAHA.107.156554.

Zhong, H.; De Marzo, A M; Laughner, E.; Lim, M.; Hilton, D. A.; Zagzag, D. et al. (1999): Overexpression of hypoxia-inducible factor 1 alpha in common human cancers and their metastases. In: *Cancer Res.* 59 (22), S. 5830–5835.

Zhou, A. L.; Egginton, S.; Brown, M. D.; Hudlicka, O. (1998): Capillary growth in overloaded, hypertrophic adult rat skeletal muscle: an ultrastructural study. In: *Anat. Rec.* 252 (1), S. 49–63.

Zhou, Hong-Zhi; Yu, Hua; Xue, Yang (2009): In vivo self-expanding engineering of bone. In: *Med. Hypotheses* 73 (4), S. 528–530. DOI: 10.1016/j.mehy.2009.06.006.

8 List of figures

Figure 1: Scheme of tissue engineered bone regeneration constructs.....	- 2 -
Figure 2: Schematic of the process of bone fracture healing, shows the major cell and matrix types involved at each stage	- 4 -
Figure 3: Activation phase of wound healing.....	- 7 -
Figure 4: Proliferative phase of wound healing	- 8 -
Figure 5: p53 pathway	- 12 -
Figure 6: DNA damage induced cell cycle arrest	- 13 -
Figure 7: Apoptosis pathway	- 14 -
Figure 8: HIF-1 α pathway.....	- 15 -
Figure 9: β -Cyclodextrin	- 22 -
Figure 10: Drug delivery from anticancer agent treated cyclodextrin functionalized hydroxyapatite	- 23 -
Figure 11: Crosslinks in DNA formed by cisplatin	- 18 -
Figure 12: Doxorubicin	- 19 -
Figure 13: Chemical reaction of CytoTox 96® Non-Radio Cytotoxicity Assay.....	- 39 -
Figure 14: Images of light microscopy.....	- 42 -
Figure 15: Osbone® hydroxyapatite granules (HA) and cyclodextrin-functionalized hydroxyapatite granules (HACD).....	- 42 -
Figure 16: Scheme of extraction assay	- 43 -
Figure 17: Scheme of extraction assay	- 45 -
Figure 18: Scheme of extraction assay: 24/48/72h.....	- 45 -
Figure 19: Determination of cell viability of osteosarcoma cell lines and human primary cells by the MTS of cells treated for 4 days with different concentrations of cisplatin or doxorubicin.....	- 54 -
Figure 20: LIVE/DEAD® assay of MG-63 after 4 days of treatment with therapeutic agents .	- 56 -
Figure 21: LIVE/DEAD® assay of Cal-72 after 4 days of treatment with therapeutic agents .	- 57 -
Figure 22: LIVE/DEAD® assay of SaOS-2 after 4 days of treatment with therapeutic agents.....	- 57 -
Figure 23: LIVE/DEAD® assay of primary osteoblasts after 4 days of treatment with therapeutic agents	- 58 -
Figure 24: LIVE/DEAD® assay of HDMEC after 4 days of treatment with therapeutic agents.....	- 59 -
Figure 25: LIVE/DEAD® assay of fibroblast after 4 days of treatment with therapeutic agents	- 59 -
Figure 26: Determination of LD ₅₀	- 61 -
Figure 27: Determination of LD ₅₀	- 62 -
Figure 28: Determination of LD ₅₀	- 63 -
Figure 29: Determination of LD ₅₀	- 64 -
Figure 30: Determination of LD ₅₀	- 65 -

Figure 31: Determination of LD ₅₀	- 66 -
Figure 32: Release of doxorubicin from doxorubicin-treated unmodified (HA) and poly(CD)- modified hydroxyapatite (HACD) after 24h.	- 67 -
Figure 33: Extraction assay: Cell viability test: MTS assay.....	- 68 -
Figure 34: Cytotoxicity test: release of LDH.....	- 70 -
Figure 35: Cell viability test: alamarBlue®	- 72 -
Figure 36: Effect of leached medium on HUVEC after 24h, 48h and 72h analyzed by MTS cell viability assay, LDH cytotoxicity assay and crystal violet DNA quantification	- 75 -
Figure 37: Effect of leached medium on pOB after 24h, 48h and 72h analyzed by MTS cell viability assay, LDH cytotoxicity assay and crystal violet DNA quantification	- 77 -
Figure 38: Effect of leached medium on MG-63 after 24h, 48h and 72h analyzed by MTS cell viability assay, LDH cytotoxicity assay and crystal violet DNA quantification	- 78 -
Figure 39: Effect of leached medium on SaOS-2 after 24h, 48h and 72h analyzed by MTS cell viability assay, LDH cytotoxicity assay and crystal violet DNA quantification	- 80 -
Figure 40: MG-63 on functionalized and non-functionalized hydroxyapatite	- 82 -
Figure 41: HUVEC on functionalized and non-functionalized hydroxyapatite	- 83 -
Figure 42: Co-cultivation of HDMEC together with pOB after 14d.....	- 83 -
Figure 43: Microvessel-like structures formed by HDMEC	- 84 -
Figure 44: Cell viability of cisplatin- or doxorubicin-treated HUVEC in normoxia or anoxia after 24h.....	- 86 -
Figure 45: Cell viability of cisplatin- or doxorubicin-treated HUVEC in normoxia or anoxia after 48h.....	- 87 -
Figure 46: Results from western blot analysis for HIF-1 α protein after the treatment of HUVEC with anoxia, CoCl ₂ and anticancer agents	- 88 -
Figure 47: Cell viability of cisplatin- or doxorubicin-treated pOB in normoxia or anoxia after 24h	- 89 -
Figure 48: Cell viability of cisplatin- or doxorubicin-treated pOB in normoxia or anoxia after 48h	- 90 -
Figure 49: Cell viability of cisplatin- or doxorubicin-treated MG-63 in normoxia or anoxia after 24h.....	- 91 -
Figure 50: Cell viability of cisplatin- or doxorubicin-treated MG-63 in normoxia or anoxia after 48h.....	- 92 -
Figure 51: ELISA of cell cycle protein p53 in cisplatin- or doxorubicin-treated HUVEC after 24h..	- 93 -
Figure 52: Quantitative real-time PCR of the cell cycle protein p53 after 24h in HUVEC	- 94 -
Figure 53: ELISA of cell cycle protein p53 in cisplatin- or doxorubicin-treated pOB after 24h- 95 -	- 95 -
Figure 54: Quantitative real-time PCR of cell cycle protein p53 after 24h in pOB	- 95 -
Figure 55: ELISA of cell cycle protein p21 in cisplatin- or doxorubicin-treated HUVEC after 24h..	- 96 -
Figure 56: Quantitative real-time PCR of cell cycle protein p21	- 97 -

List of figures

Figure 57: ELISA of cell cycle protein p21 in cisplatin- or doxorubicin-treated MG-63 after 24h....	- 97 -
Figure 58: Regulation of p53 on proteinlevel in cisplatin- or doxorubicin-treated HIF-1 α -inhibited HUVEC under anoxic conditions after 24h using ELISA.....	- 98 -
Figure 59: Regulation of p21 on proteinlevel in cisplatin- or doxorubicin- treated HIF-1 α -inhibited HUVEC under anoxic conditions after 24h using ELISA.....	- 100 -
Figure 60: Culture conditions for triple-culture..	- 102 -
Figure 61: Immunofluorescence staining of co- and triple-cultures.....	- 103 -
Figure 62: Angiogenic structures were quantified by comparing vascular area	- 104 -
Figure 63: Proinflammatory effect of macrophage treatment on the co-culture consisting of pOB and OEC. Inflammatory cytokines Interleukin-6	- 105 -
Figure 64: IL-6 ELISA	- 106 -
Figure 65: Effect of macrophage-induced THP-1 on the expression of the adhesion molecules ..	- 107 -
Figure 66: Effect of macrophage-induced THP-1 on the expression of the pro-angiogenic growth factor VEGF	- 108 -
Figure 67: Effect of macrophage-induced THP-1 on the expression of the proangiogenic growth factor VEGF	- 109 -

9 List of tables

Table 1: Cell lines.....	- 32 -
Table 2: List of cells and medium used for extraction assay	- 44 -
Table 3: LD ₅₀ values for cisplatin or doxorubicin of various cell types, determined by MTS cell viability assay or crystal violet DNA quantification	- 66 -
Table 4: Effect of leached medium from extraction assay after 24h.....	- 74 -
Table 5: Effect of leached medium from extraction assay after 24/48/72h of medium collection...	- 81 -

10 Publications and scientific presentations

10.1 Publications

E. Dohle, I. Bischoff, T. Böse, R. E. Unger and C. J. Kirkpatrick. Macrophage-mediated angiogenic activation of outgrowth endothelial cells in co-culture with primary osteoblasts. *European Cells and Materials*. 2014; 27: 149-64.

D. Herzog, E. Dohle, **I. Bischoff** and C. J. Kirkpatrick. Cell communication in a co-culture system consisting of human outgrowth endothelial cells and human primary osteoblasts. *BioMed Research International*. 2014; in press.

10.2 Scientific presentations

Oral presentations

E. Dohle, **I. Bischoff**, R. E. Unger and C. J. Kirkpatrick. Macrophage mediated angiogenic activation of outgrowth endothelial cells in co-culture with primary osteoblasts. World Biomaterial Congress, 1st-5th June, 2012, Chengdu, China.

I. Bischoff, R. E. Unger, F. Chai, H. F. Hildebrand and C. J. Kirkpatrick. Cyclodextrin-modified hydroxyapatite bone substitute as a drug delivery system. European Conference on Biomaterials (ESB2013), 8th-12th September, 2013, Madrid, Spain.

Poster presentations

I. Bischoff, R. Rehlich, A. Sartoris, R. Tsaryk, S. Halstenberg, S. Ghanaati, R. E. Unger and C. J. Kirkpatrick. Analysis of gene expression and angiogenic potential in co-cultures of primary human endothelial cells and commonly used human osteoblast cell lines. TERMIS-EU Tissue Engineering and Regenerative Medicine International Society-EU (TERMIS2011), 7th-10th June, 2011, Granada, Spain.

I. Bischoff, E. Dohle, R. E. Unger and C. J. Kirkpatrick. Effects on the regulation of VEGF by macrophages in triple-culture with outgrowth endothelial cells and

osteoblasts. TERMIS-EU Tissue Engineering and Regenerative Medicine International Society-EU (TERMIS2012), 5th-8th September, 2012, Vienna, Austria.

I. Bischoff, R. E. Unger and C. J. Kirkpatrick. Anticancer agent effects on human primary- and osteoblast cancer-cell growth and endothelial cell angiogenic potential on bone biomaterials. World Biomaterial Congress, 1st-5th June, 2012, Chengdu, China.

I. Bischoff, Dohle, R. E. Unger and C. J. Kirkpatrick. Macrophage-mediated up regulation of VEGF in co-cultures of outgrowth endothelial cells with primary osteoblasts. TERMIS-EU Tissue Engineering and Regenerative Medicine International Society-EU (TERMIS2013), 17th-20th June, 2013, Istanbul, Turkey